Stony Brook University

Synthesis of New Generation Taxoid Anticancer Agents and Dendrimer-Based Multifunctional Conjugates for Tumor-Targeting Drug Delivery

A Thesis Presented

By

Yi Sun

to

The Graduate School

In Partial Fulfillment of the

Requirements

for the Degree of

Master of Science

in

Chemistry

Stony Brook University

May 2016

Stony Brook University
The Graduate School

Yi Sun

We, the thesis committee for the above candidate for the
Master of Science degree, hereby recommend
acceptance of this thesis.

Distinguish Professor Iwao Ojima
Advisor
Department of Chemistry

Professor Dale Dreuckhammer
Chair
Department of Chemistry

Assistant Professor Ming-Yu Ngai
Third Member
Department of Chemistry

This thesis is accepted by the Graduate School

Charles Taber
Dean of the Graduate School

Abstract of the Thesis

Synthesis of New Generation Taxoid Anticancer Agents and Dendrimer-Based Multifunctional Conjugates for Tumor-Targeting Drug Delivery

Yi Sun

Master of Science

in

Chemistry

Stony Brook University

2016

Cancer remains the second leading cause of death in the United States. Although tremendous efforts have been made in the area of cancer therapy, there is still no common cure for cancer. Paclitaxel, which is a microtubule stabilizer, is used as an antitumor agent against several cancers such as ovarian, lung, and breast cancer. However, paclitaxel shows poor antitumor activities against drug resistant cell lines, and may cause undesirable side effects. Over the past decades, significant achievements have been made in the development of new generation taxoids that exhibit increased cytotoxicity against resistant cancer cell lines. Additionally work has been done towards the development of tumor-targeting drug delivery systems (TTDDS) to selectively distinguish cancer cells from normal cells.

Based on structure-activity relationship (SAR) studies on taxanes, second generation taxoid SB-T-1214 and third generation taxoids SB-T-121202, SB-T-121302, SB-T-121402, SB-T-121602, and SB-T-121702 were synthesized *via* the Ojima-Holton coupling reaction. The biological evaluation of these novel taxoids showed excellent IC_{50} values against certain drug sensitive and drug resistant cancer cell lines by MTT assays.

Biotin receptors are overexpressed on the surface of some cancer cell lines to maintain rapid cancer cell growth. Dendrimers are well-defined three-dimensional macromolecules, which can be used to increase the payload of the drugs, targeting efficacy of the conjugate, and other biological and physiological properties. Based on this fact, two dendrimer-based multifunctional conjugates for tumor-targeting drug delivery were synthesized by employing biotin as targeting moiety and second generation taxoid SB-T-1214 as antitumor agent.

List of Contents

List of Figures VIII

List of Schemes X

List of Tables XII

List of Abbreviations XIII

Acknowledgement XVI

Chapter I

Synthesis of New Generation Taxoid Anticancer Agents

§ 1.1 Introduction 2

§ 1.1.1 Cancer 2

§ 1.1.2 Chemotherapy 3

§ 1.2 Paclitaxel 4

§ 1.2.1 Discovery of Paclitaxel and its Mechanism 4

§ 1.2.2 Semi-synthesis of Paclitaxel 5

§ 1.2.3 Drug Resistance of Paclitaxel Treatment 8

§ 1.3 Development of Next Generation Taxoids. 10

§ 1.3.1 Structure-Activity Relationship (SAR) Study of Taxoids 11

§ 1.4 Synthesis of β-Lactam 14

§ 1.4.1 β-Lactam Synthon Method to Develop New Generation Taxoids 14

§ 1.4.2 Synthesis of Chiral Ester 16

§ 1.4.3 Synthesis and Modification of β-Lactam 17

§ 1.5 Synthesis of New Generation Taxoids 21

§ 1.5.1 Synthesis of second-generation taxoid SB-T-1214 21

§ 1.5.2 Synthesis of third-generation taxoids SB-T-121202, SB-T-121302 24

SB-T-121402, SB-T-121602 and SB-T-121702 24

§ 1.6 Biological Evaluation of New Generation Taxoids 29

§ 1.7 Summary 33

§ 1.8 Experimental 33

§ 1.8.1 General Methods 33

§ 1.8.2 Materials 34

§ 1.8.3 Experimental Procedure 34

Chapter II

Synthesis of Dendrimer-Based Multifunctional Conjugates for Tumor-Targeting Drug Delivery

§ 2.1 Introduction 63

§ 2.2 Tumor-targeting modules 64

§ 2.2.1 Polyunsaturated Fatty Acids (PUFAs) 65

§ 2.2.2 Monoclonal Antibodies (mAbs) 67

§ 2.2.3 Biotin 69

§ 2.3 Enhanced Permeability and Retention (EPR) Effect for Cancer Chemotherapy 71

§ 2.4 Dendrimer 72

§2.5 Design and Synthesis of PAMAM Dendrimer-Based Biotin-Taxoid Conjugate and for Tumor-Targeting Drug Delivery 78

§ 2.5.1 Synthesis of Biotin PEGylated G3 PAMAM Dendrimer 80

§2.5.2 Synthesis of PAMAM Dendrimer-Based Biotin-Taxoid Conjugate 84

§ 2.6.1 Design and Synthesis of Asymmetric Bow-Tie Dendrimer-based (ABTD) conjugate for Tumor-Targeting Drug Delivery 87

§ 2.6.1 Synthesis of PAMAM G1 Dendrimer-Alkyne Conjugate 88

§ 2.6.2 Synthesis of ABTD Conjugate 91

§ 2.7 Conclusion 94

§ 2.8.1 General Methods 94
§ 1.8.2 Materials 95
§ 1.8.3 Experimental Procedure 95
Reference 104
Appendix 111

List of Figures

Figure 1. Chemical Structure of Paclitaxel (Taxol)..... 5
Figure 2. Mechanism of Action of Paclitaxel..... 5
Figure 3. Chemical Structure of 10-deacetylbaccain III (10-DAB III)..... 6
Figure 4. MDR Mediated by Pgp..... 9
Figure 5. Tumor shrinks but grows back if the drug do not kill cancer stem cells..... 10
Figure 6. Overview of SAR studies of taxol..... 11
Figure 7. Chemical Structure of Whitesell's Chiral auxiliary..... 14
Figure 8. Catalytic Cycle of Sharpless Asymmetric Dihydroxylation..... 16
Figure 9. Mechanism of enolate-imine condensation..... 19
Figure 10. Mechanism of CAN deprotection..... 20
Figure 11. Chemical Structure of 10-DAB and SB-T-1214..... 21
Figure 12. Chemical Structure of Third Generation Taxoids Bearing Methyl Group at meta position of C-2 Benzoyl Moiety..... 25
Figure 13. Effect of DHA-taxoid conjugates on human colon tumor xenograft DLD-1 and human ovarian tumor xenograft A121..... 67
Figure 14. Chemical Structure of mAb-SB-T-12136 conjugates, SB-T-12136 and SB-T-12136-SH..... 68
Figure 15. Antitumor activity of anti-EGFR mAb-taxoid conjugates against A431 xenografts..... 69
Figure 16. RME and intracellular drug release..... 70
Figure 17. EPR Effect for Cancer Chemotherapy..... 72
Figure 18. Structures of nanoparticles A) carbon nanotubes, B) dendrimers, C) liposomes, D) quantum dots, E) gold nanoparticles..... 73
Figure 19. Graphical representation of dendrimers from generation 0 to generation 4..... 74
Figure 20. Chemical Structure of G1 PAMAM Dendrimer..... 75
Figure 21. Schematic representation of "diblock" PAMAM cystamine core dendrimer-based conjugate for synthesis of bioactive nanoparticles..... 76

Figure 22. Structure of multifunctional PAMAM dendritic devices 77
Figure 23. Designed Structure of PAMAM Dendrimer-Based Biotin-Taxoid Conjugate 78
Figure 24. Chemical Structure of G3 PAMAM dendrimer 79
Figure 25. MALDI-TOF Result of Fully Functionalized PAMAM G3 Dendrimer 84
Figure 26. MALDI-TOF Result of Biotin-PEGlated-G3-Alkyne Conjugate 86
Figure 27. The Designed ABTD Conjugate for Tumor Targeting Drug Delivery 88
Figure 28. MALDI-TOF Result of Fully Functionalized G1 PAMAM Dendrimer 90
Figure 29. MALDI-TOF result of Alkyne-G1-Linker Conjugate 92
Figure 30. MALDI-TOF Result of G1 Half Dendron-Linker-G3 Half Dendron Construct 93

List of Schemes

Scheme 1. Semi-synthesis of Paclitaxel by Potier 7
Scheme 2. Ojima-Houlton Coupling Reaction to afford Paclitaxel 8
Scheme 3. Sharpless Asymmetric Dihydroxylation to afford **1-1** 15
Scheme 4. Reductive benzylic dehydroxylation of crude diol 16
Scheme 5. Synthetic route to β-Lactam 17
Scheme 6. Synthesis of β-Lactam 18
Scheme 7. PMP was removed by employing CAN 20
Scheme 8. Modification on β-Lactam 21
Scheme 9. Initial Protection at the C-7 Position of 10-DAB 22
Scheme 10. Synthesis of 10-modified 7-TES-DAB 23
Scheme 11. Coupling reaction of the baccatin with enantiomerically pure β-Lactam 23
Scheme 12. Protecting Groups were Removed to Afford Target Molecule **SB-T-1214** 24
Scheme 13. Synthesis of C-2-modified 10-DAB III 25
Scheme 14. Synthetic Route to SB-T-121402, SB-T-121602 and SB-T-121702 . 27
Scheme 15. Synthetic route to SB-T-121202 and SB-T-121302 28
Scheme 16. Synthesis of DHA-taxoid conjugates 66
Scheme 17. Mono-Protection of Triethylene Glycol 80
Scheme 18. Hydroxyl Group was Converted to Azide Group 80
Scheme 19. Azide Group was Reduced to Amine Group Staudinger Reaction 81
Scheme 20. Biotin was Activated *via* DIC Coupling to Afford Biotin-OSu 81
Scheme 21. Biotin-PEG conjugate was generated 82
Scheme 22. *Tert*-butyl Ester was Deprotected by TFA 82
Scheme 23. Synthesis of Biotin-PEG-OSu conjugate 82
Scheme 24. Fully functionalization with PEGylated biotin on generation 3 PAMAMA dendrimer 83
Scheme 25. Synthesis of Biotin-PEGlated-G3-Alkyne Conjugate 85
Scheme 26. Synthesis of PAMAM G3 Dendrimer-Based Biotin-Taxoid Conjugate

..... 87
Scheme 27. Synthesis of PEG-Alkyne Conjugate..... 88
Scheme 28. Deprotection of *tert*-Butyl Group to afford 2-11 89
Scheme 29. Synthesis of Alkyne-PEG Activated Ester 89
Scheme 30. Synthesis of Functonalized G1-Alkyne Conjugate..... 90
Scheme 31. Synthesis of Alkyne-G1-Linker Conjugate 91
Scheme 32. Synthesis of "Click-Ready" Intermediate for ABTD Conjugate..... 93

List of Tables

Table 1. Cytotoxicity of New-Generation Taxoids against MCF-7 cell line and MCF-7R cell line 30

Table 2. Cytotoxicity of New-Generation Taxoids against LCC6-WT cell line and LCC6-MDR cell line 31

Table 3. Cytotoxicity of New-Generation Taxoids against PANC-1 cell line and CFPAC-1 cell line 32

List of Abbreviations

ABC- ATP-binding cassette

Ac- acetyl

AcOH- acetic acid

ATP- adenosine triphosphate

Bn- benzyl

Boc- tert-butoxycarbonyl

Bz- benzoyl

C- carbon

CAN- cerium(IV) ammonium nitrate

CSC-enriched cells– cancer stem cell-enriched cells

d- doublet

DAB- Deacetyl baccatin

dd- doublet of doublet

DCM- dichloromethane

DIC- *N,N*-diisopropylcarbodiimide

DMAP- 4-*N,N′*-dimethylaminopyridine

DMF- *N,N′*-dimethylformamide

ee- enantiomeric excess

eq- equivalent

Et- ethyl

et al.- and others

EtOAc- ethyl acetate

EtOH- ethanol

FDA- Food and Drug Administration

g- gram

HEX- hexanes

HOSu- *N*-hydroxysuccinimide

HPLC- high performance liquid chromatography

h – hour

NHS- *N*-hydroxysuccinimide

Hz- hertz

IC_{50} - concentration for 50 % inhibition

iPr- isopropyl

J- coupling constant

Kg- kilogram

L- liter

LDA- lithium diisopropylamide

LiHMDS- lithium bis(trimethylsilyl)amide

m- multiplet

M- molar or molarity

MDR- multi-drug resistance

Me- methyl

MeOH- methanol

mg- milligram

min- minute

mL- milliliter

mM- millimolar

mmol- millimole

mol - mole

m.p. - melting point

MS-mass spectrometry

n-BuLi- n-butyllithium

NCI- National Cancer Institute

nM- nanomolar

NMR- nuclear magnetic resonance

o/n- overnight

PBS- phosphate buffered saline

Pgp- P-glycoprotein

Ph- phenyl

PMP- p-methoxyphenyl

ppm- parts per million

Py- pyridine

q- quartet

RME- receptor-mediated endocytosis

rt- room temperature

s- singlet

SAR- structure-activity relationship

t- triplet

t-Bu- tert-butyl

TEA- triethylamine

Tert- tertiary

TES- triethylsilyl

THF- tetrahydrofuran

TIPS- triisopropylsilyl

TLC- thin layer chromatography

U.S.- United States

UV- ultraviolet-visible

[α]- specific optical rotation

δ- chemical shift

μL- microliter

Acknowledgement

First and foremost, I would like to express my sincere and deepest gratitude to my dissertation advisor Distinguish Professor Iwao Ojima for his full support, expert guidance and encouragement throughout my graduate study. Without his incredible patience and timely wisdom and counsel, my thesis work would have been a frustrating work. And I also would like to than both you and Mrs.Yoko Ojima for your generous hospitality during annual July BBQ and Thanksgiving Eve parties at your home.

I would also like to thank my committee members, Professor Dale Dreuckhammer and Professor Ming-Yu Ngai, for providing me numerous advices and finding time for me in their busy schedule.

I want to express my true appreciation to my mentor, Longfei Wei, for all the guidance and training I received from him. The good advice, support and friendship of him has been invaluable on both an academic and a personal level, for which I am extremely grateful.

I would like to acknowledge members in Ojima research group: Dr. Kongzhen Hu, Simon Tong, Krupa Haranahalli, Changwei Wang, Xin Wang, Su Yan, Yaozhong Zhang, Yao Zong, Katherine Maffucci, Qianwen Gan and Christie Shea. It was a great pleasure working with you and I think only our friendship can surpass your help. I also want to thank past Ojima group member: Dr. Gary Teng,

Dr. Chih-Wei Chien, Dr. Siyeon Lee, Dr. Tao Wang, Brendan Lichtenthal and Jonathan Khan. I wish you all the best of luck in your future endeavors. I would also like to give a special thank you to Mrs. Patricia Marinaccio and Ms. Roxanne Brockner for their kindness and support.

I would also like to thank Dr. Béla Ruzsicska, for all the analytical support and help; Dr. Jim Marecek and Dr. Francis Picart, for teaching me how to use NMR spectrometry.

I am most grateful to my family members and friends for their love and support. To both of my parents, Chengshun and Di, I am so lucky to have you as my parents. Your continuous support and encouragement accompany me throughout my entire life. I also want to express my appreciation to my friends both in United States and China. Thank you for always be there for me.

Chapter I

Synthesis of New Generation Taxoid Anticancer Agents

§ 1.1 Introduction 2
§ 1.1.1 Cancer 2
§ 1.1.2 Chemotherapy 3
§ 1.2 Paclitaxel 4
§ 1.2.1 Discovery of Paclitaxel and its Mechanism 4
§ 1.2.2 Semi-synthesis of Paclitaxel 5
§ 1.2.3 Drug Resistance of Paclitaxel Treatment 8
§ 1.3 Development of Next Generation Taxoids. 10
§ 1.3.1 Structure-Activity Relationship (SAR) Study of Taxoids 11
§ 1.4 Synthesis of β-Lactam 14
§ 1.4.1 β-Lactam Synthon Method to Develop New Generation Taxoids 14
§ 1.4.2 Synthesis of Chiral Ester 16
§ 1.4.3 Synthesis and Modification of β-Lactam 17
§ 1.5 Synthesis of New Generation Taxoids 21
§ 1.5.1 Synthesis of second-generation taxoid SB-T-1214 21
§ 1.5.2 Synthesis of third-generation taxoids SB-T-121202, SB-T-121302 24
SB-T-121402, SB-T-121602 and SB-T-121702 24
§ 1.6 Biological Evaluation of New Generation Taxoids 29
§ 1.7 Summary 33
§ 1.8 Experimental 33
§ 1.8.1 General Methods 33
§ 1.8.2 Materials 34
§ 1.8.3 Experimental Procedure 34

§ 1.1 Introduction

§ 1.1.1 Cancer

Cancer is a group of diseases characterized by fast growth and spread of certain abnormal cells. It remains the second leading cause of death in the United States and is about to surpass heart disease as the first leading cause in the next few years.[1] Cancers of the lung, breast, prostate, and colon have become more frequently diagnosed over the past few years due to common risk factors such as cigarette smoking, unhealthy dietary habits, and exposure to environmental or workplace toxins.[2] It is estimated that 595,690 Americans are expected to die of cancer in 2016, that's about 1,630 people per day.[1] The number of new cancer patients is expected to more than double from 1.36 million in 2000 to almost 3.0 million in 2050.[3]

Over the past several decades, tremendous efforts have been made in the area of cancer therapy. The 5-year relative survival rate for all cancers diagnosed during 2005-2011 was 69%, up from 49% during 1975 to 1977.[1] On the other hand, awareness of cancer and external risk factors have contributed to a reduction in cancer incidence rates. Over the past 40 years, a 50% reduction in per capita cigarette consumption has led to a 30% reduction in the male lung cancer death rate.[4]

There are various types of cancer treatment such as chemotherapy, radiation therapy, immunotherapy, targeting therapy and hormone therapy. Most people prefer to have a

combination of treatment. These treatments not only affect tumor tissues but also affect healthy tissues and organs causing a variety of side effects.

§ 1.1.2 Chemotherapy

Chemotherapy is a traditional cancer treatment that employs drugs to stop or slow the growth and division of cancer cells. Traditional chemotherapeutic drugs can be divided into several groups based on their mechanisms of action such as alkylating agents (i.e., nitrosoureas, alkyl sulfonates), antimetabolites (i.e., 5-fluorouracil, methotrexate), antitumor antibiotics (i.e., daunorubicin), topoisomerase inhibitors (i.e., topotecan, etoposide), microtubule stabilizing agents (i.e., paclitaxel), corticosteroids (i.e., prednisone). In many cases, two or more drugs are used in combination based on the non-overlapping mechanisms of action.

A long-standing problem with traditional chemotherapeutic drug is that chemotherapeutic drugs could not differentiate cancer cells and normal cells well enough. That is to say, these antitumor agents would not only kill cancer cells, but also normal cells. These drugs could therefore cause severe side effects such as hair loss, appetite loss, anemia, constipation, fatigue, and sleep problems.

§ 1.2 Paclitaxel

§ 1.2.1 Discovery of Paclitaxel and its Mechanism

Paclitaxel (Taxol) (**Figure 1**), a diterpenoid natural product, was first extracted from the bark of Pacific Yew (*Taxus brevifolia*) in 1963 by M.C. Wani and Monre E. Wall.[5] The molecule contains an oxatane ring and an ester side chain at C-13 position. Taxol was found to be an excellent cytotoxic agent against certain cancer cell lines such as B16 murine melanoma cell lines and the leukemia cell lines.[6] Paclitaxel was approved by FDA for the treatment of the ovarian cancer in 1992 and for the treatment of breast cancer in 1996.[7]

Paclitaxel's mechanism of treating cancer cells is illustrated in **Figure 2**. It interferes the normal breakdown of microtubules during cell division. During cell replication, paclitaxel binds to β-tublin after the β-tublin forms a heterodimer with α-tublin. Paclitaxel follows the heterodimer undergo further polymerization. Unlike microtubule destabilizing agents such as colchicine, combrestatin and vinfluine, paclitaxel is a microtubule stabilizer and works as a tubulin depolymerization inhibitor. Evidence shows that paclitaxel can enhance this polymerization, and stabilizes the microtubule polymer thus preventing disassembly. Chromosomes are thus unable to form a metaphase spindle configuration. That is to say, chromosomes cannot move to the opposite side of

the dividing cells. This blocks progression of mitosis and will lead to cell apoptosis or reversion to the G-phase of the cell cycle without cell division eventually.[8, 9]

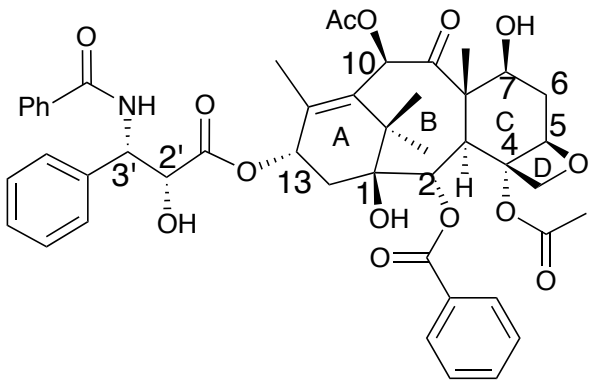

Figure 1. Chemical Structure of Paclitaxel (Taxol)

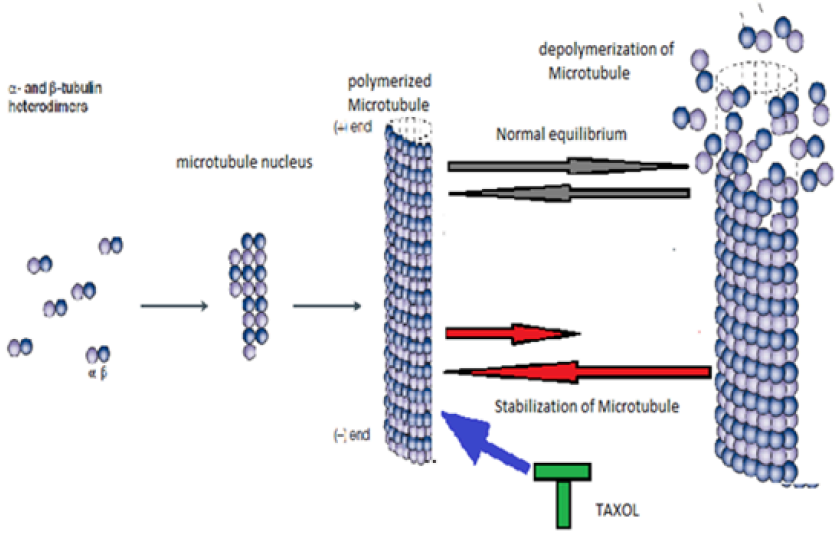

Figure 2. Mechanism of Action of Paclitaxel (Adapted from Ref. 8.)

§ 1.2.2 Semi-synthesis of Paclitaxel

In previous years, paclitaxel was isolated from the bark of Pacific Yew, which is a very slow-growing tree. The yield of the extraction is low: 10,000 kg of bark produces

only 1 kg of paclitaxel.[10] By the reasons of the low yield and the increasing demand for paclitaxel, organic chemists started to work on the synthetic routes to get this complex molecule. In 1988, Potier and Greene reported the semisynthesis of paclitaxel by employing 10-deacetylbaccatin III (10-DAB III) (**Figure 3**) as the starting material, which has the exact tetracyclic diterpene skeleton of taxol[11].

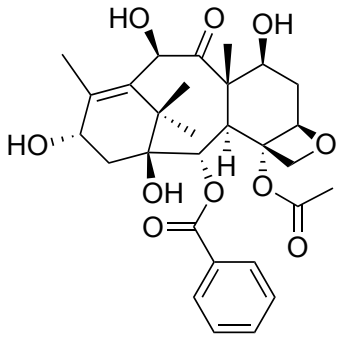

Figure 3. Chemical Structure of 10-deacetylbaccain III (10-DAB III)

10-DAB III could be extracted from the needles and leaves of European yew. Compared to paclitaxel, 10-DAB is much more easily obtained, not only because of the large quantity of needles but also the yield of the extraction is higher.[12] The semisynthesis of Potier's method started from commercially available 3-phenyl-2-propen-1-ol to obtain the side chain precursor of C-13 position by 8 steps. Then the side chain precursor was coupled to C-7 protected and C-10 modified 10-DAB III in the presence of DCP and DMAP.[11] (**Scheme 1**)

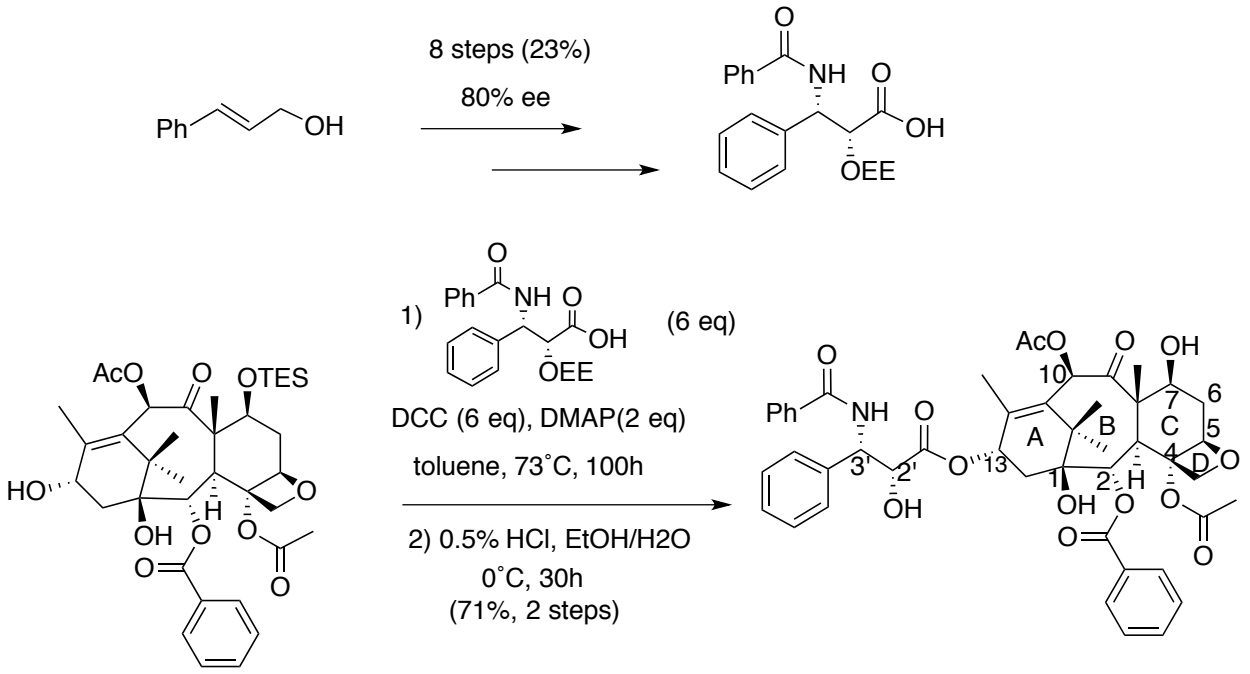

Scheme 1. Semi-synthesis of Paclitaxel by Potier[11]

Potier's semisynthesis of paclitaxel included harsh conditions due to the less reactive C-13 hydroxyl group in 10-DAB III. Only 50% conversion was achieved and the epimerization of hydroxyl group can be observed at the C-2' position. In this case, Ojima-Holton coupling reaction was invented. This method is a more efficient and applicable synthetic approach because it maintained the C2' hydroxyl group's stereochemistry and yielded higher amounts of product (**Scheme 2**). The releasing strain of β-Lactam induces the reaction proceeding to completion under much milder conditions.[13, 14]

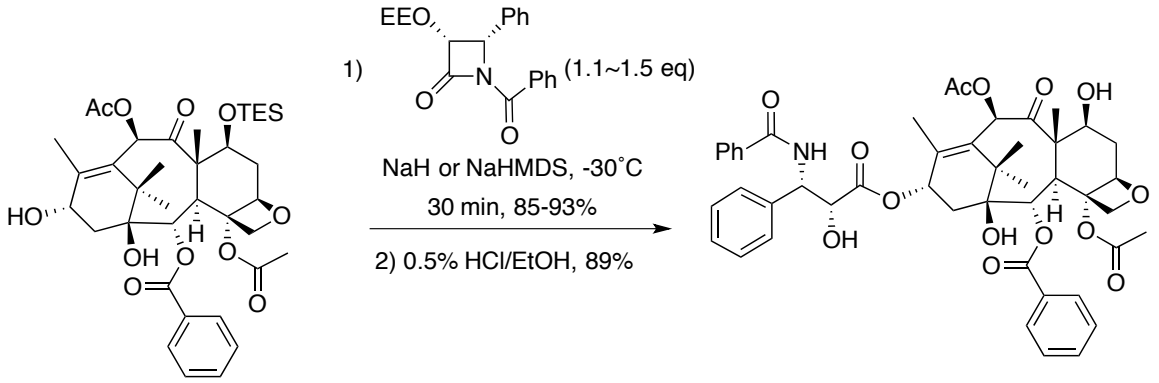

Scheme 2. Ojima-Houlton Coupling Reaction to afford Paclitaxel[13]

§ 1.2.3 Drug Resistance of Paclitaxel Treatment

Although paclitaxel shows profound antitumor activity against many cancer cell lines, there still exists some resistance in certain cancer cell lines such as non-small-cell lung (NSCL) cancer cell line and ovarian cancer cell line.[15] This muti-drug resistance (MDR) is characterized by the overexpression of P-glycoprotein (Pgp) which is an ATP-dependent efflux pump. Pgp, an important transmembrane protein, is able to pump out foreign substances from cells.[16] Not only paclitaxel but also other traditional cancer chemotherapeutic drugs such as etoposide, daunomycin, vinblastine, and doxorubicin are easily pumped out due to the existence of Pgp which results in a poor cytotoxicity (**Figure 4**).[17]

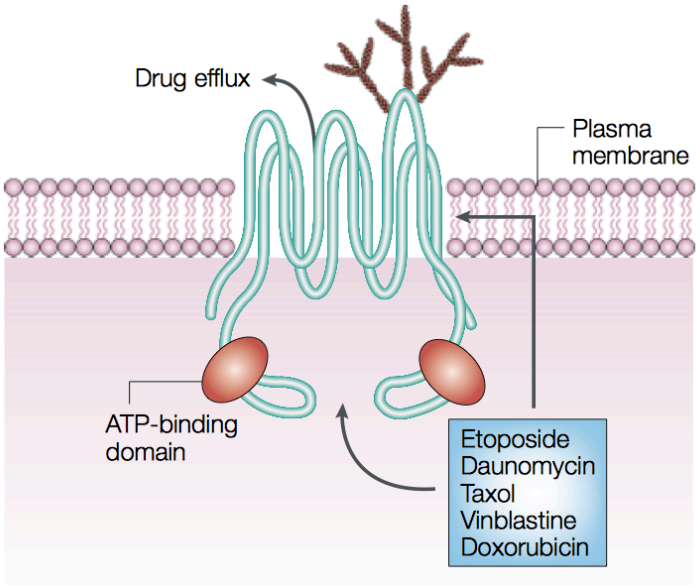

Figure 4. MDR Mediated by Pgp (Adapted from Ref. 16.)

Other mechanisms are also involved in the resistance to paclitaxel. They are related to the structure and function of cellular target tubulin/microtubules.[18] Point mutations in the paclitaxel binding pocket have been observed in ovarian and cervical cancer cell lines.[18,19] These cell lines show poor sensitivity during exposure to paclitaxel.

On the other hand, the existence of cancer stem cells (CSCs) is another intractable problem during treatment with paclitaxel. Based on the cancer stem cell theory, tumors contain three different kinds of cancer cells: CSCs, transient amplifying cells and differentiated cells.[20] CSCs have profound self-renewal capacity and the ability to produce more mature cells called transient amplifying cells. These transient amplying cells divide a certain of times and then differentiate into specialized tumor cells. Specialized tumor cells do not divide and do not contribute to tumor growth. So if the cancer treatment destroys the bulk of a tumor but leaves behind cancer stem cells, the

existence of these cancer stem cells will still cause the growth of tumor tissue as shown in **Figure 5**.[21] However, CSCs are naturally resistant to chemotherapy due to multiple mechanisms, including their relative quiescence, excellent capacity for DNA repair, activation of the ATP-binding cassette (ABC) transporters, resistance to apoptosis and others.

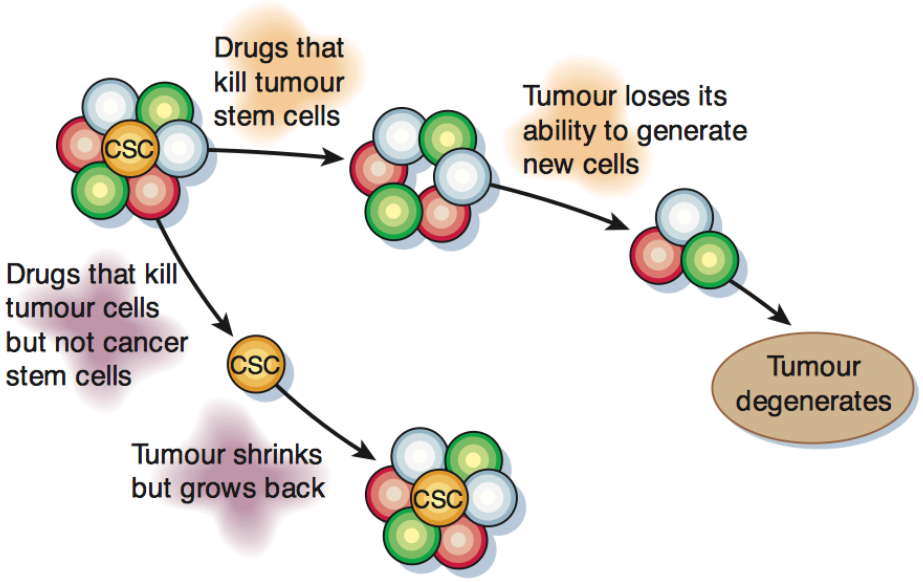

Figure 5. Tumor shrinks but grows back if the drug do not kill cancer stem cells (Adapted from Ref. 20.)

§ 1.3 Development of Next Generation Taxoids.

Although paclitaxel possesses potent antitumor activity, it has been shown that treatment with it often produces undesirable side effects as well as drug resistance.[22] Accordingly, there is a strong demand to develop new taxane anticancer agents with

fewer side effects, superior pharmacological properties, and improved activity against drug resistant tumors. [23]

§ 1.3.1 Structure-Activity Relationship (SAR) Study of Taxoids

Over the past several decades, tremendous efforts have been made on the SAR study of Taxol.[24, 25, 26] An overview of SAR studies of taxol was shown in **Figure 6**.[27] SAR studies of the baccatin core and C-13 side chain of taxol are discussed below.

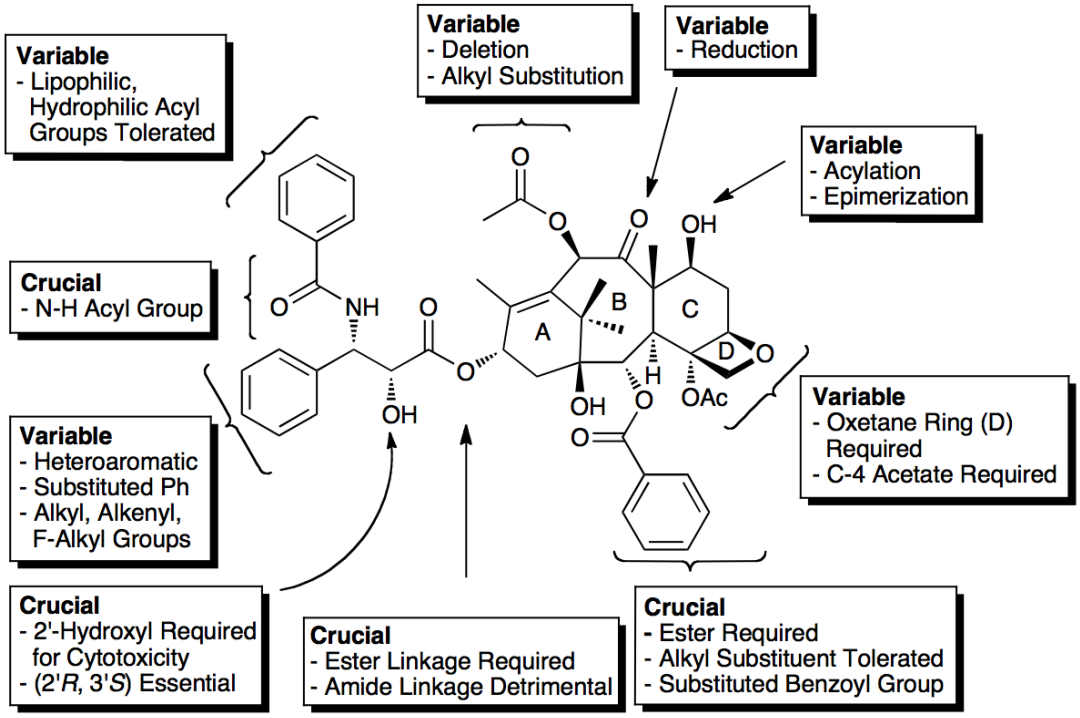

Figure 6. Overview of SAR studies of taxol (Adapted from Ref. 26.)

For the baccatin core of taxol, modification or contraction of the A ring or the C ring will significantly decrease the cytotoxic effect compared to the original structure.[28] Modification of the B ring still presents in existence of some antitumor activity against

certain cancer cell lines.[29] The D ring is more crucial as compared to the other rings. Modifications on the D ring will dramatically decrease the activity.[29, 30] The replacement of oxetane ring with a cyclopropane ring, however, maintains similar cytotoxicity compared to original compound.[31] More importantly, based on Ojima's group's SAR studies, it was found that introduction of certain groups (e.g., MeO, N_3, F, Cl, etc.) to the *meta* position of the C-2 benzoyl moiety significantly increase the cytotoxicity against some drug resistant cancer cell lines such as MCF-7R and MCC6-MDR and drug sensitive cancer cell lines such as MCF-7 and MCC6-WT.[23] Introduction of certain group at *para* position of the C-2 benzoyl will lead to a poor activity compared to *meta* substitution patterns. It is believed that the substitution at *para* position of C-2 benzoyl group will break the hydrophobic interaction with C-3' phenyl moiety which is essential to maintain the conformation of the compound, while the introduction of certain group at *meta* position enhances this interaction.[32] The C-4 acetoxy group is also critical for the antitumor activity of the compound. Hydrolysis or loss will lead to a significant decrease in cytotoxicity.[33, 34] Groups at C-7, C-9 and C-10 are more tolerable to modification as compared to the C-2 benzoyl moiety, C-4 acetoxy group and oxetane D ring. The resulting analogs possess cytotoxicities which are similar or better than that of taxol.[35, 36] It has been reported that modifications such as epimerization, deoxygenation, and acylation at C-7 position do not dramatically affect the activity against cancer cell lines.[37] For the C-10 position, evidence suggest that

modification of this position has little effect on the *in vitro* cytotoxicity. However, based on SAR studies carried by the Ojima research group, a combination of modifications at the C-10 and C-2 position will significantly increase cytotoxic activity against certain Pgp-mediated drug resistant cancer cell lines.[38]

For C-13 side chain of taxol, the isoserine moiety is important to maintain the cytotoxicity against cancer cells. Evidence suggest that if the paclitaxel does not have this isoserine moiety, the antitumor potency will decrease more than 1,000 fold.[39] Loss of any part of isoserine moiety will also induce poor antitumor activity against certain cancer cell lines.[40] C-2' hydroxyl group is essential for the antitumor activity of taxol. Recent SAR studies point out that there exists hydrogen bonding between the C-2' hydroxyl group and Arg 369 or Gly 270 of the *β*-tubulin backbone.[41] However, this C-2' hydroxyl group can form certain chemical bonds and further undergo hydrolysis in the cells meaning that the C-2' hydroxyl group can be employed to develop a "prodrug" if there are esterases in the cells.[42, 43] For the C-3'-N position, evidence showed that replacement of phenyl group to *t*-butoxycarbonyl group will increase the potency of paclitaxel.[44, 45] For the C-3' phenyl group, it has been showed that bearing C-3' alkyl or alkenyl group other than phenyl will increase the antitumor activity dramatically.[46] It is considered to be a significant step in the SAR study of taxol, because these modified drugs were found to be extremely potent against certain MDR cancer cell lines.[47] The stereochemistry at C-2'

and C-3' are also very important for the cytotoxic effects of taxol. Evidence suggests that departure of configuration will result in poor antitumor activity.

The roles of each part of paclitaxel are not completely clear so far. Thus further studies on SAR of paclitaxel still need to be conducted in order to develop new antitumor agents.

§ 1.4 Synthesis of *β*-Lactam

§ 1.4.1 *β*-Lactam Synthon Method to Develop New Generation Taxoids

The *β*-Lactam Synthon Method is widely used in the development of next generation taxoids and further SAR studies. The resulting *β*-Lactam Synthon was employed as a precursor in the semisynthesis of taxol. The *β*-Lactam could be synthesized in a good yield and extremely high enantiomeric purity *via* an enolate-imine cyclocondensation.[48, 13] The stereochemistry of this precursor was controlled by Whitesell's chiral auxiliary (**Figure 7**).[49]

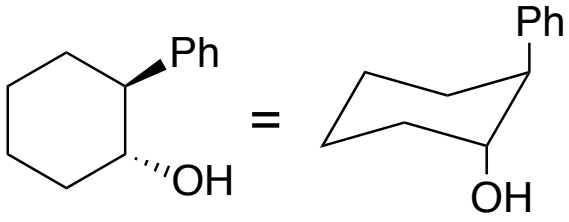

Figure 7. Chemical Structure of Whitesell's Chiral auxiliary

§ 1.4.2 Synthesis of Chiral Auxiliary

The synthesis of Whitesell's chiral auxiliary started from commercial available 1-phenyl-1-cyclohexene. At first, Sharpless asymmetric dihydroxylation reaction, also called Bishydroxylation, was conducted by employing AD-mix-β reagent to afford **1-1 (Scheme 3)**. This reaction was first investigated by King and Sharpless in 1988.[50]

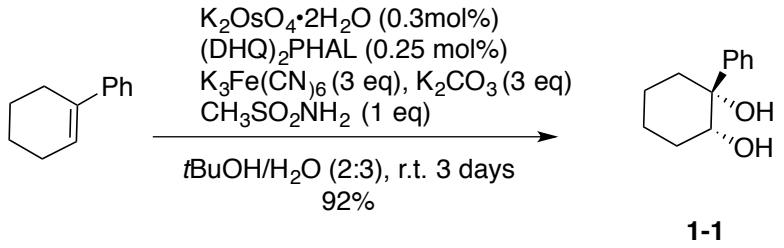

Scheme 3. Sharpless Asymmetric Dihydroxylation to afford **1-1**

The mechanism of Sharpless asymmetric dihydroxylation reaction was showed in **Figure 8**.[51] This reaction begins with the formation of the osmium tetroxide – ligand complex, followed by a [3 + 2] cycloaddition with alkyne. The expecting diol and reduced osmate are then formed after hydrolysis. At last, osmium tetroxide – ligand complex is regenerated by employing oxidant.

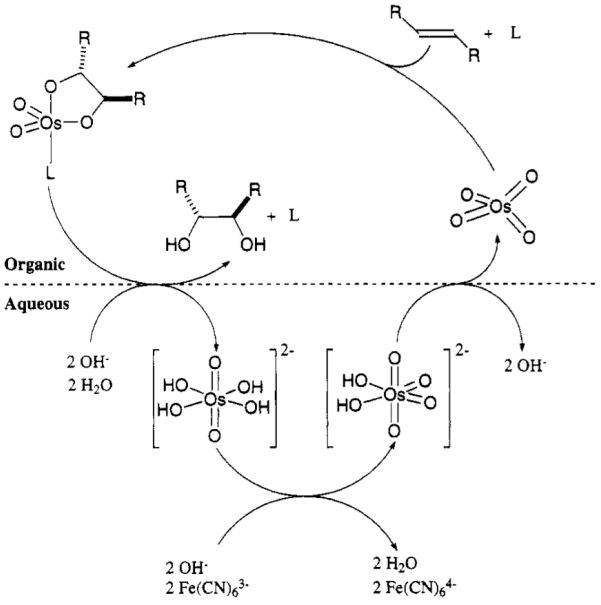

Figure 8. Catalytic Cycle of Sharpless Asymmetric Dihydroxylation (Adapted from Ref. 50.)

The resulting **1-1** was then selectively reduced by Raney nickel and gave the desired chiral auxiliary **1-2** in high enantiopurity (> 99% *ee*) (**Scheme 4**). Raney Nickel needed to be preserved in wet ethanol or wet water as it is highly pyrophoric. The desired product **1-2** was then recrystallized from pentane as white needle crystals.

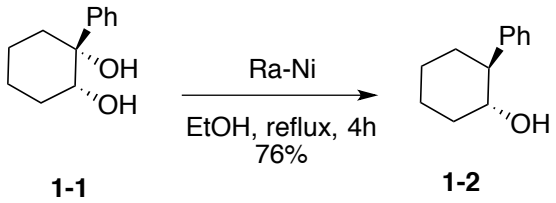

1-1 **1-2**

Scheme 4. Reductive benzylic dehydroxylation of crude diol

§ 1.4.2 Synthesis of Chiral Ester

The synthetic route of chiral ester is shown in **Scheme 5**.

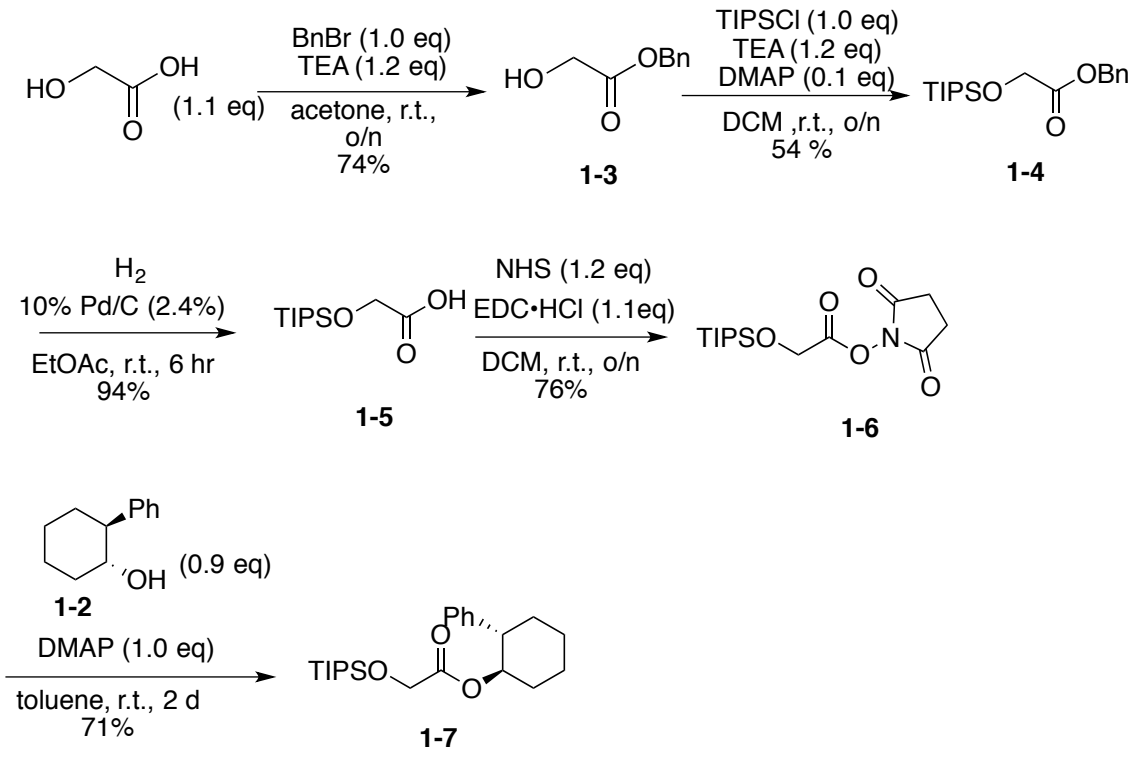

Scheme 5. Synthetic route to *β*-Lactam

The synthesis of chiral ester started from selective benzylation of commericially available glycolic acid, followed by further protection of another hydroxyl group by triisopropylsilyl chloride (TIPSCl). Carboxyl group was then regenerated from hydrogenolysis by employing H_2 and Pd/C. The intermediate **1-5** was not stable and thus was used immediately in the next step without purification. It was activated by *N*-hydroxyl succinimide (NHS) *via* EDC coupling. The resulting compound was Coupled to chiral auxiliary **1-2** under basic conditions gave chiral ester **1-7** in a good yield (71%).

§ 1.4.3 Synthesis and Modification of β-Lactam

The synthetic route of β-Lactam was illustrated in **Scheme 6**.

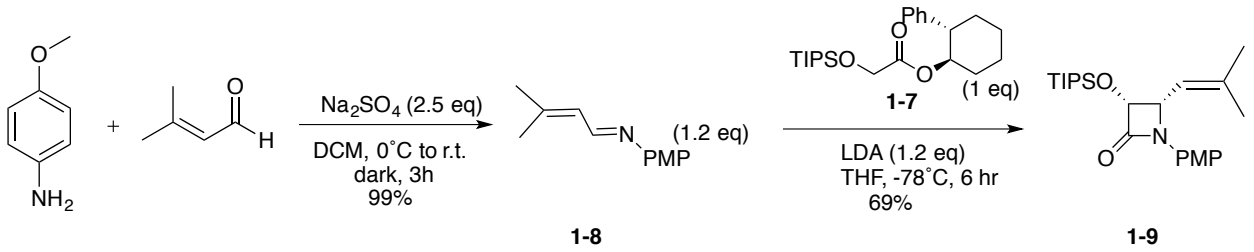

Scheme 6. Synthesis of *β*-Lactam

First of all, imine **1-8** was synthesized by employing *p*-anisidine and 3-methyl-2-butenal. 2.5 equivalents of Na_2SO_4 was added in the reaction mixture as a drying agent, and was used to push the reaction equilibrium forward. The reaction was conducted under the protection of aluminum foil as well as all the work up procedure since the product was sensitive to light. The crude product was directly used in the next step to react with chiral ester **1-7**. To avoid generation of side product in the next step, the crude **1-8** was put under *vaccum* for more than 4 hours to get rid of the excessive 3-methyl-2-butenal. The enantiopure *β*-Lactam was then synthesized by the cyclocondensation of the imine **1-8** and *E*-enolate generated *in situ* from chiral ester **1-7**. The mechanism of synthesis the *cis*-*β*-Lactam with high enantiomeric purity was shown in **Figure 9**.

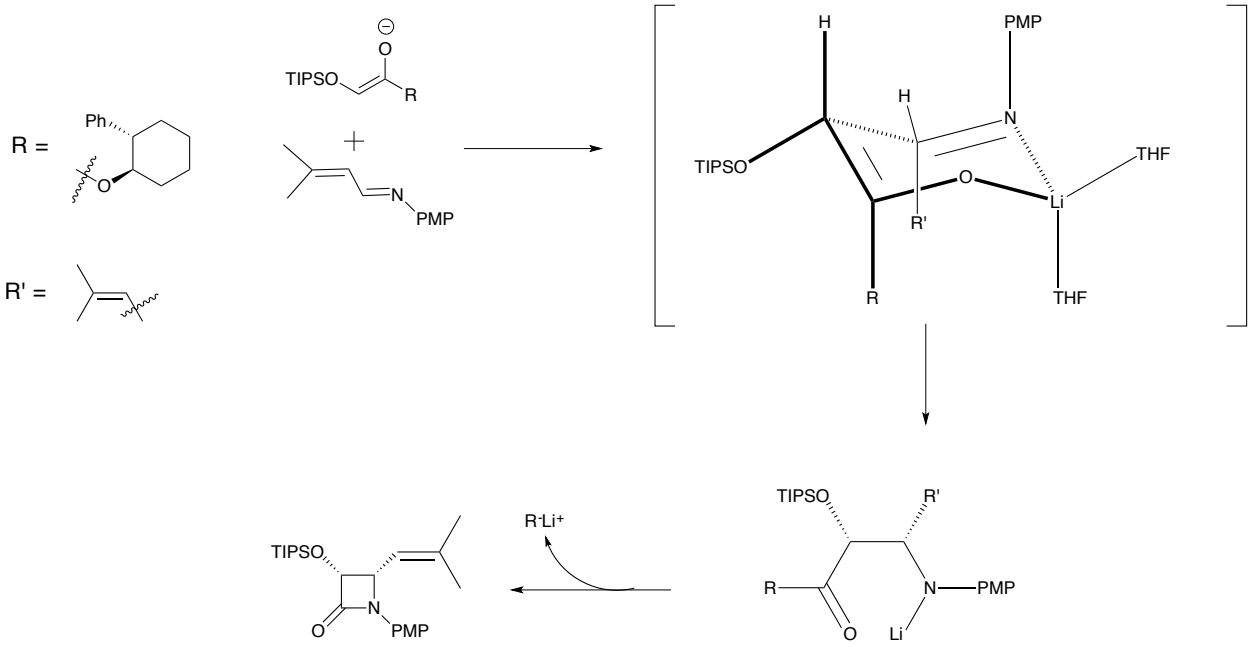

Figure 9. Mechanism of enolate-imine condensation

This enolate-imine condensation was performed in a very low temperature. *E*-enolate is predominantly formed and reacted with imine from the least hindered face to generate six-member-ring transition state as illustrated in **Figure 9**. The crude product was purified by column chromatography and recrystallized *via* hexanes to give **1-9** as a white solid in 99% *ee*.

p-methoxyphenyl (PMP) group was then removed by employing cerium ammonium nitrate (CAN) as an oxidizing agent (**Scheme 7**). CAN took two electrons from starting material, and itself was reduced to Ce (III).

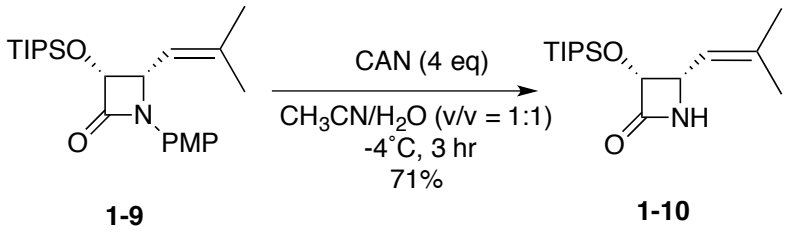

1-9 **1-10**

Scheme 7. PMP was removed by employing CAN

The mechanism of the removal of the PMP group is shown below (**Figure 10**). The mechanism involves two times of single electron transfer. First, the PMP group donates one electron to cerium (IV), forming a radical cation intermediate. After hydrolysis of the methoxy group by water, a second electron donates to another CAN molecule. In this reaction quinone was generated as a side product.

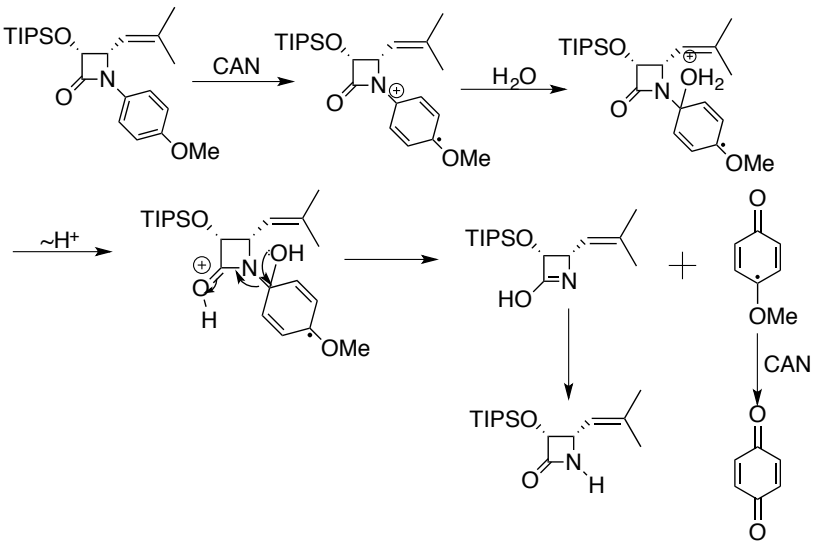

Figure 10. Mechanism of CAN deprotection

The resulting **1-9** was then reacted with di-*tert*-butyl dicarbonate to give target molecule 4-isobutenyl-1-(*tert*-butxoycarbonyl)-3-(triisopropylsilyl) oxyazetidine-2-one **1-10** in 79% yield as a colorless liquid (**Scheme 8**).

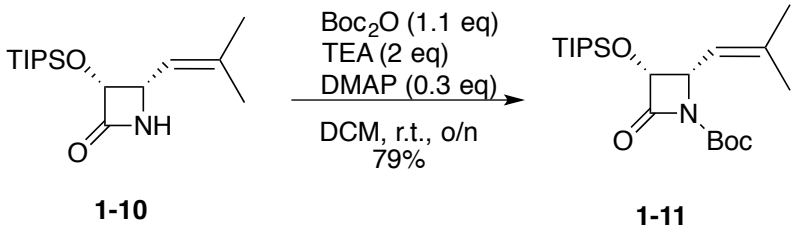

1-10 1-11

Scheme 8. Boc-protection of *β*-Lactam

§ 1.5 Synthesis of New Generation Taxoids

§ 1.5.1 Synthesis of second-generation taxoid SB-T-1214

Based on the SAR studies of paclitaxel preformed in Ojima lab, a new-generation taxoid SB-T-1214 was designed. This compound has a cyclopropanecarbonyl group at C-10 position, *t*-Boc group at C-3'-N position as well as an alkenyl group at C-3' position compared to paclitaxel. The synthesis of second-generation taxoid SB-T-1214 started from commercially available 10-Deacetylbaccatin III (10-DAB). The chemical structures of SB-T-1214 and 10-DAB were shown in **Figure 11**.

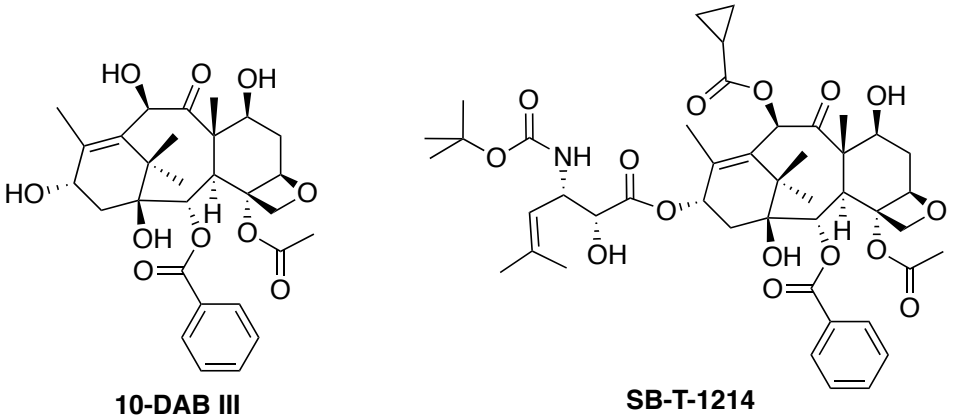

10-DAB III SB-T-1214

Figure 11. Chemical Structure of 10-DAB and SB-T-1214

To synthesize the second-generation taxoid SB-T-1214, the hydroxyl group at the C-7 position should be protected first so that the C-10 hydroxyl group can be selectively acylated by cyclopropanecarbonyl chloride in the next step. The chemical structure of 10-DAB III (**Figure 11**) contains four hydroxy groups at C-1, C-7, C-10 and C-13 separately, among which C-7 hydroxyl group is the most acidic one and can be specifically protected by chlorotriethylsilane (TESCl) (**Scheme 9**). The C-1 hydroxyl group is the most inactive one because it is buried in the core of paclitaxel. The condition was carefully monitored by TLC to avoid multiple protections. The product was purified by column chromatography to afford **1-12** as a white solid in 83% yield.

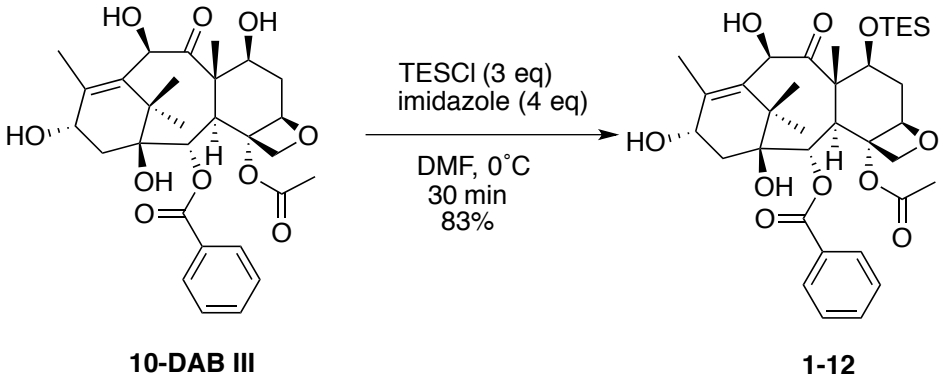

Scheme 9. Initial Protection at the C-7 Position of 10-DAB

After the protection of C-7, the C-10 hydroxyl group became the most reactive site. So the acylation at the C-10 position was able to happen with cyclopropanecarbonyl chloride in the presence of lithium bis(trimethylsilyl)amide (LiHMDS) to afford **1-13** (**Scheme 10**) as a white solid in 83% yield. The reaction mixture was carefully

monitored by TLC for the possible reaction happened at the C-13 hydroxyl group. Cold temperature is maintained to avoid side reactions.

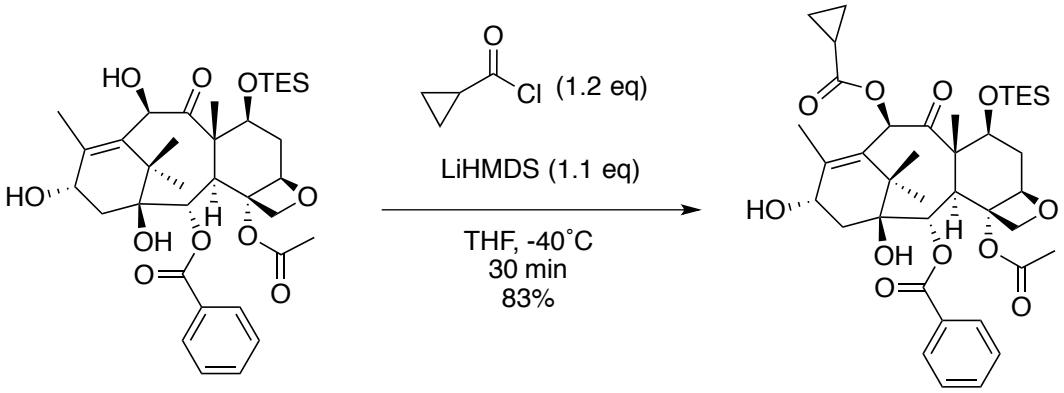

1-12 **1-13**

Scheme 10. Synthesis of 10-modified 7-TES-DAB

After acylation at the C-10 position, the C-13 hydroxyl group became the most reactive site and the Ojima-Holton coupling reaction was conducted with *N*-Boc-*β*-Lactam **1-11** to afford **1-14** (**Scheme 11**) as a white solid in 72% yield.

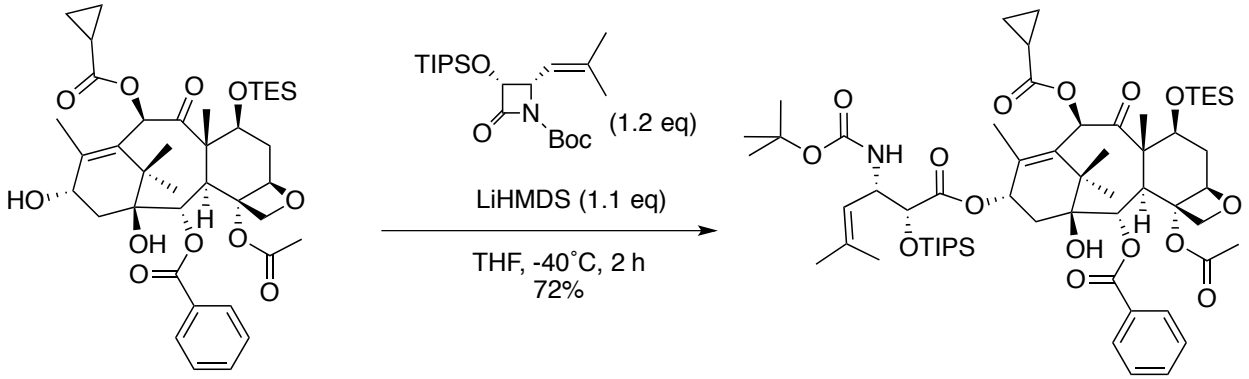

1-13 **1-14**

Scheme 11. Coupling reaction of the baccatin with enantiomerically pure *β*-Lactam

At last, All the protecting groups were removed by hydrogen fluoride in pyridine to generate the final product **SB-T-1214** (**Scheme 12**) in 90% yield. The product was afforded as a white solid with over 99% purity after recrystallization in ethyl acetate – hexanes solution.

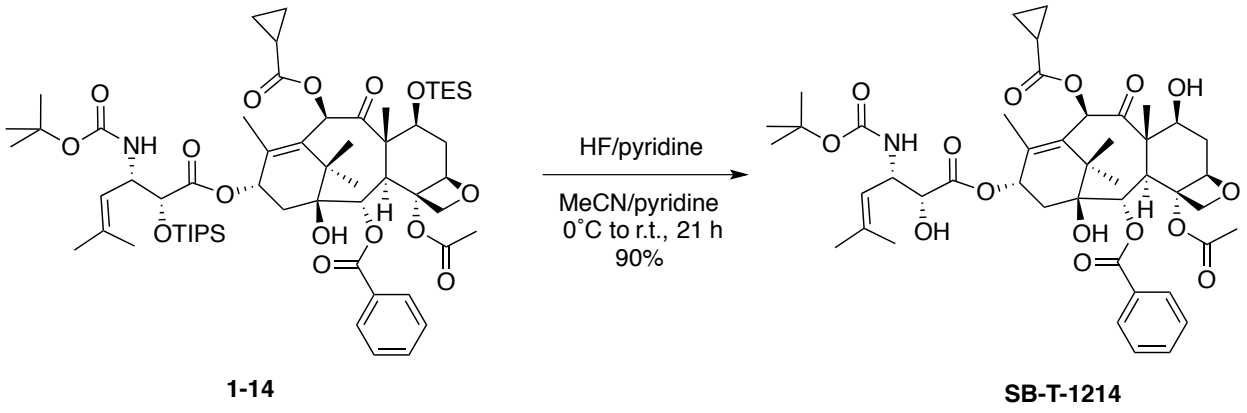

Scheme 12. Protecting Groups were Removed to Afford Target Molecule **SB-T-1214**

§ 1.5.2 Synthesis of third-generation taxoids SB-T-121202, SB-T-121302 SB-T-121402, SB-T-121602 and SB-T-121702

Chemical structure of SB-T-121202, SB-T-121302, SB-T-121402, SB-T-121602 and SB-T-121702 were shown in **Figure 12**. Both of them were semi-synthesized from 10-DAB III. Compared to second generation taxoid SB-T-1214, these new designed taxoids were introduced a methyl group to the *meta* position of the C-2-benzoyl moiety.

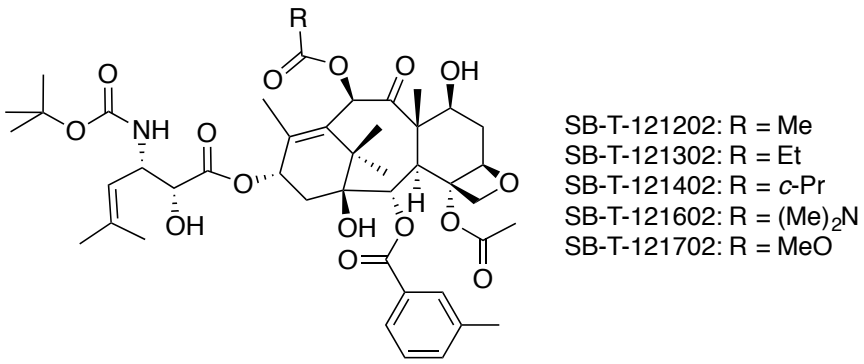

Figure 12. Chemical structure of designed third generation taxoids bearing methyl group at *meta* position of C-2 benzoyl moiety

To get final target molecules, C-2-modified-10-DAB III (**1-18**) need to be synthesized first. The synthetic route to get this key intermediate is illustrated in **Scheme 13**.

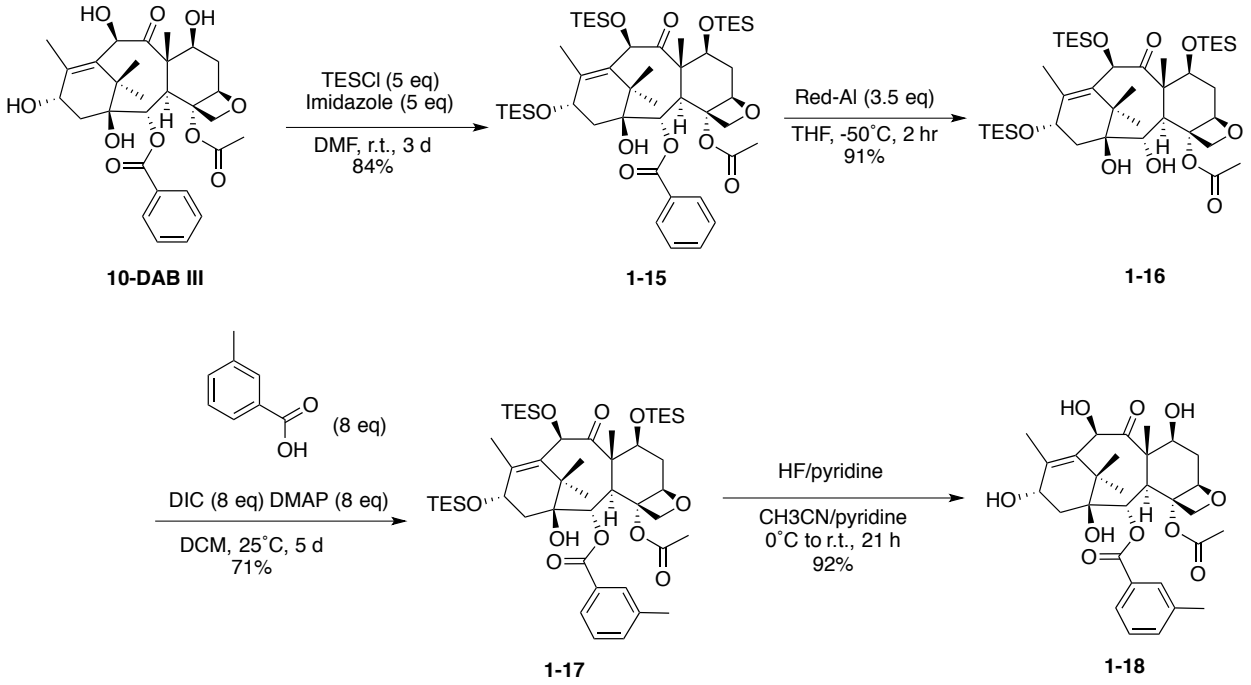

Scheme 13. Synthesis of C-2-modified 10-DAB III

The hydroxyl group at the C-7, C-10 and C-13 position of the starting material 10-DAB III should be protected first so that the C2-benzoyl moiety can be selectively removed by Sodium bis(2-methoxyethoxy)aluminumhydride (Red-Al) in the next step. The C-1 hydroxyl group can not be protected by TESCl due to its special configuration in the structure of baccatin. Red-Al was able to coordinate to the C-1 hydroxyl and deliver the hydride to the C-2-ester while preserving the C-4 acetate. The resulting product **1-16** after two steps was then coupled with 3-methyl benzoic acid, followed by removal of all protecting groups by employing hydrogen fluoride (HF) in pyridine to afford C-2-modified 10-DAB III as a white solid in quantitative yield.

The synthetic route for SB-T-121402, SB-T-121602 and SB-T-121702 was shown in **Scheme 14** started from C-2-modified 10-DAB III **1-18**.

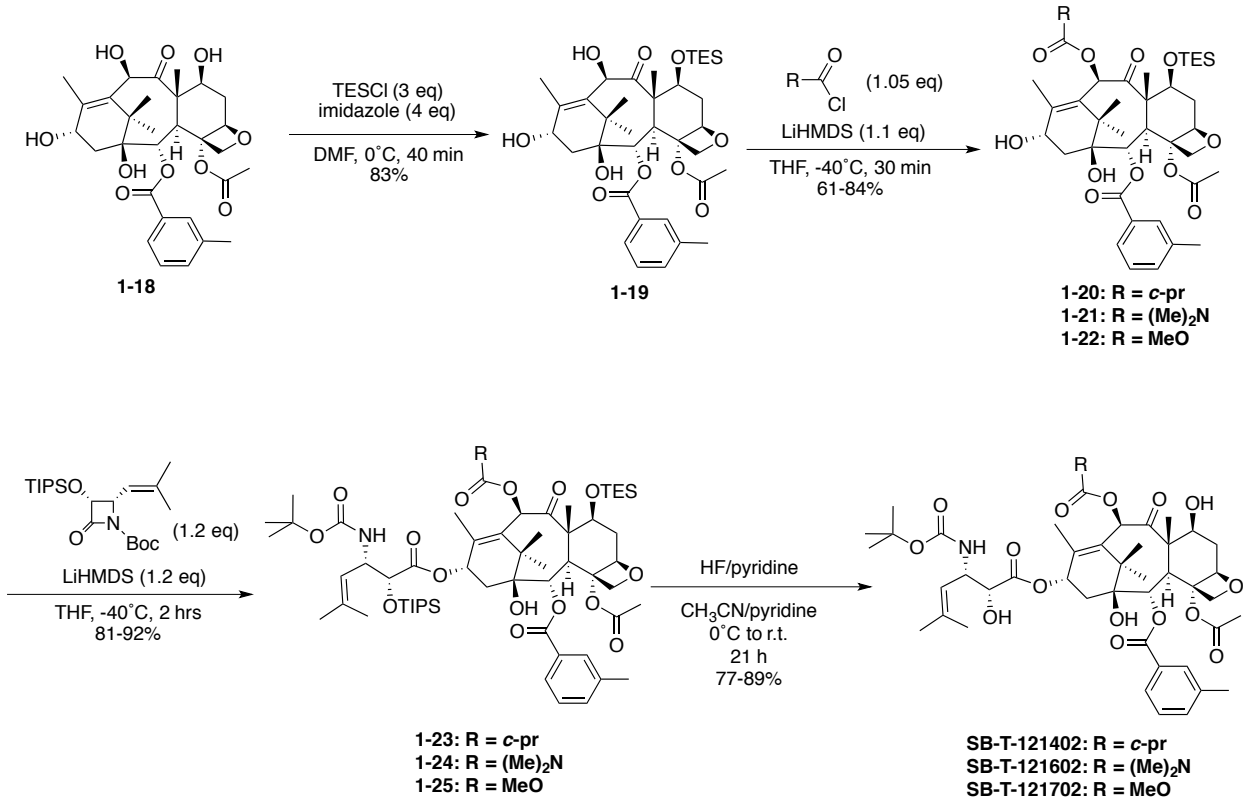

Scheme 14. Synthetic Route to SB-T-121402, SB-T-121602 and SB-T-121702

The C-2-modified baccatin **1-18** was first selectively protected by TESCl at C-7 hydroxyl group. The reaction mixture was monitored carefully by TLC to avoid multi-protected products. The acylation of the C-10 hydroxyl with certain acyl chloride was conducted in the presence of LiHMDS gave corresponded 10-modified products in good yields (61-84%). The C-13 isoserine side chain was then introduced by Ojima-Holton coupling with *N*-Boc-*β*-Lactam **1-11** in excellent yields (81-92%). Target molecules SB-T-121402, SB-T-121602 and SB-T-121702 were afforded after deprotection of the silyl groups. All the final compounds were recrystallized from

hexanes and ethyl acetate solutions, and the purity of them were 95–98% determined by reverse-phase HPLC.

A different synthetic route was applied to SB-T-121202 and SB-T-121302 (**Scheme 15**). Acetylation of C-10 hydroxyl group was conducted first instead of TES protection of C-7 hydroxyl group by employing catalyst amount of cerium trichloride and corresponded acetic anhydride in good yields (72-77%).

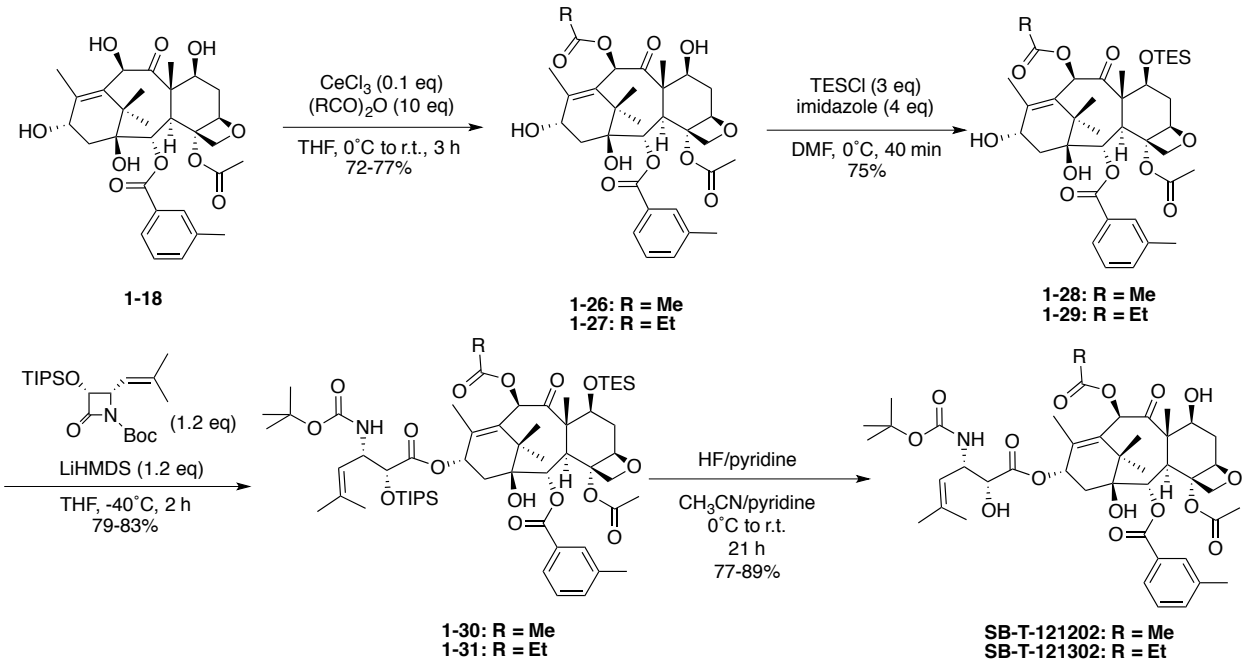

Scheme 15. Synthetic route to SB-T-121202 and SB-T-121302

The 2,10-modified baccatins were protected by TESCl at C-7 hydroxyl group in the presence of imidazole. The reaction mixture was monitored carefully by TLC to avoid multi-protected products. The resulting products were then coupled with *N*-Boc *β*-Lactam **1-11** in good yield (79%-83%). The subsequent removal of all protecting groups by

employing hydrogen fluoride in pyridine gave target molecule SB-T-121202 and SB-T-121702 in excellent yield (77-89%). The purity of SB-T-121202 and SB-T-121302 were 94% and 91% separately after recrystallization from hexanes and ethyl acetate.

§ 1.6 Biological Evaluation of New Generation Taxoids

The *in vitro* cytotoxicity of these new taxoids was evaluated against MCF-7 and drug-resistant carcinoma cell line MCF-7R. The concentrations of compounds which inhibits 50% ($IC_{50,}$ nM) of the growth of human tumor cell line after 72 hours drug exposure were illustrated in Table 1. All of these new-generation taxoids exhibit remarkable potency against Pgp-mediated drug-resistant carcinoma cell line MCF-7R and similar activity against normal cell line MCF-7 compared to paclitaxel. SB-T-121702 is exceptionally potent against MCF-7 cell line and SB-T-121302 shows the best activity against MCF-7R. It is also interesting to see the dramatic decrease in the R/S ratio of these new-generation taxoids compared to paclitaxel. The "resistance factor" (R/S) is defined as the ratio of the IC_{50} value against drug-resistant cancer cell line to that against drug-sensitive cell line which is a good indicator for the susceptibility of a compound to MDR.[23] Based on that, it is obvious to see that the Pgp-mediated MDR is totally circumvented by SB-T-121202.

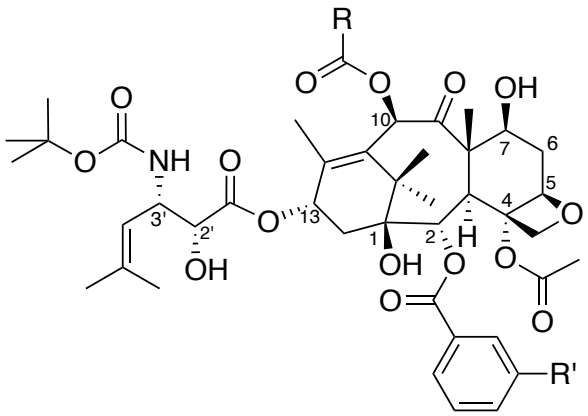

Drug	R	R'	MCF-7 (nM)	MCF-7R (nM)	R/S
Paclitaxel	--	--	1.7	300	180
SB-T-1214	*c*-pr	H	3.6	18	5.0
SB-T-121202	Me	Me	3.4	6.8	2.0
SB-T-121302	Et	Me	1.1	4.1	3.7
SB-T-121402	*c*-pr	Me	1.5	9.5	6.3
SB-T-121602	$(Me)_2N$	Me	1.2	13	11
SB-T-121702	MeO	Me	0.71	9.7	14

Table 1. Cytotoxicity of New-Generation Taxoids against MCF-7 cell line and MCF-7R cell line

On the other hand, the cytotoxic activity against LCC6-WT cell line and LCC6-MDR cell line were also evaluated by MTT assay. The result is showed in **Table 2**. All the new compounds showed better activity against these two cell lines compared to paclitaxel. It is noteworthy to see that all new taxoids showed 2 order magnitude higher potencies than paclitaxel. Among them, SB-T-121302 exhibits extremely potent anticancer activity in both cell lines, i.e., 0.34 for LCC6-WT and 1.4 for LCC6-MDR.

The dramatic decrease in R/S ratio also indicates that the Pgp-mediated MDR was circumvented by these new-generation taxoids.

Based on the IC_{50} results in Table 1 and Table 2, we can concluded that the tumor cell lines are very sensitive to the modification on C-10 position. For example, the antitumor activity decreases in the order MeO > Et > $(Me)_2N$ > cyclo-PrCO > Me against MCF-7 cancer cell line, while the order changes to Et > Me > cyclo-PrCO > MeO > $(Me)_2N$ against MCF-7R.

Drug	R	R'	LCC6-WT (nM)	LCC6-MDR (nM)	R/S
Paclitaxel	--	--	3.1	350	110
SB-T-1214	*c*-pr	H	1.1	2.4	2.2
SB-T-121202	Me	Me	0.46	2.4	5.2
SB-T-121302	Et	Me	0.34	1.4	4.1
SB-T-121402	*c*-pr	Me	0.66	4.1	6.2
SB-T-121602	$(Me)_2N$	Me	0.78	2.5	3.2
SB-T-121702	MeO	Me	0.8	5.3	6.6

Table 2. Cytotoxicity of New-Generation Taxoids against LCC6-WT cell line and LCC6-MDR cell line

Currently there are no effective chemotherapeutic treatments for pancreatic cancer due to the expression of various mutidrug resistance proteins.[23] The antitumor potency of the new synthesized taxoids were also being evaluated against pancreatic cancer cell line PANC-1 and CFPAC-1 (Table 3). It is impressive to see that all new-generation taxoids

exhibit excellent antitumor activity against these two cell lines with subnanomolar to single-digit nanomolar IC_{50} value apart from one case for SB-T-121702 against PANC-1. Among them, SB-T-121202 is the most potency taxoid against PANC-1 cell line and CFPAC-1 cell line.

Drug	R	R'	PANC-1	CFPAC-1
SB-T-1214	c-pr	H	5.0	0.9
SB-T-121202	Me	Me	4.98	0.38
SB-T-121302	Et	Me	9.86	0.94
SB-T-121402	*c*-pr	Me	6.77	1.18
SB-T-121602	$(Me)_2N$	Me	7.02	0.73
SB-T-121702	MeO	Me	14.6	1.47

Table 3. Cytotoxicity of New-Generation Taxoids against PANC-1 cell line and CFPAC-1 cell line

It is noteworthy to mention that SB-T-121302 showed excellent antitumor activity against all drug resistant cell lines except for PANC-1 and CFPAC-1. This result may suggest that taxoid SB-T-121302 cannot modulate a combination of multidrug-resistant proteins so efficiently as Pgp alone. However it is still exhibit high potency against pancreatic cell lines.

Accordingly, all these new-generation taxoids are excellent candidates for further preclinical studies. These biological results can be employed as good data for SAR studies of paclitaxel.

§ 1.7 Summary

Paclitaxel is one of the most promising anti-cancer agent widely used in many types of cancer. It works as microtubule-stabilizing agent and exhibits potent activity against cancer cell lines. However, it also induces many side effects and encounters drug resistance. Based on SAR studies on paclitaxel, second-generation taxoid SB-T-1214, third-generation taxoids SB-T-121202, SB-T-121302, SB-T-121402, SB-T-121602 and SB-T-121702 were designed and synthesized successfully. Ojima-Holton coupling protocol was applied to the semisynthesis of these new taxoids. The *in vitro* cytotoxicity of these new taxoids were evaluated against MCF-7, MCF-7R, LCC6-WT, LCC6-MDR, PANC-1 and CFPAC-1 cell lines. All of them showed a dramatic increase in cytotoxicity compared to paclitaxel, especially those against drug resistant cancer cell lines.

§ 1.8 Experimental

§ 1.8.1 General Methods

^{1}H NMR and ^{13}C NMR data were obtained on a Bruker 300, 400, 500 or 700 MHz NMR spectrometer. Chemical shifts(δ) are reported in ppm and standardized with solvent as internal standard based on literature reported values. Melting points were measured on a Thomas-Hoover capillary melting point apparatus. Optical rotations were measured on a Perkin-Elmer Model 241 polarimeter. High resolution mass spectrometry analysis was

conducted on an Agilent LC-UV-TOF mass spectrometer at the Institute of Chemical Biology and Drug Discovery (ICBDD), Stony Brook, NY. TLC analyses were performed on Merck DC- alufolien with Kieselgel 60F-254 and were visualized with UV light, sulfuric acid-EtOH, 10 % PMA-EtOH or 10 % Vanillin-EtOH with 1% sulfuric acid. Column chromatography was carried out on silica gel 60 (Merck, 230-400 mesh ASTM) with hexanes-ethyl acetate solvent system or dichloromethane-methanol solvent system. Purity of compounds were determined by a Shimadzu L-2010A HPLC with acetonitrile-water solvent system.

§ 1.8.2 Materials

The chemicals were purchased from Sigma-Aldrich Company, Fisher Scientific Company and VWR International Company. 10-Deacetylbaccatin III (10-DAB) was donated by Indena, SpA, Italy. Tetrohydrofuran was distilled from sodium and benzophenone under nitrogen. Dichloromethane was distilled from calcium hydride under nitrogen.

§ 1.8.3 Experimental Procedure

(+)-(1*R*,2*R*)-1-Phenylcyclohexanes-cis-1,2-diol (1-1)[52]

Preparation of **1-1** was started from adding the following reagents in a glassware instrument: 3 equivalents of potassium ferricyanide (49.7 g), 3 equivalents of K_2CO_3 (20.8 g), 1 equivalent of methanesulfonamide (4.79 g), *t*-BuOH/H_2O (40 ml : 60 ml), 3

equivalents of potassium osmate (VI) dehydrate (55.6 mg) and 0.25 mol% $(DHDQ)_2PHAL$ (98.0 mg). The mixture was stirred for 10 minutes at 0˚C followed by addition of 1-phenyl-1-cyclohexanes (7.97 g). Upon completion, the reaction mixture was treated with ethyl acetate with stirring to dissolve the product. The organic layer was collected and washed with 2M KOH with vigorous shaking to remove methanesulfonamide. Then the crude product was dried over $MgSO_4$, and concentrated *in vacuo* to afford crude **1-1** in 94% yield. ^{1}H NMR (400 MHz, $CDCl_3$): δ 1.41-2.20 (m, 8H), 2.60 (d, J = 1.9 Hz, 1H), 4.02 (m, 1H), 7.28- 7.52 (m, 5H). All data are consistent with literature values.[52]

(-)-(1*R*,2*S*)-trans-2-Phenyl-1-cyclohexanol(1-2)[52]

To a solution of resulting **1-1** (4.73 g, 24.6 mmol) in ethanol was added Raney Nickel which preserved in wet ethanol (70% v/v) (70 mL). The reaction mixture was equipped with a condenser and mechanical stirrer. The mixture was heated to 100˚C for 3 hours while stirring and refluxing. The reaction mixture was monitored *via* TLC and upon completion, it was cooled to 40-50 ˚C and filtered by 1-1.2 cm layer of Celite. The resulting liquid was concentrated *in vacuo* to get white solid and recrystallized with pentane at room temperature in 76% yield. ^{1}H NMR (400 MHz, $CDCl_3$): δ 1.31-1.54 (m, 5H), 1.80-1.90 (m, 3H), 2.13 (m, 1H), 2.43 (m, 1H), 3.68 (m, 1H), 7.21-7.36 (m, 5H). All data are consistent with literature values.[52]

Benzyl 2-hydroxyacetate (benzyl glycolate) (1-3)[23]

To a solution of glycolic acid (6.01 g, 78.9 mmol) dissolved in acetone (80 ml) was added 1.2 equivalents of TEA (11.6 ml, 83.5 mmol), followed by addition of benzyl bromide (8.40 ml, 70.6 mmol). White precipitate came out after 6 ml benzyl bromide was added. The mixture was monitored by TLC (Hexanes:EA = 2:1). Upon completion, the reaction mixture was concentrated to afford crude product. Then dissolved the product in 75 ml H_2O and extracted with ethyl acetate (3 x 20 ml). The organic layer was washed with saturated brine (3 x 20 ml), dried with $MgSO_4$, and concentrated *in vacuo* to afford pale yellow oil **1-1** in 74% yield. ^{1}H NMR (300 MHz, CDCl3): δ 2.455 (br s, 1H), 4.198 (s, 2H), 5.230 (s, 2H), 7.364-7.366 (m, 5H). All data are in agreement with literature values.[23]

2-(Triisopropylsiloxy)acetic acid benzyl ester (1-4)[53]

The resulting **1-3** (6.74 g, 40.6 mmol) as well as 0.1 equivalent of DMAP (0.495 g, 4.06 mmol) were dissolved in DCM (80 ml) followed by addition of 1.2 equivalents of TEA (4.93 g, 6.77 ml, 48.7 mmol). Kept the solution stir, 1.0 equivalent of TIPSCl (7.82 g, 8.68 ml, 40.6 mmol) was added dropwise. White precipitate came out at the same time. The reaction mixture was monitored by TLC (Hexanes:EA = 10:1). Upon completion, the reaction mixture was quenched by saturated NH_4Cl (30 ml), diluted with H_2O (10 ml) followed by extracting with ethyl acetate (3 x 30 ml). The combined organic layer was washed with brine (3 x 30 ml) and concentrated *in vacuo* to yield pale brown oil. The

crude product was further purified by column chromatography on silica gel with increasing amounts of eluent (Hexanes:ethyl acetate) to give pure **1-4** as a colorless oil in 54% yield. ^{1}H NMR (400 MHz, $CDCl_3$): δ 1.05 (m, 21H), 4.36 (s, 2H), 5.18 (s, 2H), 7.35 (s, 5H). All data are consistent with literature values.[53]

2-(Triisopropylsiloxy)acetic acid (1-5)[53]

The resulting **1-4** (6.00g) was dissolved in EtOAc (90 ml) followed by addition of 2.4% mol equivalents of 10% w/w palladium on carbon (480 mg). The mixture was purged with N_2 and set under H_2 at room temperature with stirring and monitored by TLC. Upon completion, the catalyst was removed by filtration *via* celite and concentrated *in vacuo* to give **1-5** as pale yellow oil in 94% yield. The crude product was directly used in the next step without further purification. ^{1}H NMR (400 MHz, $CDCl_3$): δ 1.08 (m, 24H), 4.29 (s, 2H). All data are consistent with literature values.[53]

2-(Triisopropylsiloxy)acetoxysuccinimide (1-6)[52]

To a solution of **1-5** (4.32 g) as well as 1.2 equivalents of *N*-Hydroxysuccinimide (2.36 g) was dissolved in DCM (45 ml) was added 1.1 equivalents of N-(3-Dimethylaminopropyl)-N′-ethylcarbodiimide hydrochloride (EDC•HCl) (1.437 g). Upon completion, saturated NH_4Cl (30 ml) was added in the reaction system to quench the reaction and diluted with H_2O (50 ml) followed by extracting by DCM (3 x 50ml). The organic layer was washed with brine (3 x 50ml), dried over $MgSO_4$, and then

concentrated *in vacuo* to afford crude product. The crude product was recrystallized by hexanes and filtered by employing Buchner funnel to get product **1-6** as a colorless oil in 76% yield. ^{1}H NMR (400 MHz, $CDCl_3$): δ1.08 (m, 20H), 4.83 (s, 4H), 4.66 (s, 2H). All data are consistent with literature values.[52]

2-(Triisopropylsiloxy)acetic acid (1*R*,2*S*)-2-phenylcyclohexyl ester (1-7)[52]

To a solution of **1-2** (1.95 g, 11.1 mmol) and DMAP (2.05 g, 16.6 mmol) dissolved in anhydrous toluene (32 ml) under inert conditions, followed by addition of 1.2 equivalents of **1-6** (4.37 g, 13.3 mmol) by dropwise. The reaction was kept stirred and monitored by TLC (Hexanes:EA = 1:1). Upon completion the reaction was quenched by saturated NH_4Cl (20 mL), extracted with ethyl acetate (3 x 25 mL), washed with saturated brine (3 x 25 mL), dried over anhydrous $MgSO_4$, and concentrated *in vacuo* to get crude product. Further purification was conducted by column chromatography on silica gel to get pure **1-7** as a colorless oil in 71% yield. ^{1}H NMR (400 MHz, $CDCl_3$) δ 0.97 (m, 21H), 1.25-1.56 (m, 4H), 1.61-2.15 (m, 3H), 2.14 (d, 1H), 2.66 (dt, 1H), 3.91 (d, 1H), 4.07 (d, 1H), 5.07 (dt, 1H), 7.18 (m, 3H), 7.24 (m, 2H). All data are consistent with literature values.[52]

***N*-PMP-3-methylbut-2-en-1-imine (1-8)[52]**

To a solution of recrystallized *p*-anisidine (275 mg, 2.24 mmol) and anhydrous Na_2SO_4 (783 mg, 5.51 mmol) dissolved in anhydrous DCM (5.5 ml) was added

3-methyl-2-butenal in dark. The reaction mixture was monitored *via* TLC and upon completion, the mixture was filtrated and the organic layer was concentrated *in vacuo*. Without further purification, the product was directly used in the next step as a brown oil in 99% yield. ^{1}H NMR (400 MHz, $CDCl_3$) δ 1.97 (d, 5H), 3.8 (s, 3H), 6.19 (d, 1H), 6.87 (d, 2H), 7.09 (d, 2H), 8.37 (d, 1H). All data are consistent with literature values.[52]

(3*R*,4*S*)-1-(4-methoxyphenyl)-3-triisopropylsiloxy-4-(2-methylprop-1-nyl)azetidin-2-one (1-9)[52]

To a solution of diisopropylamine (0.28 ml) in THF (5.46 ml) at -78˚C was added *n*-BuLi (0.67 ml). After stirring for 10 min, the reaction mixture was allowed to cool down to -78˚C by acetone-dry ice bath. The *in situ* LDA solution was added chiral ester **1-7** (497 mg, 1.27 mmol) dropwise with stirring, followed by addition of 1-8 (420 mg, 2.1 mmol) dissolved in THF (3.3 ml). The reaction mixture was carefully monitored by TLC. Upon completion, the system was quenched with saturated NH_4Cl and the mixture was extracted with DCM. After the collection of organic layer, the system was washed with brine, dried over $MgSO_4$, and concentrated *in vacuo* to afford product **1-9**. Column chromatography on silica gel was conducted for further purification. The pure product was afforded as a white solid in 69% yield. ^{1}H NMR (400 MHz, $CDCl_3$) δ 1.08 (m, 21H), 1.82 (d, *J*=20.0 Hz, 6H), 3.77 (s, 3H), 4.80 (dd, *J*=5.0Hz, J_2 =8.0Hz, 1H), 5.05 (d, *J*=5.0 Hz, 1H), 5.32 (d, *J* = 5.0 Hz, 1H), 6.83 (d, *J* = 8.9 Hz, 2H), 7.31 (m, 2H). All data are consistent with literature values.[52]

(3*R*,4*S*)-3-Triisopropylsiloxy-4-(2-methylprop-1-enyl)azetidin-2-one (1-10)[52]

To a solution of **1-9** (173 mg, 0.43 mmol) in acetonitrile (11.5 ml) at -10˚C was added cerium ammonium nitrate (CAN) dissolved in H_2O (11.5 ml) drop wise *via* an addition funnel. The reaction was kept stirring and monitored by TLC (Hexanes:EA=3:1). Upon completion, the reaction was quenched by saturated Na_2SO_3 (20 mL). The reaction mixture was filtrated by celite, extracted by ethyl acetate, washed by brine, dried over anhydrous $MgSO_4$, and concentrated *in vacuo*. Further purification was conducted by column chromatography on silica gel [Hex:EA = 2:1] to afford pure **1-10** as a white solid in 71% yield. ^{1}H NMR (400 MHz, $CDCl_3$) δ 1.03 (m, 21H), 1.66 (s, 3H), 1.73 (s, 3H), 4.42 (dd, *J* = 4.8 Hz, *J* = 4.8 Hz, 1H), 4.96 (d, *J* = 4.8 Hz, 1H), 5.28 (d, *J* = 4.8 Hz, 1H), 6.45 (s, 1H). All data are consistent with literature values.[52]

(3*R*,4*S*)-1-(*tert*-Butoxycarbonyl)-3-triisopropylsiloxy-4-(2-methylprop-1-enyl)azetidi n-2-one (1-11)[52]

To a solution of **1-10** (105 mg, 0.35 mmol), 0.3 equivalent DMAP (14 mg, 0.11 mmol) and 1.5 equivalents di-*tert*-butyl dicarbonate (90 mg, 0.42 mmol) dissolved in anhydrous DCM (3 ml) in 0˚C was added (76 mg, 0.11 ml, 0.75 mmol) under inert conditions. The reaction mixture was monitored *via* TLC and upon completion, the reaction was quenched by saturated NH_4Cl (2 mL). The reaction mixture was extracted by ethyl acetate, washed with saturated brine, dried over anhydrous $MgSO_4$ and concentrated *in vacuo* to give crude product. Further purification was conducted by column

chromatography on silica gel to give pure **1-10** as a colorless oil in 79% yield. ^{1}H NMR (400 MHz, $CDCl_3$) δ 1.02 (m, 22 H), 1.46 (s, 9H), 1.75(d, *J*=7.8Hz, 6H), 4.74(dd, *J*=5.1Hz, *J*=4.1Hz, 1H), 4.94(d, *J*=5.1Hz, 1H), 5.25(d, *J*=4.1Hz, 1H). All data are consistent with literature values.[52]

7-Triethylsilyl-10-deacetylbaccatin (1-12)[52]

To a solution of 10-DAB III (200 mg, 0.36 mmol) and imidazole (109 mg, 1.47 mmol) in DMF at 0˚C was added TESCl (181 mg, 0.20 ml, 1.19 mmol) dropwise. The reaction mixture was monitored by TLC (Hexanes: EA = 1:1). Once completion, the reaction was quenched with saturated NH_4Cl and extracted with ethyl acetate (3 x 20 mL). The organic layers was collected, treated with brine (3 x 20 mL), dried over $MgSO_4$, and concentrated *in vacuo.* Further purification was conducted by column chromatography on silica gel to afford product **2-1** as a white solid in 83% yield. ^{1}H NMR (400 MHz, $CDCl_3$) δ 0.56 (m, 6H), 0.95 (t, *J* =6.4 Hz, 9H), 1.08 (s, 6H), 1.26 (m, 1H), 1.73 (s, 3H), 1.94 (t, *J* = 1.8 Hz, 1H), 2.07 (m, 4H), 2.27 (d, *J* = 9 Hz, 5H), 3.94 (d, *J* = 5.4 Hz, 1H), 4.13 (t, *J* = 4.2 Hz, 2H), 4.17 (t, *J* = 4.2 Hz, 2H), 4.26 (t, *J* = 7.5 Hz, 1H), 4.89 (m, 1H), 4.95 (d, *J* = 14.0 Hz, 1H), 5.17 (s, 1H), 5.61 (d, *J* =8.2 Hz, 1H), 7.48 (t, *J* = 9.4 Hz, 2H), 7.58 (t, *J* = 5.2 Hz, 1H), 8.10 (d, *J* = 5.2 Hz, 2H). All data are consistent with literature values.[52]

10-(Cyclopropanecarbonyl)-7-triethylsilyl-10-deacetylbaccatin (1-13)[52]

To a solution of **1-12** (202 mg, 0.328 mmol) in THF (6.00 ml) at -40˚C was added cyclopropanecarbonyl chloride (42 mg, 0.040 ml), followed by the addition LiHMDS (0.36 ml) in THF dropwise. The reaction was monitored by TLC rigorously to avoid side product. Once completion, the reaction mixture was quenched with saturated NH_4Cl and extracted with ethyl acetate. The organic layer was collected, washed with brine, dried over $MgSO_4$, and concentrated *in vacuo* to afford crude product **1-13**. Further purification was conducted by column chromatography on silica gel to afford pure **1-13** as a white solid in 83% yield. ^1H NMR (400 MHz, $CDCl_3$) δ 0.56 (m, 6H), 0.91 (t, *J* = 5.2 Hz, 9H), 1.05 (s, 4H), 1.21 (s, 3H), 1.68 (s, 2H), 2.01 (s, 1H), 2.19 (s, 2H), 2.27 (d, 4H), 3.78 (d, *J* = 1.2 Hz, 2H), 3.79 (d, *J* = 1.8 Hz, 2H), 3.88 (d, *J* = 1.0 Hz, 2H), 4.94 (d, *J* = 1.0 Hz, 3H), 4.98 (d, *J* = 8.0 Hz, 2H), 5.63 (d, *J* = 15 Hz, 2H), 6.46 (s, 1H), 7.48 (t, *J* = 0.7 Hz, 2H), 7.60 (m, 1H), 8.11 (d, *J* = 5.4 Hz, 2H). All data are consistent with literature values.[52]

2'-Triisopropylsilane-3'-dephenyl-10-(cyclopropanecarbonyl)-3'-(2-methyl-2-propenyl)docetaxel (1-14)[52]

To a solution of **1-13** (112 mg, 0.216 mmol) in THF at -40˚C was added 1.1 equivalents of LiHMDS (0.282 ml), followed by the addition of (3*R*,4*S*)-1-(*tert*-butoxycarbonyl)-3-Triisopropylsiloxy-4-(2-methylprop-1-enyl)az-etidin-2-one (**1-11**) in THF dropwise. The reaction was monitored by TLC until complete conversion. Once completion, the reaction was quenched with saturated NH_4Cl and

extracted with ethyl acetate. The organic layers was collected, washed with brine, dried over $MgSO_4$, and concentrated *in vacuo* to afford crude product. The product was purified by column chromatography to afford pure **1-14** as a white solid in 72% yield. ^{1}H NMR (400 MHz, $CDCl_3$) δ 0.55 (m, 6H), 0.90 (t, J = 8.0 Hz, 9H), 1.10 (s, 21H), 1.18 (s, 3H), 1.22 (s, 3H), 1.32 (s, 9H), 1.68 (s, 3H), 1.76 (m, 5H), 1.83 (s, 3H), 1.86 (m, 1H), 2.18 (s, 3H), 2.37 (m, 5H), 2.49 (m, 1H), 3.83 (d, 7.2 Hz, 1H), 4.23 (dd, J = 44 Hz, J = 8 Hz, 2H), 4.42 (d, J = 2.9 Hz, 1H), 4.46 (d, J = 6.6 Hz, 1H), 4.78 (m, 2H), 4.92 (d, J = 7.8 Hz, 1H), 5.33, (d, J = 8.7 Hz, 1H), 5.68, (d, J = 7.2 Hz, 1H), 6.08 (t, J = 8.7 Hz, 1H), 6.47 (s, 1H), 7.44 (t, J = 8.0 Hz, 2H), 7.57 (t, J = 1.2 Hz, 1H), 8.08 (d, J = 7.1 Hz, 2H).

3'-Dephenyl-10-(cyclopropanecarbonyl)-3'-(2-methyl-2-propenyl)docetaxel (SB-T-1214)[52]

To a solution of **1-14** (105 mg) in acetonitrile (2.18 ml) and pyridine (2.18 ml) under 0˚C was added HF/pyridine (0.980 ml). The reaction system was kept stirring and monitored by TLC. Once completion, the reaction was quenched with saturated $NaHCO_3$ and extracted with ethyl acetate. The aqueous phase was added KOH to change the PH to neutral and then extracted with ethyl acetate. The collected organic phase was treated with $CuSO_4$ to remove pyridine, washed with brine, dried over $MgSO_4$ and concentrated *in vacuo* to afford final product (SB-T-1214). The product was purified by column chromatography as a wthite solid in 90% yield. The purity of the compound was higher than 99% which was determined by HPLC. ^{1}H NMR (400 MHz, CDCl3) δ 0.98 (m, 2H),

1.12 (m, 5H), 1.23 (m, 5H), 1.34 (s, 9H), 1.66 (s, 3H), 1.75 (m, 6H), 1.88 (m, 4H), 2.34 (s, 3H), 2.37 (s, 2H), 2.52 (m, 1H), 3.79 (d, J = 7.0 Hz, 1H), 4.13 (m, 2H), 4.27 (d, J = 8.3Hz, 1H), 4.40(dd, J = 8.0 Hz, J = 6.7 Hz, 1H), 4.72 (m, 2H), 4.96 (d, J = 1.8 Hz, 1H), 5.29 (d, J = 8.5 Hz, 1H), 5.65 (d, J = 7.1 Hz, 1H), 6.16 (m, 1H), 6.29 (s,1H), 7.45 (t, J = 7.8 Hz, 2H), 7.56 (t, J = 1.2 Hz, 1 H), 8.07 (d, J = 7.1 Hz, 2 H). HPLC: t = 7.3 min, purity >98%.

7,10,13-Tris(triethylsilyl)-10-deacetylbaccatin III (1-15)[23]

To a solution of 10-DAB III (500 mg, 0.917 mmol) and imidazole (325 mg, 4.590 mmol) in DMF at 0˚C was added 5 equivalents of TESCl (0.77 ml, 4.590 mmol) dropwise. Upon completion, the reaction was quenched with saturated NH_4Cl (10 ml) and extracted with ethyl acetate (3 x 30 mL). The organic layers was collected, washed with brine (3 x 30 mL), dried over $MgSO_4$ and concentrated *in vacuo* to afford crude product. Further purification was done by column chromatography on silica gel to give product **1-15** as a white solid in 84% yield. The product was characterized by ^{1}H NMR. ^{1}H NMR (400 MHz, $CDCl_3$) δ 0.62 (m, 18H), 0.97 (m, 27H), 1.12 (s, 3H), 1.18 (s, 3H), 1.37 (s, 1H), 1.55 (s, 5H), 1.57 (s, 1H), 1.65 (s, 3H), 1.88 (m, 1H), 1.98 (d, *J* = 1.2 Hz, 3H), 2.10 (m, 1H), 2.22 (m, 1H), 2.27 (s, 3H), 2.52 (m, 1H), 3.82 (d, *J* = 7.0 Hz, 1H), 4.14 (d, *J* = 8.3 Hz, 1H), 4.28 (d, *J* = 8.4 Hz, 1H), 4.41 (dd, *J* = 6.6 Hz, *J* = 10.5 Hz, 1H), 4.93 (t, *J* = 9.7 Hz, 2H), 5.19 (s, 1H), 5.62 (d, *J* = 6.8 Hz, 1H), 7.46 (t, *J* = 7.7 Hz, 2H), 7.58 (t, *J* = 6.2 Hz, 1H), 8.08 (d, *J* = 1.4 Hz, 1H), 8.10 (s, 1H). All data are consistent with literature values.[23]

2-Debenzoyl-7,10,13-tris(triethylsilyl)-10-deacetylbaccatin III (1-16)[23]

To a cooled solution of **1-15** (740 mg) in THF (13.00 ml) was added 5 equivalents of Sodium bis(2-methoxyethoxy)aluminumhydride (0.65 ml), and the mixture was allowed to react for 1.5 hours at -50˚C with stirring. The reaction was monitored by TLC (Hexanes: EA = 3:1) rigorously. Upon completion, the reaction was quenched with saturated NH_4Cl (10 ml) and extracted with ethyl acetate (3 x 30 mL). The organic layers was collected, washed with brine (3 x 30 mL), dried over $MgSO_4$ and concentrated *in vacuo* to afford crude product. Further purification was done by column chromatography on silica gel to give product **1-16** as a white solid 588 mg in 91% yield. ^{1}H NMR (500 MHz, $CDCl_3$) δ 0.61 (m, 18H), 0.98 (m, 27H), 1.09 (s, 3H), 1.16 (s, 3H), 1.54 (s, 3H), 1.62 (s, 3H), 1.90 (m, 5H), 2.05 (m, 1H), 2.17 (s, 3H), 2.28 (s, 1H), 2.43 (d, *J* = 8.0 Hz, 1H), 2.52 (m, 1H), 3.46 (d, *J* = 8.4 Hz, 1H), 3.87 (t, *J* = 8.4 Hz, 1H), 4.36 (dd, *J* = 8.4 Hz, *J* = 13 Hz, 1H), 4.59 (dd, *J* = 11 Hz, *J* = 35 Hz, 1H) 4.96(t, *J* = 11 Hz, 2H), 5.12 (s, 1H), 5.62 (d, *J* = 6.8 Hz, 1H). All data are consistent with literature values.[23]

2-Debenzoyl-2-(3-methylbenzoyl)-7,10,13-tris(triethylsilyl)-10-deacetylbaccatin III (1-17)[23]

To a solution of 2-2 (588 mg), 3-methylbenzoic acid (732 mg) and DMAP (656 mg) in DCM (6 ml) was added DIC (0.87 ml). The mixture was allowed to react for 7 days at room temperature with stirring. Upon completion, the reaction was quenched with saturated NH_4Cl (10 ml) and extracted with DCM (3 x 30 mL). The organic layers was

collected, washed with brine (3 x 30 mL), dried over $MgSO_4$ and concentrated *in vacuo* to afford crude product. Further purification was conducted by column chromatography on silica gel to give product **1-17** as a white solid 411 mg in 47% yield. ^{1}H NMR (500 MHz, $CDCl_3$) δ 0.62 (m, 18H), 0.99 (m, 27H), 1.12 (s, 3H), 1.19 (s, 3H), 1.56 (s, 3H), 1.65 (s, 3H), 1.92 (m, 1H), 2.08 (s, 3H), 2.10 (m, 1H), 2.23 (m, 1H), 2.28 (s, 3H), 2.40 (s, 3H), 2.52 (m, 1H), 3.35 (d, *J* = 7.1 Hz, 1H), 4.14 (d, *J* = 8.3 Hz, 1H), 4.28 (d, *J* = 8.4 Hz, 1H), 4.1 (dd, *J* = 6.7 Hz, *J* = 11 Hz, 1H), 4.93 (m, 1H), 5.19 (s, 1H), 5.59 (d, *J* = 7.1 Hz, 1H). 7.34 (t, *J* = 7.6 Hz, 1H), 7.39 (d, *J* = 7.5 Hz, 1H), 7.88 (d, 7.6 Hz, 1H), 7.92 (s, 1H). All data are consistent with literature values.[23]

10-Deacetyl-2-debenzoyl-2-(3-methylbenzoyl)baccatin III (1-18)[23]

To a cooled solution of **1-17** (403 mg) in CH_3CN-pyridine 1:1 (25 ml) was added HF-pyridine (4 ml), and the reaction mixture was allowed to warm from 0˚C to room temperature for 21 hours with stirring. Upon completion, the reaction was quenched with saturated NH_4Cl (10 ml) and extracted with ethyl acetate (3 x 30 mL). The organic layers was collected, washed with saturated $CuSO_4$ (3 x 30 mL) and brine (3 x 30 mL), dried over $MgSO_4$ and concentrated in *vacuo* to afford crude product. Further purification was done by column chromatography on silica gel to give product **1-18** as a white solid in 92% yield. The product was characterized by ^{1}H NMR. ^{1}H NMR (500 MHz, $CDCl_3$) δ 1.10 (s, 6H), 1.41 (d, *J* = 7.9 Hz, 1H), 1.56 (m, 5 H), 1.83 (m, 1H), 2.02 (d, *J* = 4.9 Hz, 1 H), 2.08 (d, *J* = 1.2 Hz, 3H), 2.27 (m, 5H), 2.43 (s, 3H), 2.60 (m, 1H), 4.00 (d, *J* = 7 Hz, 1H), 4.17

(m, 1H), 4.29 (m, 2H), 4.87 (m, 1H), 4.98 (d, *J* = 7.8 Hz, 1H), 5.25 (d, *J* = 1.8 Hz, 1H), 5.62 (d, *J* = 7.1 Hz, 1H). 7.34 (t, *J* = 7.6 Hz, 1H), 7.42 (d, *J* = 7.6 Hz, 1H), 7.90 (d, *J* = 7.7 Hz, 1H), 7.93 (s, 1H). All data are consistent with literature values.[23]

2-Debenzoyl-2-(3-methylbenzoyl)-7-triethylsilyl-10-deacetylbaccatin III (1-19)

To a cooled solution of **1-18** (230 mg) and imidazole (118 mg) in DMF (5 ml) was added TESCl (0.23 ml). The mixture was allowed at 0˚C with stirring. Upon completion, the reaction was quenched with saturated NH_4Cl (10 ml) and extracted with ethyl acetate (3 x 30 mL). The organic layers was collected, washed with brine (3 x 30 mL), dried over $MgSO_4$ and concentrated *in vacuo* to afford crude product. Further purification was done by column chromatography on silica gel to give product **1-19** as a white solid in 72% yield. ^{1}H NMR (500 MHz, $CDCl_3$) δ 0.57 (m, 6H), 0.93 (t, *J* = 8.0 Hz, 9H), 1.08 (s, 6H), 1.59 (m, 3H), 1.73 (s, 3H), 1.89 (m, 1H), 2.03 (m, 1H), 2.08 (d, *J* = 1 Hz, 3H), 2.27 (m, 5H), 2.42 (s, 3H), 2.46 (m, 1H), 3.94 (d, *J* = 7 Hz, 1H), 4.15 (d, *J* = 8.4 Hz, 1H), 4.25 (d, *J* = 2.1 Hz, 1H), 4.32 (d, *J* = 8.4 Hz, 1H), 4.40 (dd, *J* = 6.7 Hz, *J* = 10.6 Hz, 1H), 4.87 (m, 1H), 4.96 (d, *J* = 7.9 Hz, 1H), 5.17 (d, *J* = 2.1 Hz, 1H), 5.58 (d, *J* = 7.0 Hz, 1H), 7.35 (t, *J* = 7.2 Hz, 1H), 7.40 (d, *J* = 7.2 Hz, 1H), 7.89 (d, *J* = 7.8 Hz, 1H), 7.93 (s, 1H).

2-Debenzoyl-10-(cyclopropanecarbonyl)-2-(3-methylbenzoyl)-7-triethylsilyl-10-deacetylbaccatin III (1-20)

To a cooled solution of **1-19** (193 mg) in THF (6 ml) was added 1M LiHMDS (0.29 ml) followed by cyclopropanecarbonyl chloride (24µl). The reaction mixture was allowed to react at -40˚C with stirring. Upon completion, the reaction was quenched with saturated NH_4Cl (10 ml) and extracted with ethyl acetate (3 x 30 mL). The organic layers was collected, washed with brine (3 x 30 mL), dried over $MgSO_4$ and concentrated *in vacuo* to afford crude product. Further purification was done by column chromatography on silica gel to give product **1-20** as a white solid in 84% yield. ^{1}H NMR (500 MHz, $CDCl_3$) δ 0.56 (m, 6H), 0.91 (t, *J* = 9.6 Hz, 9H), 1.04 (m, 4H), 1.19 (m, 4H), 1.65 (m, 6H), 1.75 (m, 1H), 1.86 (m, 1H), 2.12 (d, *J* = 4.5 Hz, 1H), 2.17 (s, 3H), 2.26 (m, 5H), 2.41 (s, 3H), 2.51 (m, 1H), 3.87 (d, *J* = 7.1 Hz, 1H), 4.13 (d, *J* = 8.7 Hz, 1H), 4.30 (d, *J* = 8.4 Hz, 1H), 4.47 (dd, *J* = 6.8 Hz, *J* = 10.5 Hz, 1H), 4.82 (br s, 1H), 4.96 (d, *J* = 9.0 Hz, 1H), 5.61 (d, *J* = 7.1 Hz, 1H), 6.45 (s, 1H), 7.35 (t, *J* = 7.6 Hz, 1H), 7.40 (d, *J* = 7.5 Hz, 1H), 7.89 (d, *J* = 7.8 Hz, 1H), 7.93 (s, 1H).

2-Debenzoyl-10-(*N,N*-dimethylcarbamoyl)-2-(3-methylbenzoyl)-7-triethylsilyl-10-deacetylbaccatin III (1-21)

To a cooled solution of **1-19** (101 mg) in THF (3 ml) was added 1M LiHMDS (0.16 ml) followed by cyclopropanecarbonyl chloride (15 µl). The reaction mixture was allowed to react at -40˚C with stirring. Upon completion, the reaction was quenched with saturated NH_4Cl (10 ml) and extracted with ethyl acetate (3 x 30 mL). The organic layers was collected, washed with brine (3 x 30 mL), dried over $MgSO_4$ and concentrated *in vacuo*

to afford crude product. Further purification was conducted by column chromatography on silica gel to give pure product as a white solid in 61% yield. ^{1}H NMR (500 MHz, $CDCl_3$) δ 0.59 (m, 6H), 0.92 (t, *J* = 8.1 Hz, 9H), 1.04 (s, 3H), 1.67 (s, 3H), 1.87 (m, 1H), 2.09 (m, 1H), 2.24 (d, J = 1.2 Hz, 3H), 2.27 (m, 3H), 2.42 (s, 3H), 2.52 (m, 1H), 2.93 (s, 3H), 3.07 (s, 3H), 3.90 (d, J = 7 Hz, 1H), 4.14 (d, 8.3 Hz, 1H), 4.30 (d, J = 8.3 Hz, 1H), 4.48 (dd, J = 6.8 Hz, J = 10.5 Hz, 1H), 4.83 (br s, 1H), 4.96 (d, J = 7.9 Hz, 1H), 6.38 (s, 1H), 7.35 (t, *J* = 7.7 Hz, 1H), 7.40 (d, *J* = 7.5 Hz, 1H), 7.89 (d, *J* = 7.8 Hz, 1H), 7.93 (s, 1H).

2-Debenzoyl-10-(methoxycarbonyl)-2-(3-methylbenzoyl)-7-triethylsilyl-10-deacetylbaccatin III (1-22)

To a cooled solution of **1-19** (102 mg) in THF (2 ml) was added 1M LiHMDS (0.16 ml) followed by cyclopropanecarbonyl chloride (13 μl). The reaction mixture was allowed to react at -40˚C with stirring. Upon completion, the reaction was quenched with saturated NH_4Cl (10 ml) and extracted with ethyl acetate (3 x 30 mL). The organic layers was collected, washed with brine (3 x 30 mL), dried over $MgSO_4$ and concentrated *in vacuo* to afford crude product. Further purification was done by column chromatography on silica gel to give product 2-6 as a white solid in 62% yield. ^{1}H NMR (500 MHz, $CDCl_3$) δ 0.59 (m, 6H), 0.93 (t, *J* = 8.2 Hz, 9H), 1.05 (s, 3H), 1.17 (s, 3H), 1.63 (s, 1H), 1.68 (s, 3H), 1.88 (m, 1H), 2.10 (br s, 1H), 2.20 (s, 3H), 2.27 (m, 5H), 2.42 (s, 3H), 2.53 (m, 1H), 3.81 (s, 3H), 3.84 (d, J = 7.1 Hz, 1H), 4.13 (d, J = 8.4 Hz, 1H), 4.30 (d, J = 8.4 Hz, 1H),

4.48 (dd, J = 6.9 Hz, J = 10.5 Hz, 1H), 4.86 (m, 1H), 4.96 (d, J = 8.2 Hz, 1H), 5.60 (d, J = 7.1 Hz, 1H), 6.28 (s, 1H), 7.35 (t, *J* = 7.7 Hz, 1H), 7.41 (d, *J* = 7.5 Hz, 1H), 7.89 (d, *J* = 7.8 Hz, 1H), 7.93 (s, 1H).

2-Debenzoyl-3'-dephenyl-10-(cyclopropanecarbonyl)-2-(3-methylbenzoyl)-3'-(2-methyl-2-propen-1-yl)-7- triethylsilyl-2'- triisopropylsilyldocetaxel (1-23)

To a cooled solution **1-20** (178 mg) and β-Lactam (+) (115 mg) in THF (5 ml) was added 1M LiHMDS (0.36 ml). The mixture was allowed to react at -40˚C with stirring. Upon the reaction completion, the reaction was quenched with saturated NH_4Cl (10 ml) and extracted with ethyl acetate (3 x 30 mL). The organic layers was collected, washed with brine (3 x 30 mL), dried over $MgSO_4$ and concentrated *in vacuo* to afford crude product. Further purification was done by column chromatography on silica gel to give product **1-23** as a white solid in 81% yield. ^{1}H NMR (500 MHz, $CDCl_3$) δ 0.56 (m, 6H), 0.91 (t, *J* = 8.0 Hz, 9H), 1.10 (m, 21H), 1.18 (s, 3H), 1.22 (s, 3H), 1.33 (s, 9H), 1.67 (s, 3H), 1.75 (m, 5H), 1.77 (s, 3H), 1.87 (t, *J* = 13.6 Hz, 1H), 2.00 (s, 3H), 2.36 (s, 3H), 2.41 (s, 3H), 2.49 (m, 1H), 3.83 (d, *J* = 7.1 Hz, 1H), 4.17 (d, *J* = 8.4 Hz, 1H), 4.30 (d, *J* = 8.4 Hz, 1H), 4.44 (m, 2H), 4.75 (br s, 1H), 4.82 (m, 1H), 4.93 (d, *J* = 8.9 Hz, 1H), 5.33 (d, *J* = 8.7 Hz, 1H), 5.66 (d, *J* = 7.1 Hz, 1H), 6.07 (t, *J* = 9.0 Hz, 1H), 6.47 (s, 1H), 7.33 (t, *J* = 7.6 Hz, 1H), 7.39 (d, *J* = 7.5 Hz, 1H), 7.89 (d, *J* = 7.8 Hz, 1H), 7.93 (s, 1H).

2-Debenzoyl-3'-dephenyl-10-(*N,N*-dimethylcarbamoyl)-2-(3-methylbenzoyl)-3'-(2-methyl-2-propen-1-yl)-7- triethylsilyl-2'- triisopropylsilyldocetaxel (1-24)

To a cooled solution **1-21** (67 mg) and β-Lactam (+) (43 mg) in THF (2 ml) was added 1M LiHMDS (0.19 ml). The mixture was allowed to react at -40˚C with stirring. Upon completion, the reaction was quenched with saturated NH_4Cl (10 ml) and extracted with ethyl acetate (3 x 30 mL). The organic layers was collected, washed with brine (3 x 30 mL), dried over $MgSO_4$ and concentrated *in vacuo* to afford crude product. Further purification was done by column chromatography on silica gel to give product **1-24** as a white solid in 92% yield. The product was characterized by ^{1}H NMR. ^{1}H NMR (500 MHz, $CDCl_3$) δ 0.58 (m, 6H), 0.91 (t, *J* = 8.1 Hz, 9H), 1.10 (m, 21H), 1.19 (s, 3H), 1.22 (s, 3H), 1.33 (s, 9H), 1.68 (s, 3H), 1.74 (d, J = 0.9 Hz, 3H), 1.77 (d, J = 1.0 Hz, 1H), 1.88 (m, 1H), 2.05 (s, 3H), 2.36 (s, 3H), 2.41 (s, 3H), 2.50 (s, 1H), 2.93 (s, 3H), 3.06 (s, 3H), 3.86 (d, J = 7.1 Hz, 1H), 4.18 (d, 8.4 Hz, 1H), 4.30 (d, J = 8.4 Hz, 1H), 4.43 (d, J = 2.9 Hz, 1H), 4.47 (dd, J = 6.8 Hz, J = 10.5 Hz, 1H), 4.75 (br s, 1H), 4.81 (br s, 1H), 4.94 (d, J = 7.9 Hz, 1H), 5.33 (d, J = 8.8 Hz, 1H), 5.67 (d, J = 7.2 Hz, 1H), 6.09 (t, J = 8.6 Hz, 1H), 6.40 (s, 1H), 7.34 (t, *J* = 7.7 Hz, 1H), 7.40 (d, *J* = 7.5 Hz, 1H), 7.89 (d, *J* = 7.8 Hz, 1H), 7.93 (s, 1H).

2-Debenzoyl-3'-dephenyl-10-(methoxycarbonyl)-2-(3-methylbenzoyl)-3'-(2-methyl-2-propen-1-yl)-7- triethylsilyl-2'- triisopropylsilyldocetaxel (1-25)

To a cooled solution **1-22** (67 mg) and *β*-Lactam (+) (43 mg) in THF (2 ml) was added 1M LiHMDS (0.16 ml). The mixture was allowed to react at -40˚C with stirring. Upon completion, the reaction was quenched with saturated NH_4Cl (10 ml) and extracted with ethyl acetate (3 x 30 mL). The organic layers was collected, washed with brine (3 x 30 mL), dried over $MgSO_4$ and concentrated *in vacuo* to afford crude product. Further purification was done by column chromatography on silica gel to give product **1-25** as a white solid in 84% yield. ^{1}H NMR (500 MHz, $CDCl_3$) δ 0.58 (m, 6H), 0.92 (t, *J* = 8.1 Hz, 9H), 1.11 (m, 21H), 1.19 (m, 6H), 1.33 (s, 9H), 1.68 (s, 3H), 1.74 (s, 3H), 1.77 (s, 1H), 1.89 (m, 1H), 2.02 (s, 3H), 2.36 (s, 3H), 2.40 (s, 3H), 2.50 (m, 1H), 3.80 (m, 4H), 4.17 (d, 8.4 Hz, 1H), 4.30 (d, J = 8.4 Hz, 1H), 4.45 (m, 2H), 4.76 (br s, 1H), 4.81 (br s, 1H), 4.93 (d, J = 8.3 Hz, 1H), 5.33 (d, J = 8.8 Hz, 1H), 5.66 (d, J = 7.2 Hz, 1H), 6.08 (t, J = 8.6 Hz, 1H), 6.27 (s, 1H), 7.33 (t, *J* = 7.7 Hz, 1H), 7.40 (d, *J* = 7.5 Hz, 1H), 7.89 (d, *J* = 7.8 Hz, 1H), 7.92 (s, 1H).

2-Debenzoyl-3'-dephenyl-10-(cyclopropanecarbonyl)-2-(3-methylbenzoyl)-3'-(2-met hyl- 2-propen-1-yl)docetaxel (SB-T-121402)

To a cooled solution of **1-23** (195 mg) in CH_3CN-pyridine 1:1 (2.2 ml) was added HF-pyridine, and the reaction mixture was allowed to warm from 0˚C to room temperature for 21 hours with stirring. Upon completion, the reaction was quenched with 0.2 M citric acid (10 mL) and extracted with ethyl acetate (3 x 30 mL). The organic layers was collected, washed with saturated $CuSO_4$ (3 x 30 mL) and brine (3 x 30 mL),

dried over $MgSO_4$ and concentrated *in vacuo* to afford crude product. Further purification was done by column chromatography on silica gel to give product **SB-T-121402** as a white solid in 77% yield. ^{1}H NMR (500 MHz, $CDCl_3$) δ 0.99 (m, 2H), 1.14 (m, 5H), 1.34 (s, 9H), 1.67 (s, 3H), 1.75 (m, 6H), 1.79 (m, 2H), 1.86 (m, 4H), 2.37 (m, 5H), 2.41 (s, 3H), 2.52 (m, 1H), 2.60 (br s, 1H), 3.41 (br s, 1H), 3.80 (d, *J* = 7.1 Hz, 1H), 4.17 (d, *J* = 8.4 Hz, 1H), 4.20 (s, 1H), 4.30 (d, *J* = 8.4 Hz, 1H), 4.40 (dd, *J* = 8.8 Hz, *J* = 11 Hz, 1H), 4.74 (m, 1H), 4.97 (d, *J* = 4.3 Hz), 5.32 (d, *J* = 8.4 Hz, 1H), 5.64 (d, *J* = 7.1 Hz, 1H), 6.16 (t, *J* = 9.0 Hz, 1H), 6.30 (s, 1H), 7.35 (t, *J* = 7.7 Hz, 1H), 7.41 (d, *J* = 3.8 Hz, 1H), 7.89 (d, *J* = 7.7 Hz, 1H), 7.93 (s, 1H). ^{13}C NMR (100 MHz) δ 9.2, 9.4, 9.5, 13.0, 14.2, 15.0, 18.6, 21.1, 21.4, 22.0, 22.4, 25.8, 26.7, 28.2, 35.5, 35.6, 43.2, 45.7, 58.6, 72.2, 72.4, 73.7, 75.0, 75.5, 76.5, 76.8, 77.0, 77.3, 79.2, 81.1, 84.4, 127.3, 128.5, 129.1, 130.8, 134.5, 138.3,167.1, 170.0, 175.1, 203.9. HPLC: t = 5.8 min, purity >98%. HRMS for C46H62NO15+ calcd: 868.4119. Found: 868.4122 (Δ = 0.3 ppm). mp 178 – 179˚C. $[\alpha]^d$ -80 (*c* 1.16, DCM).

2-Debenzoyl-3'-dephenyl-10-(*N,N*-dimethylcarbamoyl)-2-(3-methylbenzoyl)-3'-(2-methyl- 2-propen-1-yl)docetaxel (SB-T-121602)

To a cooled solution of 2-7 (93 mg) in CH_3CN-pyridine 1:1 (5.6 ml) was added HF-pyridine (1 ml), and the reaction mixture was allowed to warm from 0˚C to room temperature for 21 hours with stirring. Upon completion, the reaction was quenched with saturated NH_4Cl (10 ml) and extracted with ethyl acetate (3 x 30 mL). The organic layers

was collected, washed with saturated $CuSO_4$ (3 x 30 mL) and brine (3 x 30 mL), dried over $MgSO_4$ and concentrated in *vacuo* to afford crude product. Further purification was done by column chromatography on silica gel to give product **SB-T-121602** as a white solid in 89% yield. ^{1}H NMR (700 MHz, $CDCl_3$) δ 1.15 (s, 3H), 1.24 (s, 3H), 1.37 (s, 9H), 1.66 (s, 3H), 1.75 (d, J = 7.3 Hz, 6H), 1.85 (m, 3H), 1.91 (s, 3H), 2.36 (m, 5H), 2.41 (s, 3H), 2.52 (m, 1H), 2.95 (s, 3H), 3.04 (s, 3H), 3.24 (br s, 1H), 3.46 (br s, 1H), 3.80 (d, J = 7.0 Hz, 1H), 4.17 (d, 8.5 Hz, 1H), 4.20 (d, J = 3.9 Hz, 1H), 4.30 (d, J = 8.5 Hz, 1H), 4.44 (dd, J = 6.8 Hz, J = 10.9 Hz, 1H), 4.74 (t, J = 7.6 Hz, 1H), 4.83 (d, J = 8.6 Hz, 1H), 4.97 (d, J = 8.4 Hz, 1H), 5.32 (d, J = 7.8 Hz, 1H), 5.63 (d, J = 7.1 Hz, 1H), 6.17 (t, J = 8.9 Hz, 1H), 6.25 (s, 1H), 7.34 (t, *J* = 7.7 Hz, 1H), 7.40 (d, *J* = 7.5 Hz, 1H), 7.89 (d, *J* = 7.8 Hz, 1H), 7.92 (s, 1H). ^{13}C NMR (700 MHz) δ 9.5, 15.2, 18.7, 21.5, 22.5, 25.9, 27.0, 28.4, 35.6, 35.8, 36.2, 36.8, 43.4, 45.8, 51.7, 58.6, 72.7, 73.9, 75.2, 76.4, 76.6, 77.0, 77.2, 77.4, 79.4, 80.1, 81.3, 84.8, 120.8, 127.5, 128.7, 129.3, 131.0, 133.4, 134.6, 138.0, 138.5, 143.1, 155.6, 156.3, 167.2, 170.1, 173.3, 205.9. HPLC: t = 6.7 min, purity > 95 in 220 nm, > 97% in 254 nm. HRMS for C45H62N2O15Na+ calcd: 893.4047. Found: 893.4054 (Δ = 0.8 ppm). mp 158 – 160˚C. $[\alpha]^d$ -62.5 (*c* 1.03, DCM).

2-Debenzoyl-3'-dephenyl-10-(methoxycarbonyl)-2-(3-methylbenzoyl)-3'-(2-methyl-2-propen-1-yl)docetaxel (SB-T-121702)

To a cooled solution of 2-9 (81 mg) in CH_3CN-pyridine 1:1 (5.0 ml) was added HF-pyridine (0.90 ml), and the reaction mixture was allowed to warm from 0˚C to room

temperature for 21 hours with stirring. Upon completion, the reaction was quenched with saturated NH_4Cl (10 ml) and extracted with ethyl acetate (3 x 30 mL). The organic layers was collected, washed with saturated $CuSO_4$ (3 x 30 mL) and brine (3 x 30 mL), dried over $MgSO_4$ and concentrated in *vacuo* to afford crude product. Further purification was done by column chromatography on silica gel to give product **SB-T-121702** as a white solid in 84% yield. ^{1}H NMR (700 MHz, $CDCl_3$) δ 1.15 (s, 3H), 1.24 (s, 3H), 1.34 (s, 9H), 1.64 (s, 1H), 1.69 (s, 3H), 1.71 (s, 1H), 1.75 (d, J = 10.6 Hz, 6H), 1.88 (m, 1H), 1.93 (s, 3H), 2.36 (m, 5H), 2.42 (s, 3H), 2.46 (d, J = 4.1 Hz, 1H), 2.56 (m, 1H), 3.39 (br s, 1H), 3.78 (d, J = 7.1 Hz, 1H), 3.87 (s, 3H), 4.17 (d, 8.5 Hz, 1H), 4.21 (dd, J = 2.7 Hz, J = 7.1 Hz, 1H), 4.31 (d, J = 8.5 Hz, 1H), 4.39 (m, 1H), 4.75 (m, 2H), 5.32 (d, J = 7.4 Hz, 1H), 5.65 (d, J = 7.1 Hz, 1H), 6.12 (s, 1H), 6.16 (t, J = 9.0 Hz, 1H), 7.35 (t, *J* = 7.7 Hz, 1H), 7.41 (d, *J* = 7.5 Hz, 1H), 7.89 (d, *J* = 7.8 Hz, 1H), 7.93 (s, 1H). ^{13}C NMR (700 MHz) δ 9.6, 15.2, 18.7, 21.5, 21.9, 22.5, 25.9, 26.7, 28.4, 35.7, 35.8, 43.3, 45.8, 51.7, 55.8, 58.7, 72.3, 72.5, 73.9, 75.0, 76.6, 77.0, 77.2, 77.4, 78.5, 79.3, 80.1, 81.2, 84.5, 120.8, 127.5, 128.7, 129.3, 131.0, 132.7, 134.7, 138.0, 138.5, 143.7, 155.6, 156.0, 167.2, 170.3, 173.3, 204.2. HPLC: t = 12.7 min, purity > 97% in 220 nm, > 95% in 254 nm. HRMS for C44H59NO16Na+ calcd: 880.3732. Found: 880.3742 (Δ = 1.1 ppm). mp 150 – 152˚C. $[\alpha]^d$ -25 (*c* 0.83, DCM).

2-Debenzoyl-10-acetyl-2-(3-methylbenzoyl)baccatin III (1-26)

To a cooled solution of **1-18** (84 mg) and $CeCl_3$ (4 mg) in THF was added acetic anhydride (0.10 ml). The mixture was allowed at room temperature with stirring. Upon completion, the reaction was quenched with saturated NH_4Cl (10 ml) and extracted with ethyl acetate (3 x 30 mL). The organic layers was collected, washed with brine (3 x 30 mL), dried over $MgSO_4$ and concentrated *in vacuo* to afford crude product. Further purification was done by column chromatography on silica gel to give product **1-26** as a white solid in 77% yield. The product was characterized by ^1H NMR. ^1H NMR (500 MHz, $CDCl_3$) δ 1.00 (m, 1H), 1.09 (s, 5H), 1.65 (s, 3H), 1.84 (m, 1H), 2.22 (s, 3H), 2.27 (m, 4H), 2.41 (m, 3H), 2.54 (m, 1H), 3.85 (d, *J* = 7.1 Hz, 1H), 4.13 (d, *J* = 6.4 Hz, 1H), 4.29 (d, *J* = 8.4 Hz, 1H), 4.44 (dd, *J* = 6.8 Hz, *J* = 10.8 Hz, 1H), 4.85 (t, J = 7.9 Hz, 1H), 4.97 (d, *J* = 8.4 Hz, 1H), 6.31 (s, 1H), 7.35 (t, *J* = 7.6 Hz, 1H), 7.40 (d, *J* = 7.2 Hz, 1H), 7.88 (d, *J* = 7.8 Hz, 1H), 7.91 (s, 1H).

2-Debenzoyl-10-propanoyl -2-(3-methylbenzoyl)-10-deacetylbaccatin III (1-27)

To a cooled solution of **1-18** (92 mg) and $CeCl_3$ (6 mg) in THF (4 ml) was added acetic anhydride (0.21 ml). The mixture was allowed at room temperature with stirring. Upon completion, the reaction was quenched with saturated NH_4Cl (10 ml) and extracted with ethyl acetate (3 x 30 mL). The organic layers was collected, washed with brine (3 x 30 mL), dried over $MgSO_4$ and concentrated *in vacuo* to afford crude product. Further purification was done by column chromatography on silica gel to give product **1-27** as a white solid in 77% yield. The product was characterized by ^1H NMR. ^1H NMR (500

MHz, $CDCl_3$) δ1.19 (s, 5H), 1.23 (t, J = 3.4 Hz, 3H), 1.55 (s, 3H), 1.61 (s, 1H), 1.66 (s, 3H), 1.86 (m, 1H), 2.06 (s, 3H), 2.28 (s, 3H), 2.30 (s, 1H), 2.48 (s, 3H), 2.54 (m, 4H), 3.88 (d, *J* = 7.1 Hz, 1H), 4.14 (d, *J* = 6.4 Hz, 1H), 4.31 (d, *J* = 8.4 Hz, 1H), 4.47 (m, 1H), 4.89 (br s, 1H), 4.99 (d, *J* = 7.7 Hz, 1H), 6.33 (s, 1H), 7.36 (t, *J* = 7.6 Hz, 1H), 7.42 (d, *J* = 7.6 Hz, 1H), 7.90 (d, *J* = 5.4 Hz, 1H), 7.93 (s, 1H).

2-Debenzoyl-2-(3-methylbenzoyl)-7-triethylsilyl-10-acetylbaccatin III (1-28)

To a cooled solution of **1-26** (70 mg) and imidazole (35 mg) in DMF was added TESCl (0.08 ml). The mixture was allowed at 0˚C with stirring. Upon completion, the reaction was quenched with saturated NH_4Cl (10 ml) and extracted with ethyl acetate (3 x 30 mL). The organic layers was collected, washed with brine (3 x 30 mL), dried over $MgSO_4$ and concentrated *in vacuo* to afford crude product. Further purification was done by column chromatography on silica gel to give product **1-28** as a white solid in 75% yield. The product was characterized by ^{1}H NMR. ^{1}H NMR (500 MHz, $CDCl_3$) δ 0.57 (m, 6H), 0.92 (t, *J* = 8.0 Hz, 9H), 1.03 (s, 3H), 1.19 (s, 3H), 1.66 (m, 4H), 1.87 (m, 1H), 2.17 (s, 3H), 2.26 (m, 5H), 2.41 (s, 3H), 2.52 (m, 1H), 3.87 (d, *J* = 7.0 Hz, 1H), 4.14 (d, *J* = 6.4 Hz, 1H), 4.30 (d, *J* = 8.4 Hz, 1H), 4.48 (dd, *J* = 6.8 Hz, *J* = 10.8 Hz, 1H), 4.82 (t, J = 7.9 Hz, 1H), 4.96 (d, *J* = 8.4 Hz, 1H), 5.60 (d, J = 6.7 Hz, 1H), 6.45 (s, 1H), 7.35 (t, *J* = 7.6 Hz, 1H), 7.41 (d, *J* = 7.2 Hz, 1H), 7.90 (d, *J* = 7.7 Hz, 1H), 7.93 (s, 1H).

2-Debenzoyl-10-propanoyl-2-(3-methylbenzoyl)-7-O-(triethylsilyl)-10-deacetylbaccatin III (1-29)

To a cooled solution of **1-27** (72 mg) and imidazole (35 mg) in DMF was added TESCl (0.08 ml). The mixture was allowed at 0˚C with stirring. Upon completion, the reaction was quenched with saturated NH_4Cl (10 ml) and extracted with ethyl acetate (3 x 30 mL). The organic layers was collected, washed with brine (3 x 30 mL), dried over $MgSO_4$ and concentrated *in vacuo* to afford crude product. Further purification was done by column chromatography on silica gel to give product **1-29** as a white solid in 75% yield. The product was characterized by ^{1}H NMR. ^{1}H NMR (500 MHz, $CDCl_3$) δ 0.57 (m, 6H), 0.92 (t, *J* = 8.0 Hz, 9H), 1.03 (s, 3H), 1.21 (m, 6H), 1.54 (s, 3H), 1.62 (s, 1H), 1.68 (s, 3H), 1.87 (m, 1H), 2.00 (d, J = 4.9 Hz), 2.20 (d, J = 1.0 Hz, 3H), 2.28 (m, 5H), 2.41 (s, 3H), 2.52 (m, 3H), 3.89 (d, *J* = 6.8 Hz, 1H), 4.14 (d, *J* = 9.3 Hz, 1H), 4.30 (d, *J* = 9.3 Hz, 1H), 4.48 (dd, *J* = 6.8 Hz, *J* = 10.8 Hz, 1H), 4.83 (t, J = 7.9 Hz, 1H), 4.96 (d, *J* = 8.4 Hz, 1H), 5.61 (d, J = 6.7 Hz, 1H), 6.48 (s, 1H), 7.36 (t, *J* = 7.6 Hz, 1H), 7.41 (d, *J* = 7.2 Hz, 1H), 7.90 (d, *J* = 7.7 Hz, 1H), 7.94 (s, 1H).

2-Debenzoyl-3'-dephenyl-10-acetyl-2-(3-methylbenzoyl)-3'-(2-methyl-2-propen-1-yl) -7- triethylsilyl-2'-triisopropylsilyldocetaxel (1-30)

To a cooled solution **1-28** (62 mg) and β-Lactam (+) (40 mg) in THF (2 ml) was added 1M LiHMDS (0.13 ml). The mixture was allowed to react at -40˚C with stirring. Upon completion, the reaction was quenched with saturated NH_4Cl (10 ml) and extracted with

ethyl acetate (3 x 30 mL). The organic layers was collected, washed with brine (3 x 30 mL), dried over $MgSO_4$ and concentrated *in vacuo* to afford crude product. Further purification was done by column chromatography on silica gel to give product **1-30** as a white solid in 83% yield. The product was characterized by ^{1}H NMR. ^{1}H NMR (500 MHz, $CDCl_3$) δ 0.57 (m, 6H), 0.91 (t, *J* = 8.1 Hz, 9H), 1.13 (m, 21H), 1.18 (s, 3H), 1.22 (s, 3H), 1.33 (s, 9H), 1.68 (s, 3H), 1.74 (s, 3H), 1.77 (d, J = 0.9 Hz, 3H), 1.89 (m, 1H), 2.17 (s, 3H), 2.36 (s, 3H), 2.41 (s, 3H), 2.52 (m, 1H), 3.83 (d, *J* = 7.0 Hz, 1H), 4.17 (d, *J* = 8.5 Hz, 1H), 4.30 (d, *J* = 8.5 Hz, 1H), 4.42 (d, J = 3.0 Hz, 1H), 4.46 (dd, *J* = 6.7 Hz, *J* = 10.6 Hz, 1H), 4.76 (br s, 1H), 4.82 (m, 1H), 4.94 (d, *J* = 8.0 Hz, 1H), 5.33 (d, J = 8.8 Hz, 1H), 5.66 (d, J = 7.1 Hz, 1H), 6.08 (t, J = 8.8 Hz, 1H), 6.46 (s, 1H), 7.33 (t, *J* = 7.6 Hz, 1H), 7.41 (d, *J* = 7.2 Hz, 1H), 7.90 (d, *J* = 7.7 Hz, 1H), 7.93 (s, 1H).

2-Debenzoyl-3'-dephenyl-10-propanoyl-2-(3-methylbenzoyl)-3'-(2-methyl-2-propen-1-yl)-7-triethylsilyl-2'-triisopropylsilyldocetaxel (1-31)

To a cooled solution **1-29** (64 mg) and β-Lactam (+) (40 mg) in THF (2 ml) was added 1M LiHMDS (0.13 ml). The mixture was allowed to react at -40˚C with stirring. Upon completion, the reaction was quenched with saturated NH_4Cl (10 ml) and extracted with ethyl acetate (3 x 30 mL). The organic layers was collected, washed with brine (3 x 30 mL), dried over $MgSO_4$ and concentrated *in vacuo* to afford crude product. Further purification was done by column chromatography on silica gel to give product **1-31** as a white solid in 77% yield. The product was characterized by ^{1}H NMR. ^{1}H NMR (500

MHz, $CDCl_3$) δ 0.57 (m, 6H), 0.91 (t, *J* = 8.1 Hz, 9H), 1.11 (m, 21H), 1.17 (s, 3H), 1.20 (s, 3H), 1.22 (s, 3H), 1.33 (s, 9H), 1.66 (m, 4H), 1.74 (s, 3H), 1.77 (s, 3H), 1.88 (m, 1H), 2.01 (s, 3H), 2.37 (m, 4H), 2.43 (s, 3H), 2.52 (m, 3H), 3.84 (d, *J* = 7.2 Hz, 1H), 4.17 (d, *J* = 8.5 Hz, 1H), 4.30 (d, *J* = 8.5 Hz, 1H), 4.42 (d, J = 3.0 Hz, 1H), 4.46 (dd, *J* = 6.7 Hz, *J* = 10.6 Hz, 1H), 4.80 (m, 2H), 4.94 (d, *J* = 8.0 Hz, 1H), 5.32 (d, J = 8.8 Hz, 1H), 5.66 (d, J = 7.1 Hz, 1H), 6.08 (t, J = 8.8 Hz, 1H), 6.49 (s, 1H), 7.33 (t, *J* = 7.6 Hz, 1H), 7.41 (d, *J* = 7.2 Hz, 1H), 7.90 (d, *J* = 7.7 Hz, 1H), 7.93 (s, 1H).

2-Debenzoyl-3'-dephenyl-10-acetyl-2-(3-methylbenzoyl)-3'-(2-methyl-2-propen-1-yl)docetaxel (SB-T-121202)

To a cooled solution of **1-30** (76 mg) in CH_3CN-pyridine 1:1 (4.6 ml) was added HF-pyridine (0.74 ml), and the reaction mixture was allowed to warm from 0˚C to room temperature for 21 hours with stirring. Upon completion, the reaction was quenched with saturated NH_4Cl (10 ml) and extracted with ethyl acetate (3 x 30 mL). The organic layers was collected, washed with saturated $CuSO_4$ (3 x 30 mL) and brine (3 x 30 mL), dried over $MgSO_4$ and concentrated *in vacuo* to afford crude product. Further purification was done by column chromatography on silica gel to give product **SB-T-121202** as a white solid 52 mg in 89% yield. ^{1}H NMR (700 MHz, $CDCl_3$) δ 1.14 (s, 3H), 1.25 (s, 3H), 1.34 (s, 9H), 1.67 (s, 1H), 1.74 (d, J = 0.7 Hz, 3H), 1.76 (s, 3H), 1.87 (m, 4H), 2.23 (s, 3H), 2.35 (s, 3H), 2.41 (s, 3H), 2.54 (m, 1H), 3.44 (br s, 1H), 3.80 (d, J = 7.1 Hz, 1H), 4.17 (d, 8.5 Hz, 1H), 4.20 (s, 1H), 4.30 (d, J = 6.1 Hz, 1H), 4.41 (dd, J = 6.8 Hz, J = 10.8 Hz, 1H),

4.74 (t, J = 6.9 Hz, 1H), 4.82 (d, J = 7.6 Hz, 1H), 4.96 (d, J = 7.9 Hz, 1H), 5.31 (d, J = 7.4 Hz, 1H), 5.63 (d, J = 7.1 Hz, 1H), 6.16 (t, J = 9.0 Hz, 1H), 6.30 (s, 1H), 7.34 (t, *J* = 7.7 Hz, 1H), 7.40 (d, *J* = 7.5 Hz, 1H), 7.88 (d, *J* = 7.8 Hz, 1H), 7.92 (s, 1H). ^{13}C NMR (700 MHz) δ 9.7, 15.2, 18.7, 21.1, 21.6, 22.5, 25.9, 26.8, 28.4, 35.8, 35.8, 43.4, 45.9, 51.7, 58.7, 72.4, 73.9, 75.1, 75.9, 76.7, 77.1, 77.2, 77.4, 79.3, 81.3, 84.6, 120.9, 127.5, 128.7, 129.3, 131.0, 134.7, 138.5, 142.8, 155.6, 167.3, 170.2, 171.5, 173.4, 204.0. HPLC: t = 12.9 min, purity > 94% in 220 nm, > 94% in 254 nm. HRMS for C44H60NO15+ calcd: 842.3967. Found: 842.3965 (Δ = -0.2 ppm). mp 160 – 162˚C. $[\alpha]^d$ -85 (*c* 0.81, DCM).

2-Debenzoyl-3'-dephenyl-10-propanoyl-2-(3-methylbenzoyl)-3'-(2-methyl-2-propen-1-yl)docetaxel (SB-T-121302)

To a cooled solution of **1-31** (74 mg) in CH_3CN-pyridine 1:1 (4.6 ml) was added HF-pyridine (0.74 ml), and the reaction mixture was allowed to warm from 0˚C to room temperature for 21 hours with stirring. Upon completion, the reaction was quenched with saturated NH_4Cl (10 ml) and extracted with ethyl acetate (3 x 30 mL). The organic layers was collected, washed with saturated $CuSO_4$ (3 x 30 mL) and brine (3 x 30 mL), dried over $MgSO_4$ and concentrated *in vacuo* to afford crude product. Further purification was done by column chromatography on silica gel to give product **SB-T-121302** as a white solid in 77% yield. ^{1}H NMR (700 MHz, $CDCl_3$) δ 1.14 (s, 3H), 1.23 (m, 6H), 1.34 (s, 9H), 1.67 (s, 3H), 1.75 (s, 3H), 1.76 (s, 3H), 1.87 (m, 4H), 2.37 (m, 5H), 2.42 (s, 3H), 2.53 (m, 4H), 3.39 (br s, 1H), 3.81 (d, J = 7.1 Hz, 1H), 4.17 (d, 8.5 Hz, 1H), 4.20 (dd, J = 2.5 Hz, J

= 6.7 Hz, 1H), 4.30 (d, J = 8.5 Hz, 1H), 4.42 (m, 1H), 4.74 (t, J = 6.9 Hz, 1H), 4.78 (d, J = 8.7 Hz, 1H), 5.32 (d, J = 7.6 Hz, 1H), 5.64 (d, J = 7.1 Hz, 1H), 6.16 (t, J = 9.0 Hz, 1H), 6.31 (s, 1H), 7.35 (t, *J* = 7.7 Hz, 1H), 7.42 (d, *J* = 7.6 Hz, 1H), 7.89 (d, *J* = 7.7 Hz, 1H), 7.93 (s, 1H). ^{13}C NMR (700 MHz) δ 9.3, 9.8, 15.2, 18.8, 21.6, 22.6, 25.9, 26.8, 27.8, 28.4, 35.8, 35.8, 43.4, 45.9, 51.7, 58.8, 72.5, 72.6, 74.0, 75.1, 75.7, 76.7, 79.4, 80.2, 81.3, 84.6, 120.9, 127.5, 128.8, 131.0, 134.7, 138.6, 142.7, 155.7, 167.3, 170.2, 173.4, 174.9, 204.1. HPLC: t = 7.3 min, purity > 91% in 220 nm, > 94% in 254 nm. HRMS for C45H62NO15+ calcd: 856.4129. Found: 856.4129 (Δ = 0 ppm). mp 169 – 172˚C. $[\alpha]^{d}$ -45 (*c* 0.67, DCM).

Chapter II

Synthesis of Dendrimer-Based Multifunctional Conjugates for Tumor-Targeting Drug Delivery

§ 2.1 Introduction 63

§ 2.2 Tumor-targeting modules 64

§ 2.2.1 Polyunsaturated Fatty Acids (PUFAs) 65

§ 2.2.2 Monoclonal Antibodies (mAbs) 67

§ 2.2.3 Biotin 69

§ 2.3 Enhanced Permeability and Retention (EPR) Effect for Cancer Chemotherapy 71

§ 2.4 Dendrimer 72

§2.5 Design and Synthesis of PAMAM Dendrimer-Based Biotin-Taxoid Conjugate and for Tumor-Targeting Drug Delivery 78

§ 2.5.1 Synthesis of Biotin PEGylated G3 PAMAM Dendrimer 80

§2.5.2 Synthesis of PAMAM Dendrimer-Based Biotin-Taxoid Conjugate 84

§ 2.6.1 Design and Synthesis of Asymmetric Bow-Tie Dendrimer-based (ABTD) conjugate for Tumor-Targeting Drug Delivery 87

§ 2.6.1 Synthesis of PAMAM G1 Dendrimer-Alkyne Conjugate 88

§ 2.6.2 Synthesis of ABTD Conjugate 91

§ 2.7 Conclusion 94

§ 2.8.1 General Methods 94

§ 1.8.2 Materials 95

§ 1.8.3 Experimental Procedure 95

§ 2.1 Introduction

Traditional chemotherapy relies on potent antitumor drugs to kill fast-growing cancer cells. However, these cytotoxic agents lack specificity and kill not only tumor cells, but also rapidly dividing noncancerous tissues such as cells in blood, mouth, digestive system and hair follicles. Due to this fact, several severe side effects will be caused by the use of chemotherapeutic drugs, such as hair loss, mouth sores, diarrhea, vomiting, constipation and blood disorders.

Tremendous efforts have been made towards the development of tumor-targeting drug delivery systems (TTDDS) to alleviate the side effects induced by antitumor drugs. The designed system should contain a targeting moiety, a potent cytotoxic agent and a smart linker. This conjugate should be able to recognize the tumor tissue from normal tissue, release drugs in the cancer cell successfully, be stable in the blood circulation, and systemically nontoxic.

§ 2.2 Tumor-targeting modules

Rapid growing tumor cells require different kinds of nutrients and vitamins. Therefore, tumor cells overexpress many tumor-specific receptors, which can be employed as targets to deliver cytotoxic agents into tumor cells. In recent years, a number of targeting molecules are being used in the construction of drug conjugates, such as omega-3 polyunsaturated fatty acids, monoclonal antibodies, folic acid, biotin and

hyaluronic acid. The strategy of employ tumor-targeting modules to kill cancer cells is termed as “active targeting”.

§ 2.2.1 Polyunsaturated Fatty Acids (PUFAs)

Polyunsaturated fatty acids (PUFAs) are found in vegetable oils (n-6 PUFAs) and deep-water fish (n-3 PUFAs) as hydrocarbon chains of variable length.[54] PUFAs such as Linolenic acid (LNA), linoleic acid (LA), arachidonic acid (AA), docosahexaenoic acid (DHA), and eicosapentaenoic acid (EPA), these acids contain more than one double bond, a methyl group at one end of the chain and a carboxyl group at the other end.[55] Compared to normal tissue, PUFA uptake is elevated in tumor tissue.[56] In Ojima’s group, numerous conjugates of DHA to cytotoxic agents were designed, synthesized, and showed potent antitumor activities against certain cancer cells.[56]

On the other hand, PUFAs also exhibited antitumor activity against PANC-1, CFPAC, and Mia-Pa-Ca-2 pancreatic and HL-60 Leukemia cancer cell lines. Evidence suggests that the PUFAs are able to penetrate into the lipid bilayer of tumor cells which results in disruption of the plasma membrane structure. Thus, PUFA-targeted prodrug conjugates may lead not only to accumulation of the cytotoxic agent in the tumor microenvironment, but also synergism between the PUFA-targeting component and the drug.

The synthesis of DHA conjugates containing new-generation taxoids is illustrated in **Scheme 16**. New-generation taxoids were directly coupled with DHA *via* DIC coupling.

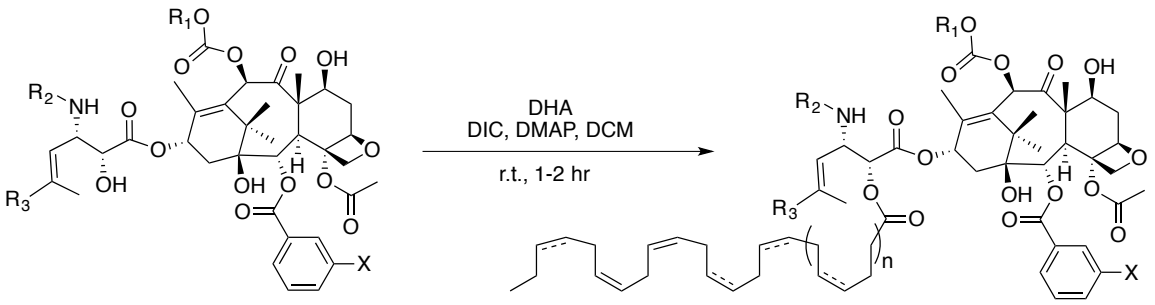

Scheme 16. Synthesis of DHA-taxoid conjugates

The cytotoxicities of PUFA-taxoid conjugates was assessed against a drug-resistant human colon tumor xenograft DLD-1 and a drug-sensitive human ovarian tumor xenograft A121 (**Figure 13**). Of these PUFA-taxoid conjugates, DHA-SB-T-1214, achieved complete regression of the DLD-1 tumor in 5 of 5 mice at a dose of 80 mg/kg administered on days 5, 8 and 11. In contrast, DHA-paclitaxel showed little antitumor activity against drug-resistant cancer xenograft DLD-1. In the case of the drug-sensitive tumor A121 xenograft, most of the DHA-taxoid conjugates showed antitumor activity. Among them, DHA-SB-T-1213 and DHA-SB-T-1216 achieved complete regression of the tumor in all surviving mice and delayed the tumor growth for more than 186 days even at the nonoptimized dose.[57]

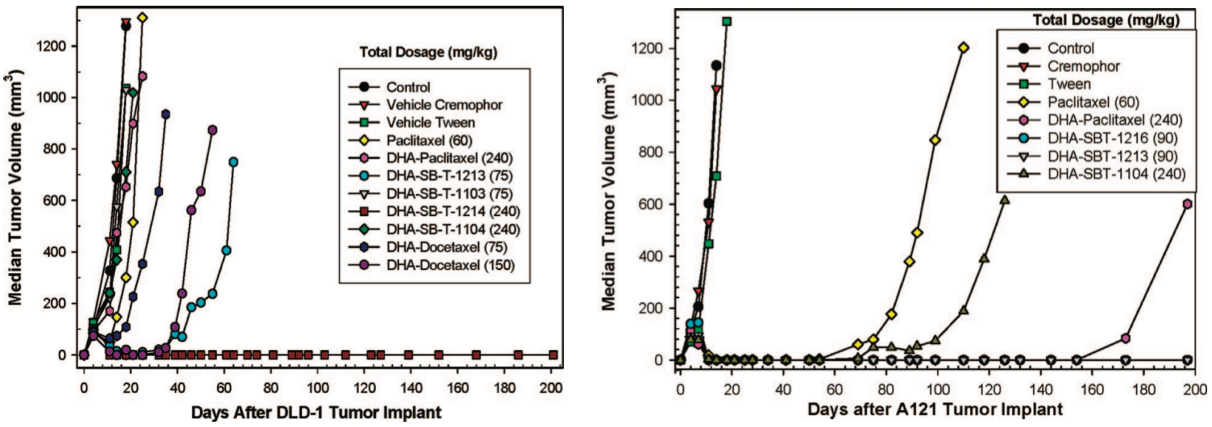

Figure 13. Effect of DHA-taxoid conjugates on human colon tumor xenograft DLD-1 and human ovarian tumor xenograft A121 (Adapted from Ref. 57.)

§ 2.2.2 Monoclonal Antibodies (mAbs)

Monoclonal antibodies (mAbs) exhibit high binding affinity for tumor-specific antigens, and thus can be selected as an ideal tumor-targeting moiety for a drug delivery system. The mAb-drug conjugate would target the tumor cells and undergo internalization and processing to release the cytotoxic agent in its active form. The epidermal growth factor receptor (EGFR) is known to be overexpressed in numerous human squamous cancer cells, such as lung and breast cancer. In this case, murine monoclonal antibodies were employed as tumor-targeting moieties because they were able to directed target EGFR. In Ojima's group, three such antibodies, KS61 (lgG2a), KS77 (lgG1) and KS78 (lgG2a) were used to link cytotoxic agent SB-T-12136 *via* disulfide bonds. The chemical structure of mAb-SB-T-12136 conjugate is showed in **Figure 14**.

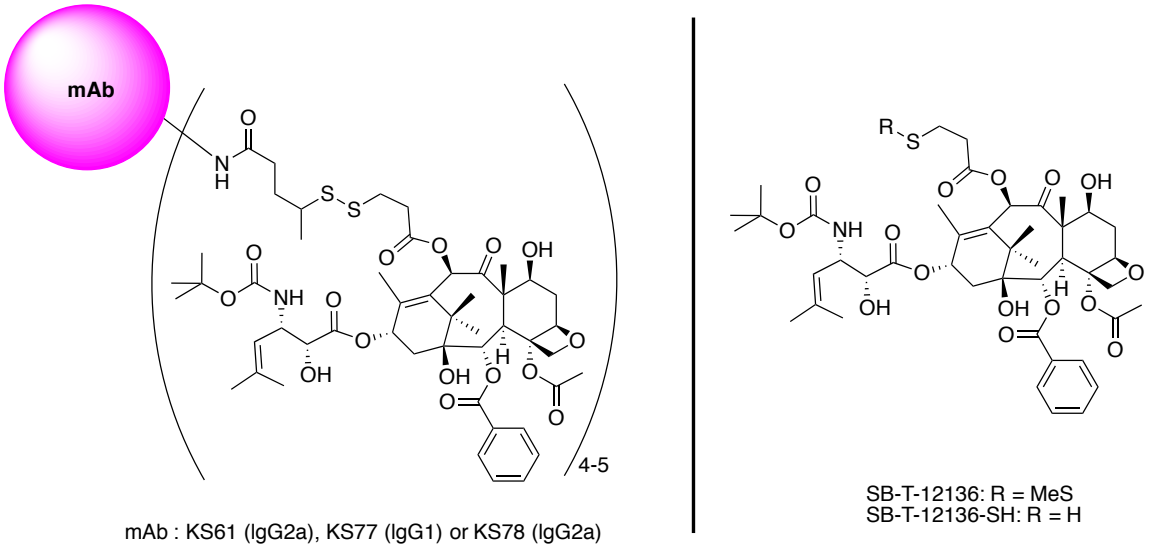

Figure 14. Chemical Structure of mAb-SB-T-12136 conjugates, SB-T-12136 and SB-T-12136-SH

The disulfide linker employed to connect taxoids and mAb (**Figure 14**) in the conjugate is non-toxic, stable in blood circulation, and readily cleaved inside the cancer cells. The use of disulfide linker is attractive due to the fact that the concentration of glutathione is much higher (> 1000 times) in tumor cells than in blood plasma. Once the conjugate is internalized into the cell, the SB-T-12136-SH will be released as the active cytotoxic agent after the disulfide linker is cleaved by glutathione. The potent antitumor activities of the anti-EGFR mAb-taxoid conjugates KS-61-SB-T-12136 and KS-77-SB-T-12136 were proved by *in vivo* tumor growth inhibition assays against EGFR expressed A431 xenografts (**Figure 15**). Both the anti-EGFR-mAb-taxoid conjugates showed potent cytotoxicity, resulting in complete inhibition of tumor growth. Additionally, the absence of any weight loss also suggested the anti-EGFR-mAb-taxoid

conjugates were non-toxic to the mice. Based on the results shown above, it can be concluded that these conjugates are remarkable anti-tumor agents with few side effects.

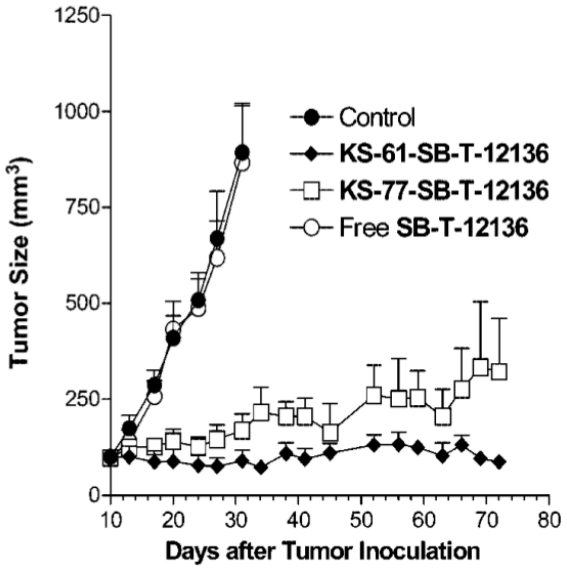

Figure 15. Antitumor activity of anti-EGFR mAb-taxoid conjugates against A431 xenografts

§ 2.2.3 Biotin

Vitamins are essential nutrients for all living cells to survive. Compared to normal cells, cancer cells require more vitamins such as vitamin B_{12}, folic acid, biotin and riboflavin in order to sustain their rapid cell growth and enhanced proliferation. Thus, these particular vitamin receptors are overexpressed on the cancer cell surface. Of these vitamins, biotin (vitamin H), is a growth promoter at the cellular level, and its content in tumor cells is much higher than in normal cells. Evidence suggests that biotin receptors are overexpressed in many cancer cell lines, e.g., leukemia (L1210FR), colon (colo-26),

lung (M109), renal (RENCA, RD 0995). Biotin uptake is Na^+, pH and temperature dependent, through the biotin receptor by receptor-mediated endocytosis (RME), shown in **Figure 16**.[57] After the biotin binds to the cell surface receptor, a signaling cascade is initiated, followed by the formation of coated vesicle containing the tumor-targeting drug conjugate. The vesicle fuses with the endosome, and the drug conjugate is cleaved in the endosome, as the concentration of glutathione (GSH) is elevated in the endosome. The cleaved pieces transfer to lysosome from endosome, followed by release of drug in its active form.[57]

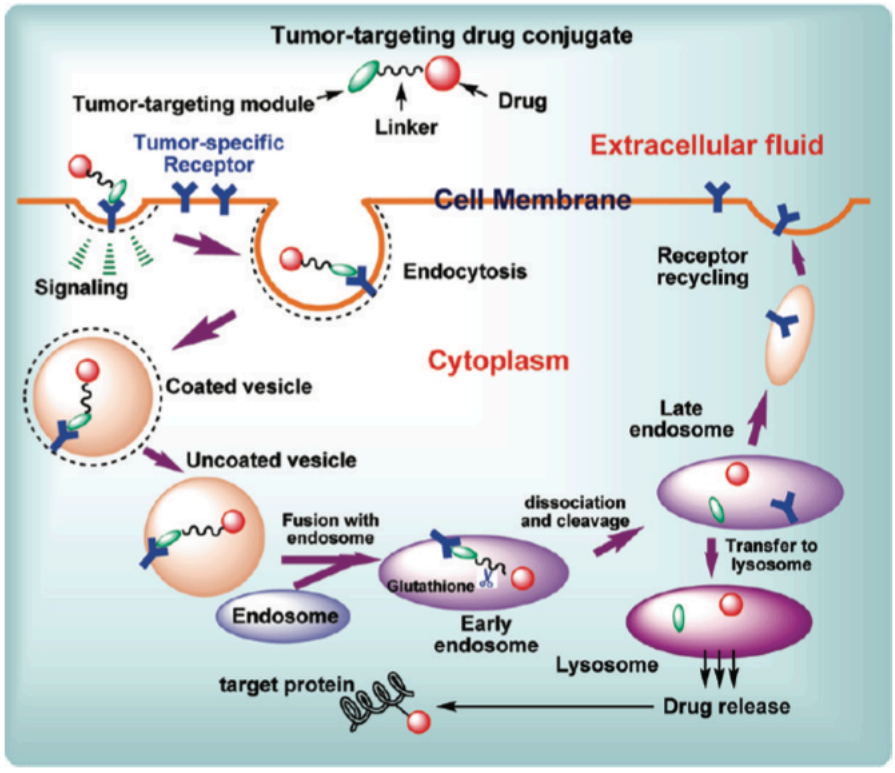

Figure 16. RME and intracellular drug release (Adapted from Ref. 57)

§ 2.3 Enhanced Permeability and Retention (EPR) Effect for Cancer Chemotherapy

Tumor are capable of building new blood vessels for getting nutrients and oxygens to support their rapid growth. These newly developed blood vessels are very different from those in the normal tissues, that is to say, they have irregular shapes, leakages and defective architectures. These abnormal tissues enable macromolecules or nanoparticles to have an increased chance to enter tumor tissues than normal tissue. Moreover, the lymphatic drainage system in tumor tissue is not well developed, resulting in bad clearance of the macromolecules or nanoparticles. Therefore, such large molecules have longer retention time in tumor tissue. This phenomenon is termed as "Enhanced Permeability and Retention" Effect which has been well studied in modern cancer chemotherapy (**Figure 17**).[58] The strategy to take advantage of this EPR effect to treat cancer cells is termed as "passive targeting".

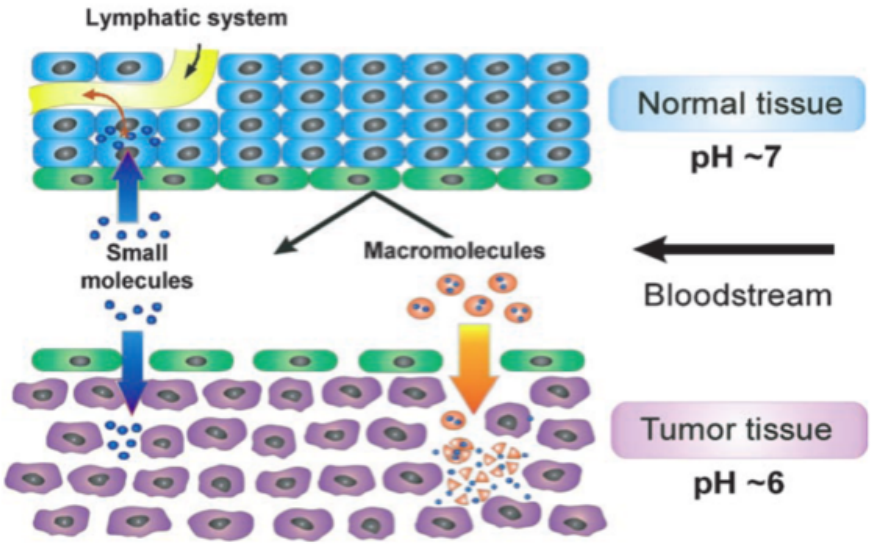

Figure 17. EPR Effect for Cancer Chemotherapy[58]

§ 2.4 Dendrimer

In recent years, numerous nanoparticles, such as dendrimers, gold nanoparticles, single-walled carbon nanotubes, liposomes, quandom dots, and nanowires were employed as the vehicle for tumor-targeting drug delivery conjugates.[59] Some nanoparticles' structures are illustrated in **Figure 18**. The area of research in this dissertation, however, was focused on polyaminoamine (PAMAM) dendrimer.

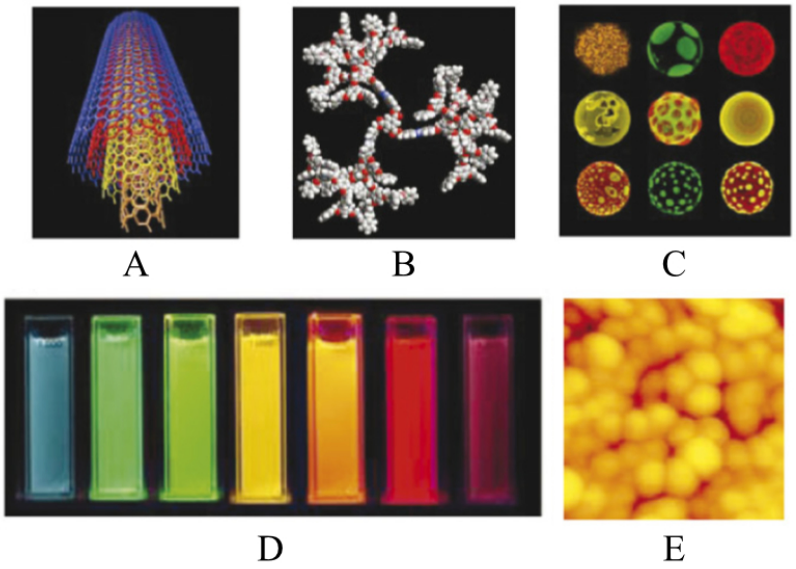

Figure 18. Structures of nanoparticles A) carbon nanotubes, B) dendrimers, C) liposomes, D) quantum dots, E) gold nanoparticles (Adapted from Ref. 59 with modifications)

Dendrimers, well-defined three-dimensional macromolecules, are highly branched synthetic polymers with a central core, an internal region and many terminal groups that determine the characteristics of the dendrimer. As shown in **Figure 19**, dendrimers usually contain three parts, namely the core molecule, the surface molecules, and branches.[60] Each layer added to a dendrimer is termed a "generation". At lower generations, the dendrimer branch may fold back on itself depending on the pH, solvent polarities and surface groups.[61, 62]

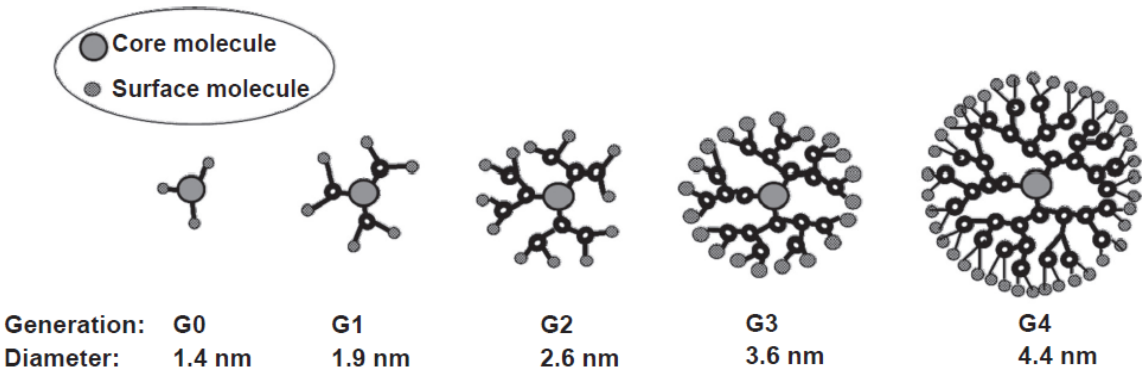

Figure 19. Graphical representation of dendrimers from generation 0 to generation 4[63]

In term of anticancer drug delivery, dendrimers are attractive platforms because of their unique properties, including: i) Well-defined architectures, molecular weights and functionalities; ii) anticancer drugs could be encapsulated into the interior space of dendrimers to greatly increase the water solubility of the drug; iii) anticancer drugs, targeting moieties and other functional groups could also be conjugated to the terminal groups on the surface of dendrimers to increase the payload of the drugs, targeting efficacy of the conjugate, and other biological and physiological properties; iv) passive targeting of the conjugate could be achieved based on the size of the functionalized dendrimers by employing the enhanced permeability and retention (EPR) effect; and v) lack of immunogenicity of certain types of dendrimers make them safer than synthetic peptides or natural proteins.[64]

PAMAM (poly(amidoamine)) dendrimer is one of the most commonly used dendrimers in the medicinal field. This star-burst synthetic compound contains surface amine groups and can be used for installing more than one drug, imaging agents, targeting moieties, and groups for biocompatibility. Accordingly, it can be used to create

a polyfunctional nanomedicine. The chemical structure of G1 PAMAM dendrimer is illustrated in **Figure 20**.

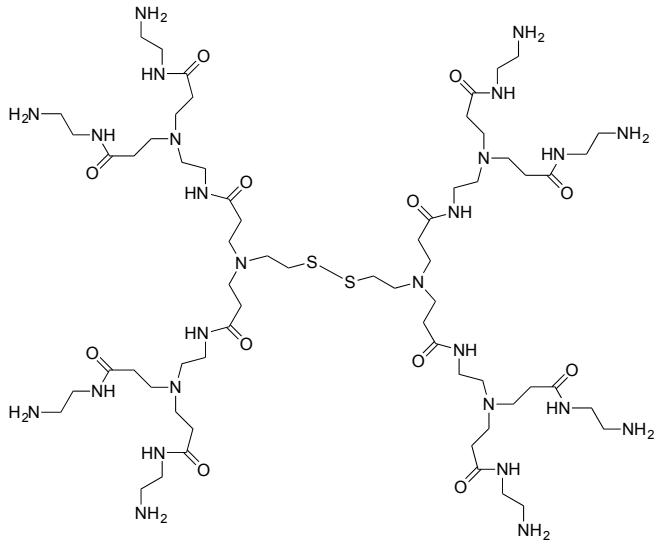

Figure 20. Chemical Structure of G1 PAMAM Dendrimer

In 2011, Hartley et al. reported a "diblock" PAMAM dendrimers with cystamine core and three functional units (**Figure 21**).[65] They chose to use mannose as the first functional unit to increase the uptake processing by sentinel cells. An array of short peptide molecules was used as the second functional unit. In order to trace the uptake of these conjugates, a fluorescent moiety was used as the third functional unit. These conjugates were used to release a peptide or protein antigen to mannose-receptor expressed sentinel cells.

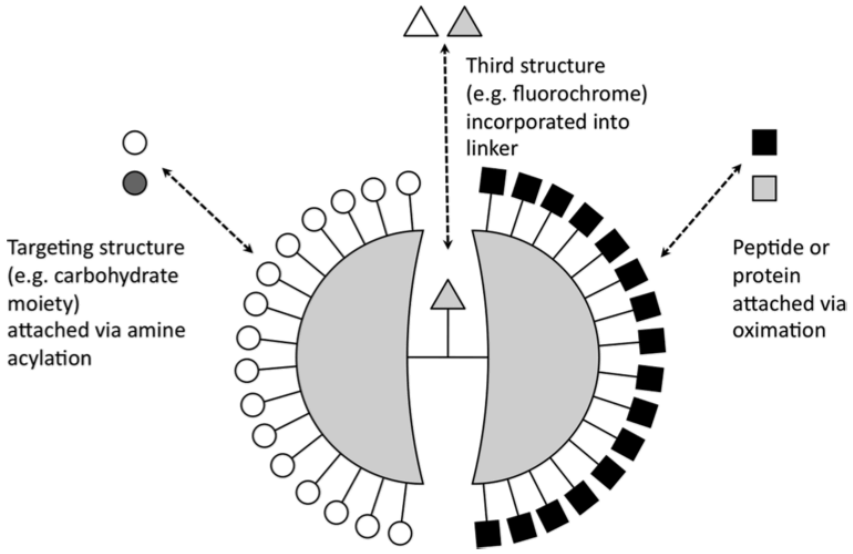

Figure 21. Schematic representation of "diblock" PAMAM cystamine core dendrimer-based conjugate for synthesis of bioactive nanoparticles (Adapted from Ref. 65)

In 2005, Baker et al. reported the synthesis of partially acetylated G5 dendrimer conjugates bearing folic acid (FA), fluorescein isothiocyanate (FITC), glycidol and methotrexate (MTX).[66] The structure of this conjugate is shown in **Figure 22**.[66] This multifunctional PAMAM dendritic conjugate was able to target the overexpressed membrane-associated folate receptors of certain cancer cells with FA and induce cytotoxicity by employing MTA. This conjugate has shown *in vitro* and *in vivo* cellular internalization through the folate receptor and improved efficacy to kill tumor cells.[67, 68] However, when they scaled up the synthesis for clinical trial studies, it was discovered to be less cytotoxicity *in vitro* and insignificant anticancer activity *in vivo* compared to small batches of the material.[69] The unsatisfactory result is mainly because of the polydispersity of the synthesized multifunctional dendrimer conjugates.[69]

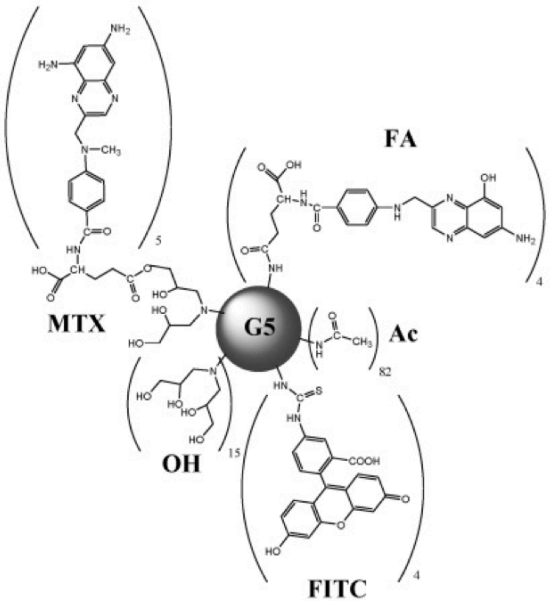

Figure 22. Structure of multifunctional PAMAM dendritic devices (Adapted from Ref. 66.)

One problem of dendrimer-based conjugates is heterogeneity, which means functionalization with multiple kinds of molecules may be distributed on the surface unevenly. It is affected by reaction conditions such as temperature, pH, concentration, and stoichiometry of reagents. Currently, dendrimer-based conjugates are presented by the average number of each type of functional molecules regardless of their distribution of on the surface. The quality of final conjugates of each batch was not guaranteed to be same. Because of that, the biological evaluation becomes unreliable by employing these dendrimer-based conjugates. The number of each functional group varies from batch to batch, mainly affected by reaction conditions.

Regardless of the heterogeneity, structural defects were also observed during the synthesis of the dendrimer. It has been described as the problem of purification and

analysis[66]. Side reactions, such as synthesis of fewer arms, combine to induce such defective PAMAM dendrimer structure. This defective problem mainly existed in higher generations (3, 4 and 5)[66]. The amount, and different form of defective dendrimers vary from batch to batch. Thus it becomes difficult to determine the exact purity and quality of resulting dendrimer drug conjugate.

§2.5 Design and Synthesis of (PAMAM Dendrimer)-Based Biotin-Taxoid Conjugate and for Tumor-Targeting Drug Delivery

To solve the problem of heterogeneity, a new dendrimer-based conjugate was designed for tumor-targeting drug delivery. The structure of PAMAM dendrimer-based biotin-taxoid conjugate for tumor-targeting drug delivery is illustrated in **Figure 23**.

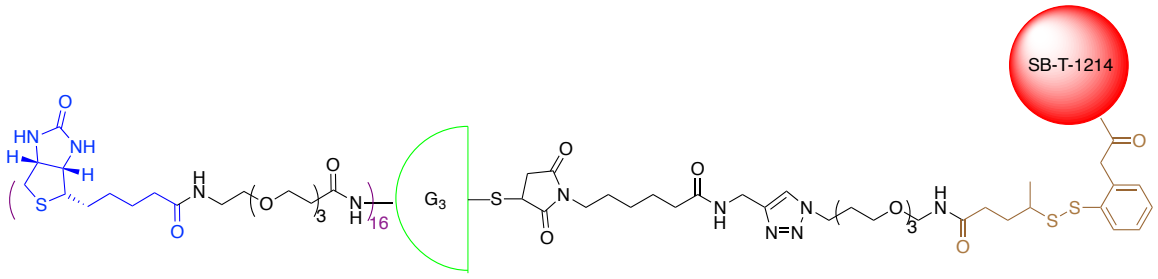

Figure 23. Designed structure of (PAMAM dendrimer)-based biotin-taxoid conjugate

Generation 3 (G3) PAMAM dendrimer (**Figure 24**), which has 32 primary amines on the surface of cystamine core, was used as the vehicle for the conjugate. The star-burst G3 dendrimer was reduced to half dendron and was connected to 16 biotin molecules. Each biotin molecule was coupled with one amine group on the surface of the half

dendron. Sceond-generation taxoid SB-T-1214, a potent antitumor activity drug against certain drug sensitive cell line and drug resistant cell line, was selected as the cytotoxic agent in the conjugate. A bifuctional maleimido-alkyne space was employed to connect targeting moiety by feasible 1,4-Michael addition and cytotoxic moiety by "Click" reaction.

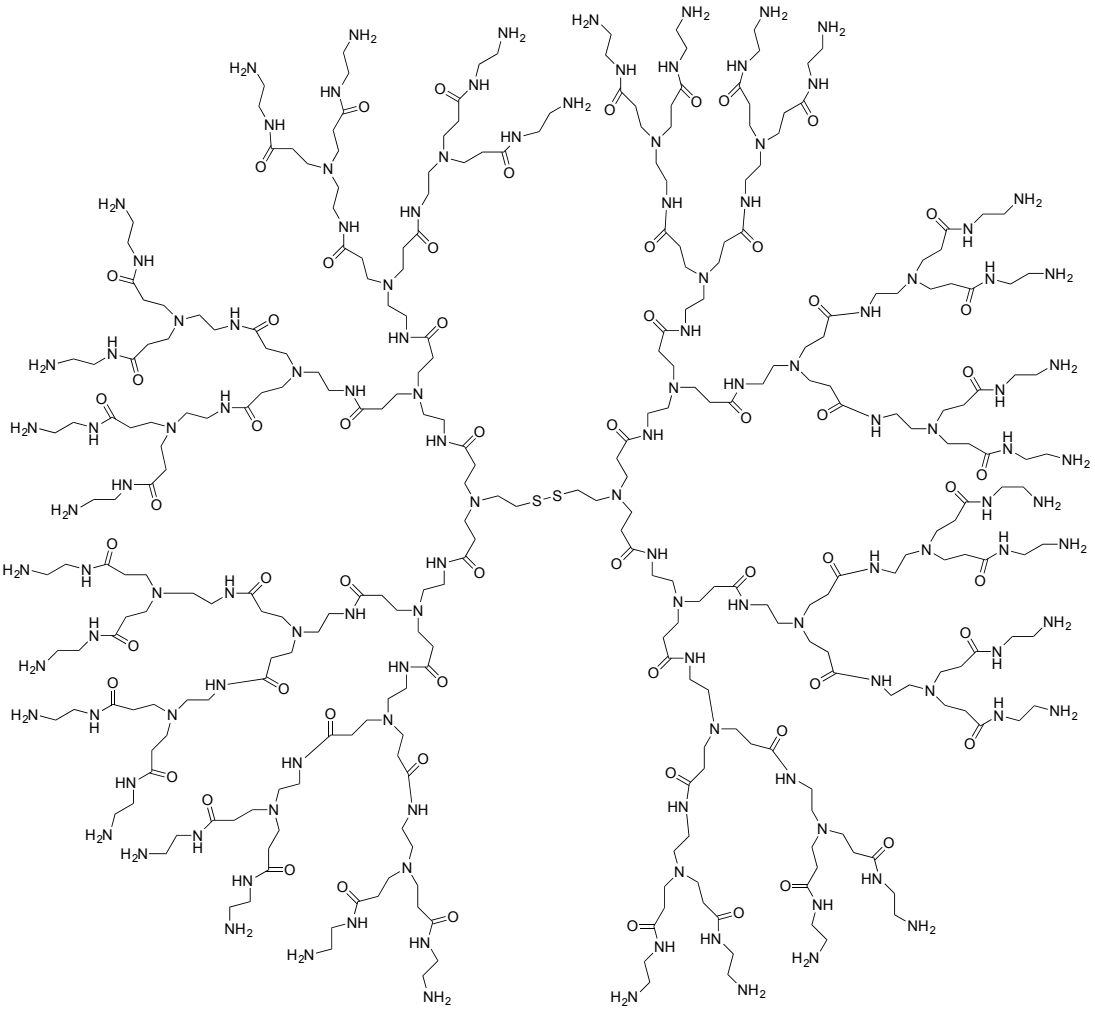

Figure 24. Chemical Structure of (G3 PAMAM)-dendrimer

§ 2.5.1 Synthesis of Biotin-PEG$_3$-(G3 PAMAM)-Dendrimer

The synthesis of functionalized G3 dendrimer begins with mono protection of commercial available triethylene glycol (**Scheme 17**). This is a Michael addition, and triethylene glycol is used in great excess to ensure mono protection is favored over di-protection. Also, *tert*-butyl acrylate should be added very slowly to favor the mono-protected product. Desired product *tert*-butyl 12-hydroxy-4,7,10-trioxadodecanoate **2-1** was obtained in 23% yield.

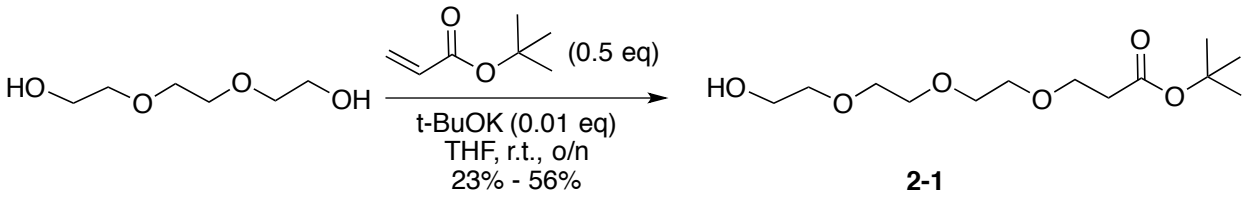

Scheme 17. Mono-protection of triethylene glycol

The hydroxyl group of **2-1** was converted to azide functional group by a two-step sequence to give *tert*-butyl 12-azido-4,7,10-trioxadocecanoate **2-2** in 44%/59% yield (**Scheme 18**) over two steps. After the first step, the pH of reaction mixture needed to be adjusted to 8 to prevent the formation of the explosive hydrazoic acid.

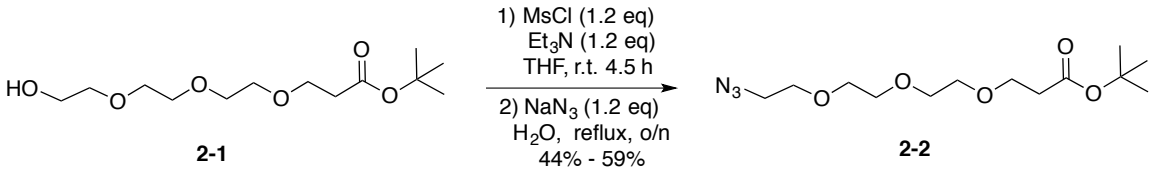

Scheme 18. Hydroxyl group was converted to azide group

The azide functional group was then reduced to primary amine group by Staudinger reaction (**Scheme 19**). Two equivalents of triphenylphosphine were employed to convert the azide group to amine group, yielding triphenylphosine oxide as the side product. The crude product was directly used in the next step after extraction with small amount of toluene.

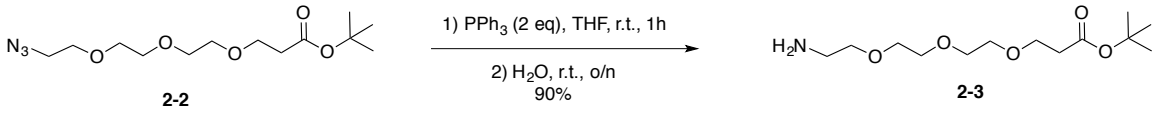

Scheme 19. Azide group was reduced to amine group by the Staudinger reaction

In addition, biotin was activated by NHS *via* DIC coupling. The reaction was conducted in 45 ˚C due to the poor solubility of biotin. The desired product **2-4** was obtained in 71% yield after purification by column chromatography.

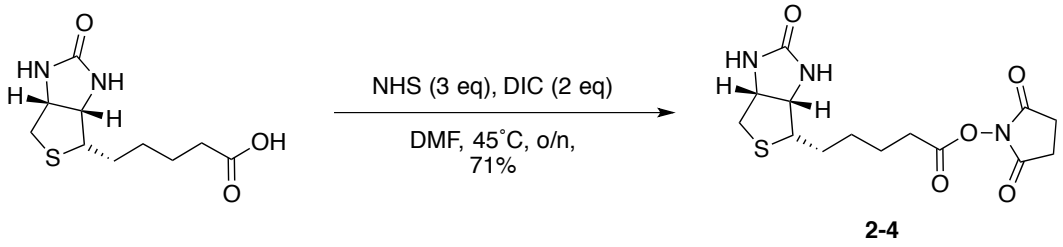

Scheme 20. Biotin was activated *via* DIC coupling to afford biotin-OSu

The activated biotin ester **2-4** was then reacted with PEG derivative tert-butyl-12-amino-4,7,10-trioxadodecanoate **2-3** to generate biotin-PEG conjugate **2-5**

in 70% yield after purification *via* column chromatography(**Scheme 21**). NHS was regenerated as the reaction's side product.

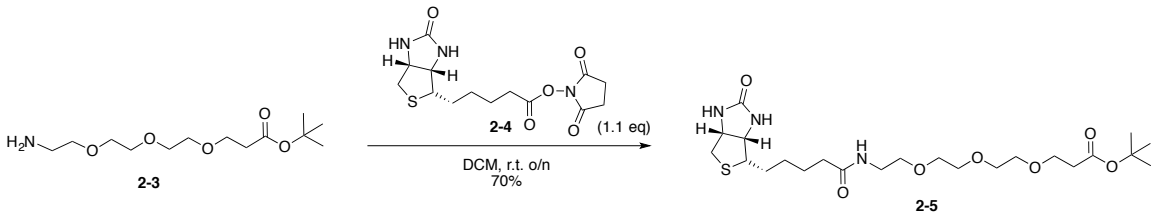

Scheme 21. Biotin-$(PEG)_3$ conjugate was generated

The resulting conjugate **2-5** was then treated with trifluoroacetic acid (TFA) in DCM to give **2-6** as a solid (**Scheme 22**). The ratio of TFA to DCM was 1:4. Upon completion, the concentrated reaction mixture was set under vacuum to remove excess TFA. The product was directly used in the next step without further purification.

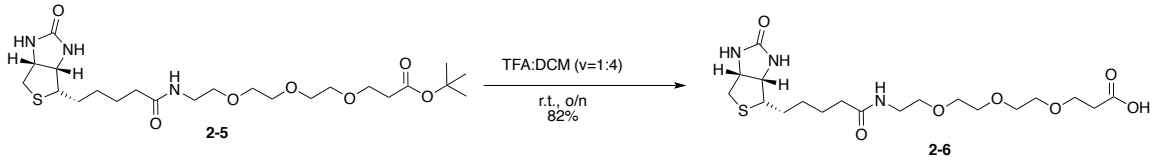

Scheme 22. *Tert*-butyl ester was deprotected by TFA

The resulting **2-6** was then reacted by NHS *via* DIC coupling to afford activated ester **2-7**. The reaction was conducted in room temperature in DCM. The crude product was purified by column chromatography to afford pure product in 68%/82% yield as a solid (**Scheme 23**).

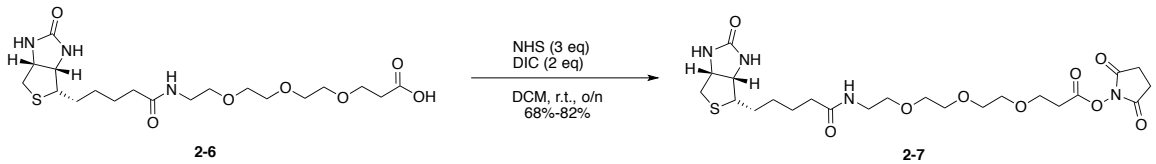

Scheme 23. Synthesis of biotin-$(PEG)_3$-OSu conjugate

The activated ester was then reacted with G3 PAMAM dendrimer with cystamine core to generate functionalied G3 dendrimer (**Scheme 24**). 32 primary amine groups on the surface of the dendrimer were converted to amide bond. The amount of biotin-PEG-OSu conjugates added to the dendrimer was determined based on the number of the primary amine group on the surface of dendrimer. The reaction was done in methanol and excess amount of **2-7** was converted to methyl ester. Once complete, the reaction mixture was purified by dialysis in methanol using MWCO 6000-8000 membrane to remove side products. The molecular weight of the compound was determined by MALDI-TOF using 2,5-dihydroxybenzoic acid (DHB) as matrix (**Figure 25**). The observed peak 20786.1 was assigned to expected product. The highest peak 10385.9 corresponded cleaved half dendron formed during the MALDI measurement. It indicated the fully functionalized product was generated successfully in good quality.

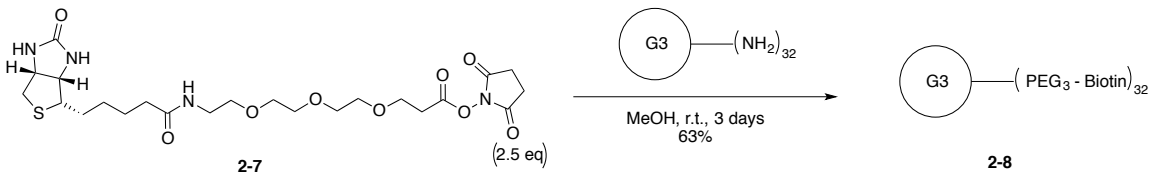

Scheme 24. Fully functionalization with PEGylated biotin on generation 3 PAMAM dendrimer

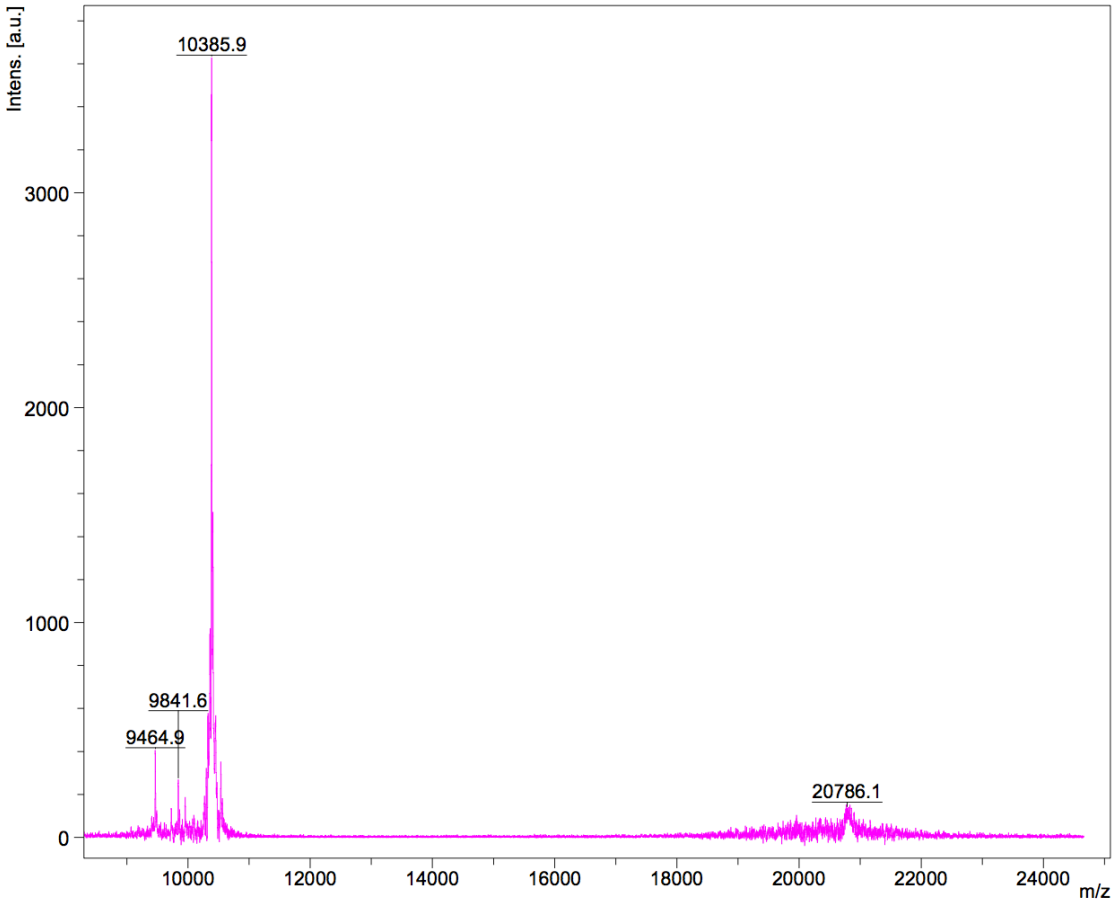

Figure 25. MALDI-TOF Result of Fully Functionalized PAMAM G3 Dendrimer

§2.5.2 Synthesis of (PAMAM-Dendrimer)-Based Biotin-Taxoid Conjugate

The disulfide bond inside the biotin-$(PEG)_3$-(G3 PAMAM)-denderimer **2-8** was then cleaved by tris(2-carboxyethyl)phosphine (TCEP). The resulting half dendron was directly connected to bifunctional maleimido-alkyne spacer to afford biotin-$(PEG)_3$-G3-alkyne conjugate **2-9** (**Scheme 25**). The product was characterized by MALDI-TOF using 2,5-dihydroxybenzoic acid (DHB) as matrix (**Figure 26**). The highest ionic peak 10654.4 was corresponded the product. By FIA mass analysis, this

peak gave 1328.6 $(M+8H^+)^{8+}/8$, 1181.2 $(M+9H^+)^{9+}/9$ and 1063.1 $(M+10H^+)^{10+}/10$ which could be deconvoluted to the designed mass number 10622.38. These results indicated that the expected product biotin-$(PEG)_3$-G3-alkyne conjugate was synthesized successfully.

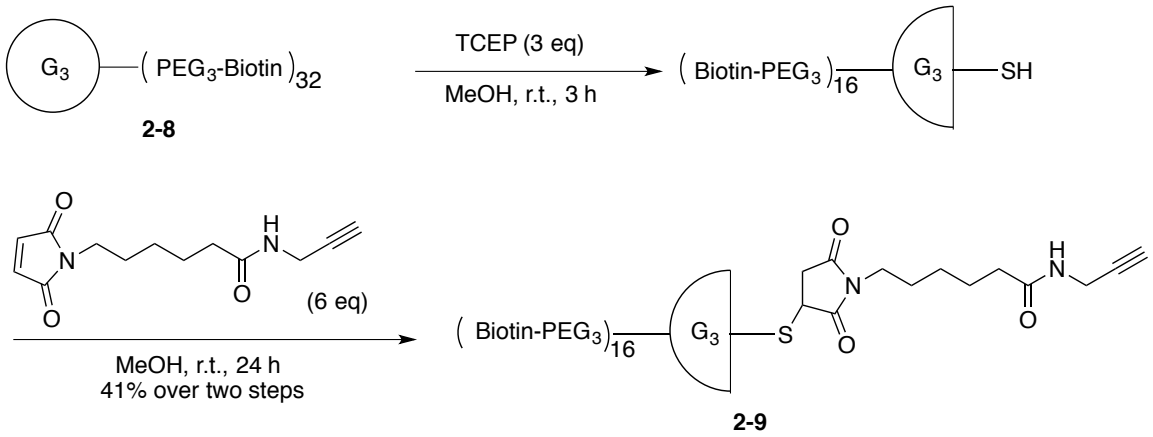

Scheme 25. Synthesis of biotin-$(PEG)_3$-G3-alkyne conjugate

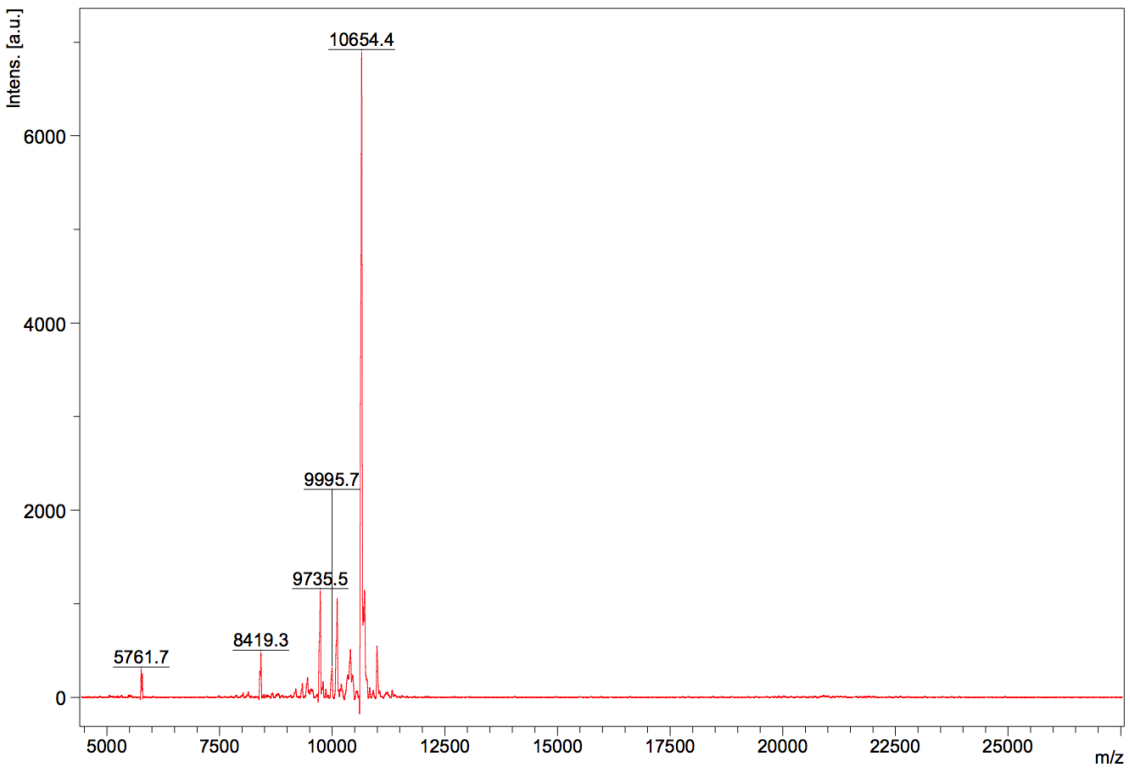

Figure 26. MALDI-TOF Result of Biotin-$(PEG)_3$-G3-Alkyne Conjugate

The resulting "click-ready" dendrimer scaffold **2-9** bearing 16 PEGlated biotin arms was then react with azide-$(PEG)_3$-drug conjugate by click reaction to afford the (PAMAM-G3)-Dendrimer-based biotin-taxoid conjugate (**Scheme 26**). The purification of target molecule was conducted by preparative HPLC *via* Jupiter C18 column. Solvents were water with 0.1% TFA (solvent A) and acetonitrile with 0.1% TFA (solvent B). The impurities and defect derivatives were removed and the product was obtained as a single component. The formation of the final compound was confirmed by FIA mass spectrometry which showed 1495.8 $(M+8H^+)^{8+}/8$, 1329.8 $(M+9H^+)^{9+}/9$.

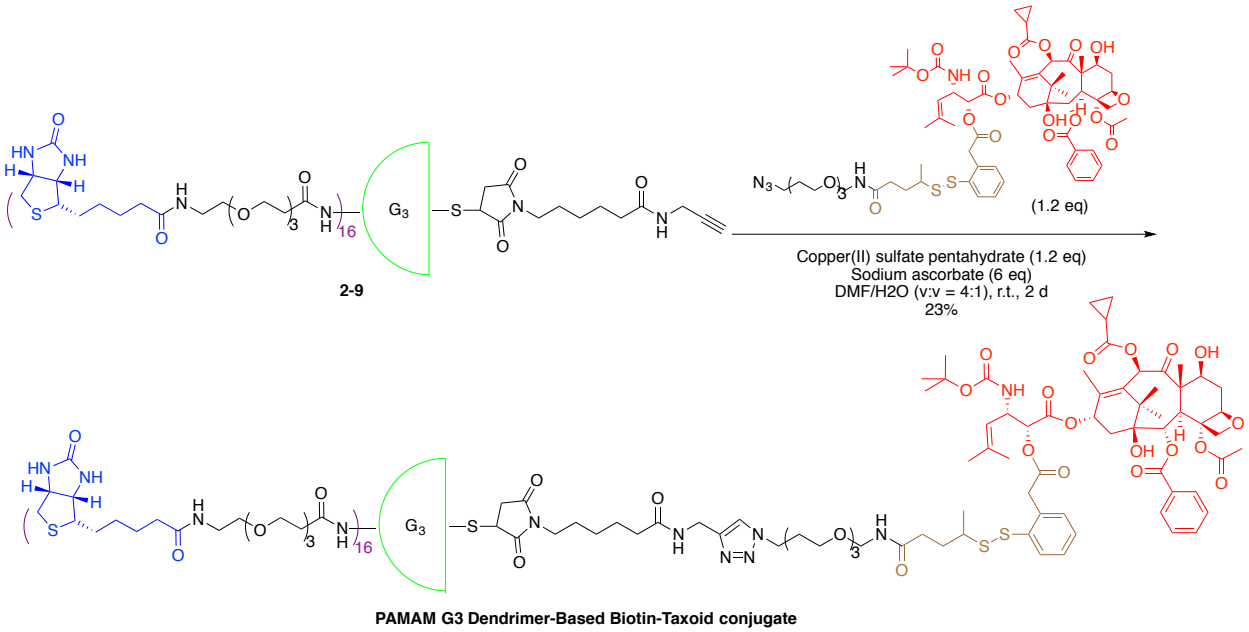

Scheme 26. Synthesis of (PAMAM G3)-(dendrimer-based) biotin-taxoid conjugate

§ 2.6.1 Design and Synthesis of Asymmetric Bow-Tie Dendrimer-based (ABTD) conjugate for Tumor-Targeting Drug Delivery

Apart from PAMAM G3 dendrimer-based biotin-taxoid conjugate, an asymmetric bow-tie dendrimer-based (ABTD) conjugate was also designed for tumor-targeting drug delivery. The structure of ABTD conjugate was illustrated in Figure 26. This asymmetric multi-functionalized dendrimer conjugate contains 3 components: a G3 PAMAM half dendron functionalized by biotin as targeting moiety, a G1 PAMAM half dendron functionalized by second generation taxoid SB-T-1214 as cytotoxic agent and a bis(maleimido) linker to conncet the two half dendrons. The surface of the asymmetric bow-tie dendrimer could be coupled with 16 targeting molecules and 4 cytotoxic agents within one conjugate, greatly increasing the payload of drug and its internalization

efficiency. PEG chains are inserted between biotin and G3 dendrimer, and also between cytotoxic agent and G1 dendrimer to increase the solubility of the conjugate.

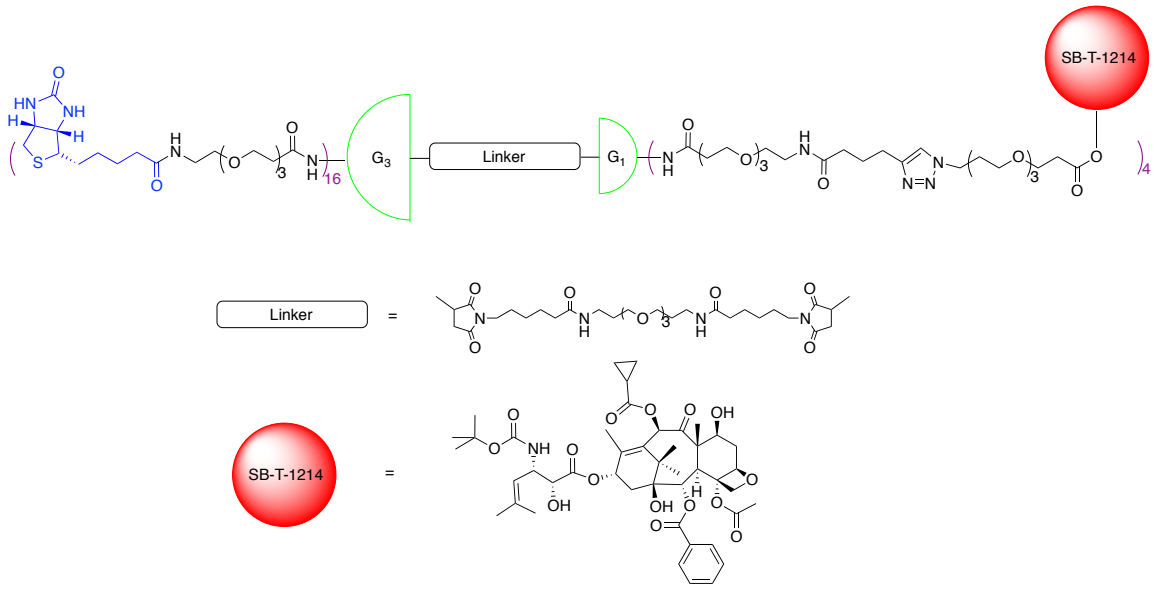

Figure 27. The Designed ABTD conjugate for tumor targeting drug delivery

§ 2.6.1 Synthesis of PAMAM G1 Dendrimer-Alkyne Conjugate

The 4-pentynoic acid was treated with **2-3** to give **2-10** as a colorless liquid in 65% crude yield (**Scheme 27**). This is a DIC coupling and DIU was produced as a side product. The product was directly used in the next step.

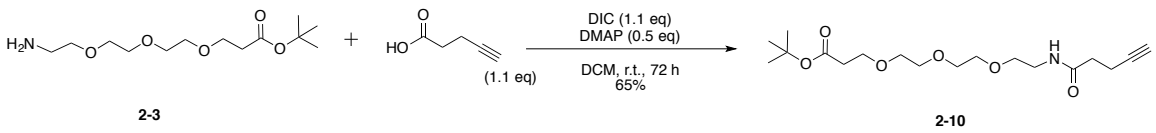

Scheme 27. Synthesis of $(PEG)_3$-alkyne conjugate

Then, deprotection of tert-butyl group was conducted by using TFA to afford 2-11 in 57% yield (**Scheme 28**), followed by activation by employing NHS *via* DIC coupling to form its activated ester 2-12 in 71% yield (**Scheme 29**).

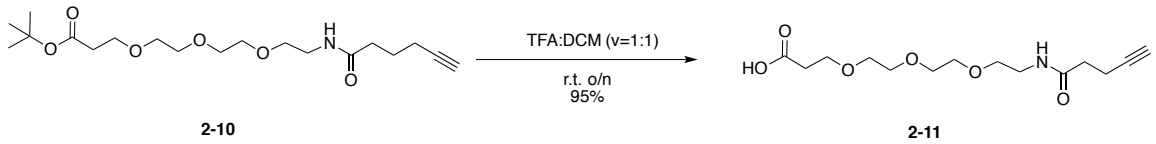

2-10 2-11

Scheme 28. Deprotection of *tert*-butyl group to afford 2-11

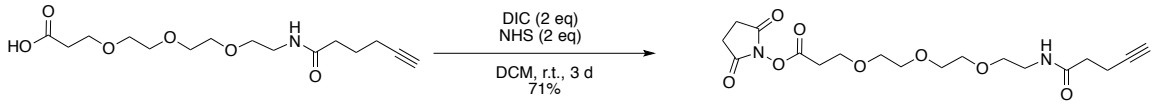

2-11 2-12

Scheme 29. Synthesis of alkyne-$(PEG)_3$ activated ester

The resulting 2-12 was then reacted with (G1 PAMAM)-dendrimer bearing cystamine core (**Scheme 30**). Eight primary amine groups on the surface of the G1 dendrimer were converted to amide bonds. The amount of alkyne-PEG-OSu conjugates added to the dendrimer was determined based on the number of the primary amine group on the surface of dendrimer. The molecular weight of the compound was determined by MALDI-TOF using 2,5-dihydroxybenzoic acid (DHB) as matrix (**Figure 28**). The observed peak 3789.343 was assigned to expected product. By FIA mass analysis, this peak gave 1263.4 $(M+3H^+)^{3+}/3$, 947.9 $(M+4H^+)^{4+}/4$, 758.5 $(M+5H^+)^{5+}/5$ and 632.3 $(M+6H^+)^{6+}/6$ which could be deconvoluted to the designed mass number 3788.13. It indicated the fully functionalized product was generated successfully in good quality.

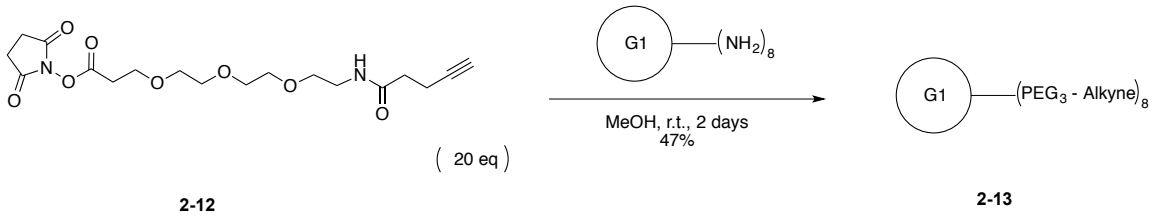

2-12 2-13

Scheme 30. Synthesis of functonalized G1-alkyne conjugate

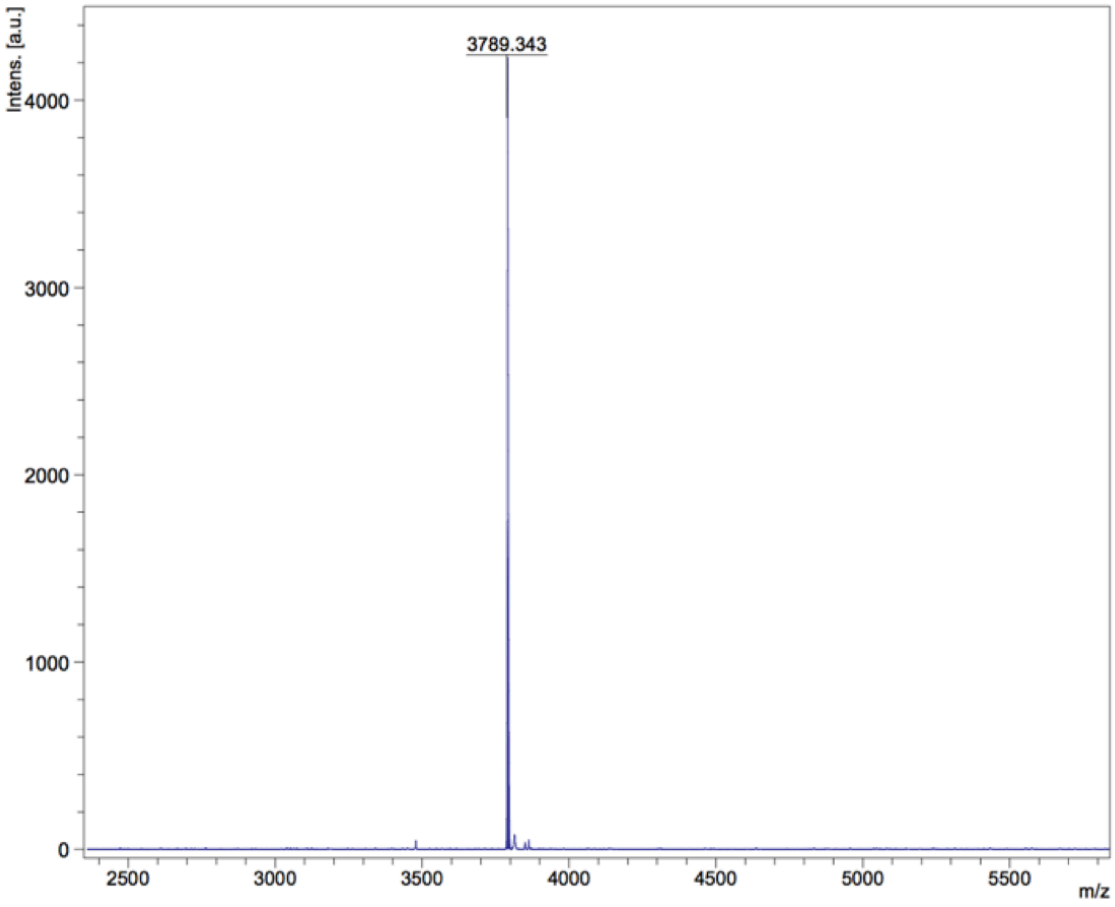

Figure 28. MALDI-TOF result of fully functionalized (G1 PAMAM)-dendrimer

§ 2.6.2 Synthesis of ABTD Conjugate

The disulfide bond inside the biotin-$(PEG)_3$-(G1 PAMAM)-denderimer **2-13** was then reduced by TCEP. The resulting half dendron was directly connected to bis(maleimido) linker to afford Alkyne-G1-linker conjugate **2-14** (**Scheme 31**). The product was purified by preparative HPLC using C18 column. The product was characterized by MALDI-TOF using 2,5-dihydroxybenzoic acid (DHB) as matrix (**Figure 29**). The highest ionic peak 2502.496 corresponded to the product. By FIA mass analysis, this peak gave 1251.8 $(M+2H^+)^{2+}/2$, 834.8 $(M+3H^+)^{3+}/3$ and 626.3 $(M+4H^+)^{4+}/4$ which could be deconvoluted to the designed mass number 3788.13. These results indicated that the expected product biotin-$(PEG)_3$-G3-alkyne conjugate was synthesized successfully.

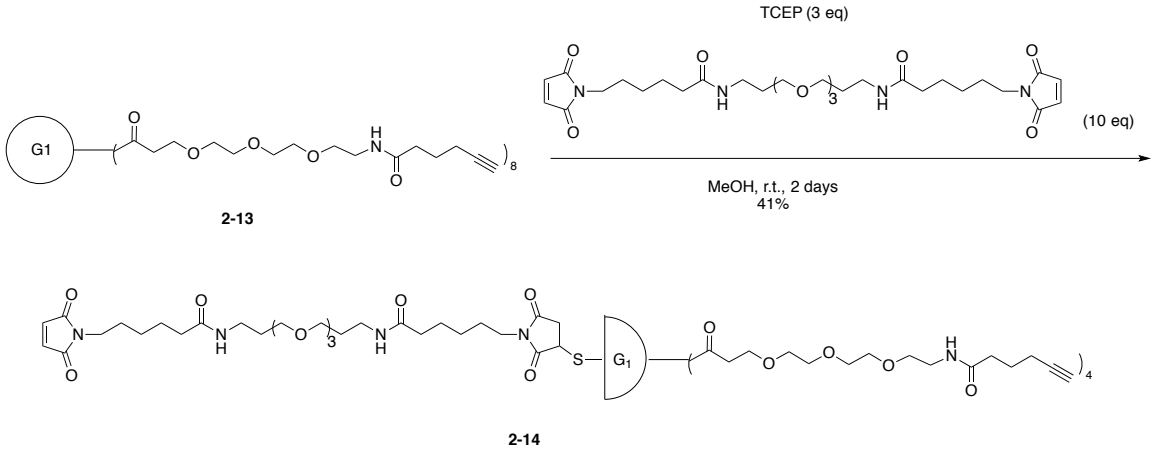

Scheme 31. Synthesis of alkyne-G1-linker conjugate

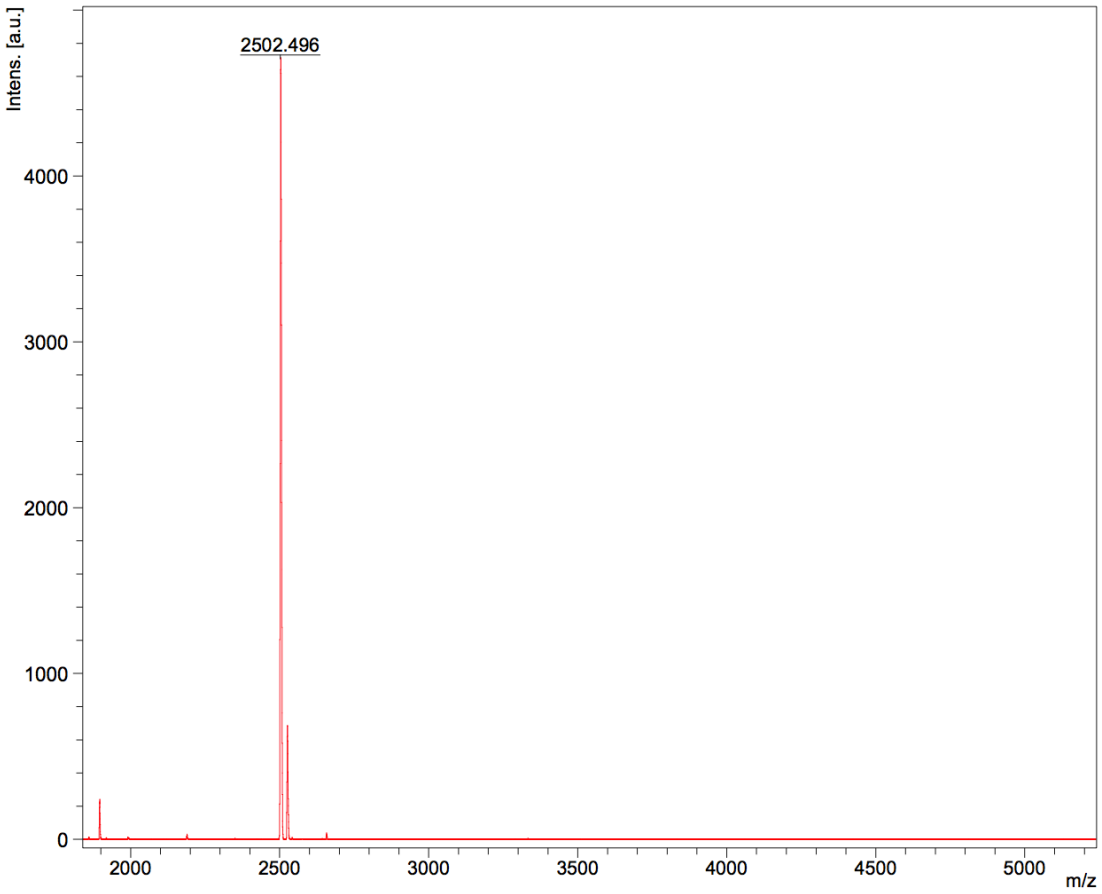

Figure 29. MALDI-TOF result of alkyne-G1-linker conjugate

To construct the "click-ready" intermediate bearing four PEGlated terminal alkyne arms and sixteen PEGlated biotin arms, biotin functionalized G3 PAMAM dendrimer **2-8** was cleaved into two half dendrons by TCEP first. The resulting half dendron was then reacted with **2-14** to generate designed bow-tie scaffold **2-15** which is used for further click reaction (**Scheme 32**). Purification of **2-15** was conducted by preparative HPLC employing ^{18}C column. The impurities and defect derivatives were removed successfully. The isolated pure product was characterized by MALDI-TOF mass spectrometry (**Figure 30**). The highest ionic peak 12878.026 corresponded to the product.

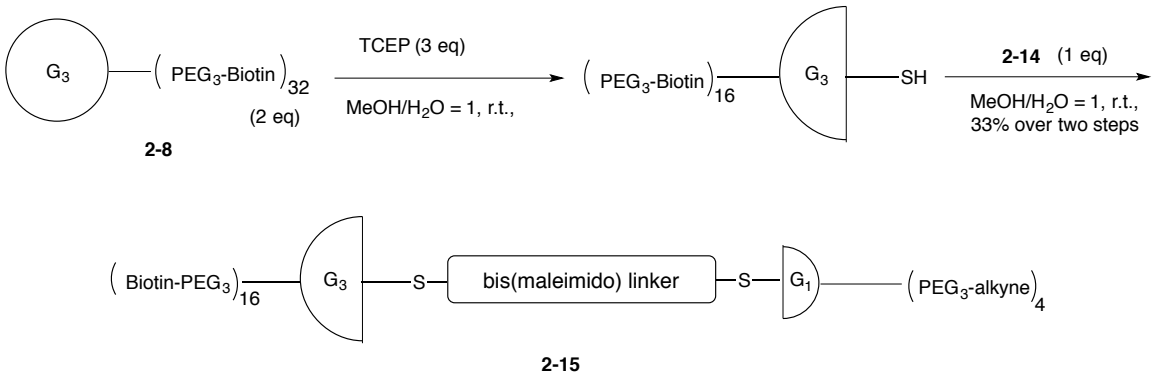

Scheme 32. Synthesis of "click-ready" intermediate for ABTD conjugate

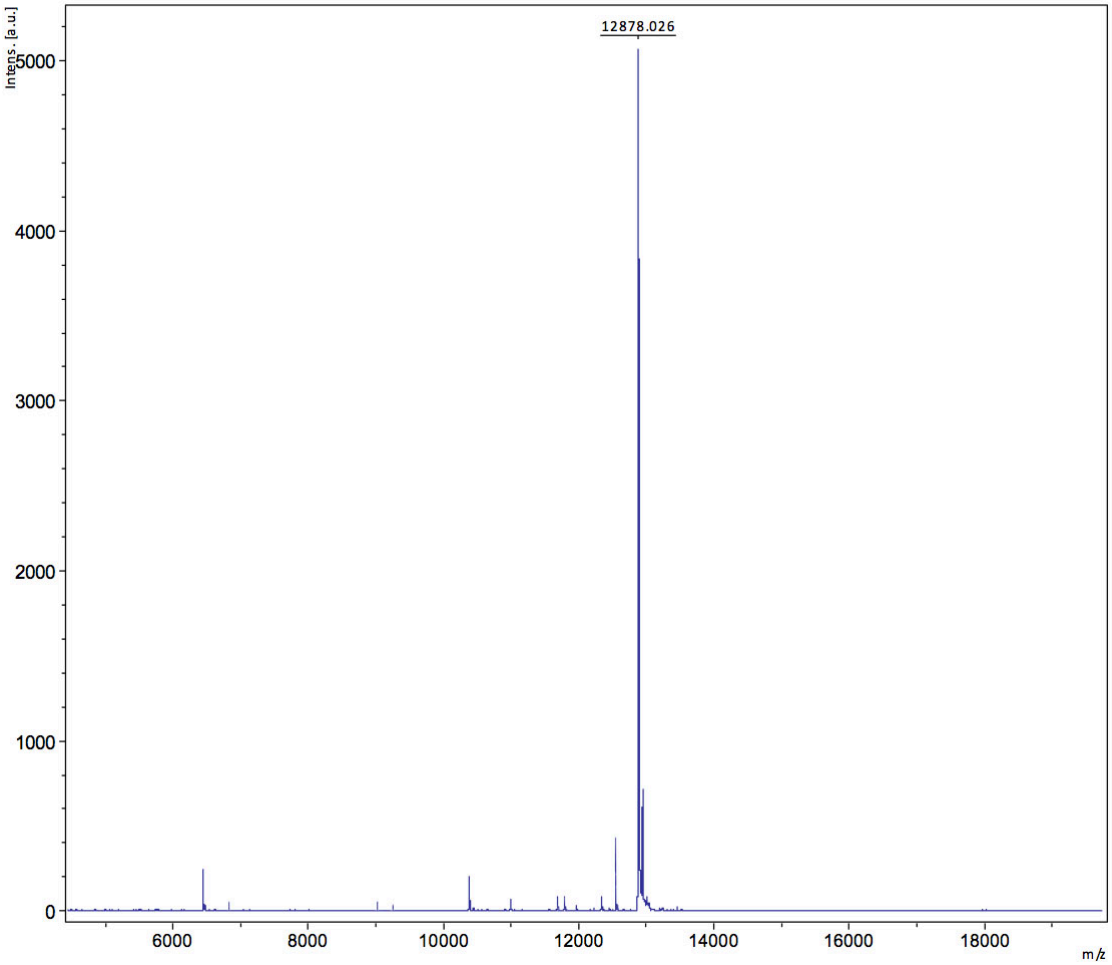

Figure 30. MALDI-TOF result of (G1 half Dendron)-linker-(G3 half Dendron) construct

§ 2.7 Conclusion

Dendrimers, well-defined three-dimensional macromolecules, are considered attractive platforms for tumor-targeting drug delivery. Two dendrimer-based tumor-targeting drug delivery conjugates, biotin-G3-linker-SB-T-1214 conjugate and biotin-G3-linker-G1-SB-T-1214 were designed and synthesized. Biotin was selected as tumor targeting moiety and new-generation taxoid SB-T-1214 was employed as anti-cancer agent. Further studies include the "click reaction" of **2-15** and azide-PEG-SB-T-1214 and the biological evaluation of dendrimer-based conjugates.

§ 2.8.1 General Methods

^{1}H NMR and ^{13}C NMR data were obtained on a Bruker 300, 400, 500 or 700 MHz NMR spectrometer. Chemical shifts(δ) are reported in ppm and standardized with solvent as internal standard based on literature reported values. FIA mass analysis was conducted on an Agilent LC-UV-TOF mass spectrometer at the Institute of Chemical Biology and Drug Discovery (ICBDD), Stony Brook, NY. TLC analyses were performed on Merck DC- alufolien with Kieselgel 60F-254 and were visualized with UV light, sulfuric acid-EtOH, 10 % PMA-EtOH or 10 % Vanillin-EtOH with 1% sulfuric acid. Column chromatography was carried out on silica gel 60 (Merck, 230-400 mesh ASTM) with hexanes-ethyl acetate solvent system or dichloromethane-methanol solvent system.

§ 1.8.2 Materials

The chemicals were purchased from Sigma-Aldrich Company, Fisher Scientific Company and VWR International Company. 10-Deacetylbaccatin III (10-DAB) was donated by Indena, SpA, Italy. Tetrohydrofuran was distilled from sodium and benzophenone under nitrogen. Dichloromethane was distilled from calcium hydride under nitrogen.

§ 1.8.3 Experimental Procedure

tert-Butyl 12-hydroxy-4,7,10-trioxadodecanoate (2-1)

To a cooled solution was added triethylene glycol (15.0 g) and potassium tert-butoxide (115mg) dissolve in THF (50 ml). A solution of tert-butyl acrylate (6.18 g) in 50 mL dry THF was then slowly added to the mixture *via* syringe pump within 2.5 h. Upon completion, the solvent was evacuated, and the crude mixture was purified by column chromatography on silica gel with increasing amounts of eluent (hexanes:ethyl acetate) to give product 3.01 g as colorless oil in 23 % yield. The product was characterized by 1H NMR. 1H NMR (400 MHz, CDCl3): δ 1.32 (s, 9H), 2.38 (t, J = 6.5 Hz, 2H), 3.50 (m, 10H), 3.58 (m, 4H). All data are in agreement with literature values.[70]

tert-Butyl 12-azido-4,7,10-trioxadocecanoate (2-2)

To a cooled solution of 3-1 (500 mg; 1.91 g), methanesulfonyl chloride (244 mg; 937 mg)

dissolved in THF (3 mL;8 mL). Then triethylamine (0.26 g; 0.83 g) was added dropwise. White precipitate came out immediately. The reaction mixture was allowed to slowly warm to room temperature and stir at room temperature overnight. Upon completion, the white precipitate was removed by vaccum filtration and washed with ether. The filtrate was concentrated to remove solvent to afford pale yellow oil. The resulting oil was diluted with 15 mL distilled water and cooled to 0 °C. Sodium bicarbonate was added to adjust the pH of the mixture to 8-9. Then sodium azide (140 mg; 531 mg) was added and the resulting solution was heated up to reflux at 100 °C overnight. Upon completion, the reaction mixture was extract with ether (3 x 30 mL). The organic layer was collected, washed with brine (3 x 30 mL), dried over magnesium sulfate, and concentrated to afford crude product. Further purification was done by column chromatography on silica gel to give product 2-2 as a colorless oil in 44% / 59% yield. The product was characterized by ^{1}H NMR.^{1}HNMR (400 MHz, $CDCl_3$): δ 1.44 (s, 9H), 2.50 (t, J = 6.6 Hz, 2H), 3.38 (t, J = 5.1 Hz, 2H), 3.67 (m, 12H). All data are in agreement with literature values.[70]

***tert*-Butyl 12-amino-4,7,10-trioxadocecanoate (2-3)**

To a cooled solution was added *tert*-butyl 3-2 (1.46 g) dissolved in 50 mL THF and triphenylphosphine (2.42 g). The mixture was allowed to stir at room temperature for 1 h. Then 16 mL distilled water was added. Upon completion, the resulting solution was concentrated to remove THF. After THF was removed, white precipitate (mixture of

triphenylphosphine and triphenylphosphine oxide) slowly crushed out and was removed by vaccum filtration and washed with water. The filtrate was washed with benzene (3 x 30 mL) to remove triphenylphosphine oxide. The water layer was concentrated by rotavapor and water was further removed by freezer drier overnight to give 2-3 1.20 g in 90% yield. The product was characterized by ^{1}H NMR. ^{1}H NMR (400 MHz, $CDCl_3$): δ 1.44 (s, 9H), 2.50 (t, J = 6.6 Hz, 2H), 2.86 (t, J = 5.2 Hz, 2H), 3.50 (t, J = 6.5 Hz, 2H), 3.63 (m, 8H), 3.71 (t, J = 8.2 Hz, 2H). All data are in agreement with literature values.[70]

D-(+)-Biotinyloxysuccinimide(2-4)

To a 100 ml round-bottomed-flask was added D-(+)-biotin (1.00 g), N-hydroxysuccinimide (NHS) (1.41 g) was dissolved in DMF (20 ml). The mixture was first heated up to 70˚C to make sure all the materials were dissolved. And then the reaction mixture was set in 45˚C with stirring. Then *N*,*N*'-diisopropylcarbodiimide (DIC) (1.06 g) was slowly added. Upon completion, the reaction mixture was slowed cooled down to room temperature. Solid was crushed out and was separated by vaccum filtration. The filtration was concentrated and was purified by colomn chromatography to afford product 2-4 951 mg in 71% yield. The product was characterized by ^{1}H NMR. ^{1}H NMR (400 MHz, d^6-DMSO): δ 1.45 (m, 3H), 1.65 (m, 3H), 2.60 (s, 1H), 2.67 (t, J = 7.4 Hz, 2H), 2.84 (m, 5H), 3.11 (m, 1H), 4.15 (m ,1H), 4.30 (t, J = 7.6 Hz, 1H), 6.36 (s, 1H), 6.42 (s, 1H). All data are in agreement with literature values.[71]

tert-Butyl D-(+)-Biotinyl-4,7,10-trioxa-13-azaoctadecan-1-oate (2-5)

To a solution of 3-3 (1.46 g) in DCM (18 mL), was added Biotin-OSu activated ester 3-4 (951 mg), followed by another 18 mL DCM. The reaction mixture was allowed to stir at room temperature under inert condition for 2 days. The reaction was monitored by TLC and stained with DACA. Upon the reaction was completed, the solvent was evacuated and the crude was purified by column chromatography on silica gel with increasing amounts of eluent (DCM : methanol) to give product **2-5** 1.21 g as pale yellow sticky solid in 71 % yield. ^{1}H NMR (400 MHz, $CDCl_3$): δ 1.42 (s, 9H), 1.67 (m, 4H), 2.21 (t, J = 7.5 Hz, 2H), 2.47 (t, J = 6.5 Hz, 2H), 2.71 (m, 1H), 2.87 (m, 1H), 3.12 (m, 1H), 3.40 (m, 2H), 3.54 (t, J = 5.1 Hz, 2H), 3.60 (s, 8H), 3.69 (t, J = 6.5 Hz), 4.29 (m, 1H), 4.48 (m, 1H), 5.71 (s, 1H), 6.61 (s, 1H), 6.80 (m, 1H). All data are in agreement with literature values.[70]

D-(+)-Biotinyl-12-amino-4,7,10-trioxadocecanoyloxysuccinimide ester (2-7)

To a solution of biotin-PEG-carboxylic acid (100 mg/478 mg) and NHS (77 mg/ 368 mg) in DCM (6 mL/ 24 mL) was added DIC (0.10 ml/ 0.34 ml). The reaction mixture was allowed to stir at room temperature under inert condition for 2 days. The reaction was monitored by TLC and stained with DACA. Upon the reaction was completed, the solvent was evacuated and the crude was purified by column chromatography on silica

gel with increasing amounts of eluent (DCM : methanol) to give product **3-1** 82 mg/ 476 mg as a yellow sticky solid in 68%/82% yield. ^{1}H NMR (400 MHz, $CDCl_3$): δ 1.44 (m, 2H), 1.68 (m, 6H), 2.21 (m, 2H), 2.27 (m, 2H), 2.28 (br s, 3H), 2.90 (m, 2H), 3.14 (m, 1H), 3.43 (m, 2H), 3.48 (s, 1H), 3.56 (t, J = 4.9 Hz, 2H), 3.64 (m, 8H), 3.76 (t, J = 6.5 Hz, 1H), 3.85 (t, 6.3 Hz, 2H), 4.33 (m, 1H), 4.51 (t, J = 6.1 Hz, 1H), 4.34 (t, J = 4.6 Hz, 1H), 4.51 (t, 6.1 Hz, 1H), 5.16 (br s, 1H), 5.90 (br s, 1H), 6.49 (br s, 1H).

Fully functionalized (PAMAM-G3) dendrimer (2-8)

To a solution of **2-7** (850 mg) in MeOH (17 ml) was added PAMAM G3 dendrimer (137 mg). The reaction mixture was allowed to stir at room temperature for 2 days. Once completion, the reaction mixture was purified by dialysis in MeOH against MWCO 6000 to 8000 membrane for 3 days. The purified product was concentrated and dried under vaccum to afford 2-8 as a white solid in 63% yield. The product was characterized by MALDI-TOF mass spectrometry (observed mass 10385.9 and 20786.1; calculated mass 20746.1).

Biotin-$(PEG)_3$-(PAMAM G3)-dendrimer-alkyne conjugate (2-9)

To a solution of **2-8** (136 mg) dissolved in MeOH (2 ml) was added TCEP (0.5 M) (0.040 ml). The reaction mixture was allowed to stir at room temperature for 1 hr. Then, maleimido-alkyne (10 mg) dissolved in MeOH (1 ml) was added in the reaction mixture.

The reaction mixture was allowed to stir overnight. Once completion, the reaction mixture was concentrated and purified by preparative HPLC to afford pure product 2-9 as a white solid in 41% yield. MALDI-TOF-MS (observed mass 10654.4; calculated mass 10622.3) ESI-MS (observed ionic peaks 1328.6 $(M+8H^+)^{8+}/8$, 1181.2 $(M+9H^+)^{9+}/9$ and 1063.1 $(M+10H^+)^{10+}/10$).

PAMAM-(G3 dendrimer)-based biotin-SB-T-1214 conjugate

To a 5 ml r.b.f. was added Biotin PEGlated PAMAM G3 dendrimer-alkyne conjugate (2-9) (10 mg) and SB-T-1214-PEG3-azide (1.7 mg). The r.b.f. was purged with nitrogen and DMF (0.4 ml) was added to dissolve the mixture. After that, sodium ascorbate (1.5 mg) dissolved in 0.05 ml H_2O was added in the reaction mixture, followed by addition of copper sulfate pentahydrate (0.3 mg) dissolved in 0.05 ml H_2O. The reaction mixture was monitored by ESI-MS. Once completion, the reaction mixture was concentrated and purified by preparative HPLC to afford product brown solid in 23% yield. ESI-MS (observed ionic peaks 1495.8 $(M+8H^+)^{8+}/8$ and 1329.8 $(M+9H^+)^{9+}/9$).

***tert*-Butyl 14-oxo-4,7,10-trioxa-13-azaoctadec-17-yroate (2-10)**

To a 10 ml r.b.f. was added 4-pentynoic acid (760 mg) and DMAP (1.36 g) dissolved in 30 ml DCM, followed by addition of 2-3 (2.06 g). The reaction mixture was allowed to stir for 10 minutes. Then, DIC (1.7 ml) was added in the reaction mixture and was

allowed to react overnight. The reaction was monitored by TLC. Once completion, the solvent was evacuated to give product 2.57 g as colorless oil in 65 % yield. The reaction mixture was diluted with 10 ml H_2O, washed with DCM (3 x 20 ml) and H_2O (3 x 20 ml). The combined organic layer was concentrated and directly used in the next step without further purification. The product was characterized by ESI-MS. ESI-MS ($(M+H^+)^{+1}$ = 358.2).

14-Oxo-4,7,10-trioxa-13-azaoctadec-17-ynoic acid (2-11)

To a solution of 2-10 (1.68 g) dissolved in DCM (60 ml) was added TFA (6 ml). The reaction mixture was allowed to stir at room temperature overnight. Once completion, the solvent was evacuated, and the crude mixture was purified by column chromatography on silica gel with increasing amounts of eluent (DCM:methanol) to give product 1.34 g as colorless oil in 95 % yield. The product was characterized by ^{1}H NMR. ^{1}H NMR (500 MHz, $CDCl_3$): δ 2.01 (t, J = 2.7 Hz, 1H), 2.44 (m, 2H), 2.53 (m, 2H), 2.63 (t, J = 6.0 Hz, 2H), 3.48 (m, 3H), 3.59 (t, J = 5.3 Hz), 3.65 (m, 8H), 3.78 (t, J = 6.0 Hz, 2H), 6.54 (br s, 1H).

2,5-Dioxpyrrolidin-1-yl 14-oxo-4,7,10-trioxa-13-azaoctadec-17-ynoate (2-12)

To a solution of **2-11**(1.34 g) and NHS (616 mg) dissolved in DCM (30 ml) was added DIC (0.83 ml) dropwise. The reaction mixture was allowed to stir at room temperature overnight and monitored by TLC. Once completion, the solvent was evacuated, and the crude mixture was purified by column chromatography on silica gel with increasing amounts of eluent (DCM:methanol) to give product 1.26 g as colorless oil in 71% yield. The product was characterized by ^{1}H NMR. ^{1}H NMR (500 MHz, $CDCl_3$): δ 1.63 (br s, 2H), 2.02 (t, J = 2.7 Hz, 1H), 2.41 (m, 2H), 2.52 (m, 2H), 2.73 (m, 1H), 2.84 (br s, 3H), 2.91 (t, J = 6.4 Hz, 2H), 3.47 (m, 2H), 3.56 (t, J = 4.9 Hz, 2H), 3.64 (m, 6H), 3.85 (t, J = 6.4 Hz, 2H), 6.27 (br s, 6.27).

Fully functionalized (PAMAM G1)-dendrimer (2-13)

To a solution of 2-12 (973 mg) dissolved in MeOH (20 ml) was added PAMAM G1 dendrimer (210 mg). The reaction mixture was allowed to stir at room temperature for 2 days and monitored by ESI-MS. Once completion, the crude mixture was purified by dialysis in MeOH *via* MWCO 2000 for 3 days. The reaction mixture was concentrated and dried under vaccum to afford product in 47% yield as a colorless oil. The product was characterized by MALDI-TOF and ESI-MS. MALDI-TOF-MS (observed mass 3789.3; calculated mass 3788.6) ESI-MS (observed ionic peaks 1263.4 $(M+3H^{+})^{3+}/3$, 947.9 $(M+4H^{+})^{4+}/4$, 758.5 $(M+5H^{+})^{5+}/5$ and 632.3 $(M+6H^{+})^{6+}/6$).

Biotin-$(PEG)_3$-(PAMAM G1)-dendrimer-alkyne conjugate (2-14)

To a solution of 2-13 (160 mg) and bis(maleimido) linker (250 mg) dissolved in MeOH (24 ml) was added TCEP (0.40 ml) dropwise. The reaction mixture was allowed to stir at room temperature for 2 days and monitored by ESI-MS. Once completion, the crude reaction mixture was concentrated and purification was conducted by preparative HPLC to gave product as a colorless oil in 41% yield. MALDI-TOF-MS (observed mass 2502.5; calculated mass 2502.1) ESI-MS (observed ionic peaks 1251.8 $(M+2H^+)^{2+}/2$, 834.8 $(M+3H^+)^{3+}/3$ and 626.3 $(M+4H^+)^{4+}/4$).

(G1 half dendron)-linker-(G3 half dendron) (2-15)

To a solution of **2-8** (50 mg) and **2-14** (6 mg) dissolved in H_2O (4.8 ml) was added TCEP (0.027 ml) dropwise. The reaction mixture was allowed to stir at room temperature for 2 days and monitored by ESI-MS. Once completion, the crude reaction mixture was concentrated and purification was conducted by preparative HPLC to gave product as a white solid in 33% yield. MALDI-TOF-MS (observed mass 12878.0; calculated mass 12876.3)

Reference

1. American Cancer Society. Cancer Facts & Figures 2016. Atlanta: American Cancer Society; 2016.
2. Trichopoulos, D.; Li, F. P.; Hunter, D. J., What causes cancer? *Sci Am* **1996,** *275* (3), 80-87.
3. Hayat, M. J.; Howlader, N.; Reichman, M. E.; Edwards, B. K., Cancer statistics, trends, and multiple primary cancer analyses from the surveillance, epidemiology, and end results (SEER) program. *Oncologist* **2007,** *12* (1), 20-37.
4. American Cancer Society. Cancer Facts & Figures 2015. Atlanta: American Cancer Society; 2015.
5. Wall, M. E.; Wani, M. C.; Cook, C. E.; Palmer, K. H.; Mcphail, A. T.; Sim, G. A., Plant Antitumor Agents .I. Isolation and Structure of Camptothecin a Novel Alkaloidal Leukemia and Tumor Inhibitor from Camptotheca Acuminata. *J Am Chem Soc* **1966,** *88* (16), 3888-3890.
6. Wall, M. E.; Wani, M. C.; Taylor, H., Isolation and Chemical Characterization of Antitumor Agents from Plants. *Cancer Treat Rep* **1976,** *60* (8), 1011-1030.
7. Ojima, I.; Slater, J. C.; Michaud, E.; Kuduk, S. D.; Bounaud, P. Y.; Vrignaud, P.; Bissery, M. C.; Veith, J. M.; Pera, P.; Bernacki, R. J., Syntheses and structure-activity relationships of the second-generation antitumor taxoids: Exceptional activity against drug-resistant cancer cells. *J Med Chem* **1996,** *39* (20), 3889-3896.
8. Schiff, P. B.; Horwitz, S. B., Taxol Stabilizes Microtubules in Mouse Fibroblast Cells. *P Natl Acad Sci-Biol* **1980,** *77* (3), 1561-1565.
9. Morris, P. G.; Fornier, M. N., Microtubule Active Agents: Beyond the Taxane Frontier. *Clin Cancer Res* **2008,** *14* (22), 7167-7172.
10. Cragg, G. M.; Schepartz, S. A.; Suffness, M.; Grever, M. R., The Taxol Supply Crisis - New Nci Policies for Handling the Large-Scale Production of Novel Natural Product Anticancer and Anti-Hiv Agents. *J Nat Prod* **1993,** *56* (10), 1657-1668.
11. Denis, J. N.; Greene, A. E.; Guenard, D.; Guerittevoegelein, F.; Mangatal, L.; Potier, P., A Highly Efficient, Practical Approach to Natural Taxol. *J Am Chem Soc* **1988,** *110* (17), 5917-5919.

12. Chauviere, G.; Guenard, D.; Picot, F.; Senilh, V.; Potier, P., Structural-Analysis and Biochemical-Study of Isolated Products of the Yew - Taxus-Baccata L (Taxaceae). *Cr Acad Sci Ii* **1981,** *293* (7), 501-503.

13. Ojima, I.; Habus, I.; Zhao, M.; Zucco, M.; Park, Y. H.; Sun, C. M.; Brigaud, T., New and Efficient Approaches to the Semisynthesis of Taxol and Its C-13 Side-Chain Analogs by Means of Beta-Lactam Synthon Method. *Tetrahedron* **1992,** *48* (34), 6985-7012.

14. Ojima, I.; Komata, T.; Qiu, X. G., Asymmetric Alkylations of a Phenylalanylglycinate Equivalent - Novel Route to Dipeptides Bearing Alpha-Alkyl-Alpha-Amino Acid Residues. *J Am Chem Soc* **1990,** *112* (2), 770-774.

15. Szakacs, G.; Paterson, J. K.; Ludwig, J. A.; Booth-Genthe, C.; Gottesman, M. M., Targeting multidrug resistance in cancer. *Nat Rev Drug Discov* **2006,** *5* (3), 219-234.

16. Gottesman, M. M.; Pastan, I., Biochemistry of Multidrug-Resistance Mediated by the Multidrug Transporter. *Annu Rev Biochem* **1993,** *62*, 385-427.

17. Sorrentino, B. R., Gene therapy to protect haematopoietic cells from cytotoxic cancer drugs. *Nat Rev Cancer* **2002,** *2* (6), 431-441.

18. Orr, G. A.; Verdier-Pinard, P.; McDaid, H.; Horwitz, S. B., Mechanisms of Taxol resistance related to microtubules. *Oncogene* **2003,** *22* (47), 7280-7295.

19. Giannakakou, P.; Gussio, R.; Nogales, E.; Downing, K. H.; Zaharevitz, D.; Bollbuck, B.; Poy, G.; Sackett, D.; Nicolaou, K. C.; Fojo, T., A common pharmacophore for epothilone and taxanes: Molecular basis for drug resistance conferred by tubulin mutations in human cancer cells. *P Natl Acad Sci USA* **2000,** *97* (6), 2904-2909.

20. Lobo, N. A.; Shimono, Y.; Qian, D.; Clarke, M. F., The biology of cancer stem cells. *Annu Rev Cell Dev Bi* **2007,** *23*, 675-699.

21. Reya, T.; Morrison, S. J.; Clarke, M. F.; Weissman, I. L., Stem cells, cancer, and cancer stem cells. *Nature* **2001,** *414* (6859), 105-111.

22. Rowinsky, E. K., The development and clinical utility of the taxane class of antimicrotubule chemotherapy agents. *Annu Rev Med* **1997,** *48*, 353-374.

23. Ojima, I.; Chen, J.; Sun, L.; Borella, C. P.; Wang, T.; Miller, M. L.; Lin, S. N.; Geng, X. D.; Kuznetsova, L. R.; Qu, C. X.; Gallager, D.; Zhao, X. R.; Zanardi, I.; Xia, S. J.; Horwitz, S. B.; Mallen-St Clair, J.; Guerriero, J. L.; Bar-Sagi, D.; Veith, J. M.; Pera, P.; Bernacki, R. J., Design,

synthesis, and biological evaluation of new-generation taxoids. *J Med Chem* **2008,** *51* (11), 3203-3221.

24. Lin, S. N.; Inoue, T.; Borella, C.; Walsh, J. J.; Chakravarty, S.; Pera, P.; Bernacki, R. J.; Ojima, I., Design and structure-activity relationships study of taxoid-epothilone hybrids. *Abstr Pap Am Chem S* **1998,** *216*, U296-U296.

25. Holton, R. A.; Zhang, Z. M.; Clarke, P. A.; Nadizadeh, H.; Procter, D. J., Protection of the C(7) and C(10) hydroxyl groups in 10-deacetyl baccatin III. *Tetrahedron Lett* **1998,** *39* (19), 2883-2886.

26. Kingston, D. G. I., Recent advances in the chemistry of taxol. *J Nat Prod* **2000,** *63* (5), 726-734.

27. Vineberg, J. G., Design, synthesis, and biological evaluation of novel taxoid-based drug conjugates and theranostic imaging agents towards tumor-targeted chemotherapy. *phD thesis* **2014**.

28. Samaranayake, G.; Magri, N. F.; Jitrangsri, C.; Kingston, D. G. I., Modified Taxols .5. Reaction of Taxol with Electrophilic Reagents and Preparation of a Rearranged Taxol Derivative with Tubulin Assembly Activity. *J Org Chem* **1991,** *56* (17), 5114-5119.

29. Wahl, A.; Guerittevoegelein, F.; Guenard, D.; Legoff, M. T.; Potier, P., Rearrangement Reactions of Taxanes - Structural Modifications of 10-Deacetylbaccatin-Iii. *Tetrahedron* **1992,** *48* (34), 6965-6974.

30. Klein, L. L.; Maring, C. J.; Li, L. P.; Yeung, C. M.; Thomas, S. A.; Grampovnik, D. J.; Plattner, J. J.; Henry, R. F., Synthesis of Ring-B Rearranged Taxane Analogs. *J Org Chem* **1994,** *59* (9), 2370-2373.

31. Gunatilaka, A. A. L.; Ramdayal, F. D.; Sarragiotto, M. H.; Kingston, D. G. I.; Sackett, D. L.; Hamel, E., Synthesis and biological evaluation of novel paclitaxel (Taxol) D-ring modified analogues. *J Org Chem* **1999,** *64* (8), 2694-2703.

32. Dubois, J.; Thoret, S.; Gueritte, F.; Guenard, D., Synthesis of 5(20)deoxydocetaxel, a new active docetaxel analogue. *Tetrahedron Lett* **2000,** *41* (18), 3331-3334.

33. daCosta, M.; Rothenberg, S. P., Purification and characterization of folate binding proteins from rat placenta. *Bba-Protein Struct M* **1996,** *1292* (1), 23-30.

34. Lu, Y. J.; Low, P. S., Folate-mediated delivery of macromolecular anticancer therapeutic

agents. *Adv Drug Deliver Rev* **2002,** *54* (5), 675-693.

35. Chen, S. H.; Wei, J. M.; Long, B. H.; Fairchild, C. A.; Carboni, J.; Mamber, S. W.; Rose, W. C.; Johnston, K.; Casazza, A. M.; Kadow, J. F.; Farina, V.; Vyas, D. M.; Doyle, T. W., Novel C-4 Paclitaxel (Taxol(R)) Analogs - Potent Antitumor Agents. *Bioorganic & medicinal chemistry letters* **1995,** *5* (22), 2741-2746.

36. Chen, S. H.; Kadow, J. F.; Farina, V.; Fairchild, C. R.; Johnston, K. A., First Syntheses of Novel Paclitaxel(Taxol) Analogs Modified at the C4-Position. *J Org Chem* **1994,** *59* (21), 6156-6158.

37. Chen, S. H.; Kant, J.; Mamber, S. W.; Roth, G. P.; Wei, J. M.; Marshall, D.; Vyas, D. M.; Farina, V.; Casazza, A.; Long, B. H.; Rose, W. C.; Johnston, K.; Fairchild, C., Taxol(R) Structure-Activity-Relationships - Synthesis and Biological Evaluation of Taxol Analogs Modified at C-7. *Bioorganic & medicinal chemistry letters* **1994,** *4* (18), 2223-2228.

38. Ojima, I.; Wang, T.; Miller, M. L.; Lin, S. N.; Borella, C. P.; Geng, X. D.; Pera, P.; Bernacki, R. J., Synthesis and structure-activity relationships of new second-generation taxoids. *Bioorganic & medicinal chemistry letters* **1999,** *9* (24), 3423-3428.

39. Kingston, D. G.; Jagtap, P. G.; Yuan, H.; Samala, L., The chemistry of taxol and related taxoids. *Fortschr Chem Org Naturst* **2002,** *84*, 53-225.

40. Georg, G. I.; Harriman, G. C. B.; Vandervelde, D. G.; Boge, T. C.; Cheruvallath, Z. S.; Datta, A.; Hepperle, M.; Park, H.; Himes, R. H.; Jayasinghe, L., Medicinal Chemistry of Paclitaxel - Chemistry, Structure-Activity-Relationships, and Conformational-Analysis. *Acs Sym Ser* **1995,** *583*, 217-232.

41. Geney, R.; Simmerling, C.; Ojima, I., Computational analysis of the paclitaxel binding site in alpha-tubulin. *Abstr Pap Am Chem S* **2001,** *222*, U650-U650.

42. Ojima, I.; Lin, S. N.; Wang, T., Recent advances in the medicinal chemistry of taxoids with novel beta-amino acid side chains. *Current medicinal chemistry* **1999,** *6* (10), 927-954.

43. Ueda, Y.; Mikkilineni, A. B.; Knipe, J. O.; Rose, W. C.; Casazza, A. M.; Vyas, D. M., Novel Water-Soluble Phosphate Prodrugs of Taxol(R) Possessing in-Vivo Antitumor-Activity. *Bioorganic & medicinal chemistry letters* **1993,** *3* (8), 1761-1766.

44. Ojima, I.; Slater, J. C.; Kuduk, S. D.; Takeuchi, C. S.; Gimi, R. H.; Sun, C. M.; Park, Y. H.; Pera, P.; Veith, J. M.; Bernacki, R. J., Syntheses and structure-activity relationships of taxoids

derived from 14 beta-hydroxy-10-deacetylbaccatin III. *J Med Chem* **1997,** *40* (3), 267-278.

45. Ojima, I.; Lin, S. N., Efficient asymmetric syntheses of beta-Lactams bearing a cyclopropane or an epoxide moiety and their application to the syntheses of novel isoserines and taxoids. *J Org Chem* **1998,** *63* (2), 224-225.

46. Ojima, I.; Fenoglio, I.; Park, Y. H.; Pera, P.; Bernacki, R. J., Synthesis and Biological-Activity of 14-Hydroxydocetaxel. *Bioorganic & medicinal chemistry letters* **1994,** *4* (13), 1571-1576.

47. Ojima, I.; Duclos, O.; Zucco, M.; Bissery, M. C.; Combeau, C.; Vrignaud, P.; Riou, J. F.; Lavelle, F., Synthesis and Structure-Activity-Relationships of New Antitumor Taxoids - Effects of Cyclohexyl Substitution at the C-3' and/or C-2 of Taxotere (Docetaxel). *J Med Chem* **1994,** *37* (16), 2602-2608.

48. Ojima, I.; Park, Y. H.; Sun, C. M.; Brigaud, T.; Zhao, M. Z., New and Efficient Routes to Norstatine and Its Analogs with High Enantiomeric Purity by Beta-Lactam Synthon Method. *Tetrahedron Lett* **1992,** *33* (39), 5737-5740.

49. Whitesell, J. K.; Lawrence, R. M., Practical Enzymatic Resolution of Chiral Auxiliaries - Enantiomerically Pure Trans-2-Phenylcyclohexanol and Trans-2-(Alpha-Cumyl)Cyclohexanol. *Chimia* **1986,** *40* (9), 318-321.

50. Jacobsen, E. N.; Marko, I.; Mungall, W. S.; Schroder, G.; Sharpless, K. B., Asymmetric Dihydroxylation Via Ligand-Accelerated Catalysis. *J Am Chem Soc* **1988,** *110* (6), 1968-1970.

51. Kolb, H. C.; Vannieuwenhze, M. S.; Sharpless, K. B., Catalytic Asymmetric Dihydroxylation. *Chem Rev* **1994,** *94* (8), 2483-2547.

52. Ojima, I.; Sun, C. M.; Zucco, M.; Park, Y. H.; Duclos, O.; Kuduk, S., A Highly Efficient Route to Taxotere(R) by the Beta-Lactam Synthon Method. *Abstr Pap Am Chem S* **1993,** *206*, 130-MEDI.

53. Yu, H. W.; Ballard, C. E.; Boyle, P. D.; Wang, B. H., An inexpensive carbohydrate derivative used as a chiral auxiliary in the synthesis of alpha-hydroxy carboxylic acids. *Tetrahedron* **2002,** *58* (38), 7663-7679.

54. Schonberg, S. A.; Lundemo, A. G.; Fladvad, T.; Holmgren, K.; Bremseth, H.; Nilsen, A.; Gederaas, O.; Tvedt, K. E.; Egeberg, K. W.; Krokan, H. E., Closely related colon cancer cell

lines display different sensitivity to polyunsaturated fatty acids, accumulate different lipid classes and downregulate sterol regulatory element-binding protein 1. *Febs J* **2006,** *273* (12), 2749-2765.

55. Lauritzen, L.; Hansen, H. S.; Jorgensen, M. H.; Michaelsen, K. F., The essentiality of long chain n-3 fatty acids in relation to development and function of the brain and retina. *Prog Lipid Res* **2001,** *40* (1-2), 1-94.

56. Seitz, J.; Ojima, I., Drug Conjugates with Polyunsaturated Fatty Acids. *Drug Delivery in Oncology: From Basic Research to Cancer Therapy, Vols 1-3* **2012**, 1323-1357.

57. Ojima, I., Guided molecular missiles for tumor-targeting chemotherapy--case studies using the second-generation taxoids as warheads. *Accounts of chemical research* **2008,** *41* (1), 108-19.

58. Kratz, F.; Muller, I. A.; Ryppa, C.; Warnecke, A., Prodrug strategies in anticancer chemotherapy. *Chemmedchem* **2008,** *3* (1), 20-53.

59. Sanvicens, N.; Marco, M. P., Multifunctional nanoparticles - properties and prospects for their use in human medicine. *Trends Biotechnol* **2008,** *26* (8), 425-433.

60. Bharali, D. J.; Khalil, M.; Gurbuz, M.; Simone, T. M.; Mousa, S. A., Nanoparticles and cancer therapy: A concise review with emphasis on dendrimers. *International journal of nanomedicine* **2009,** *4* (1), 1-7.

61. Bosman, A. W.; Janssen, H. M.; Meijer, E. W., About dendrimers: Structure, physical properties, and applications. *Chem Rev* **1999,** *99* (7), 1665-1688.

62. Lee, I.; Athey, B. D.; Wetzel, A. W.; Meixner, W.; Baker, J. R., Structural molecular dynamics studies on polyamidoamine dendrimers for a therapeutic application: Effects of pH and generation. *Macromolecules* **2002,** *35* (11), 4510-4520.

63. Bharali, D. J.; Khalil, M.; Gurbuz, M.; Simone, T. M.; Mousa, S. A., Nanoparticles and cancer therapy: a concise review with emphasis on dendrimers. *International journal of nanomedicine* **2009,** *4*, 1-7.

64. (a) Tomalia, D. A.; Reyna, L. A.; Svenson, S., Dendrimers as multi-purpose nanodevices for oncology drug delivery and diagnostic imaging. *Biochem Soc T* **2007,** *35*, 61-67; (b) Astruc, D.; Boisselier, E.; Ornelas, C., Dendrimers Designed for Functions: From Physical, Photophysical, and Supramolecular Properties to Applications in Sensing, Catalysis,

Molecular Electronics, Photonics, and Nanomedicine. *Chem Rev* **2010,** *110* (4), 1857-1959.

65. Gaertner, H. F.; Cerini, F.; Kamath, A.; Rochat, A. F.; Siegrist, C. A.; Menin, L.; Hartley, O., Efficient Orthogonal Bioconjugation of Dendrimers for Synthesis of Bioactive Nanoparticles. *Bioconjugate Chem* **2011,** *22* (6), 1103-1114.

66. Majoros, I. J.; Thomas, T. P.; Mehta, C. B.; Baker, J. R., Poly(amidoamine) dendrimer-based multifunctional engineered nanodevice for cancer therapy. *J Med Chem* **2005,** *48* (19), 5892-5899.

67. Thomas, T. P.; Majoros, I. J.; Kotlyar, A.; Kukowska-Latallo, J. F.; Bielinska, A.; Myc, A.; Baker, J. R., Targeting and inhibition of cell growth by an engineered dendritic nanodevice. *J Med Chem* **2005,** *48* (11), 3729-3735.

68. Kukowska-Latallo, J. F.; Candido, K. A.; Cao, Z. Y.; Nigavekar, S. S.; Majoros, I. J.; Thomas, T. P.; Balogh, L. P.; Khan, M. K.; Baker, J. R., Nanoparticle targeting of anticancer drug improves therapeutic response in animal model of human epithelial cancer. *Cancer Res* **2005,** *65* (12), 5317-5324.

69. Zong, H.; Thomas, T. P.; Lee, K. H.; Desai, A. M.; Li, M. H.; Kotlyar, A.; Zhang, Y. H.; Leroueil, P. R.; Gam, J. J.; Holl, M. M. B.; Baker, J. R., Bifunctional PAMAM Dendrimer Conjugates of Folic Acid and Methotrexate with Defined Ratio. *Biomacromolecules* **2012,** *13* (4), 982-991.

70. Seitz, O.; Kunz, H., HYCRON, an allylic anchor for high-efficiency solid phase synthesis of protected peptides and glycopeptides. *J. Org. Chem.* **1997,** *62* (4), 813-826.

71. Chan, E. W.; Chattopadhaya, S.; Panicker, R. C.; Huang, X.; Yao, S. Q., Developing photoactive affinity probes for proteomic profiling: hydroxamate-based probes for metalloproteases. *J Am Chem Soc* **2004,** *126* (44), 14435-46.

Appendix

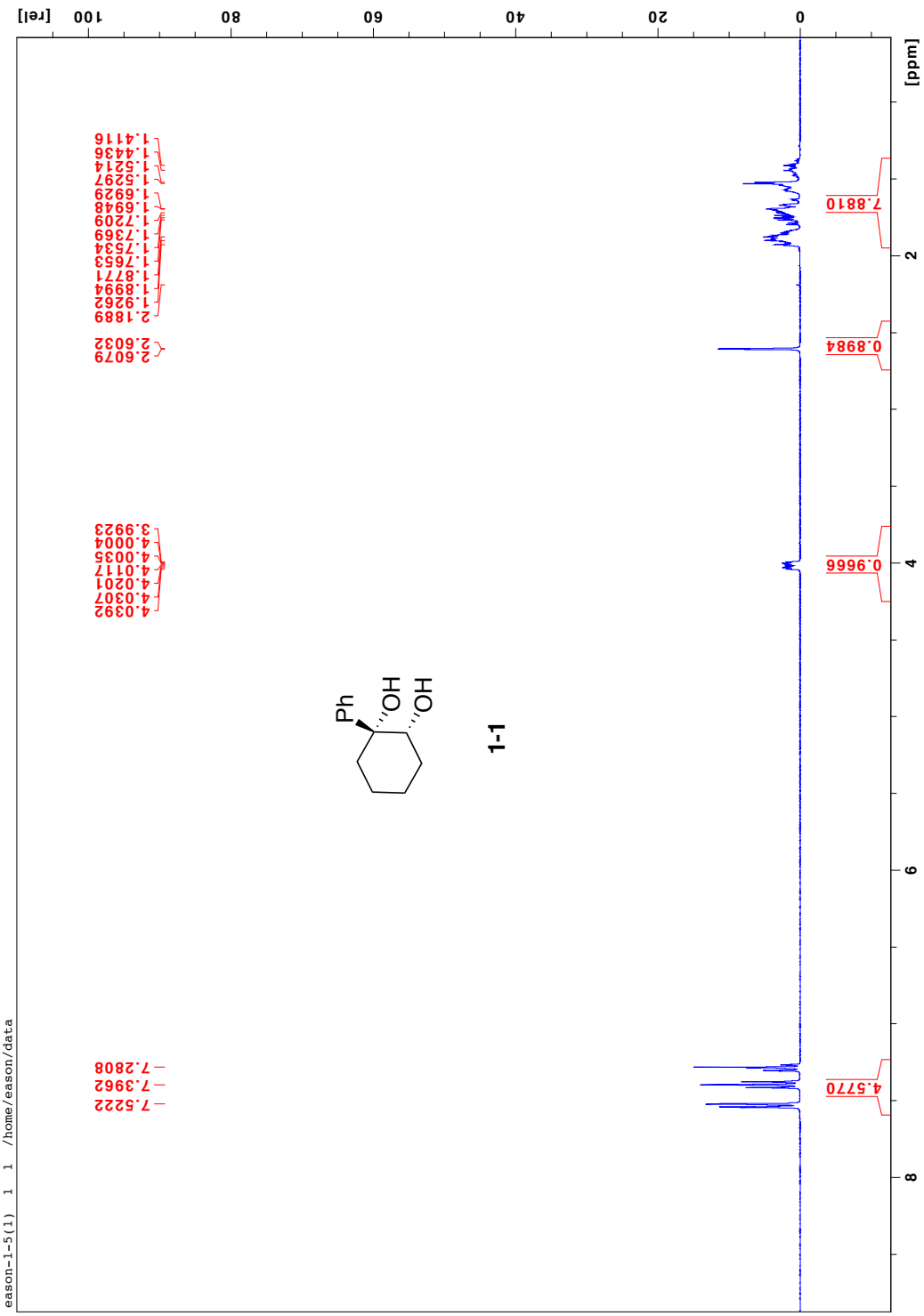
eason-1-5(1) 1 1 /home/eason/data
[rel]
100
80
60
40
20
0
[ppm]
2
4
6
8
7.8810
0.8984
0.9666
4.5770
7.5222
7.3962
7.2808
4.0392
4.0307
4.0201
4.0117
4.0035
4.0004
3.9923
2.6079
2.6032
2.1889
1.9262
1.8994
1.8771
1.7653
1.7534
1.7369
1.7209
1.6948
1.6629
1.5297
1.5214
1.4436
1.4116
Ph
HO
OH
1-1

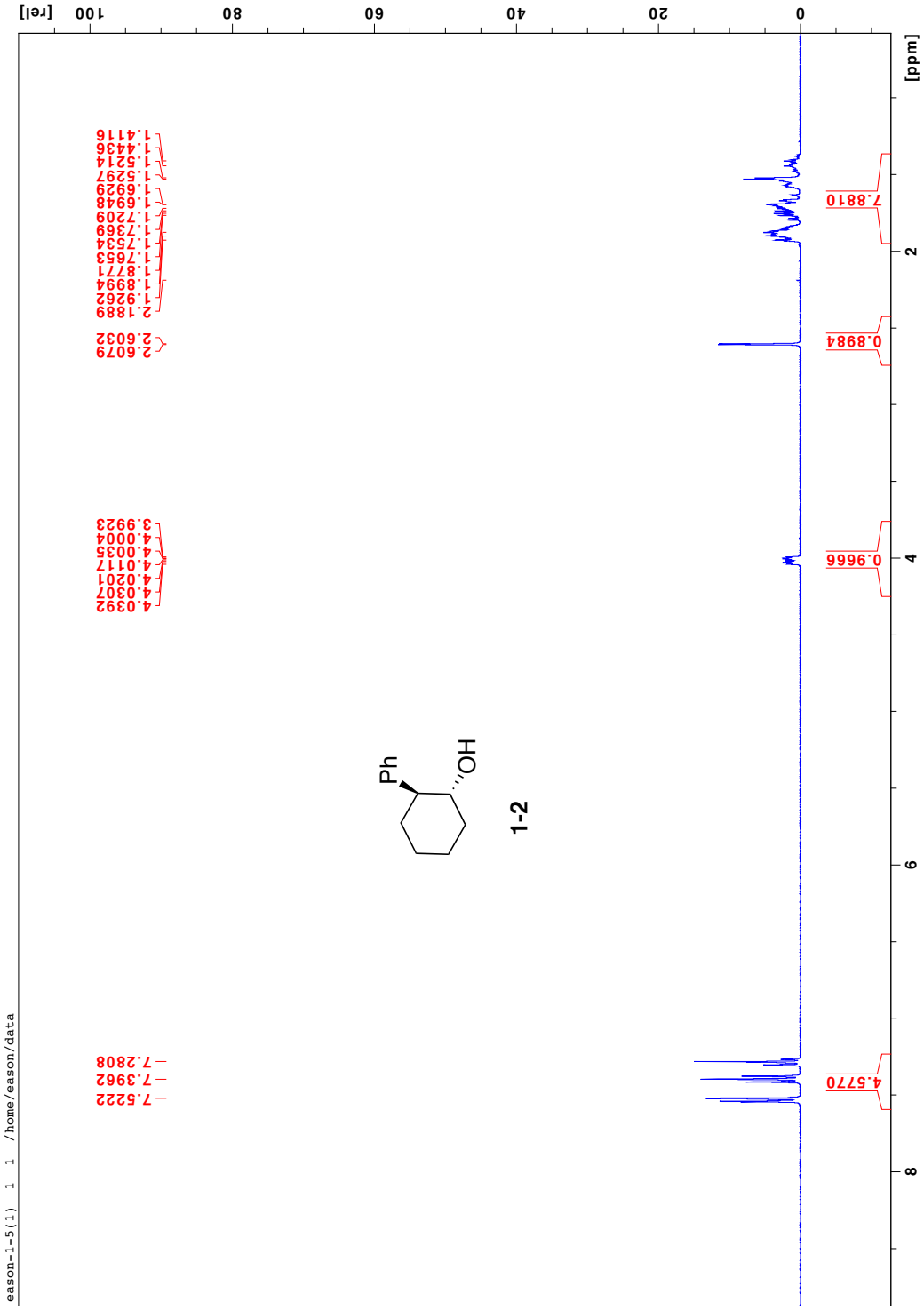
eason-1-5(1) 1 1 /home/eason/data
[rel]
100
80
60
40
20
0
[ppm]
8
6
4
2
7.5222
7.3962
7.2808
4.0392
4.0307
4.0201
4.0117
4.0035
4.0004
3.9923
2.6079
2.6032
2.1889
1.9262
1.8994
1.8771
1.7653
1.7534
1.7369
1.7209
1.6948
1.6929
1.5297
1.5214
1.4436
1.4116
4.5770
0.9666
0.8984
7.8810
Ph
OH
1-2

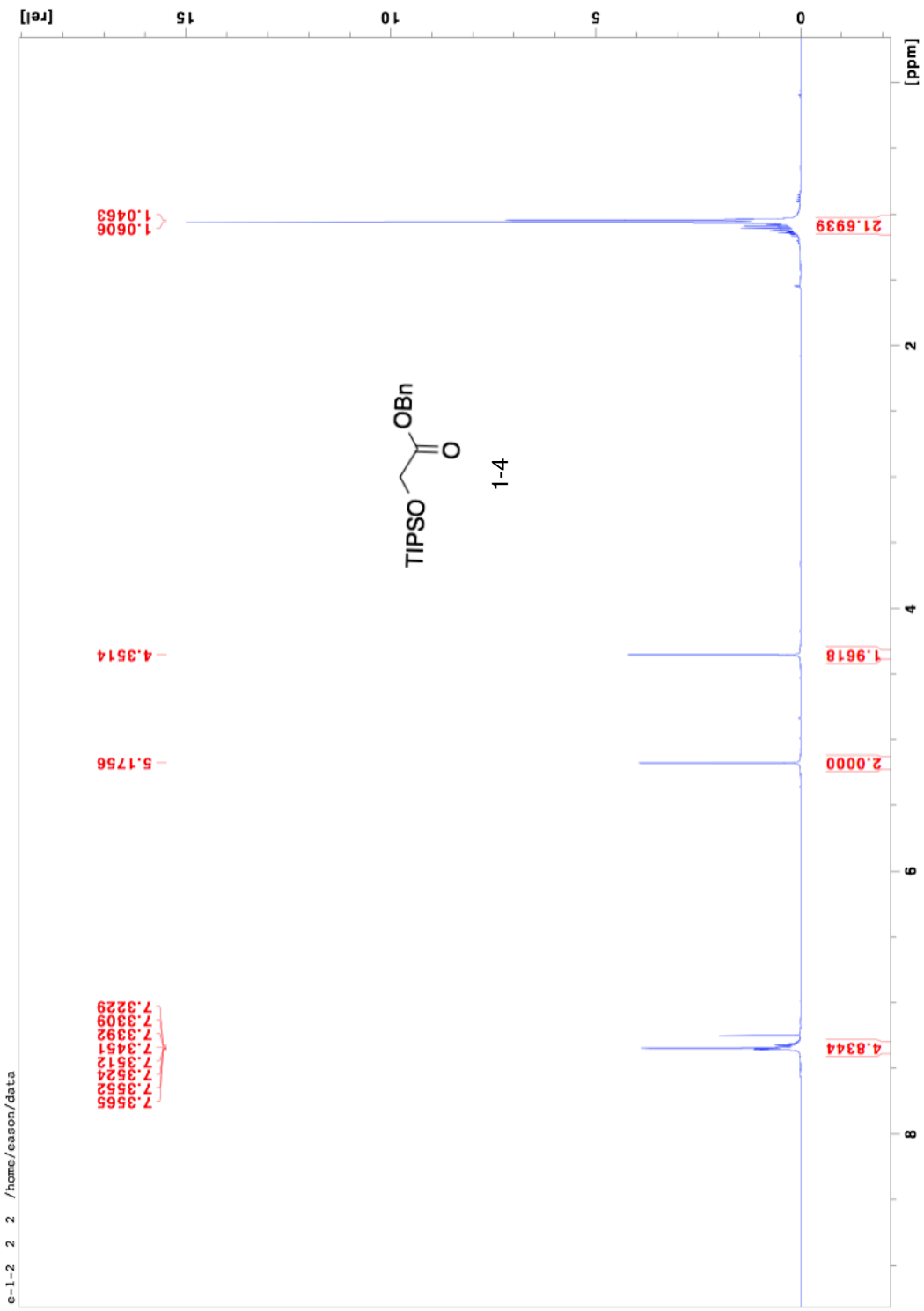
e-1-2 2 2 /home/eason/data
[rel]
15
10
5
0
[ppm]
2
4
6
8
1.0606
1.0463
21.6939
4.3514
1.9618
5.1756
2.0000
7.3565
7.3552
7.3524
7.3512
7.3451
7.3392
7.3309
7.3229
4.8344
TIPSO
OBn
O
1-4

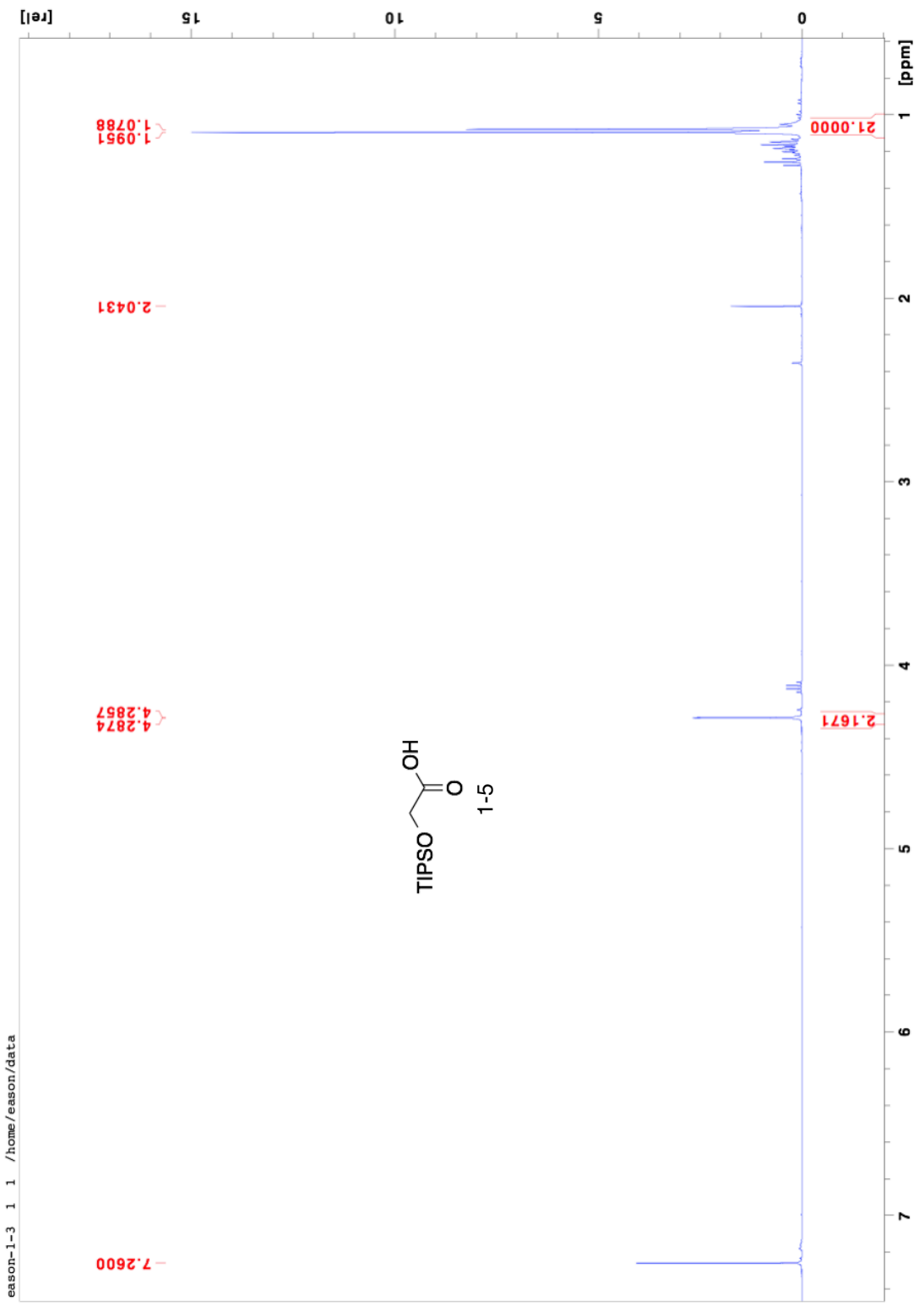
eason-1-3 1 1 /home/eason/data
[rel]
15
10
5
0
[ppm]
1
2
3
4
5
6
7
7.2600
4.2874
4.2857
2.0431
1.0951
1.0788
21.0000
2.1671
TIPSO
O
OH
1-5

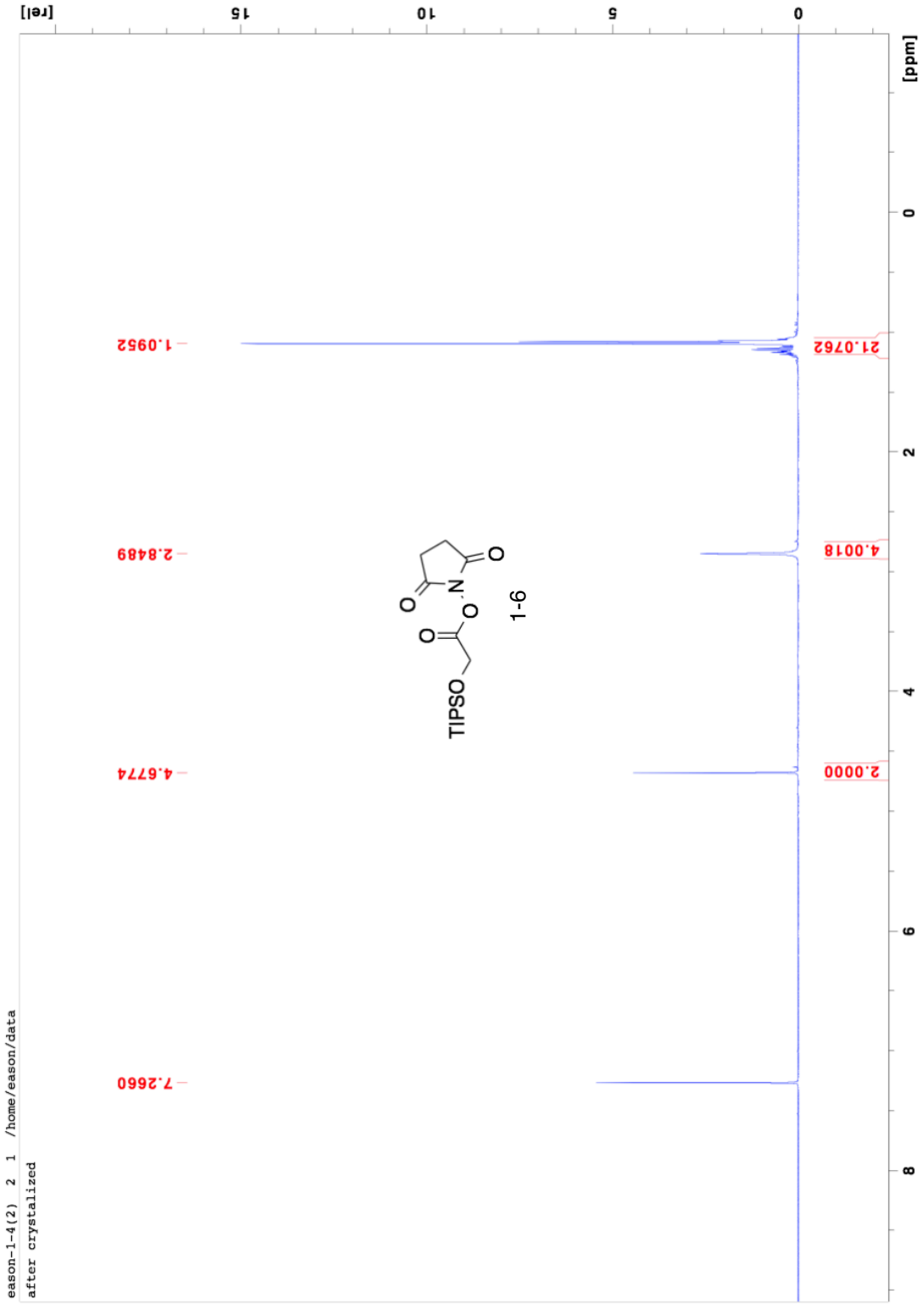
eason-1-4(2) 2 1 /home/eason/data
after crystalized
[rel]
15
10
5
0
[ppm]
0
2
4
6
8
1.0952
2.8489
4.6774
7.2660
21.0762
4.0018
2.0000
TIPSO
1-6

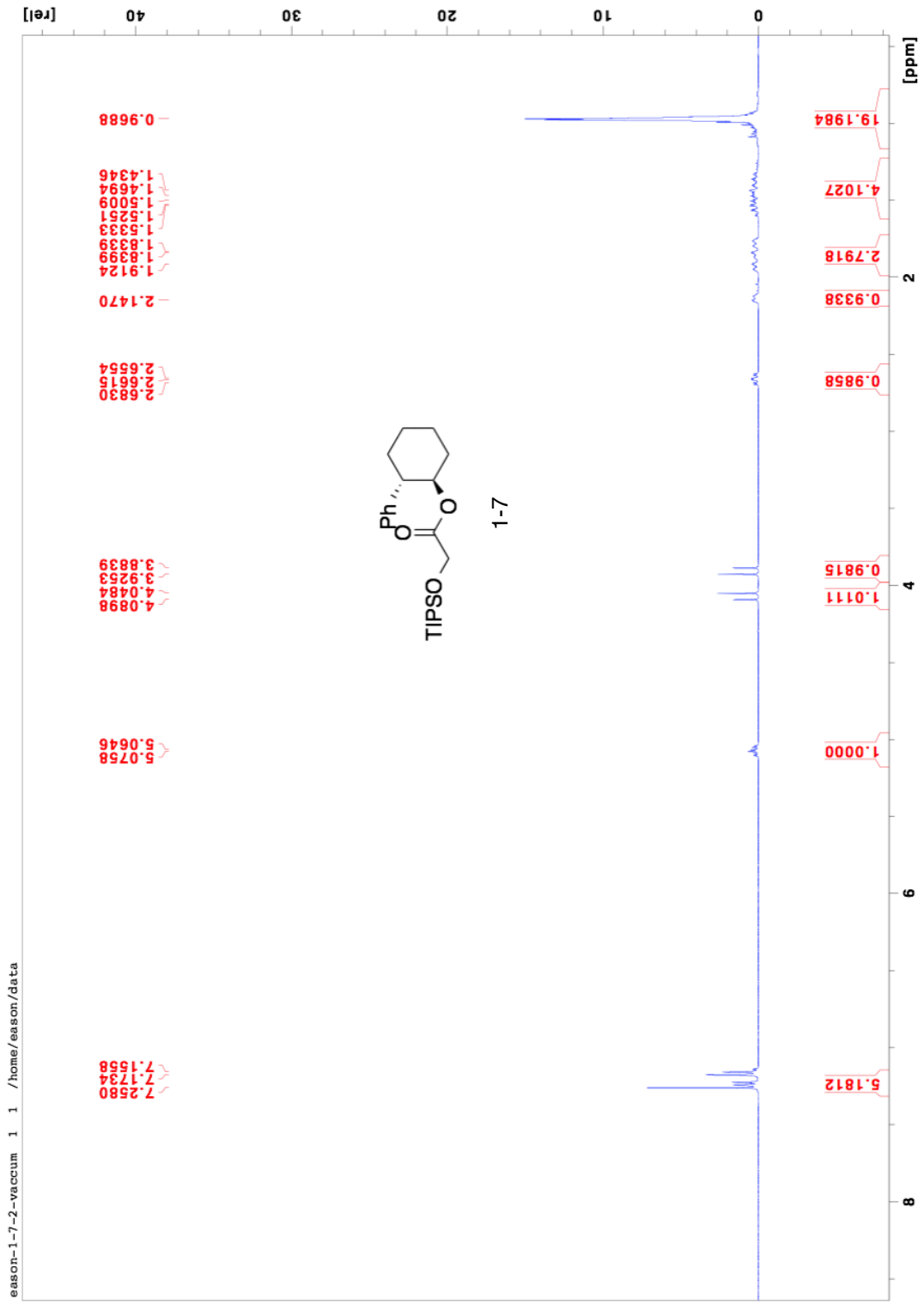
eason-1-7-2-vaccum 1 1 /home/eason/data
[rel]
40
30
20
10
0
[ppm]
2
4
6
8
19.1984
4.1027
2.7918
0.9338
0.9858
0.9815
1.0111
1.0000
5.1812
0.9688
1.4346
1.4694
1.5009
1.5251
1.5333
1.8339
1.8399
1.9124
2.1470
2.6830
2.6615
2.6554
3.8839
3.9253
4.0484
4.0898
5.0758
5.0646
7.2580
7.1734
7.1558
Ph
O
O
TIPSO
1-7

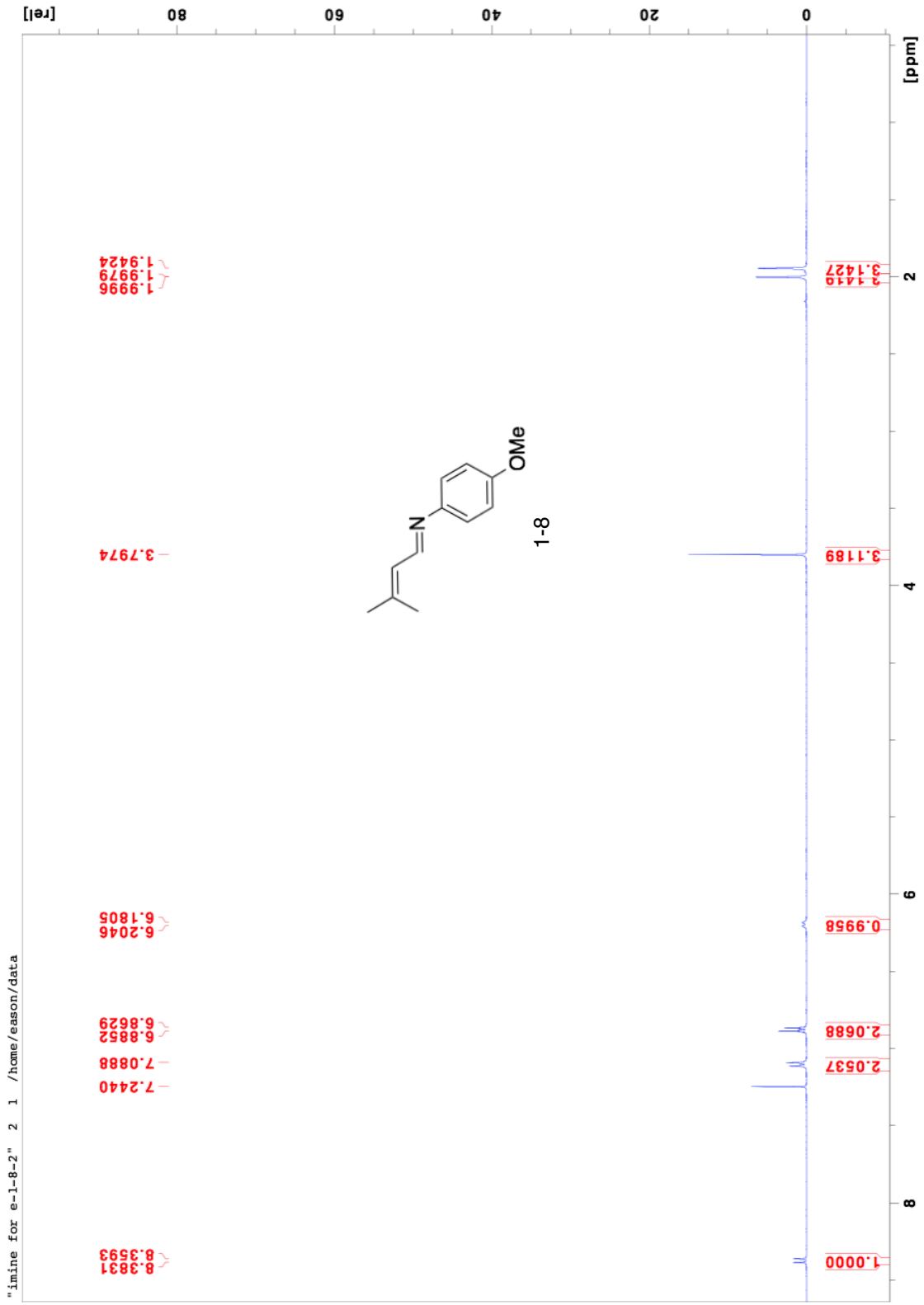
"imine for e-1-8-2" 2 1 /home/eason/data
[rel]
[ppm]
8.3831
8.3593
7.2440
7.0888
6.8852
6.8629
6.2046
6.1805
3.7974
1.9996
1.9979
1.9424
1.0000
2.0537
2.0688
0.9958
3.1189
3.1410
3.1427
OMe
N
1-8

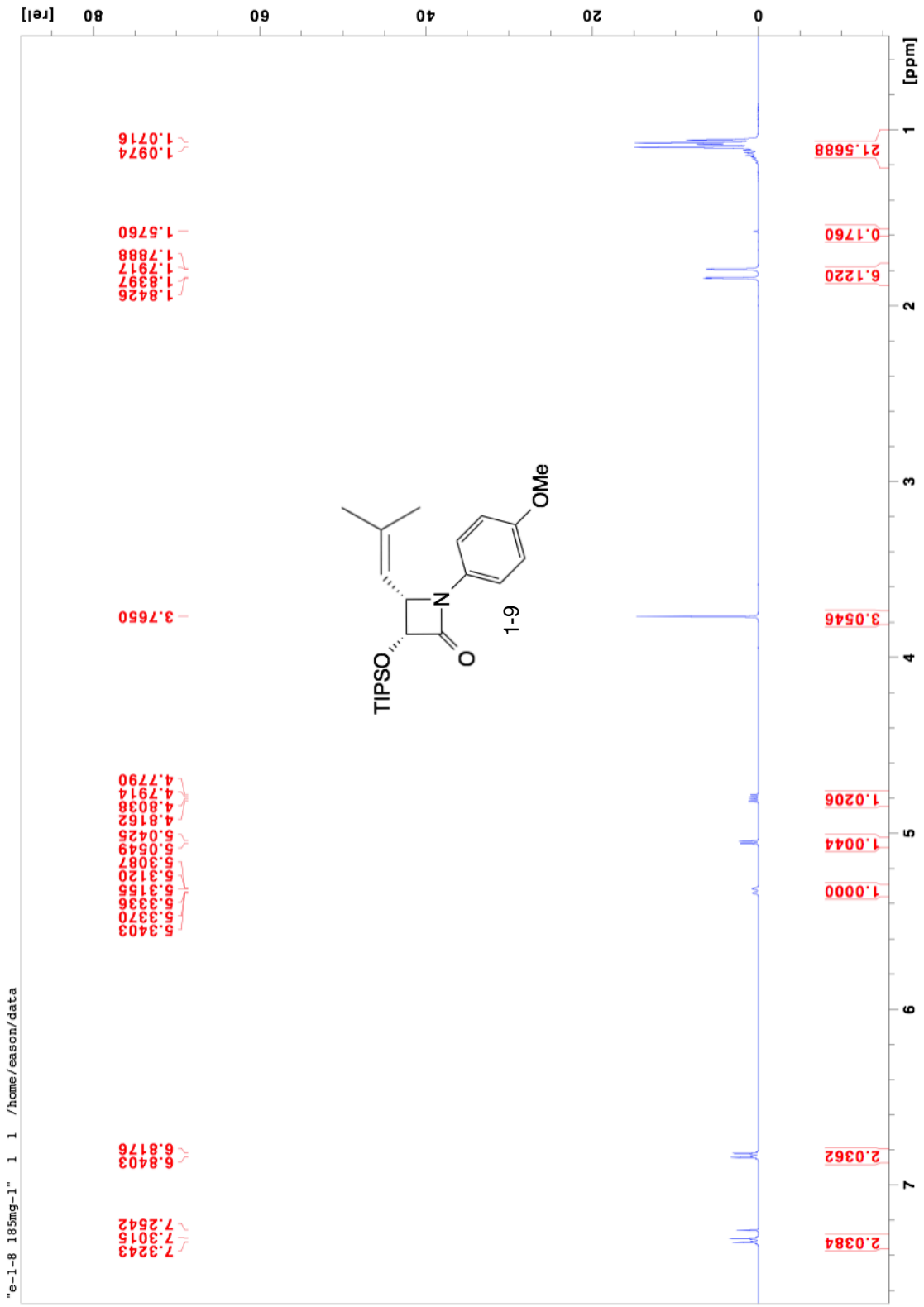
"e-1-8 185mg-1" 1 1 /home/eason/data
[rel]
80
60
40
20
0
[ppm]
1
2
3
4
5
6
7
1.0716
1.0974
1.5760
1.7888
1.7917
1.8397
1.8426
3.7650
4.7790
4.7914
4.8038
4.8162
5.0425
5.0549
5.3087
5.3120
5.3155
5.3336
5.3370
5.3403
6.8403
6.8176
7.2542
7.3015
7.3243
21.5688
0.1760
6.1220
3.0546
1.0206
1.0044
1.0000
2.0362
2.0384
TIPSO
O
N
OMe
1-9

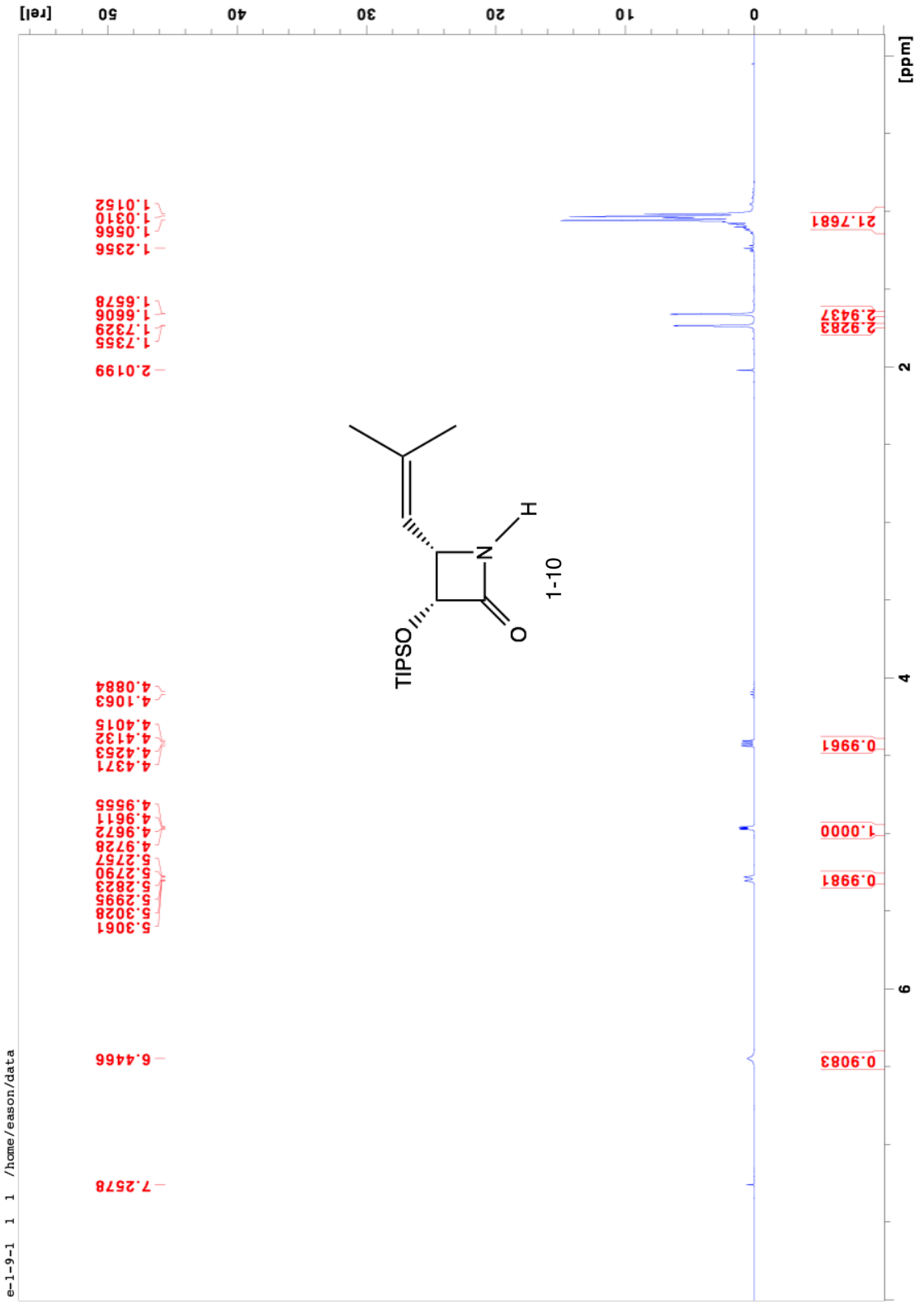
[rel]
50
40
30
20
10
0
[ppm]
2
4
6
e-1-9-1 1 1 /home/eason/data
7.2578
6.4466
5.3061
5.3028
5.2995
5.2823
5.2790
5.2757
4.9728
4.9672
4.9611
4.9555
4.4371
4.4253
4.4132
4.4015
4.1063
4.0884
2.0199
1.7355
1.7329
1.6606
1.6578
1.2356
1.0566
1.0310
1.0152
21.7681
2.9437
2.9283
0.9961
1.0000
0.9981
0.9083
TIPSO
N
H
O
1-10

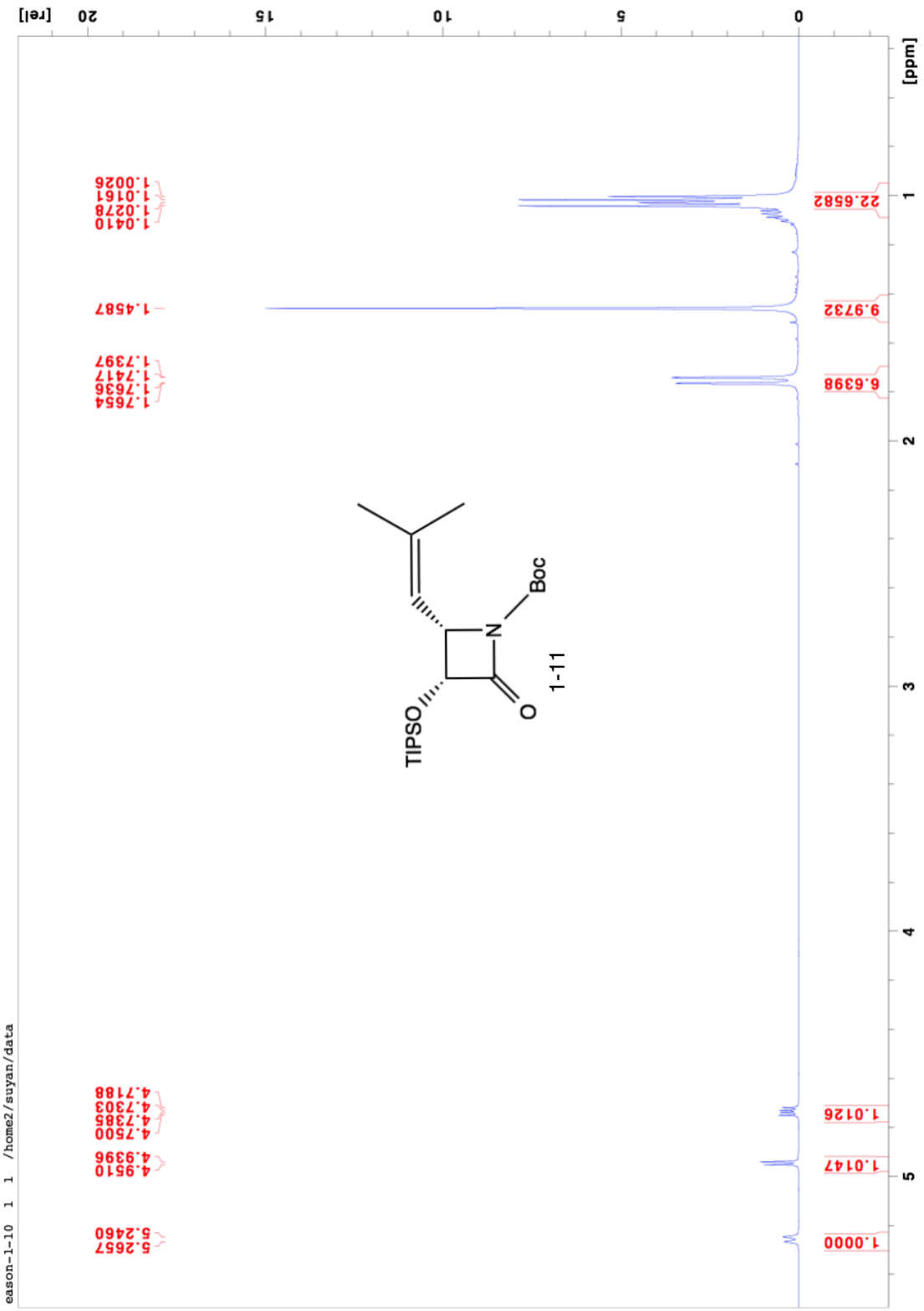
eason-1-10 1 1 /home2/suyan/data
[rel]
20
15
10
5
0
[ppm]
1
2
3
4
5
1.0000
1.0147
1.0126
22.6582
9.9732
6.6398
1.4587
1.7654
1.7636
1.7417
1.7397
1.0410
1.0278
1.0161
1.0026
5.2657
5.2460
4.9510
4.9396
4.7500
4.7385
4.7303
4.7188
TIPSO
O
N
Boc
1-11

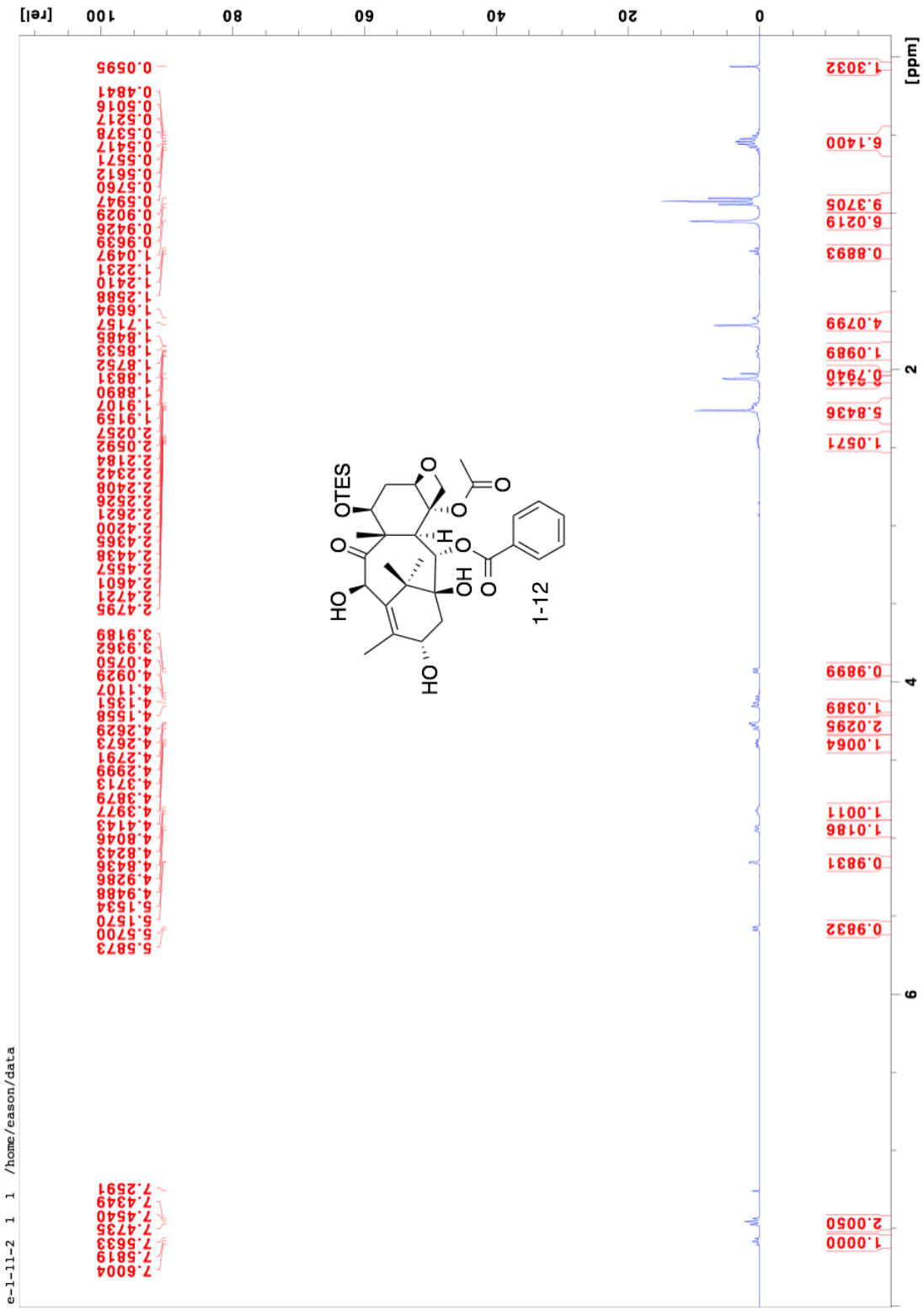
e-1-11-2 1 1 /home/eason/data
[rel]
[ppm]
1-12
OTES
HO
OH
HO

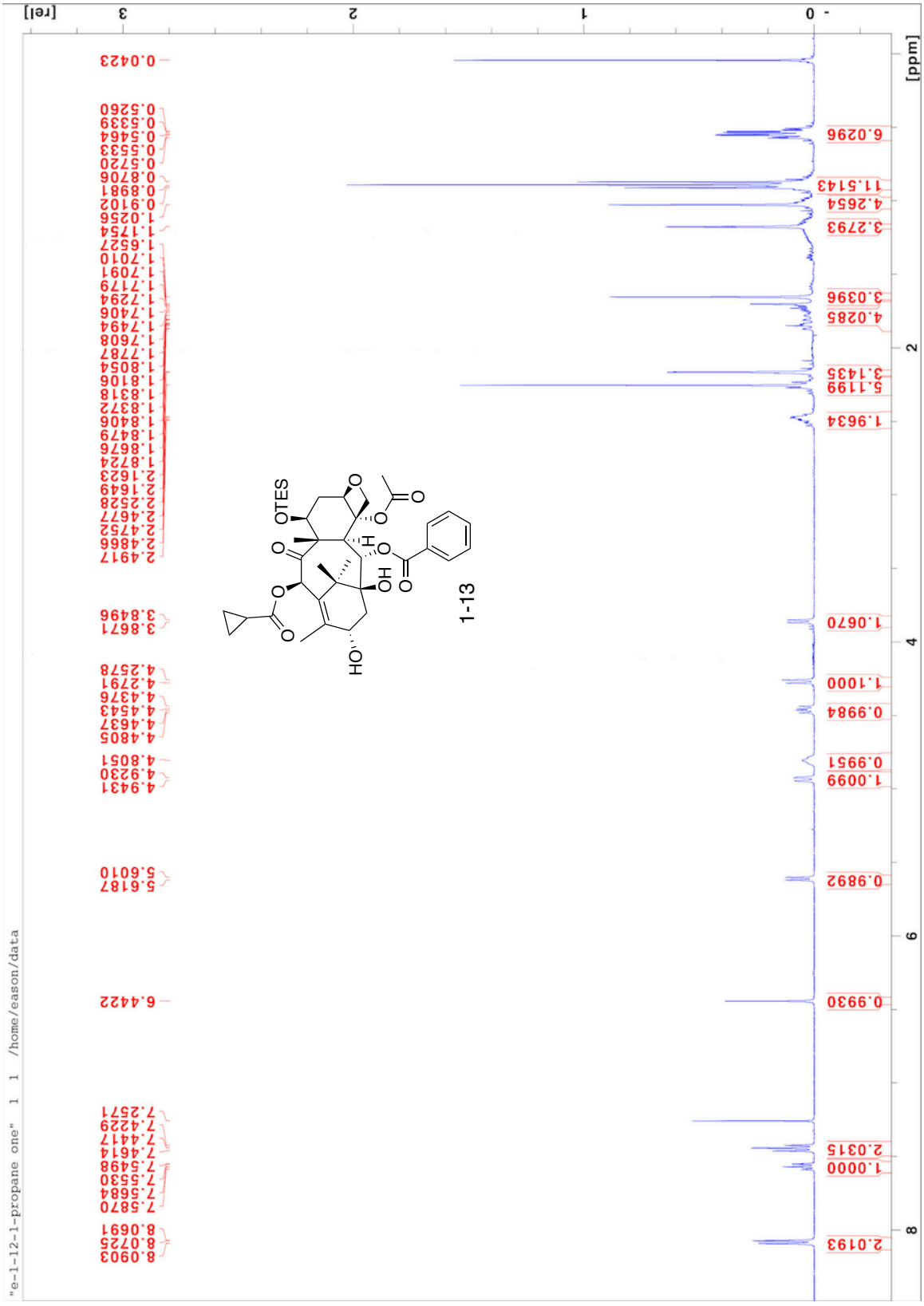
"e-1-12-1-propane one" 1 1 /home/eason/data
[rel]
[ppm]
OTES
OH
HO
1-13

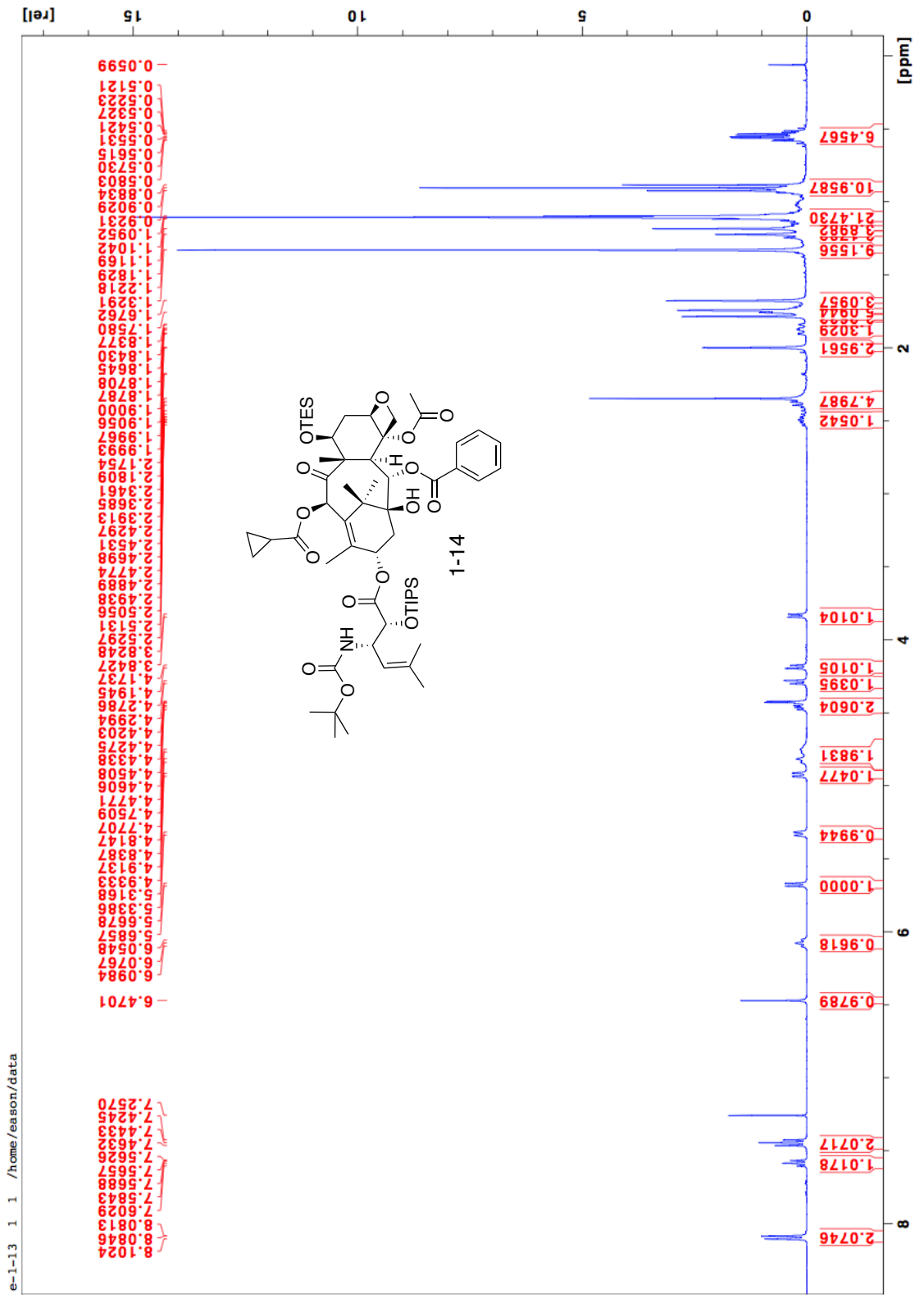
OTES
OTIPS
OH
1-14
[ppm]
[rel]
e-1-13 1 1 /home/eason/data

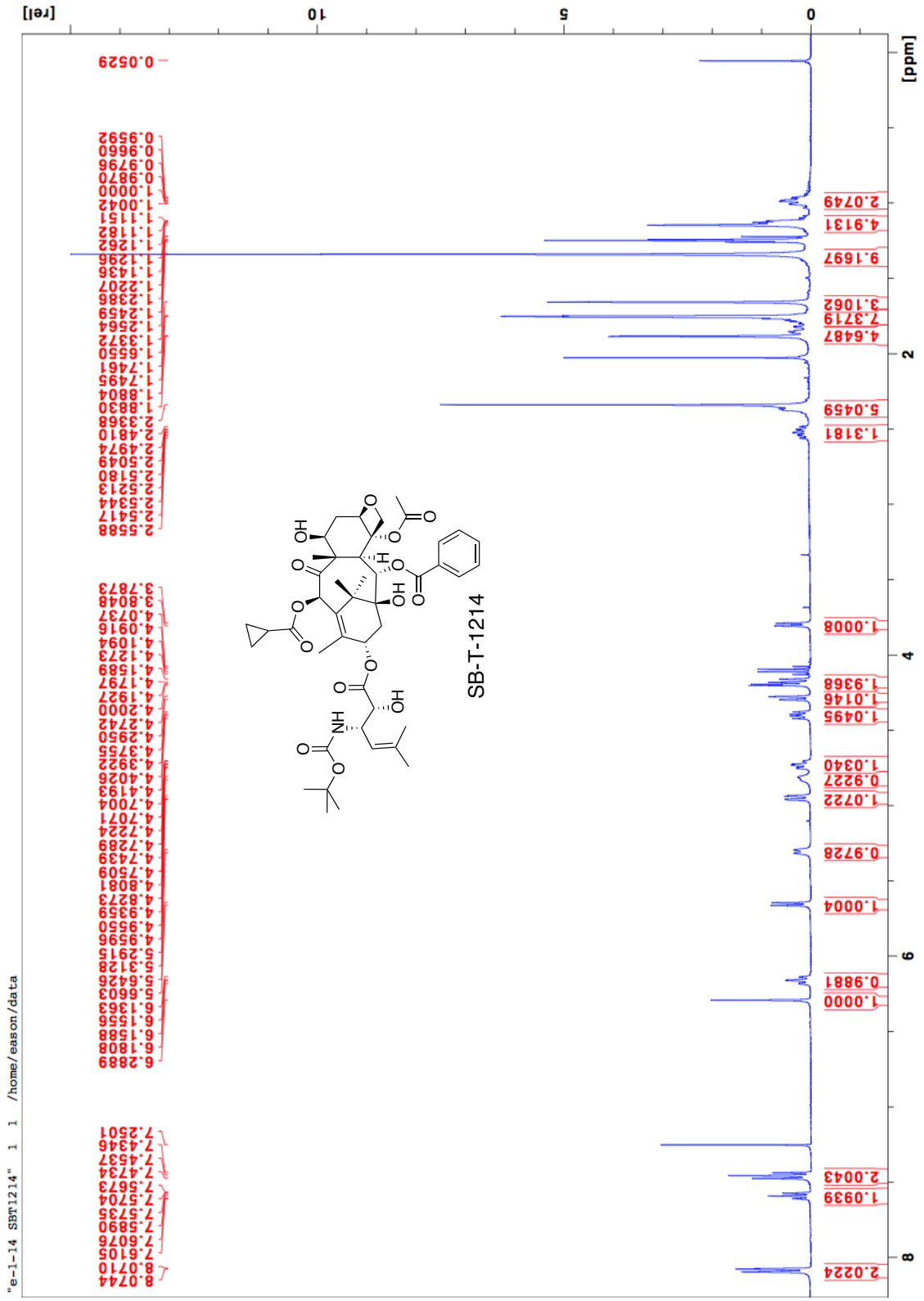
"e-1-14 SBT1214" 1 1 /home/eason/data
[rel]
[ppm]
SB-T-1214


"3tes 10 dab" 1 1 /home/eason/data
[rel]
15
10
5
0
[ppm]
2
4
6
8
19.1000
29.4974
2.8697
2.6177
0.7566
4.2695
2.7479
1.0626
2.6280
1.0158
0.9837
2.6026
1.0133
0.9342
0.9643
0.9217
0.9809
1.8367
0.8839
0.9031
1.7849
0.9266
0.8921
TESO
OTES
TESO
OH
1-15

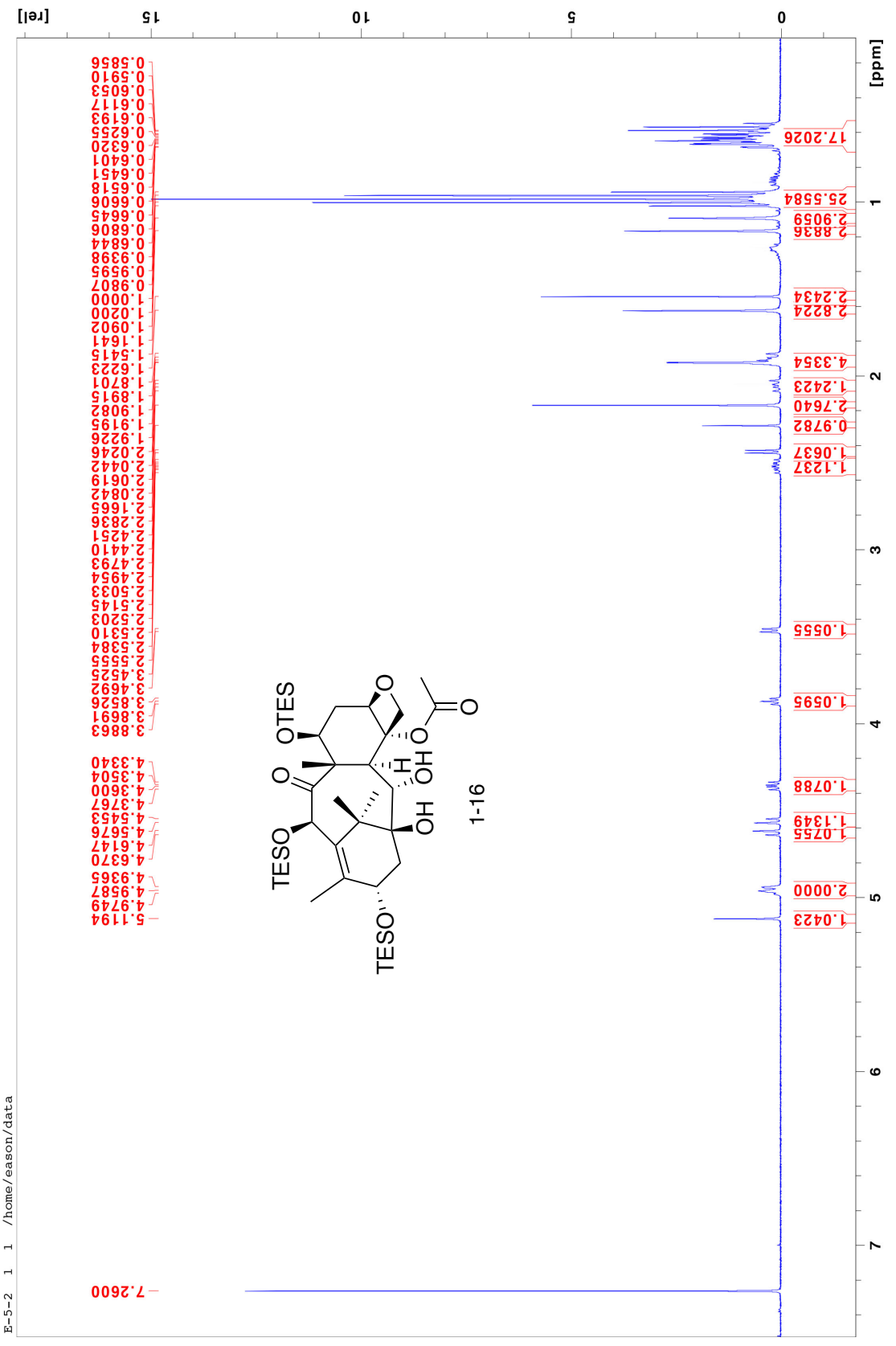
E-5-2 1 1 /home/eason/data
[rel]
[ppm]
TESO
OTES
OH
HO
TESO
1-16

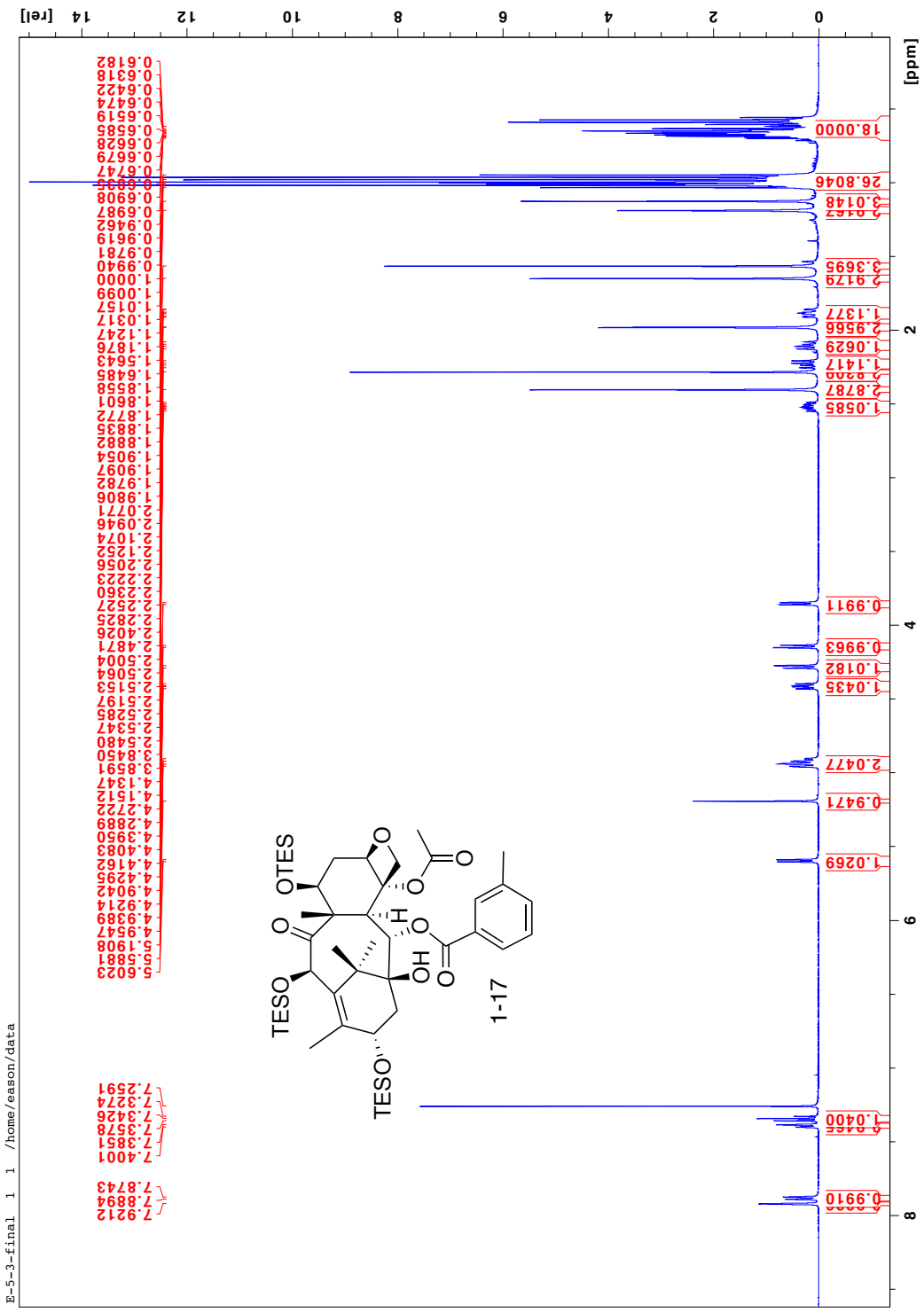
E-5-3-final 1 1 /home/eason/data
[rel]
[ppm]
TESO
OTES
OH
TESO
1-17

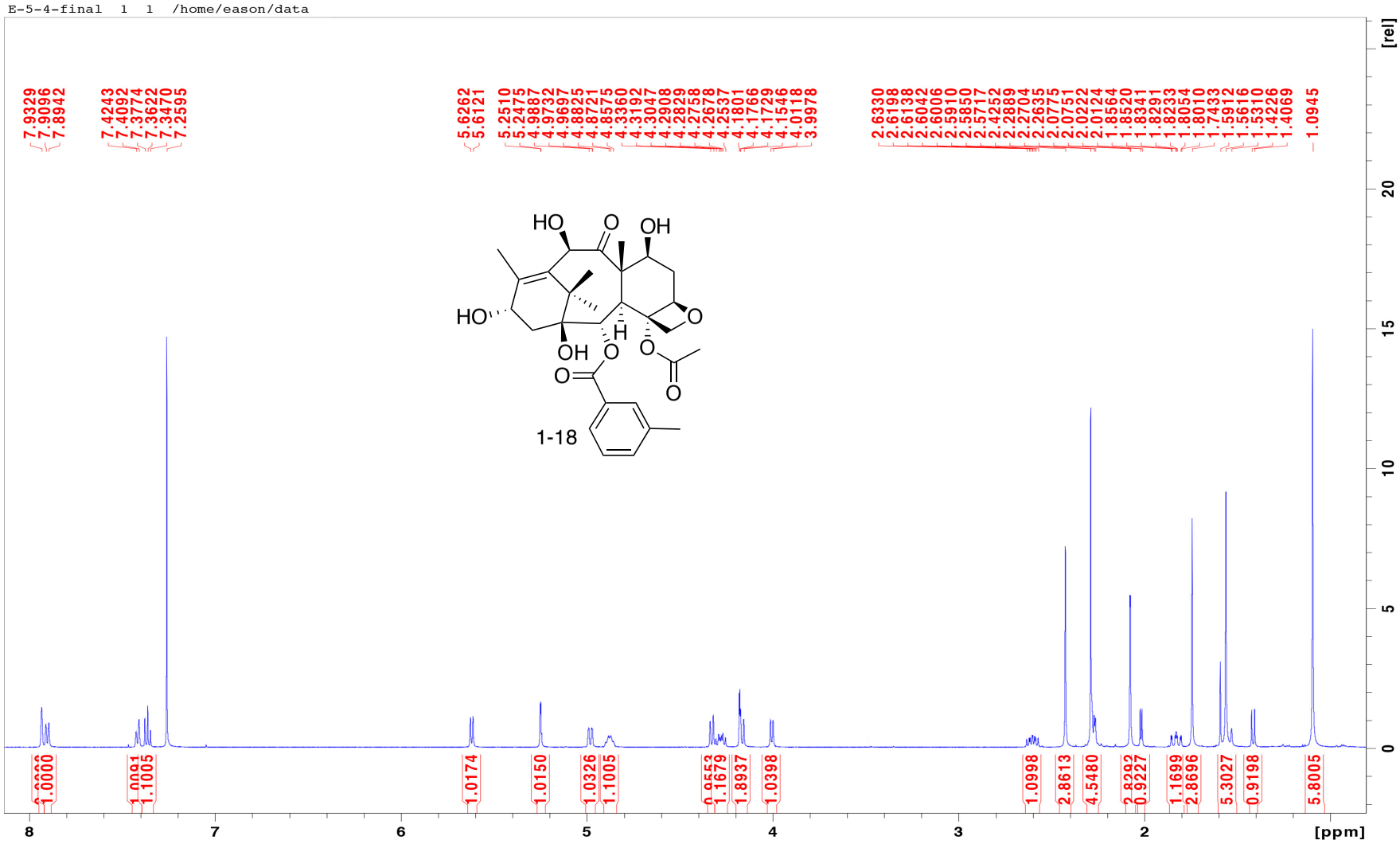
E-5-4-final 1 1 /home/eason/data
7.9329
7.9096
7.8942
7.4243
7.4092
7.3774
7.3622
7.3470
7.2595
5.6262
5.6121
5.2510
5.2475
4.9887
4.9732
4.9697
4.8825
4.8721
4.8575
4.3360
4.3192
4.3047
4.2908
4.2829
4.2758
4.2678
4.2537
4.1801
4.1766
4.1729
4.1546
4.0118
3.9978
2.6330
2.6198
2.6138
2.6042
2.6006
2.5910
2.5850
2.5717
2.4252
2.2889
2.2704
2.2635
2.0775
2.0751
2.0222
2.0124
1.8564
1.8520
1.8341
1.8291
1.8233
1.8054
1.8010
1.7433
1.5912
1.5616
1.5310
1.4226
1.4069
1.0945
HO
O
OH
HO
H
O
OH
O
O
O
O
1-18
1.0000
1.0001
1.1005
1.0174
1.0150
1.0326
1.1005
0.9552
1.1679
1.8937
1.0398
1.0998
2.8613
4.5480
2.8202
0.9227
1.1699
2.8696
5.3027
0.9198
5.8005
[rel]
[ppm]

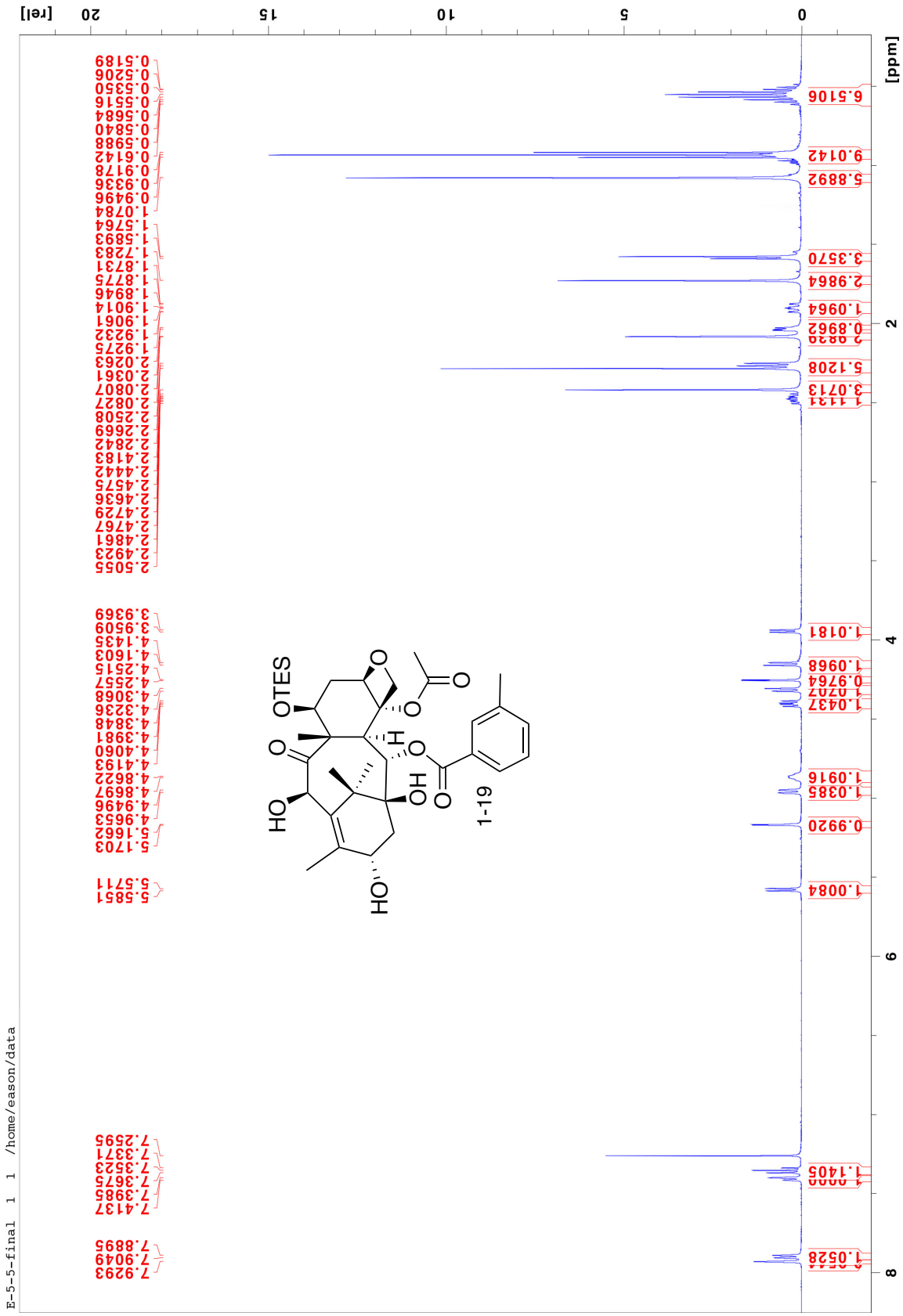
E-5-5-final 1 1 /home/eason/data
[ppm]
[rel]
OTES
HO
OH
1-19

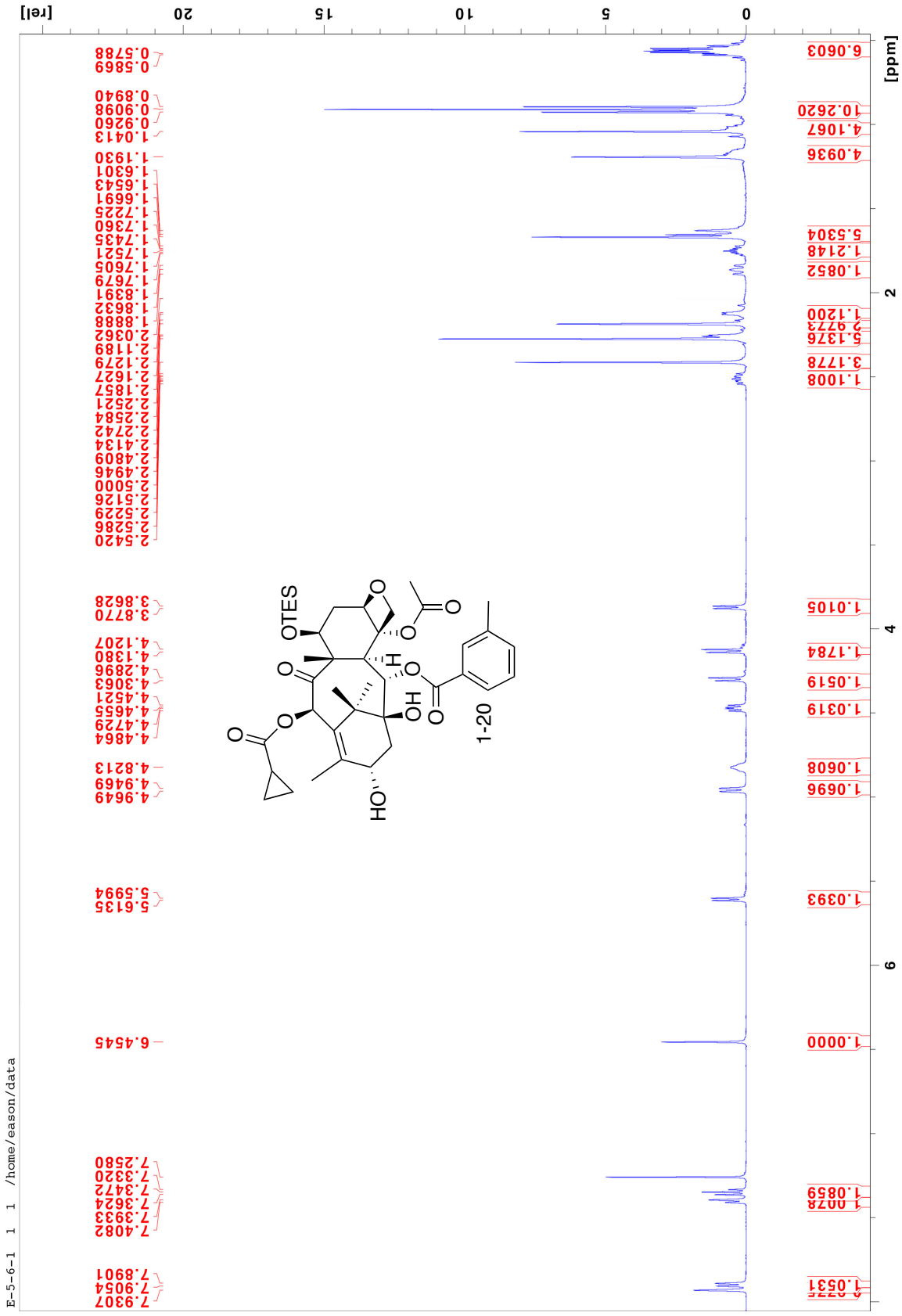
E-5-6-1 1 1 /home/eason/data
[rel]
[ppm]
OTES
OH
HO
1-20

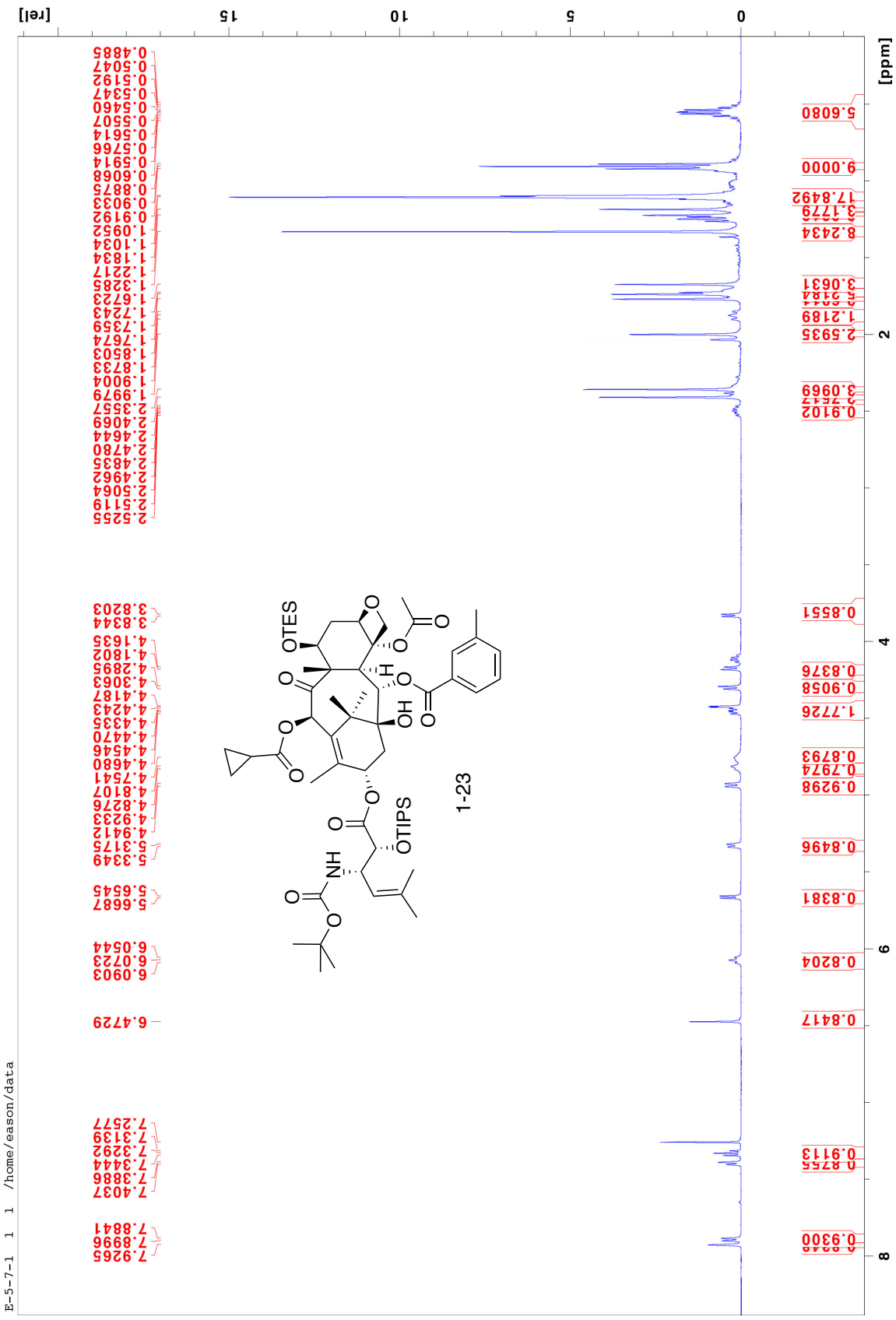
E-5-7-1 1 1 /home/eason/data
[rel]
[ppm]
OTES
OTIPS
1-23

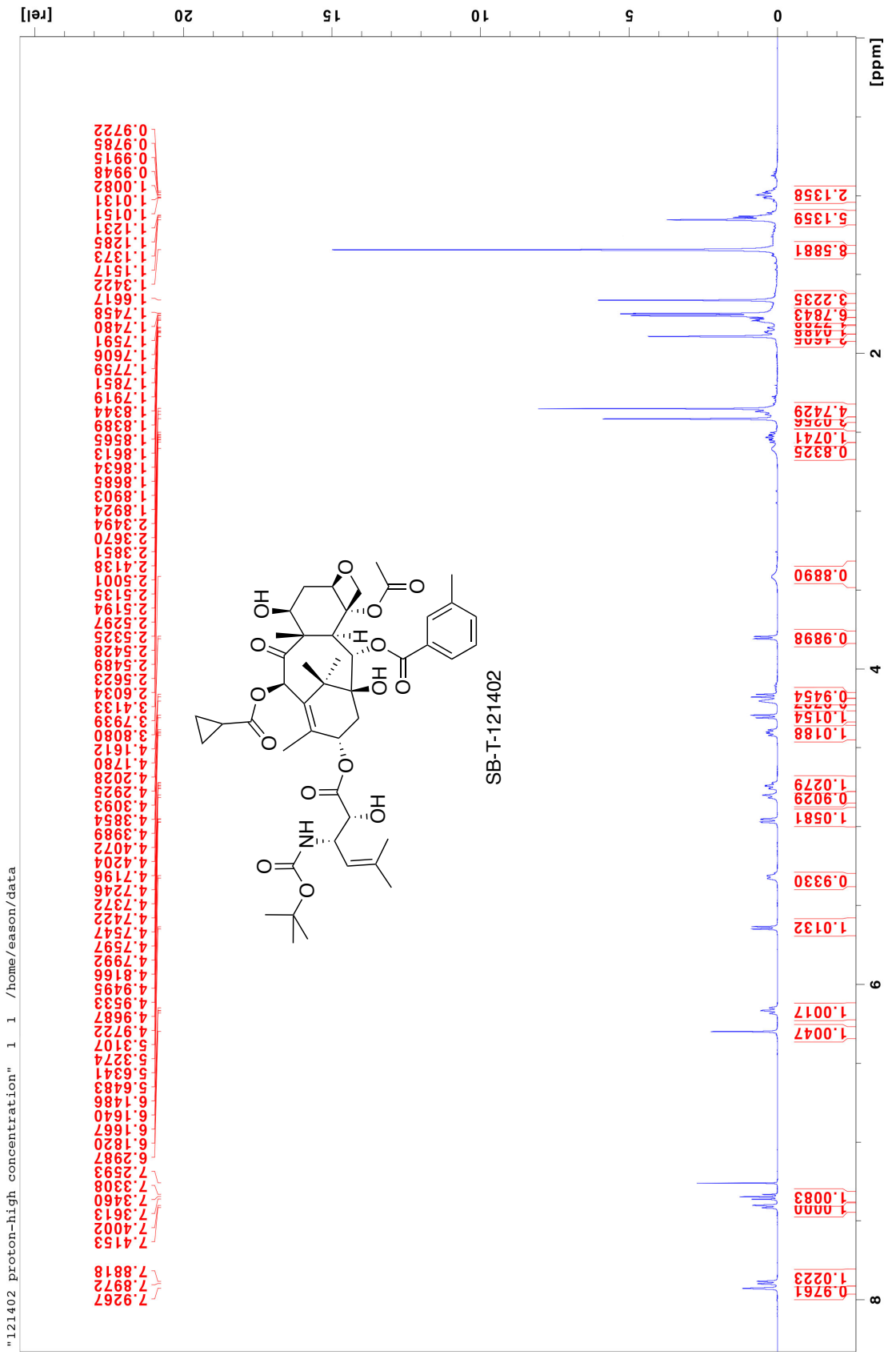
"121402 proton-high concentration" 1 1 /home/eason/data
[rel]
[ppm]
SB-T-121402

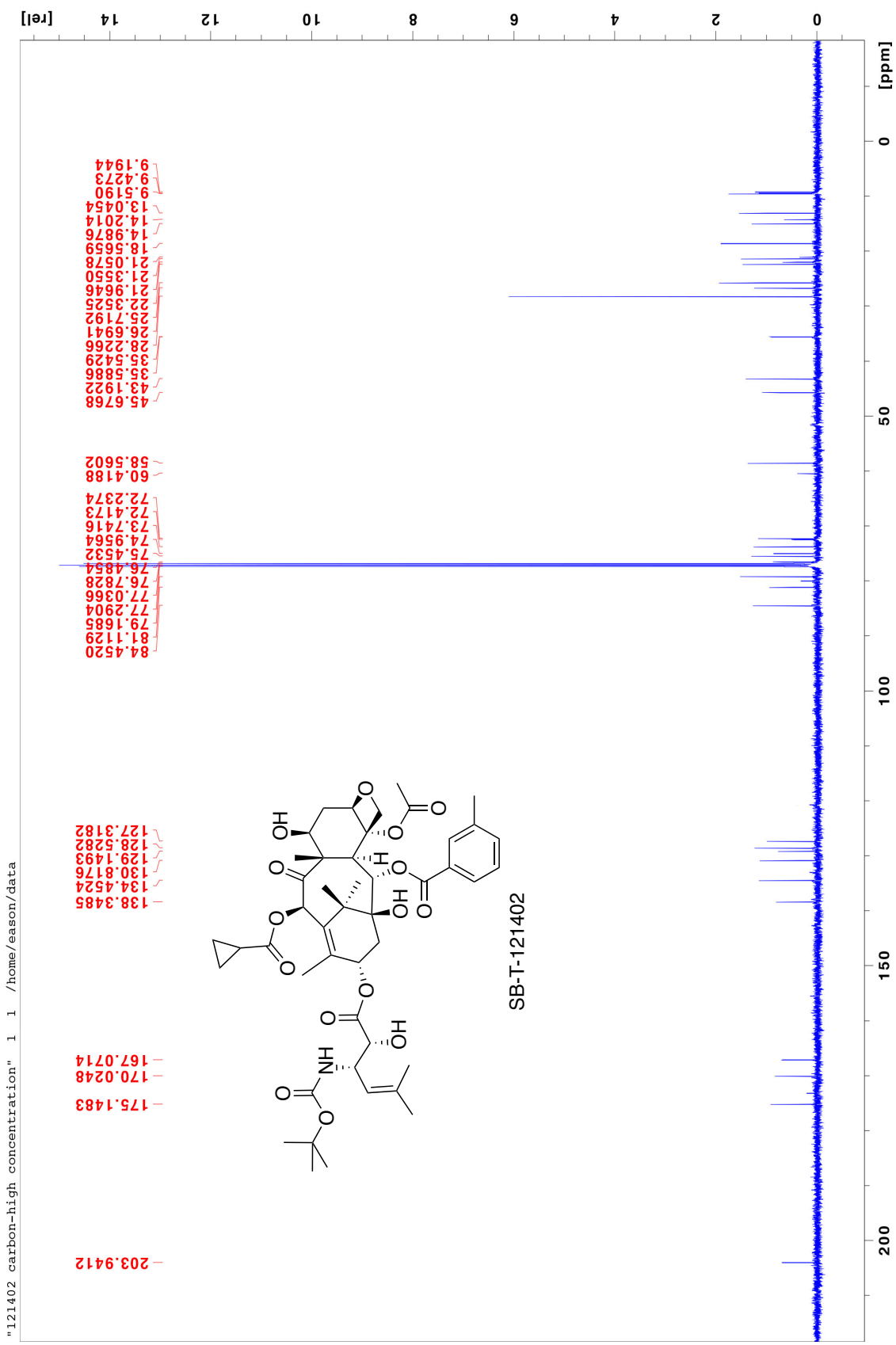
"121402 carbon-high concentration" 1 1 /home/eason/data
[rel]
[ppm]
SB-T-121402
203.9412
175.1483
170.0248
167.0714
138.3485
134.4524
130.8176
129.1493
128.5282
127.3182
84.4520
81.1129
79.1685
77.2904
77.0366
76.7828
76.4854
75.4532
74.9564
73.7416
72.4173
72.2374
60.4188
58.5602
45.6768
43.1922
35.5886
35.5429
28.2266
26.6941
25.7192
22.3525
21.9646
21.3550
21.0578
18.5659
14.9876
14.2014
13.0454
9.5190
9.4273
9.1944

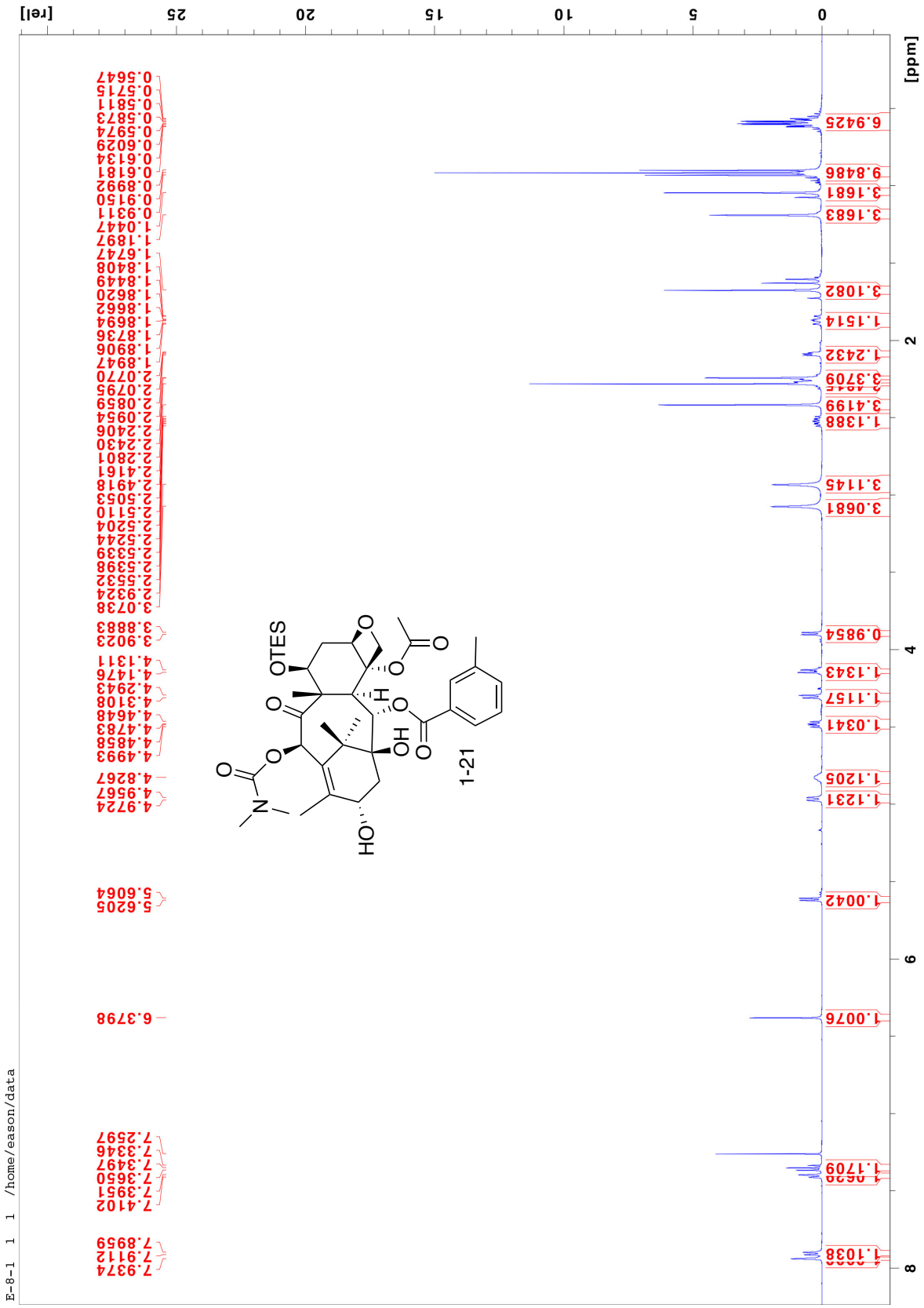
E-8-1 1 1 /home/eason/data
[rel]
[ppm]
OTES
OH
HO
1-21

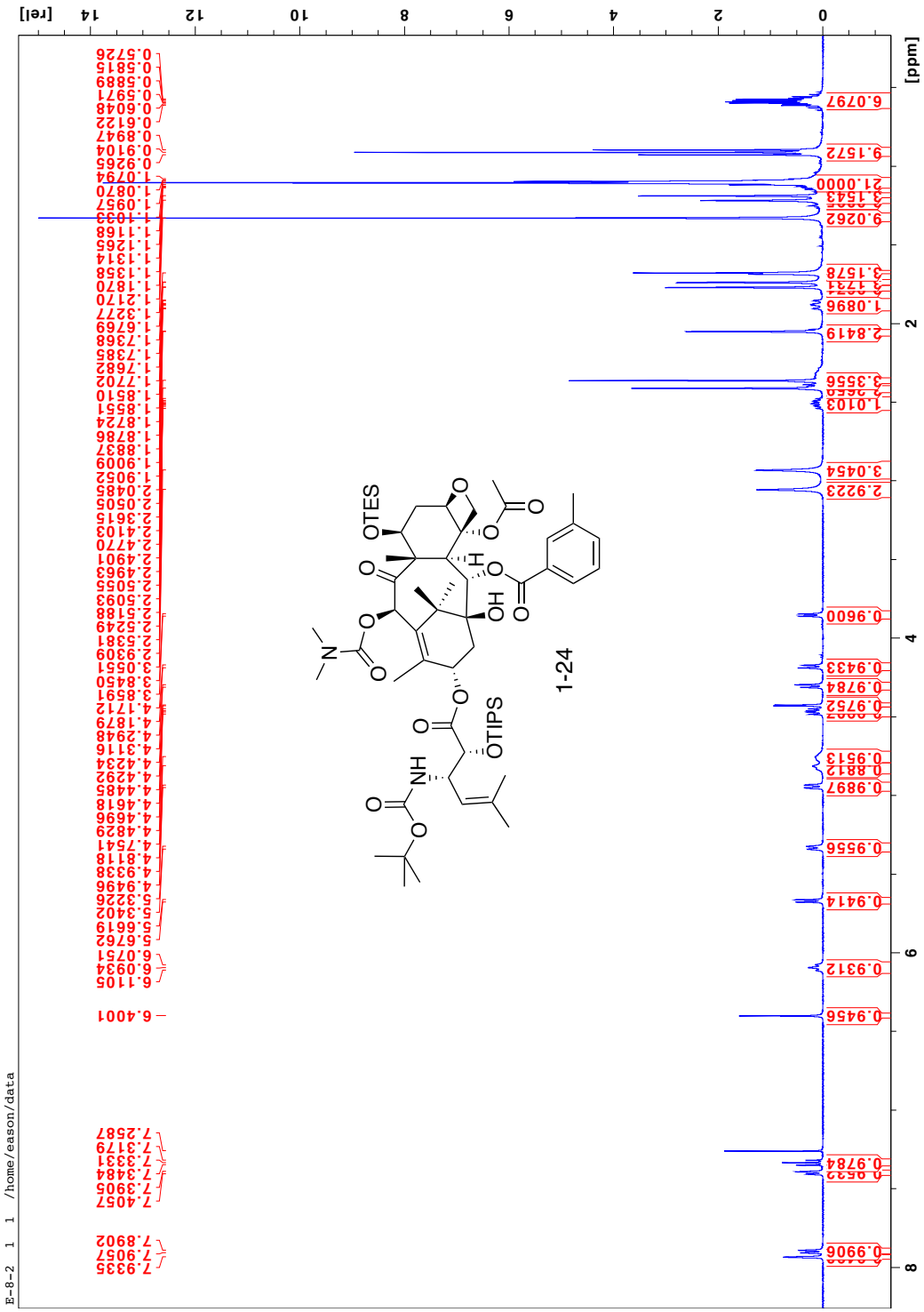
E-8-2 1 1 /home/eason/data
[rel]
[ppm]
1-24
OTES
OTIPS
OH
NH

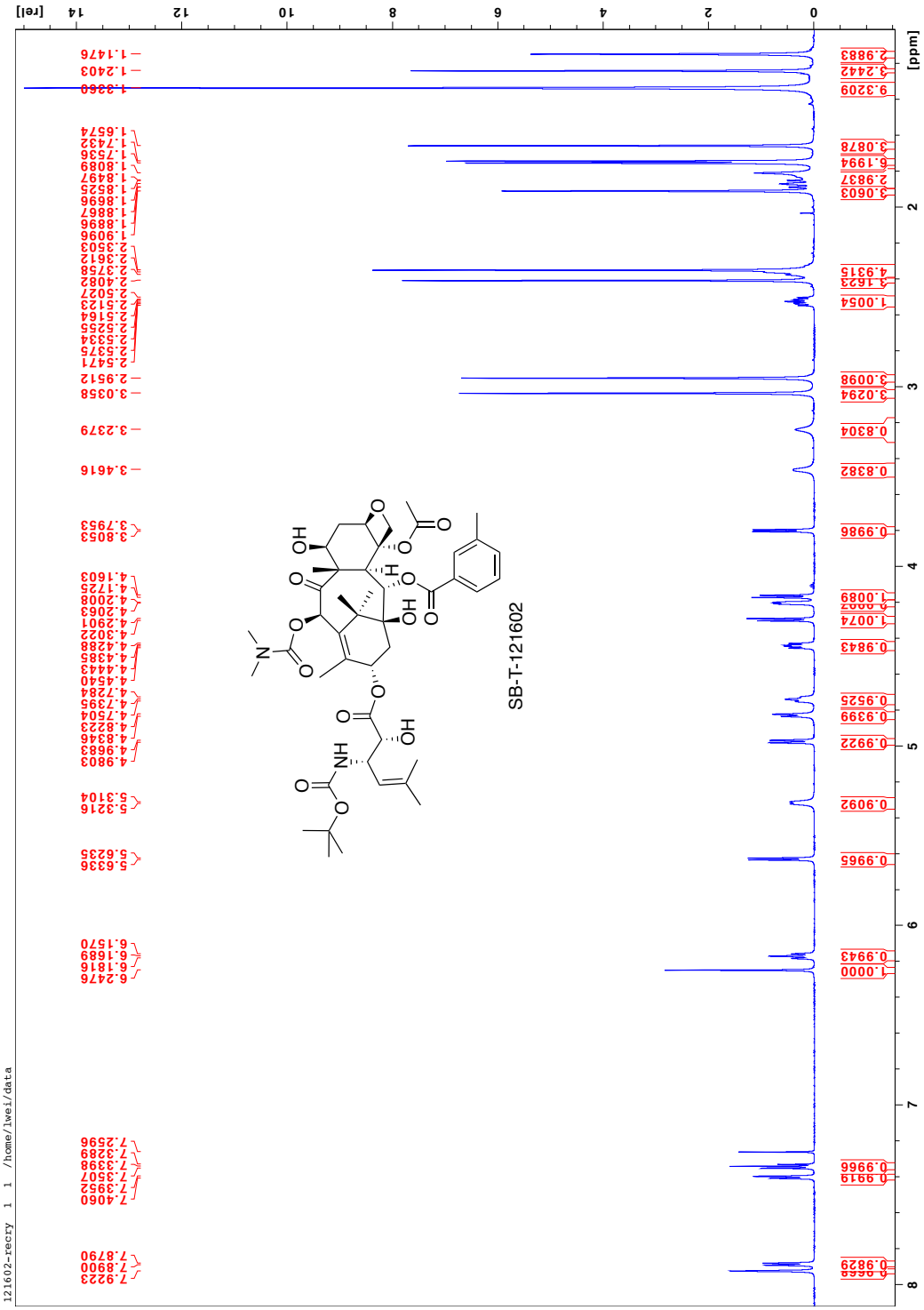
SB-T-121602
121602-recry 1 1 /home/lwei/data
[rel]
[ppm]

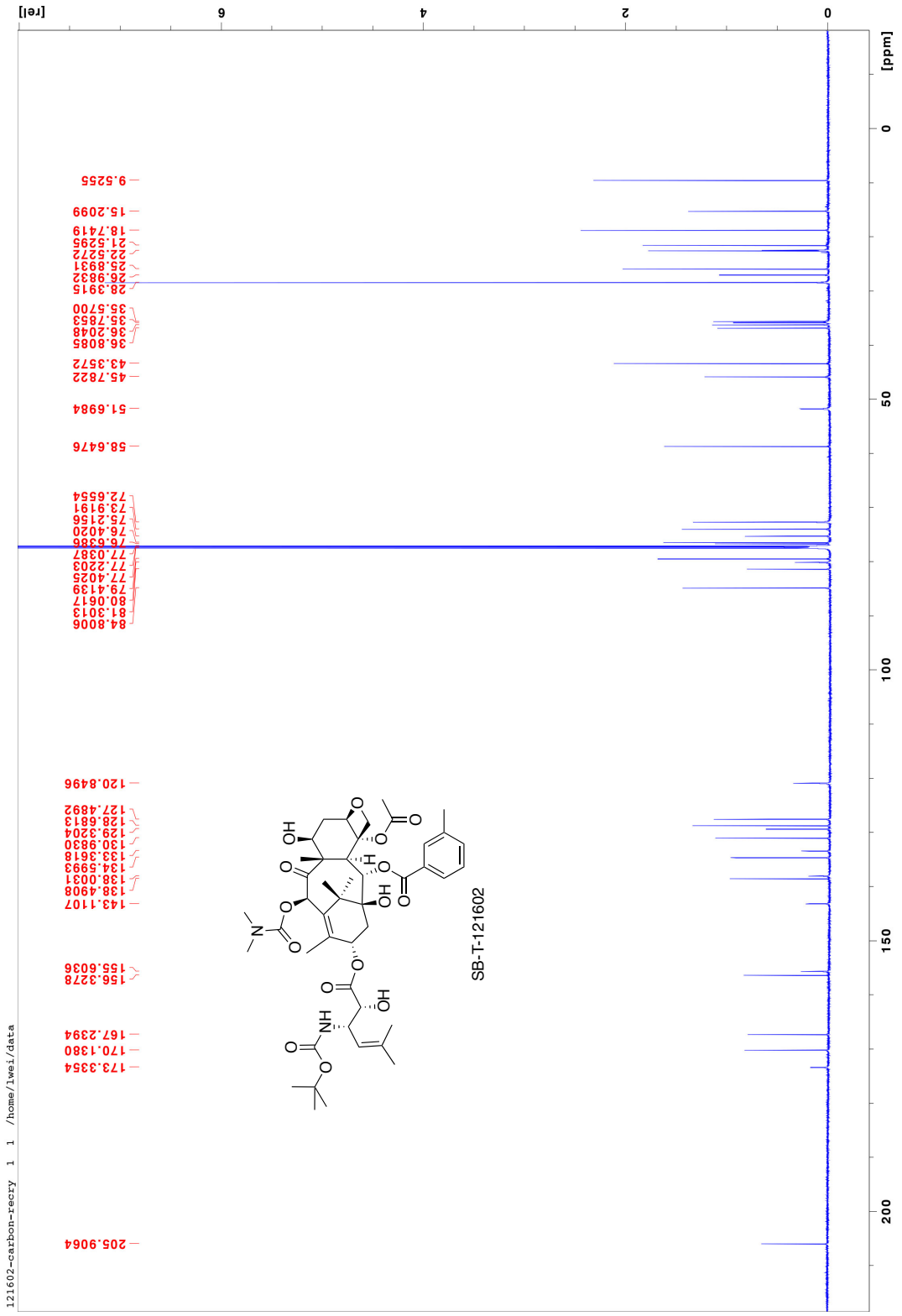
121602-carbon-recry 1 1 /home/lwei/data
[rel]
[ppm]
SB-T-121602
9.5255
15.2099
18.7419
21.5295
22.5272
25.8931
26.9832
28.3915
35.5700
35.7653
36.2048
36.8085
43.3572
45.7822
51.6984
58.6476
72.6554
73.9191
75.2156
76.4020
76.6286
77.0387
77.2203
77.4025
79.4139
80.0617
81.3013
84.8006
120.8496
127.4892
128.6813
129.3204
130.9830
133.3618
134.5993
138.0031
138.4908
143.1107
155.6036
156.3278
167.2394
170.1380
173.3354
205.9064

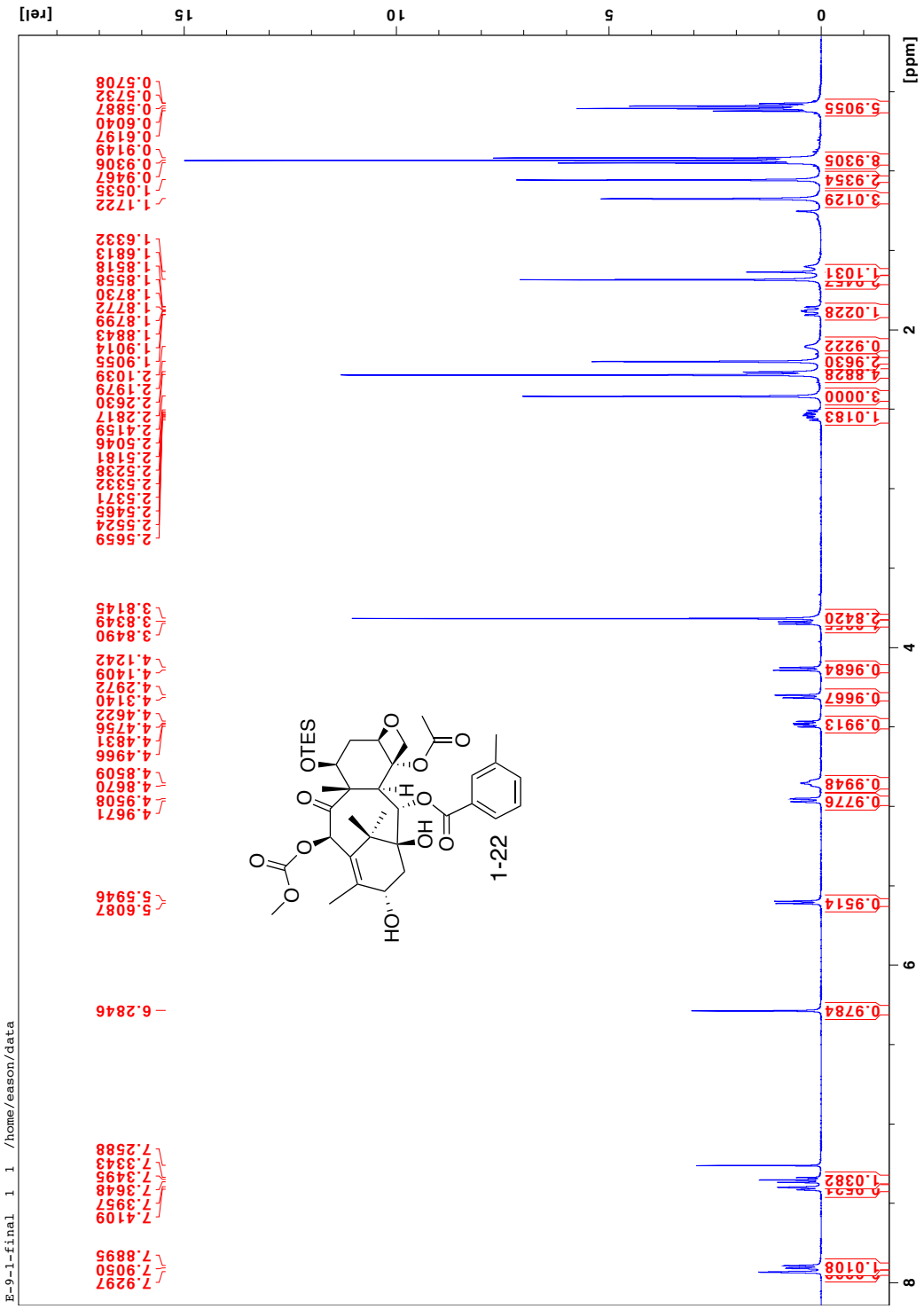
E-9-1-final 1 1 /home/eason/data
[rel]
[ppm]
OTES
OH
OH
1-22

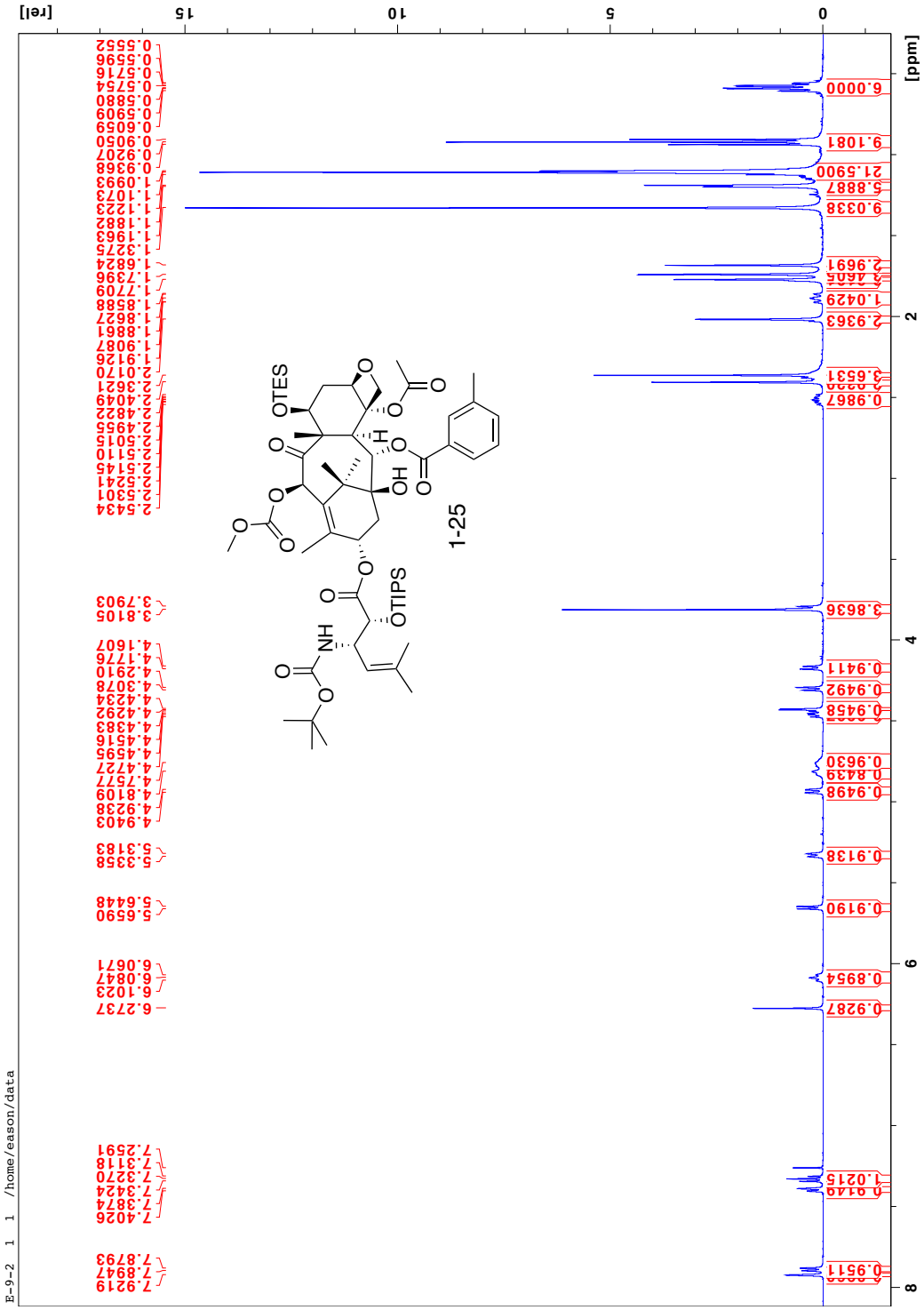
E-9-2 1 1 /home/eason/data
[rel]
[ppm]
OTES
OTIPS
1-25

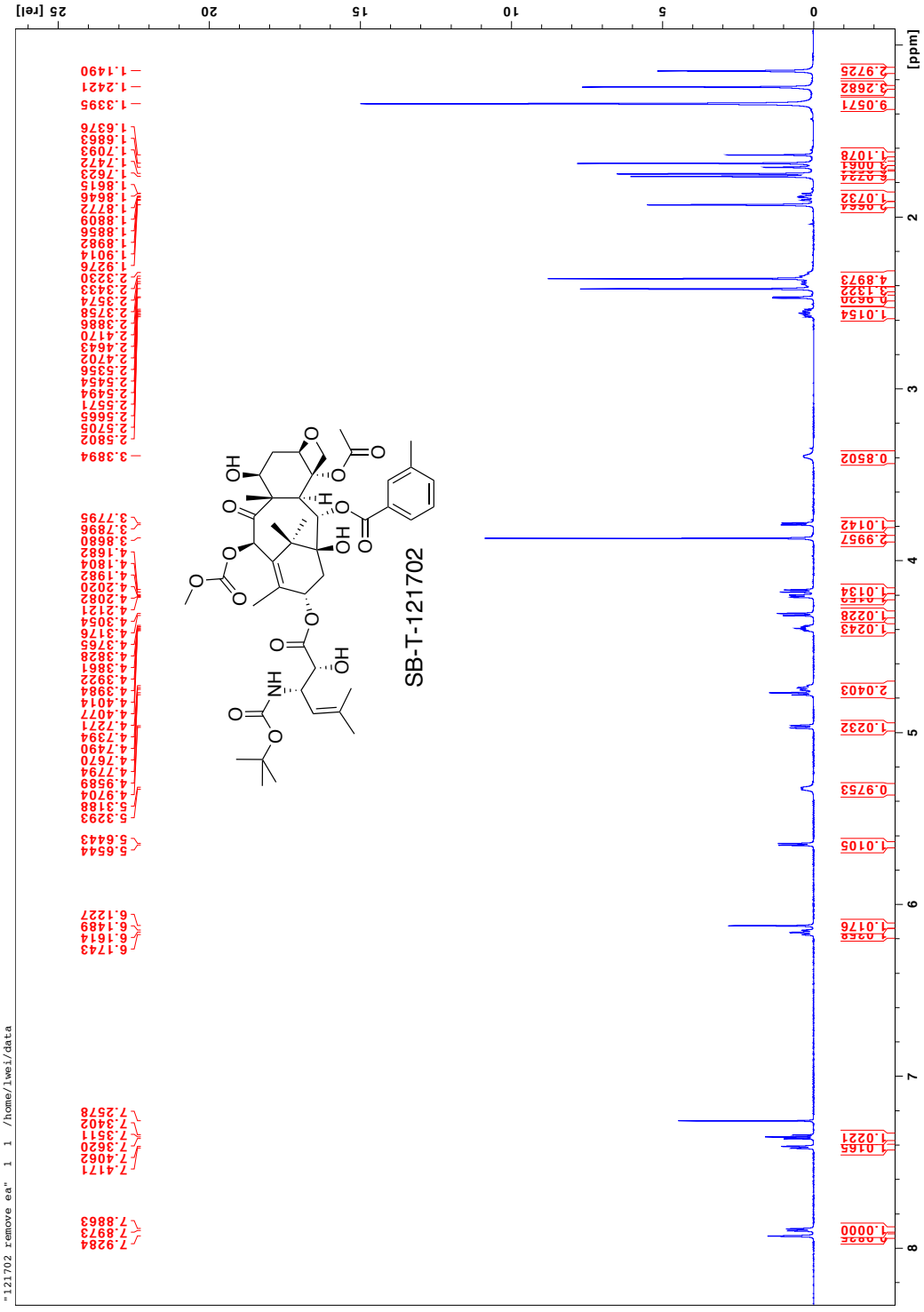
SB-T-121702
"121702 remove ea" 1 1 /home/iwei/data
[ppm]
[rel]

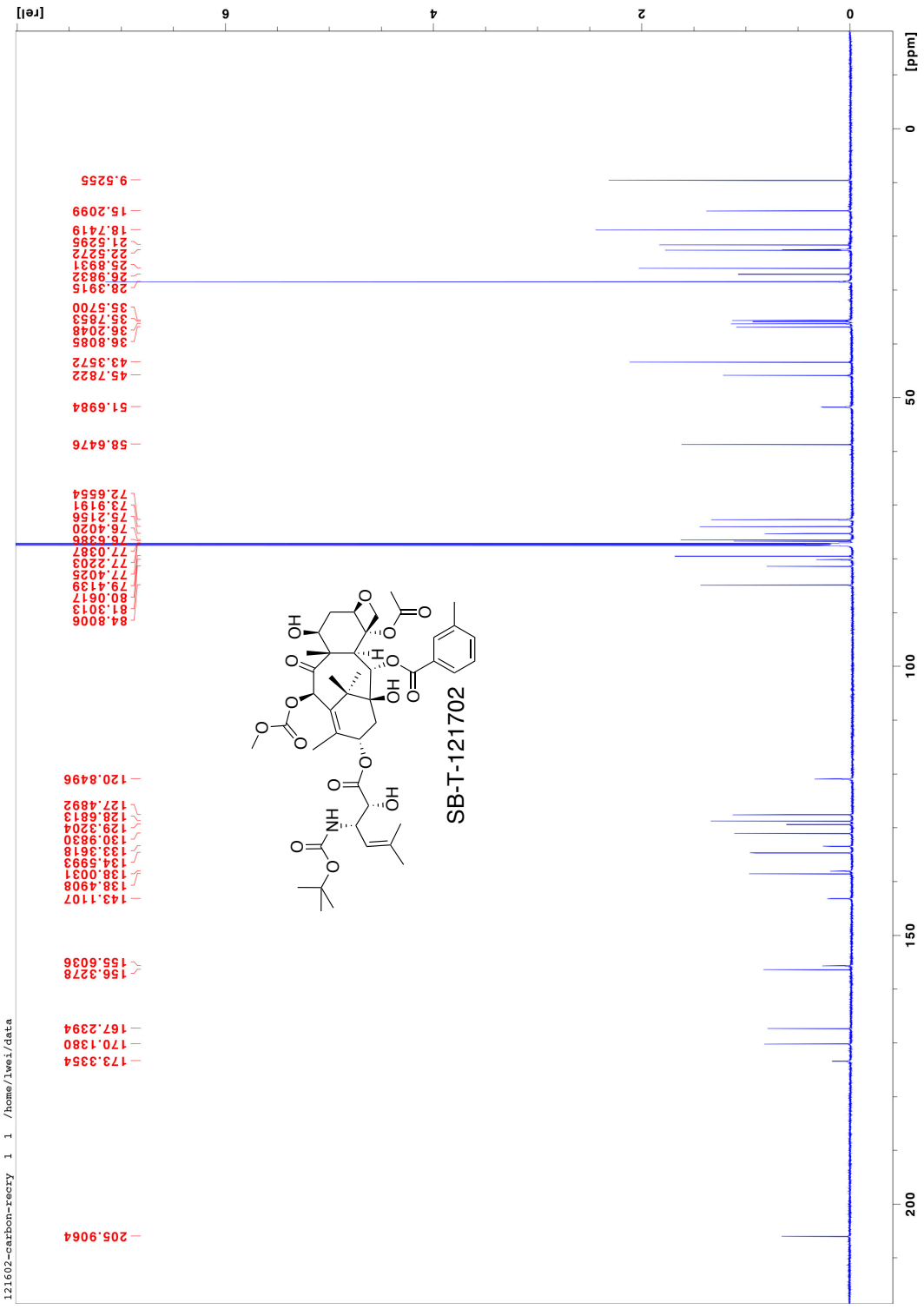
SB-T-121702
121602-carbon-reczy 1 1 /home/lwei/data
[rel]
[ppm]
9.5255
15.2099
18.7419
21.5295
22.5272
25.8931
26.9832
28.3915
35.5700
35.7853
36.2048
36.8085
43.3572
45.7822
51.6984
58.6476
72.6554
73.9191
75.2156
76.4020
76.6386
77.0387
77.2203
77.4025
79.4139
80.0617
81.3013
84.8006
120.8496
127.4892
128.6813
129.3204
130.9830
133.3618
134.5993
138.0031
138.4908
143.1107
155.6036
156.3278
167.2394
170.1380
173.3354
205.9064

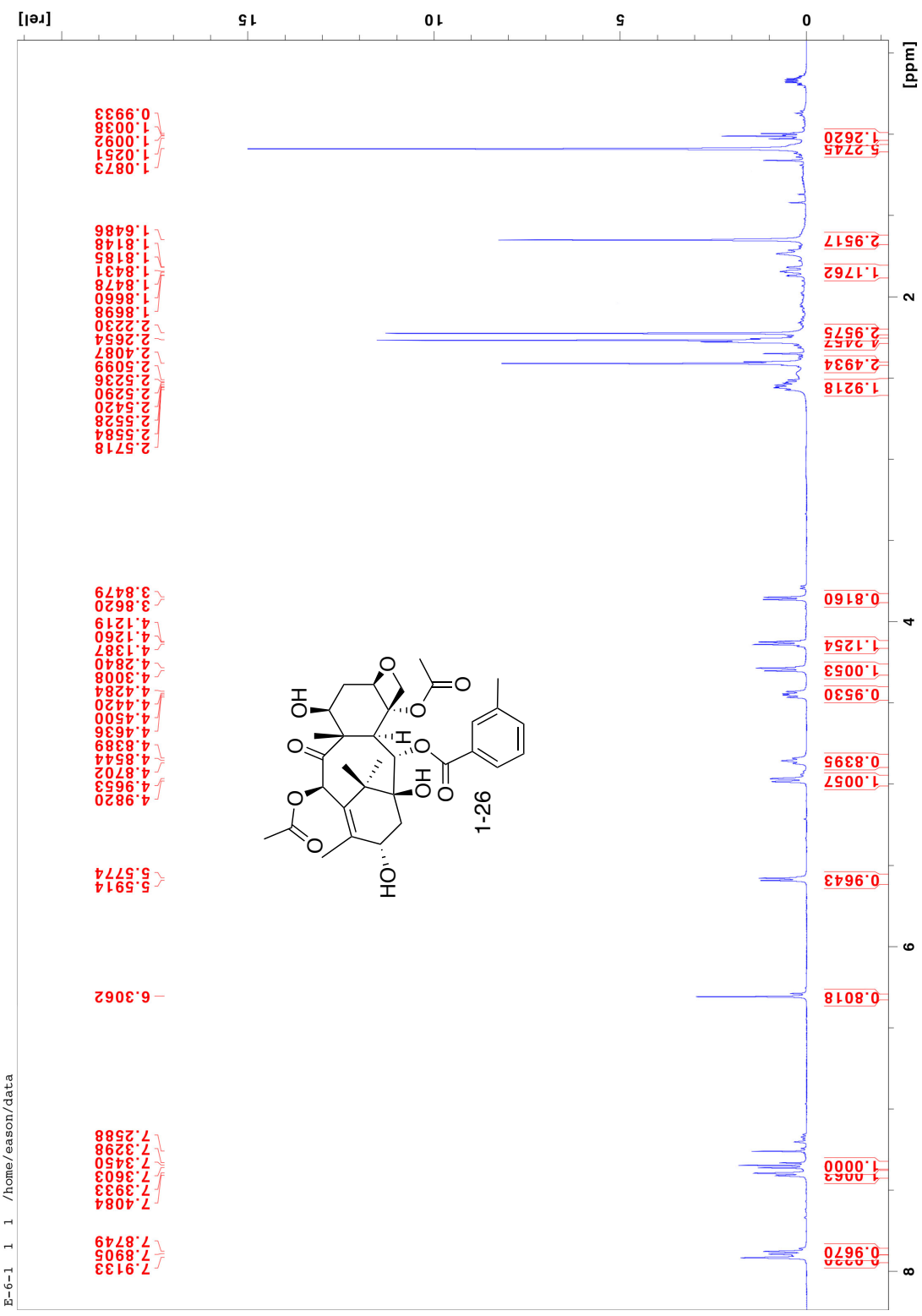
E-6-1 1 1 /home/eason/data
[rel]
[ppm]
1-26

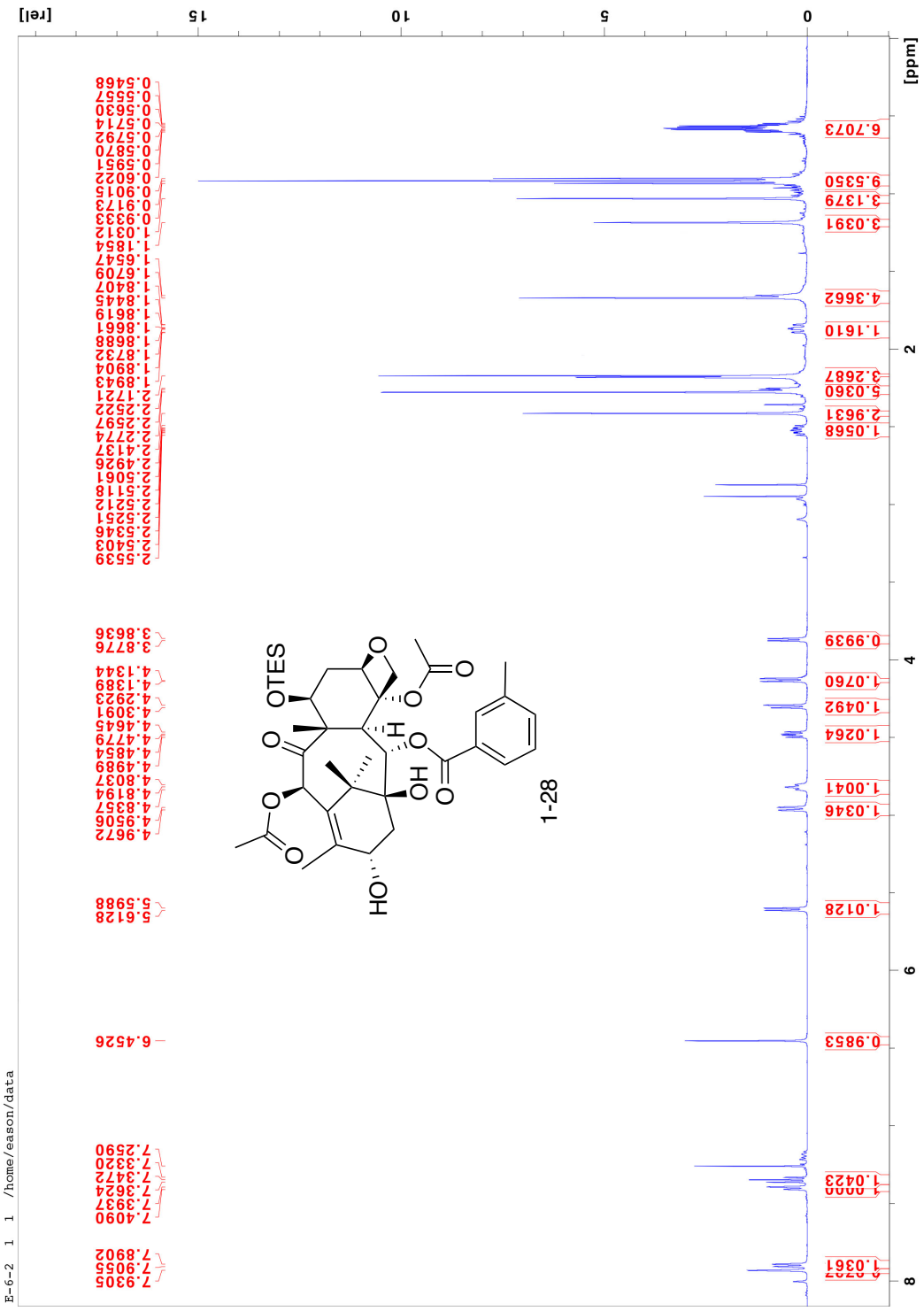
E-6-2 1 1 /home/eason/data
[rel]
15
10
5
0
[ppm]
8
6
4
2
7.9305
7.9055
7.8902
7.4090
7.3937
7.3624
7.3472
7.3320
7.2590
6.4526
5.6128
5.5988
4.9672
4.9506
4.8357
4.8194
4.8037
4.4989
4.4854
4.4779
4.4645
4.3091
4.2923
4.1389
4.1344
3.8776
3.8636
2.5539
2.5403
2.5346
2.5251
2.5212
2.5118
2.5061
2.4926
2.4137
2.2774
2.2597
2.2522
2.1721
1.8943
1.8904
1.8732
1.8688
1.8661
1.8619
1.8445
1.8407
1.6709
1.6547
1.1854
1.0312
0.9333
0.9173
0.9015
0.6022
0.5951
0.5870
0.5792
0.5714
0.5630
0.5557
0.5468
6.7073
9.5350
3.1379
3.0391
4.3662
1.1610
3.2687
5.0360
2.9631
1.0568
0.9939
1.0760
1.0492
1.0264
1.0041
1.0346
1.0128
0.9853
1.0423
1.0000
1.0361
OTES
HO
OH
1-28

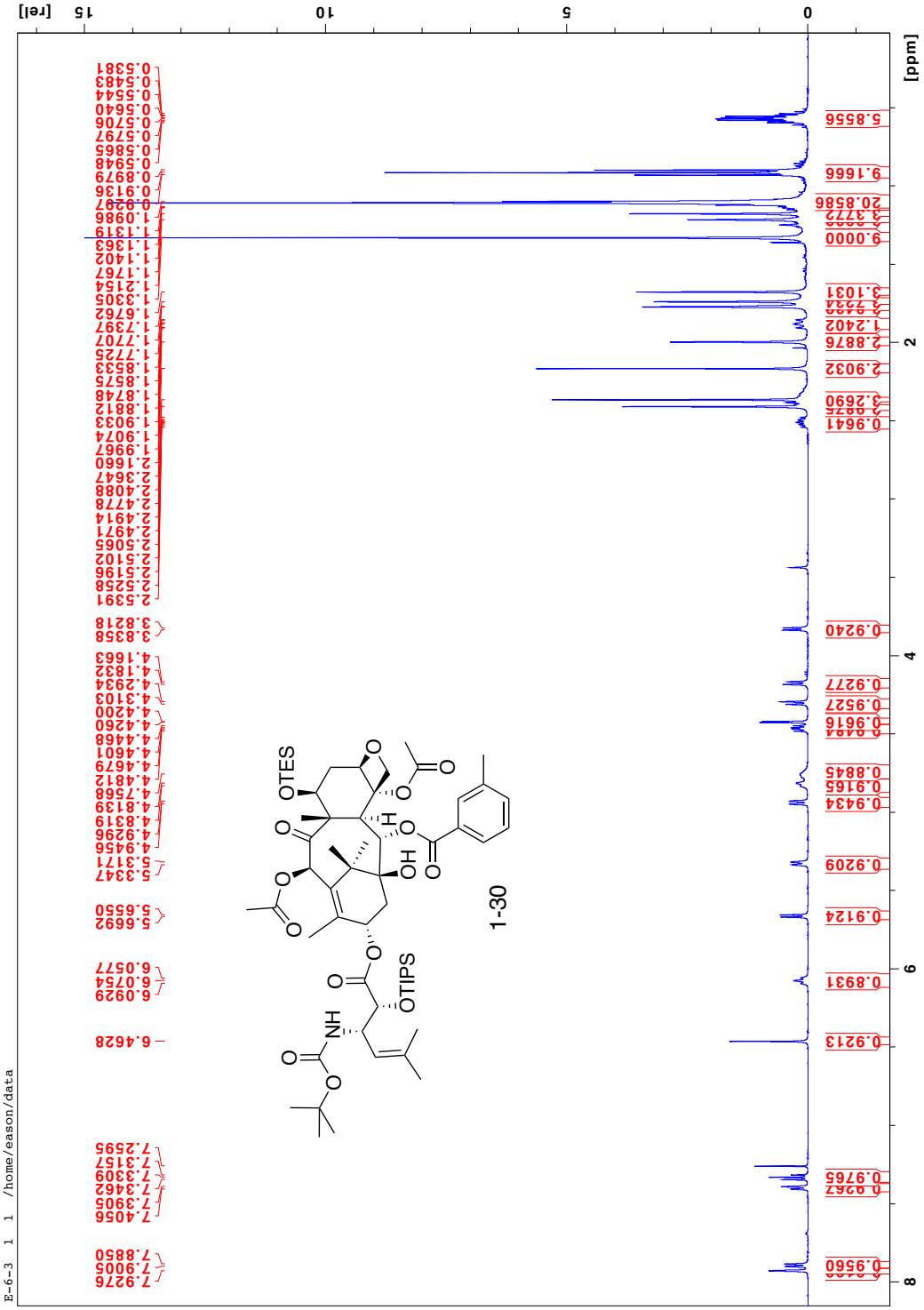
E-6-3 1 1 /home/eason/data
[rel]
[ppm]
OTES
OTIPS
OH
NH
1-30

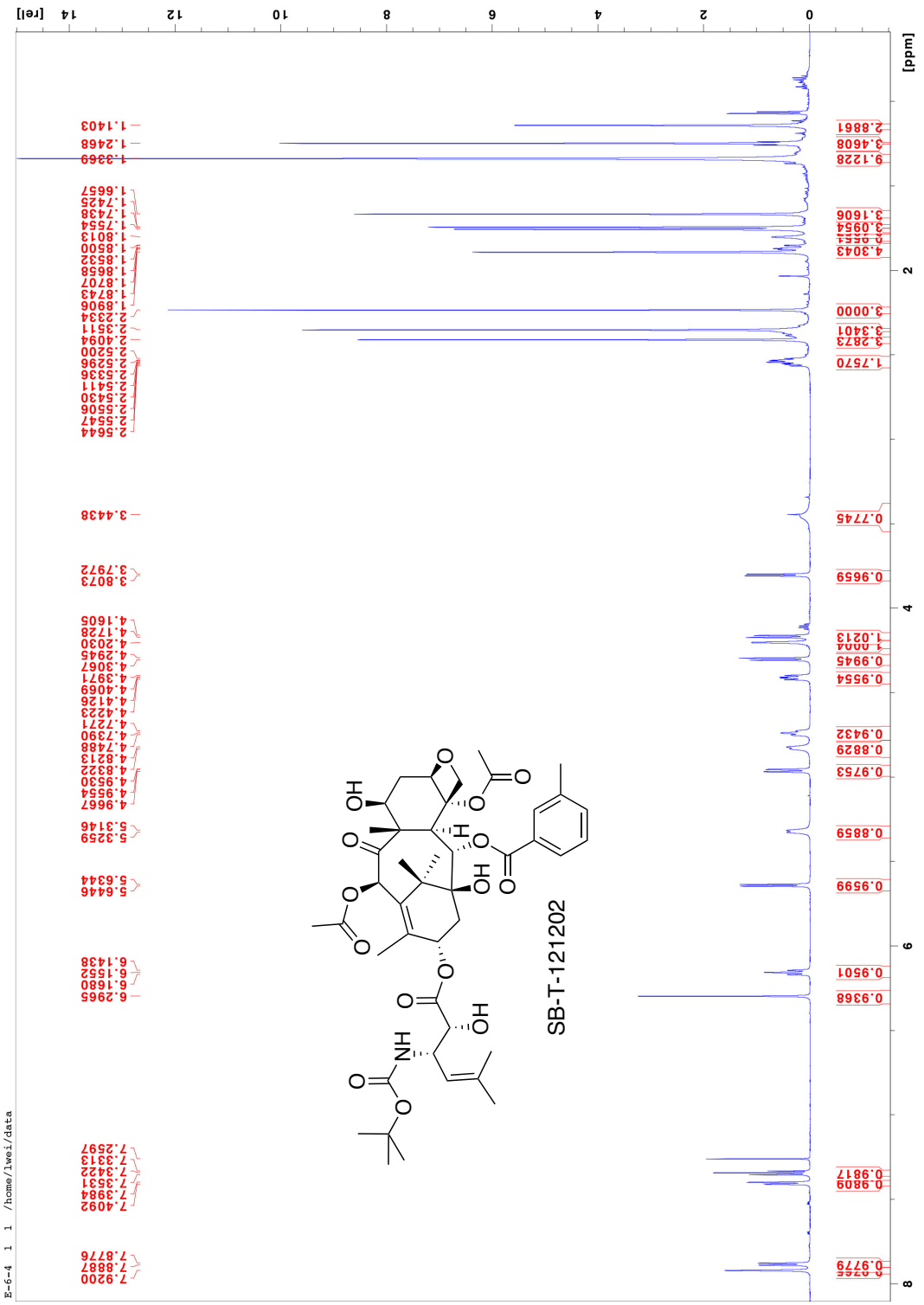
SB-T-121202
E-6-4 1 1 /home/lwei/data
[ppm]
[rel]

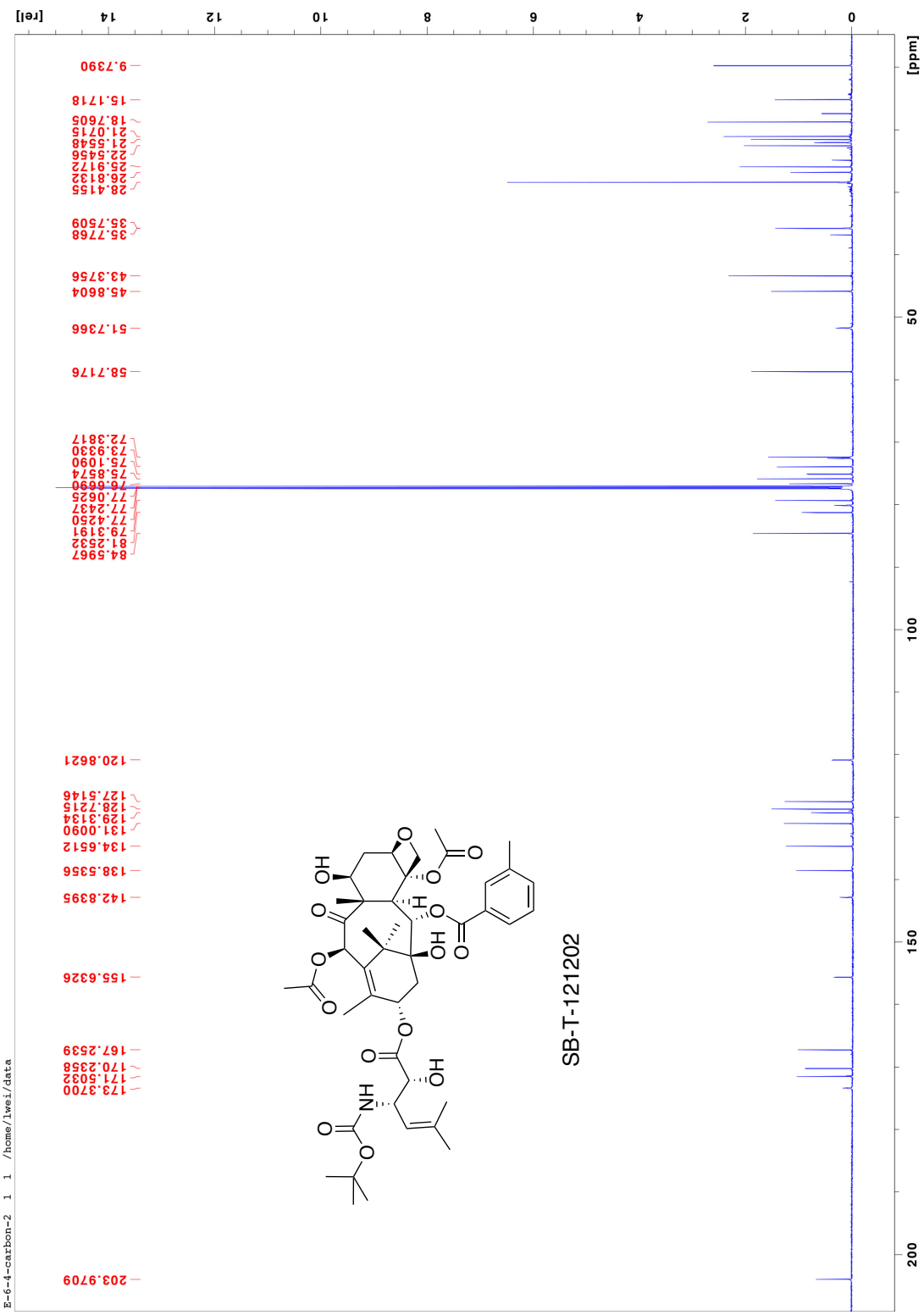
E-6-4-carbon-2 1 1 /home/lwei/data
[rel]
[ppm]
9.7390
15.1718
18.7605
21.0715
21.5548
22.5456
25.9172
26.8132
28.4155
35.7509
35.7768
43.3756
45.8604
51.7366
58.7176
72.3817
73.9330
75.1090
75.8574
76.6890
77.0625
77.2437
77.4250
79.3191
81.2532
84.5967
120.8621
127.5146
128.7215
129.3134
131.0090
134.6512
138.5356
142.8395
155.6326
167.2539
170.2358
171.5032
173.3700
203.9709
SB-T-121202

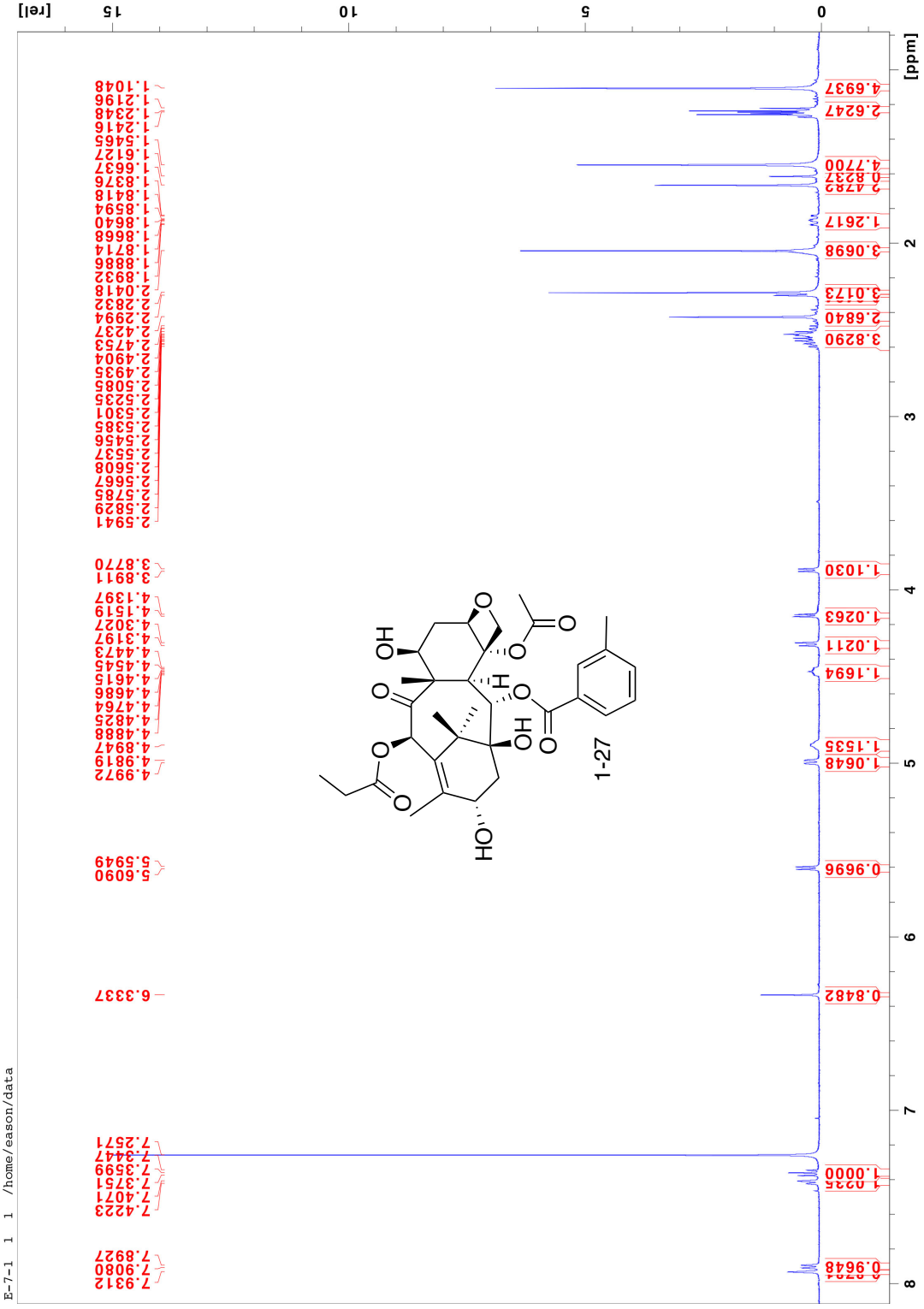
E-7-1 1 1 /home/eason/data
[rel]
[ppm]
1-27


E-7-2 1 1 /home/eason/data
[rel]
[ppm]
OTES
HO
OH
1-29

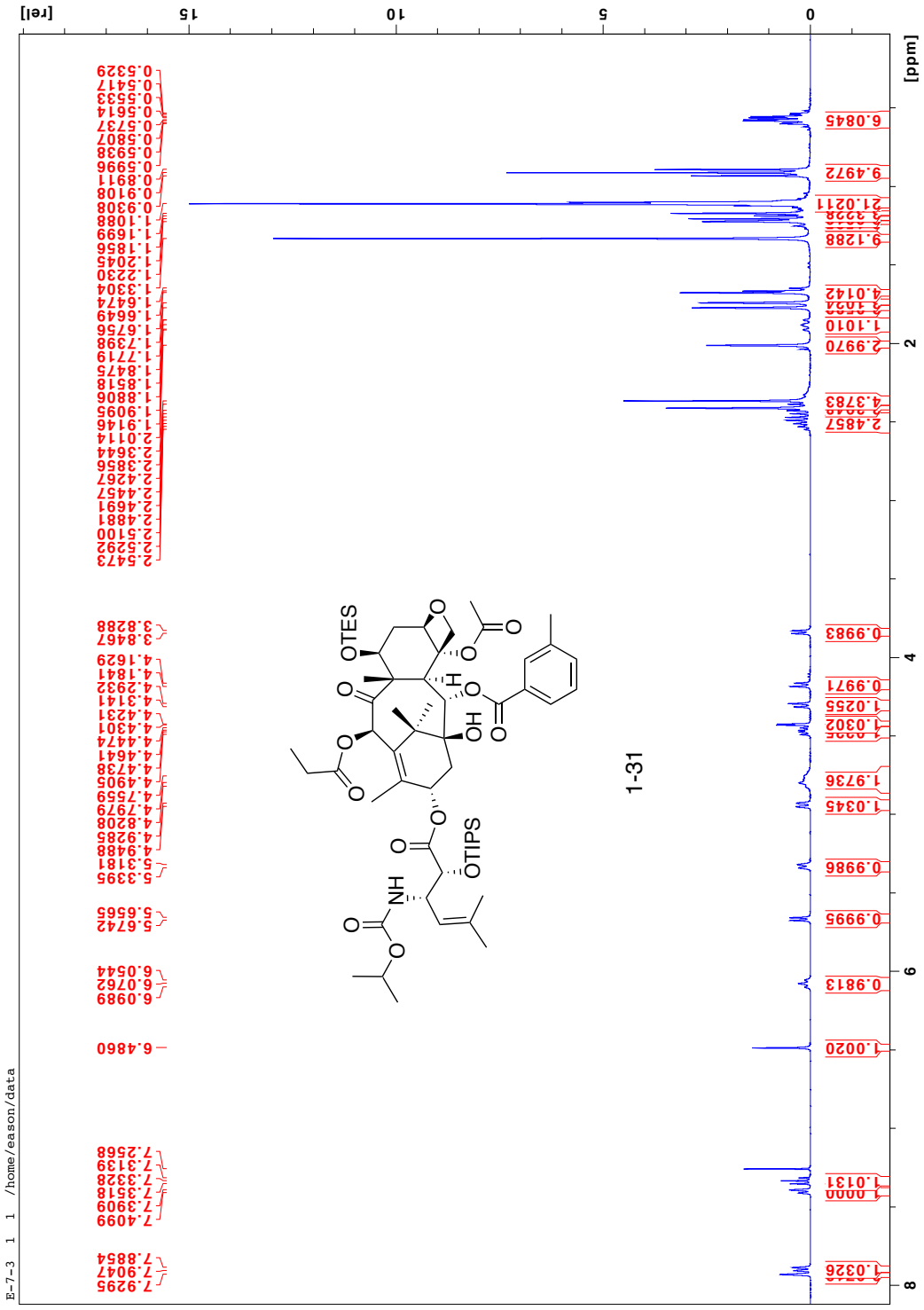
E-7-3 1 1 /home/eason/data
[rel]
[ppm]
1-31
OTES
OTIPS
OH
NH

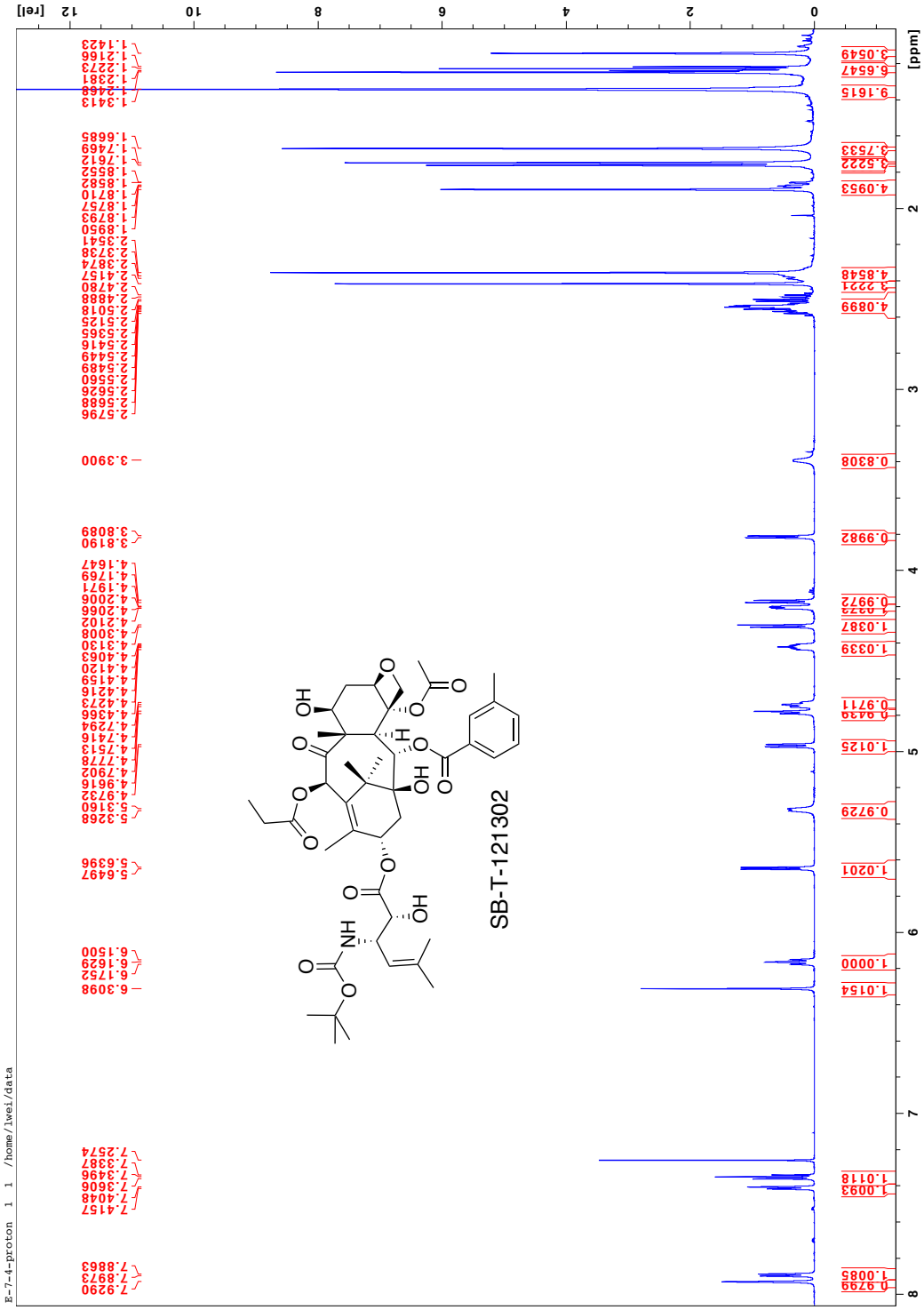
SB-T-121302
E-7-4-proton 1 1 /home/iwei/data
[ppm]
[rel]

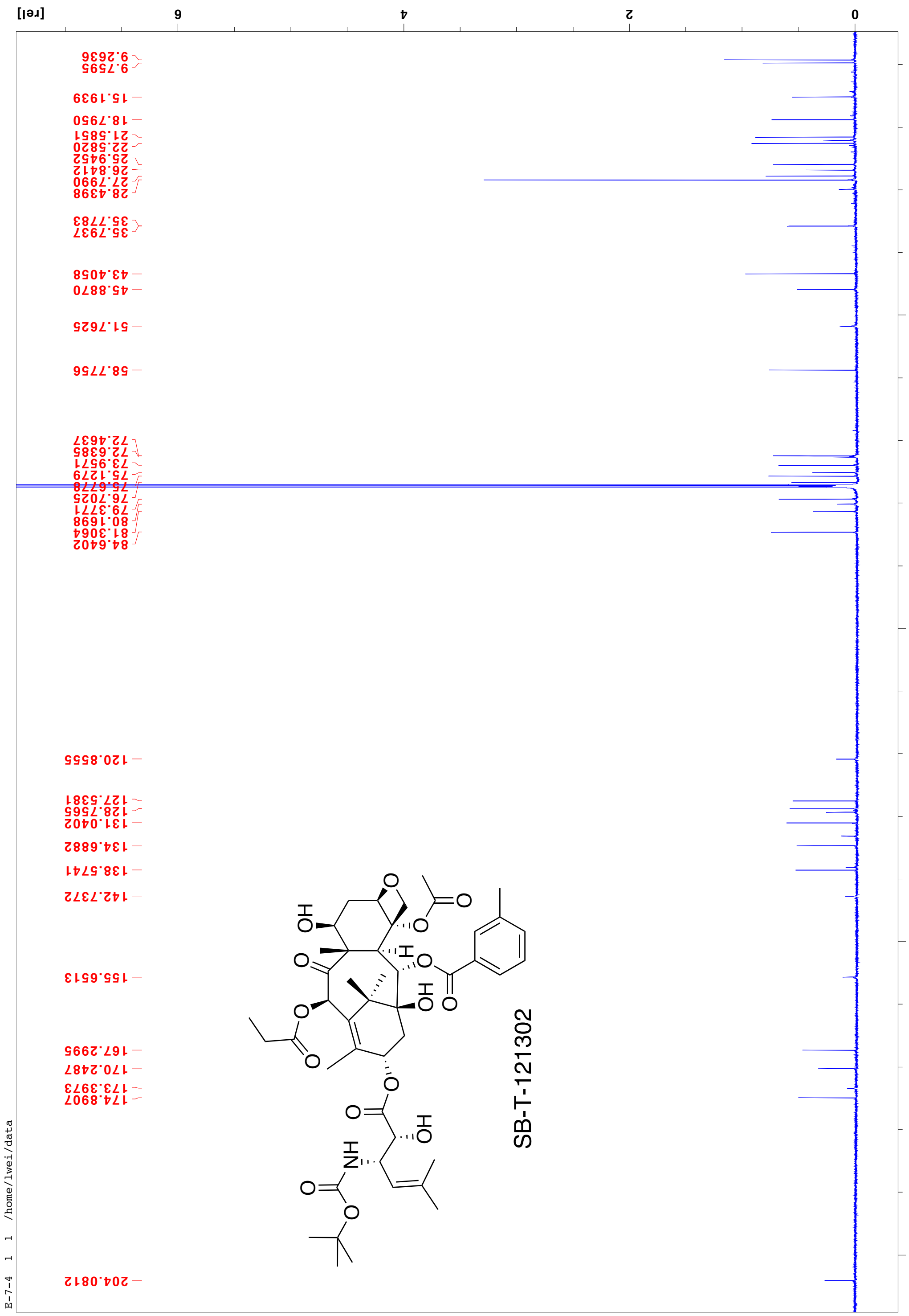
SB-T-121302
E-7-4 1 1 /home/lwei/data
[rel]
[ppm]
9.2636
9.7595
15.1939
18.7950
21.5851
22.5820
25.9452
26.8412
27.7990
28.4398
35.7783
35.7937
43.4058
45.8870
51.7625
58.7756
72.4637
72.6385
73.9571
75.1279
76.6770
76.7025
79.3771
80.1698
81.3064
84.6402
120.8555
127.5381
128.7565
131.0402
134.6882
138.5741
142.7372
155.6513
167.2995
170.2487
173.3973
174.8907
204.0812

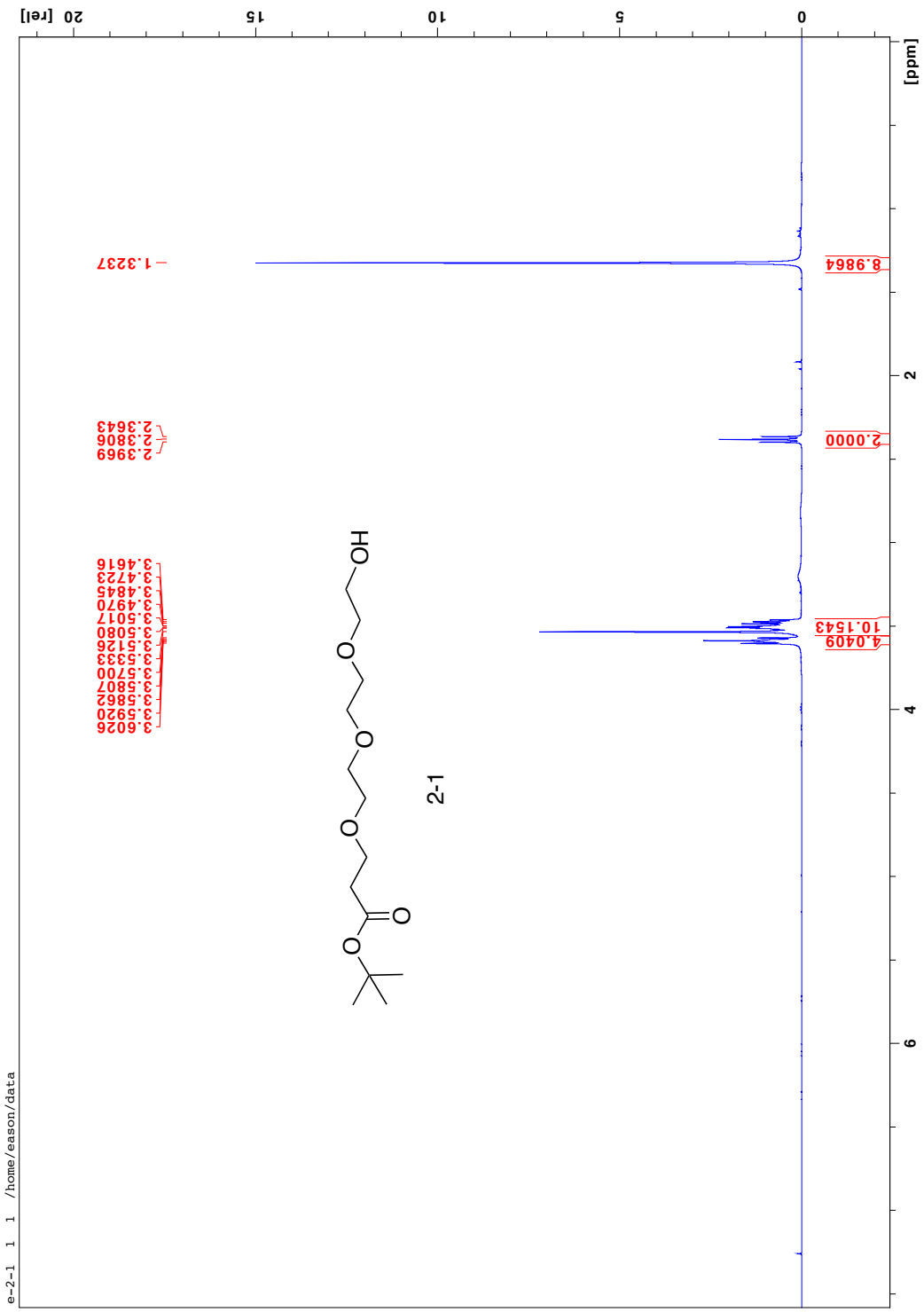
e-2-1 1 1 /home/eason/data
[rel]
20
15
10
5
0
[ppm]
6
4
2
8.9864
2.0000
10.1543
4.0409
1.3237
2.3969
2.3806
2.3643
3.4616
3.4723
3.4845
3.4970
3.5017
3.5080
3.5126
3.5333
3.5700
3.5807
3.5862
3.5920
3.6026
OH
O
O
O
O
O
O
2-1

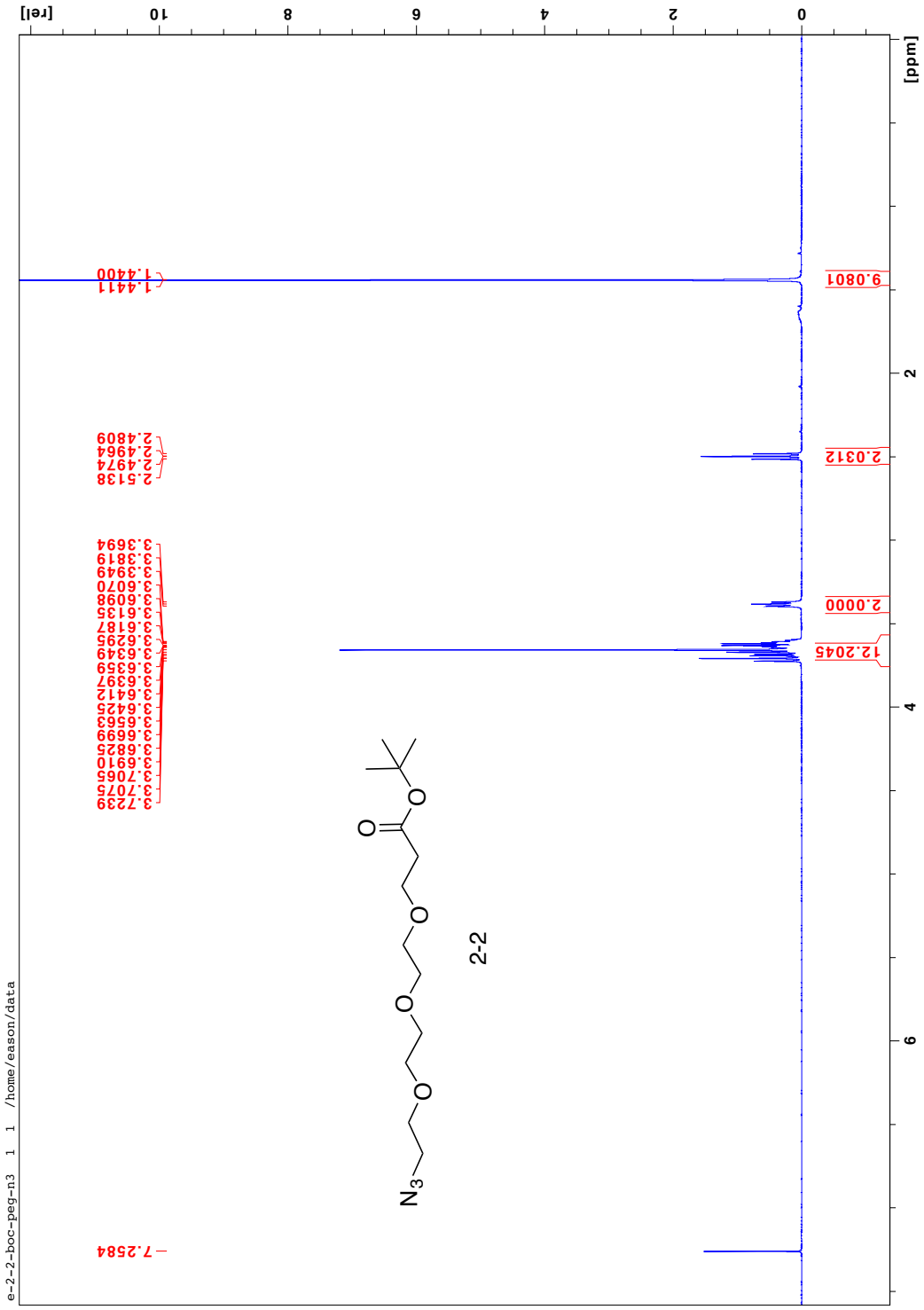
e-2-2-boc-peg-n3 1 1 /home/eason/data
[rel]
[ppm]
7.2584
3.7239
3.7075
3.7065
3.6910
3.6825
3.6699
3.6563
3.6425
3.6412
3.6397
3.6359
3.6349
3.6295
3.6187
3.6135
3.6098
3.6070
3.3949
3.3819
3.3694
2.5138
2.4974
2.4964
2.4809
1.4411
1.4400
12.2045
2.0000
2.0312
9.0801
2-2

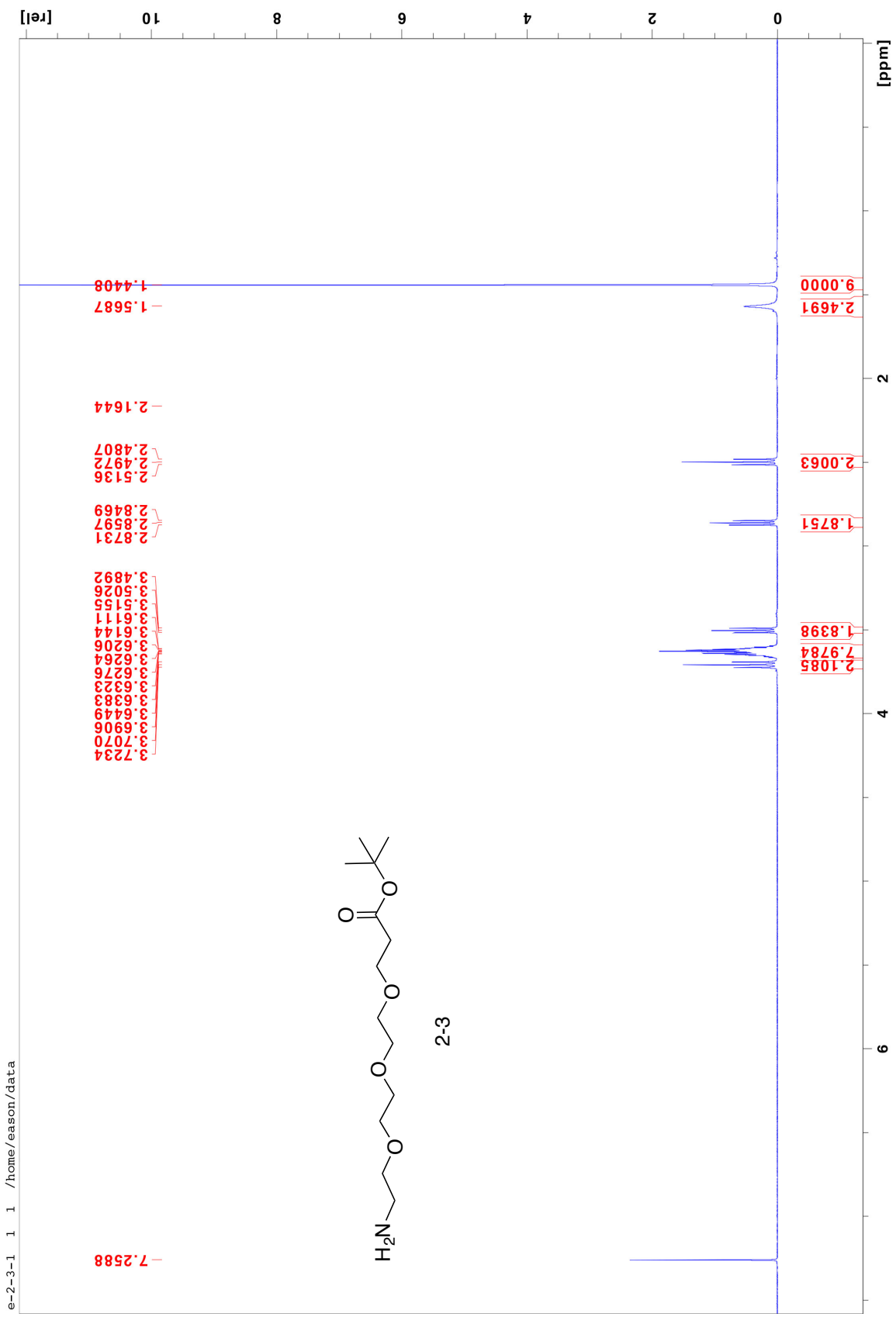
e-2-3-1 1 1 /home/eason/data
[rel]
[ppm]
0
2
4
6
8
10
7.2588
3.7234
3.7070
3.6906
3.6449
3.6383
3.6323
3.6276
3.6264
3.6206
3.6144
3.6111
3.5155
3.5026
3.4892
2.8731
2.8597
2.8469
2.5136
2.4972
2.4807
2.1644
1.5687
1.4408
9.0000
2.4691
2.0063
1.8751
1.8398
7.9784
2.1085
2-3

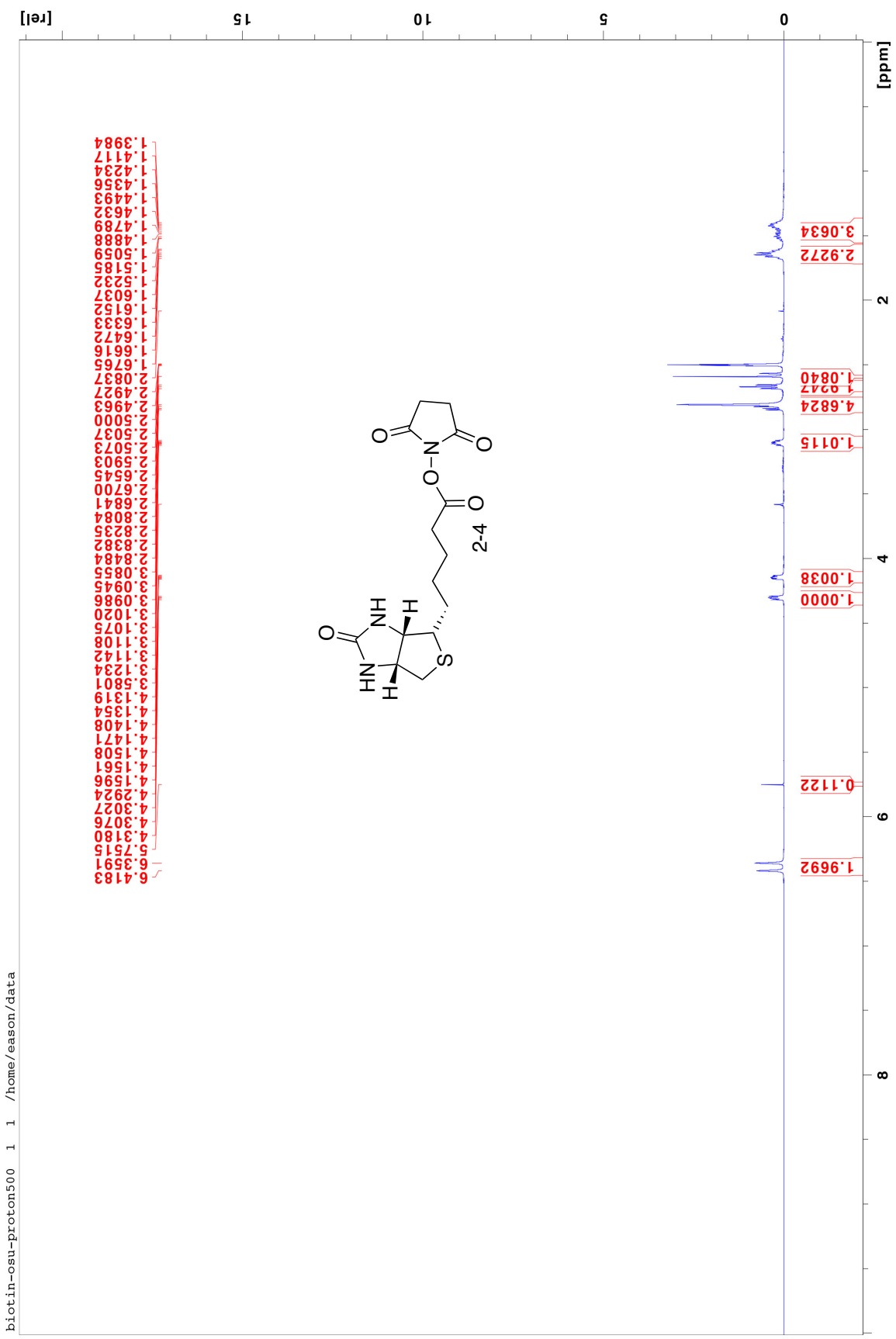
biotin-osu-proton500 1 1 /home/eason/data
[rel]
[ppm]
2-4
1.9692
0.1122
1.0038
1.0000
1.0115
4.6824
1.0840
3.0634
2.9272

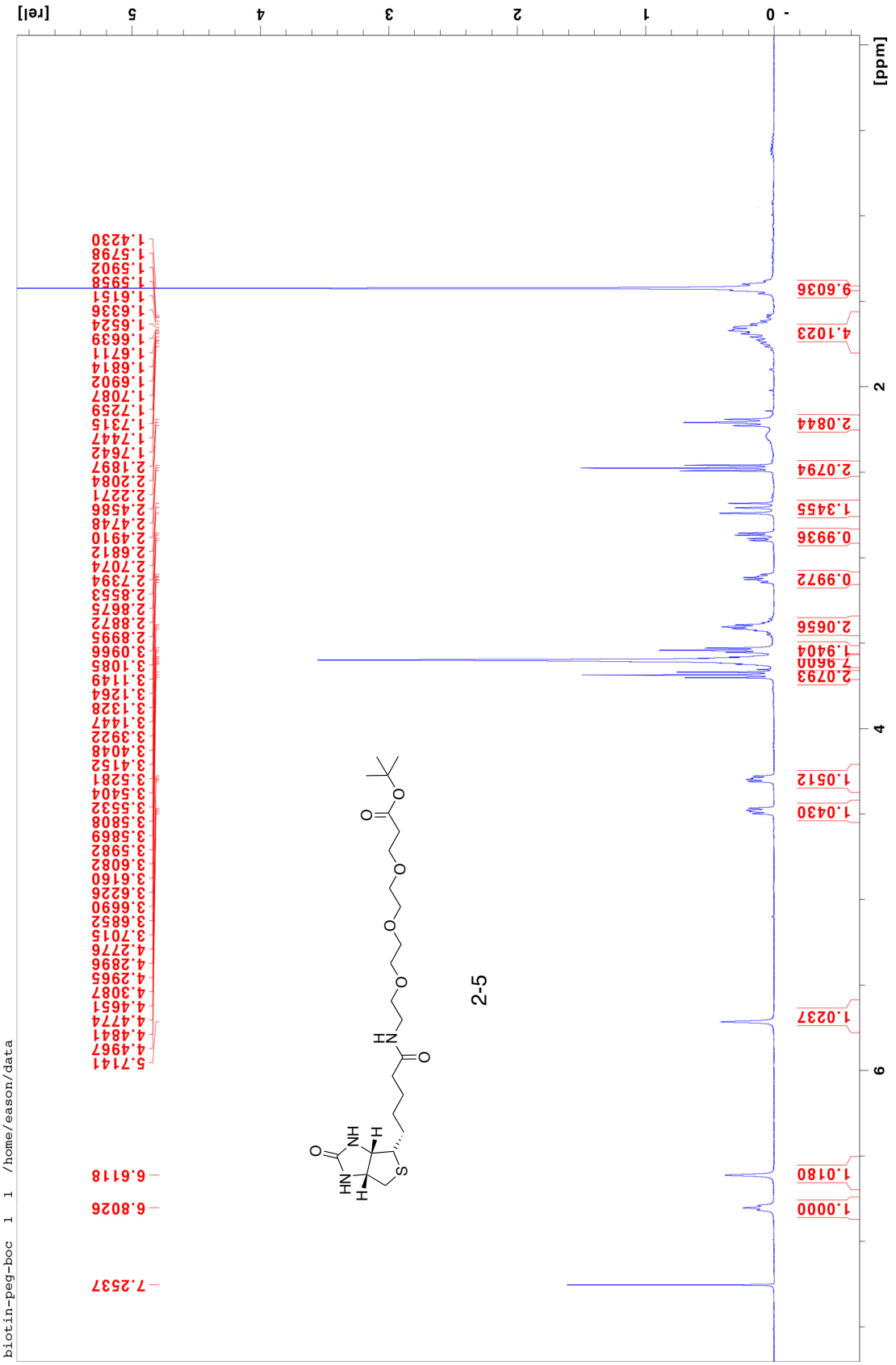
biotin-peg-boc 1 1 /home/eason/data
[rel]
[ppm]
2-5
9.6036
4.1023
2.0844
2.0794
1.3455
0.9936
0.9972
2.0656
1.9404
2.0793
1.0512
1.0430
1.0237
1.0180
1.0000
7.2537
6.8026
6.6118

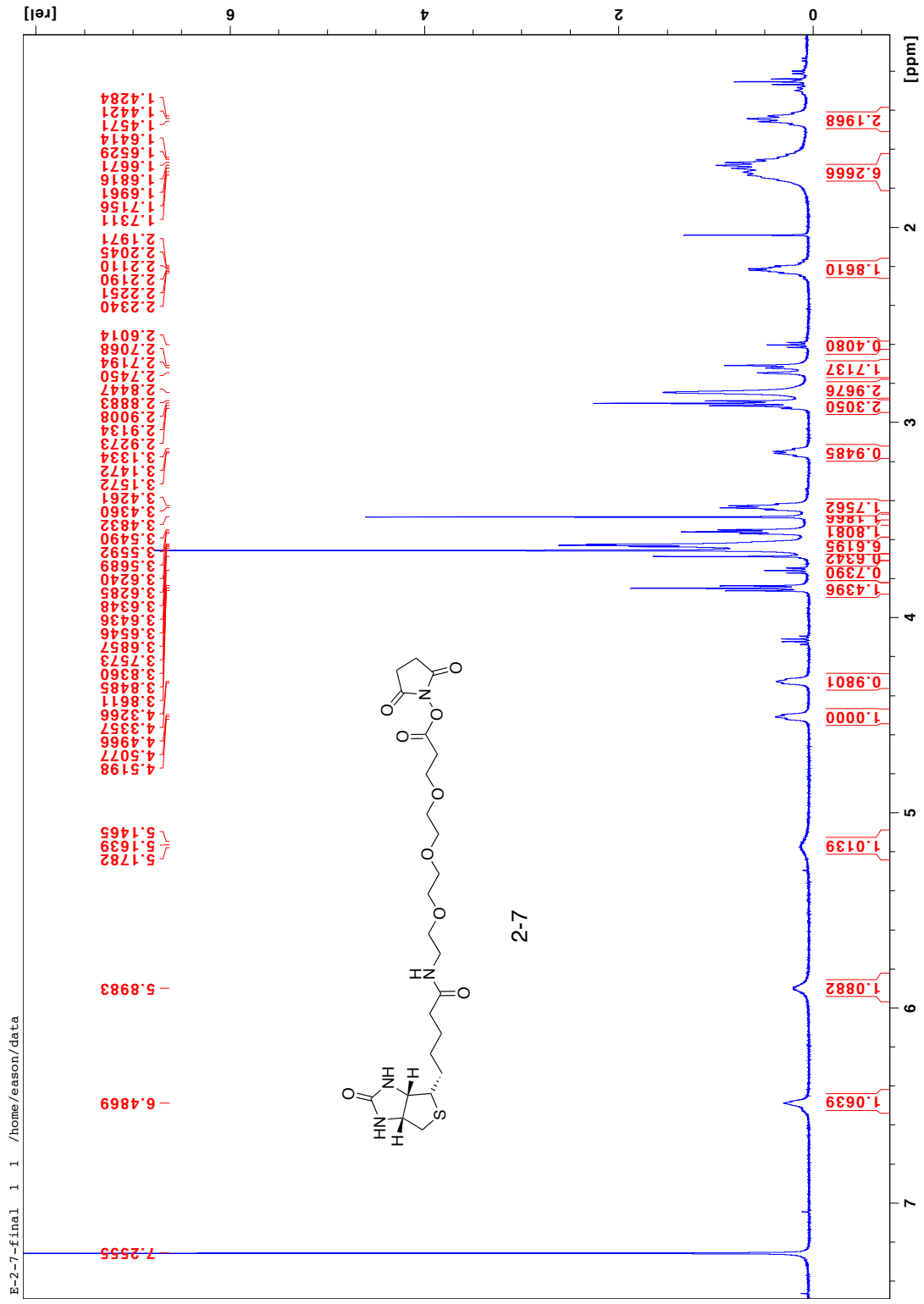
E-2-7-final 1 1 /home/eason/data
[rel]
[ppm]
2-7
7.2565
6.4869
5.8983
5.1782
5.1639
5.1465
4.5198
4.5077
4.4966
4.3357
4.3266
3.8611
3.8485
3.8360
3.7573
3.6857
3.6546
3.6436
3.6348
3.6285
3.6240
3.5689
3.5592
3.5490
3.4832
3.4360
3.4261
3.1572
3.1472
3.1334
2.9273
2.9134
2.9008
2.8883
2.8447
2.7450
2.7194
2.7068
2.6014
2.2340
2.2251
2.2190
2.2110
2.2045
2.1971
1.7311
1.7156
1.6961
1.6816
1.6671
1.6529
1.6414
1.4571
1.4421
1.4284
1.0639
1.0882
1.0139
0.9801
1.0000
1.4396
0.7390
0.6342
6.6195
1.8081
1.7562
0.9485
2.3050
2.9676
1.7137
0.4080
1.8610
6.2666
2.1968